Understanding the Origins of Haematopoietic Stem Cells in the E11.5 AGM Region using a Novel Reaggregate Culture System.

Christèle Gonneau

Thesis presented for the degree of Doctor of Philosophy

University of Edinburgh

Centre for Regenerative Medicine, Institute for Stem Cell Research

2009

I declare that the work present in this thesis is my own, except otherwise stated

Christèle Gonneau

À mes parents …

i. Acknowledgements

I thank my supervisor, Dr. Alexander Medvinsky for his guidance, support, and encouragement throughout my PhD. I also thank him for many invaluable discussions and for his genuine passion for science, both of which have been a great inspiration during difficult times. I also thank Dr. Samir Taoudi for his extreme patience, scientific teachings, and friendship; they have been invaluable assets. My sincere thanks are given to animal units members, Ray McInnes and Carol Manson and their technicians, who provided superb assistance and professionalism. I would also like to acknowledge the provision of fantastic technical assistance from Suling Zhao, Erin Taylor and Karen Anderson. Thanks to Jan Vrana and Simon Monard for their help with cell sorting, and to Dr. Adin Ross-Gillespie for his help with statistics. Thanks to Dr. David Hills, Dr. Stanislav Rybstov, Dr. Jennifer Antonchuk, Dr. Kate Moore, Dr. Sabrina Gordon-Keylock, Dr. Celine Souilhol, and Dr. Owen Davies for their post-doctoral scientific and moral support.

I would also like to thank my dear PhD fellows and friends Nick, Pedro, Laura, Ellie, Michelle, Anna, Alison, Alistair and Aga for sharing the same boat, for their support and understanding in the dark days. Many thanks to Remi, Fleur, and Sophie for their precious friendship, and for always being there for me. I would like to particularly thank my great friend Katia, who was never scared to stay by my side until late hours and whose friendship, kindness and moral support have been invaluable. I would also like to particularly thank my dear friend Adin, my rock throughout my PhD, for his patience and understanding, for his wonderful rants, his imaginative cooking, and for the many long discussions that opened my mind about many aspects of science and life.

Finally, I would like to thank my parents, Jean-Pierre and Marika, for their unwavering moral support throughout my studies and whose infinite love and trust are my greatest strengths. Merci maman et papa…

ii. Abstract

Identifying the sites and mechanisms involved in haematopoietic stem cells (HSCs) during development would improve our understanding of how to induce HSCs from alternative sources like embryonic stem cells, while offering insight into pathways involved in HSC-related diseases such as leukaemia. Adult-type HSC, or long-term reconstituting HSCs (LTR-HSCs), are widely defined as cells capable of reconstituting the entire haematopoietic system of a lethally irradiated adult recipient. The first LTR-HSCs emerge and expand in the aorta-gonad-mesonephros (AGM) region of the mid-gestation mouse embryo. Recently, the development of a novel reaggregate culture system has provided a valuable tool to identify key cell populations involved in LTR-HSC development. This system allows the mechanical dissociation of the E11.5 AGM region prior to culture whilst maintaining its ability to autonomously expand LTR-HSCs. Here, I show that reaggregate LTR-HSCs are $CD45^{+}Sca1^{+}c\text{-}kit^{+}CD31^{med}$ and that IL-3, SCF, and Flt3l are required in order to achieve an optimal 150 fold LTR-HSC expansion. I also characterise the pattern of Runx1 expression in the adult and E11.5 AGM region of our novel *Runx1*^{EGFP} reporter mouse and identify a population of $EGFP^{+}CD45^{-}VE\text{-}cadherin^{-}$ cells in the E11.5 AGM region that disappears during reaggregate culture. Finally, using the E11.5 AGM reaggregate culture, I show that while uro-genital ridges are potentially required for optimal LTR-HSC expansion, most LTR-HSCs are derived from the dorsal aorta (Ao) region, and that the dorsal aspect of the dorsal aorta (AoD) can contribute to the reaggregate LTR-HSCs compartment.

iii. Table of contents

iv. List of abbreviations

7-AAD	7-aminoactinomycin D
AGM	Aorta Gonad Mesonephros
Ao	dorsal Aorta
AoD	dorsal Aorta, Dorsal domain
AoV	dorsal Aorta, Ventral domain
BFU-E	Burst Forming Unit-Erythroid
bHLH	basic Helix Loop Helix
BL-CFC	Blast Colony Forming Cell
BrDU	Bromodeoxyuridine
CBF	Core Binding Factor
CFSE	Carboxyfluorescein Succinimidyl Esther
CFU-C	Colony Forming Unit-Culture
CFU-GEMM	Granulocyte/Erythrocyte/Macrophage/Megakaryocyte
CFU-GM	Colony Forming Unit-Granulocyte/Macrophage
CFU-mac	Colony Forming Unit-macrophage
CFU-mast	Colony Forming Unit-mast
CFU-meg	Colony Forming Unit-megakaryocyte
CFU-S	Colony Forming Unit-Spleen
CLP	Common Lymphoid Progenitor
CMP	Common Myeloid Progenitor
DAPI	4-6 Diamidino-2-phenylindole
DLP	Dorso-Lateral Plate
DMZ	Dorsal Marginal Zone
DT	Dorsal Tissue
E	Embryonic day
EB	Embryoid Body
EGFP	Enhanced Green Fluorescent Protein
ES	Embryonic Stem
FACS	Fluorescence Activated Cell Sorting
FCS	Fetal Calf Serum
FGF	Fibroblast Growth Factor
Flt3l	Fms-like tyrosine kinase 3-ligand
GFP	Green Fluorescent Protein
GM-CSF	Granulocyte-Macrophage Colony Stimulating Factor

GMP	Granulocyte Macrophage Progenitor
Hox	Homeobox
HSC	Haematopoietic Stem Cell
IAHC	Intra-Aortic Haematopoietic Cluster
IGF	Insulin Growth Factor
IL	Interleukin
IRES	Internal Ribosome Entry Site
Lin	Lineage
Lmo2	LIM domain only 2
LSK	$Lin^{-}Sca1^{+}c\text{-}kit^{+}$
LTR	Long-Term Repopulating
M-CSF	Macrophage Colony Stimulating Factor
MEP	Megakaryocyte Erythrocyte Progenitor
MFI	Median Fluorescence Intensity
NLS	Nuclear Localisation Signal
P/S	Penicillin/Streptomycin
PBC	Peripheral Blood Chimerism
PBS	Phosphate Buffered Saline
PCR	Polymerase Chain Reaction
PGC	Primordial Germ Cell
P-Sp	Para-aortic Spanchnopleura
Rd	Dose of Reaggregate
RT	Room Temperature
RT-PCR	Reverse-Transcriptase Polymerase Chain Reaction
SAP	Sub-Aortic Patch
SCL	Stem Cell Leukaemia
SLAM	Signalling Lymphocyte Activation Molecule
STR	Short Term Repopulating
TPO	Thrombopoietin
UGR	Urogenital Ridge
VBI	Ventral Blood Island
VE	Vascular Endothelial
VEGF	Vascular Endothelial Growth Factor
VMZ	Ventral Marginal Zone
WT	Wild Type
YS	Yolk Sac

1. Introduction

1.1. General Introduction

1.1.1. On stem cells…

The future of regenerative medicine, which promises treatments for complex diseases such as neurological disorders or cancers, relies mainly on the advances of stem cell research. A stem cell is widely defined as an undifferentiated cell that undergoes the processes of self-renewal and differentiation into mature cell types.

Embryonic stem (ES) cells, isolated from the inner cell mass of the pre-implantation embryo, are the only pluripotent cells with the capacity for *in vivo* and *in vitro* differentiation into cell lineages from all three germ layers (endoderm, mesoderm and, ectoderm)(Beddington and Robertson, 1989; Bradley et al., 1984). Undifferentiated ES cell lines can be maintained and expanded when either co-cultured on fibroblast feeder cells (Evans and Kaufman, 1981; Martin, 1981) or in the presence of leukaemia inhibitory factor and bone morphogenic protein 4 (Smith et al., 1988; Williams et al., 1988; Ying et al., 2003).

During embryonic development, and in the adult organism, tissue specific stem cells can be isolated (Figure 1.1). Contrary to ES cells, tissue specific stem cells can only give rise to cell lineages that are from the same germ layer and sometimes from the same tissue only.

1.1.2. On haematopoietic stem cells…

Elucidating the mechanisms by which haematopoietic stem cells (HSC) can be generated is of major scientific interest as it will improve our understanding of how to induce HSCs from alternative sources such as ES cells, while offering important insights into pathways involved in HSC-related diseases such as leukaemia. Because it is believed that long-term repopulating haematopoietic stem

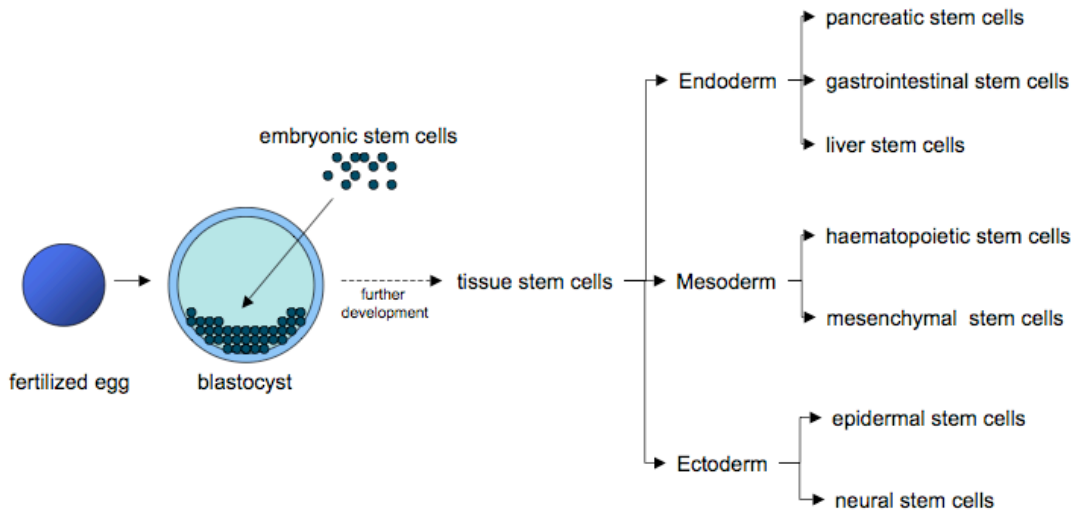

Figure 1.1: Sources and types of stem cells during development.
ES cells are the most primitive stem cells that are isolated from the inner cell mass of pre-implantation embryos and can give rise to all embryonic and extra-embryonic lineages. Further along development, only tissue specific stem cells are present in the organism and they can be isolated from most tissues of the endodermal, mesodermal, and ectodermal germ layers.

cells (LTR-HSCs) arise *de novo* during ontogeny only, the study of embryonic LTR-HSCs is under a great scrutiny. The study of embryonic LTR-HSCs is a challenge because, contrary to the adult, embryonic haematopoiesis involves a complex spatial and temporal chain of events which are characterised by successive appearance of haematopoietic progenitors in extra-embryonic tissues followed by the emergence of LTR-HSCs in intra-embryonic organs (Cumano et al., 1996; Cumano et al., 2001; Gekas et al., 2005; Medvinsky and Dzierzak, 1996; Moore and Metcalf, 1970; Muller et al., 1994; Ottersbach and Dzierzak, 2005; Yoder and Hiatt, 1997; Yoder et al., 1997b). This is further complicated by the possible existence of two ontogenetically distinct haematopoietic hierarchies during development: the primitive (embryonic) and definitive (adult) haematopoietic hierarchies.

In this introduction, current knowledge and issues associated with the ontogeny of LTR-HSCs in the murine embryo are discussed. The complex spatial and temporal emergence of the primitive and definitive waves of haematopoiesis will be extensively described with a particular focus on theories about the ancestry of LTR-HSC and their supporting evidence. After a brief overview on molecular mechanisms involved in LTR-HSCs biology, the essential role of the transcription factor Runx1 in haematopoiesis will be discussed.

1.2. The adult haematopoietic hierarchy

The adult (definitive) haematopoietic hierarchy is represented by the steady-state haematopoiesis that exists within the organism[1]. Haematopoiesis is the process by which a small number of LTR-HSCs, located in the bone marrow, is able to support and provide sufficient progeny that will progressively restrict differentiation potential and differentiate into mature blood cells (Figure 1.2).

[1] Unless stated otherwise, all discussions are presented in the context of the murine organism.

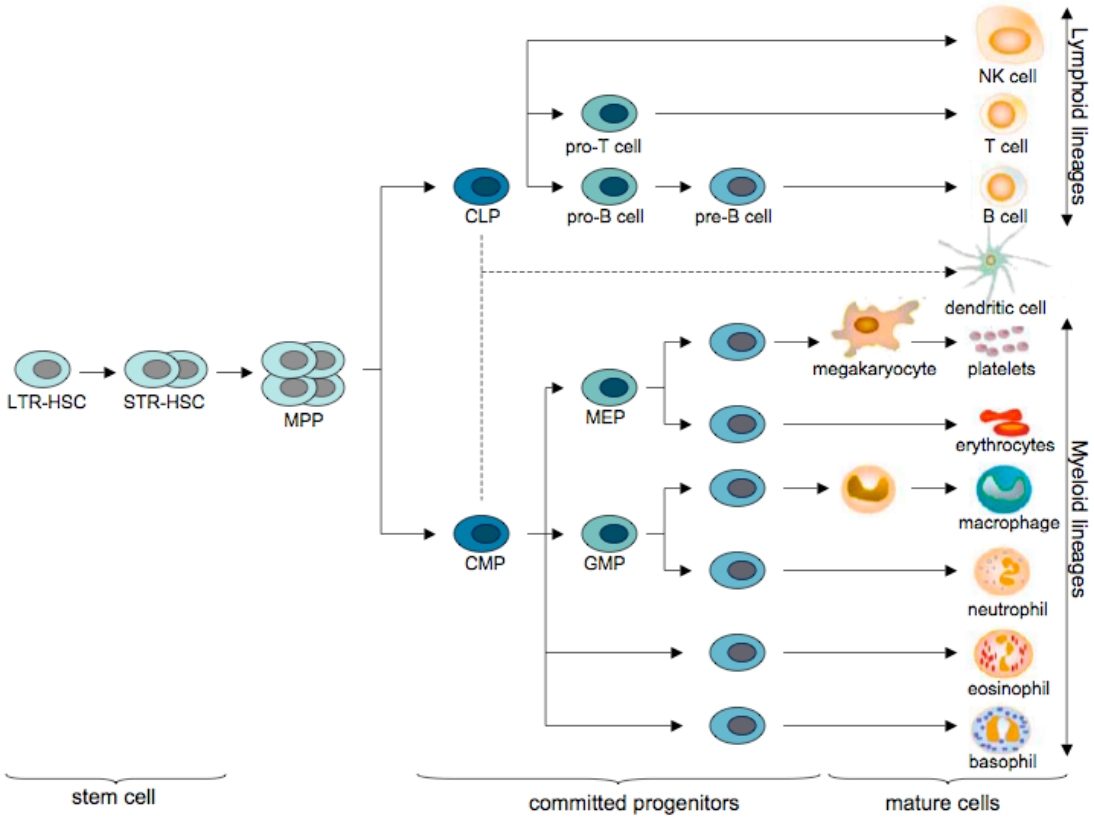

Figure 1.2: Schematic representation of the definitive haematopoietic hierarchy.
The definitive haematopoietic hierarchy is described by the LTR-HSCs compartment giving rise to progeny that sequentially loose self-renewal capacity (STR-HSC) and commit to specific lineages (CMP and CLP) before undergoing terminal differentiation and giving rise to mature blood cells.
LTR-HSC: long-term repopulating haematopoietic stem cell; STR-HSC: short term repopulating haematopoietic stem cell; MPP: multipotent progenitor; CLP: common lymphoid progenitor; CMP: common myeloid progenitor; MEP: common erythroid progenitor; GMP: granulocyte macrophage progenitor.
(adapted from Larsson and Karlsson, 2005)

1.2.1. The haematopoietic stem cell compartment

HSCs are the cells capable of simultaneously self-renewing and differentiating into more committed progeny. These cells subsequently proliferate and further differentiate into all blood cell types. In the adult bone marrow, there are two types of multipotent[2] cells with the capacity to home and engraft in adult haematopoietic organs upon transplantation, the LTR-HSCs and the short-term repopulating (STR) progenitors. STR progenitors lack life-long self-renewal capacity and thus can only provide haematopoietic reconstitution for a limited period (Zhao et al., 2000; Zhong et al., 1996). LTR-HSCs however, are capable of undergoing life-long self-renewal and robustly support haematopoiesis throughout life. Experimentally, LTR-HSCs are detected and assessed functionally by the *in vivo* competitive long-term repopulation assay and are defined by their ability to repopulate the haematopoietic system of a lethally irradiated adult recipient mouse upon serial transplantations (Szilvassy et al., 1990).

1.2.1.1. The bone marrow HSC identity

The bone marrow of an adult mouse (CBA x C57/Bl6) contains LTR-HSC at a frequency of 1 in 10, 000 nucleated cells (Kumaravelu et al., 2002). Flow cytometry have allowed the purification of bone marrow LTR-HSCs: they can either be identified by their ability to efflux the nuclear dye Hoechst 33342 (Goodell et al., 1996) or by a complex immunophenotype based on the absent/low expression of cell surface proteins expressed on mature cell lineages (Lin^-)(includes Ter119, Mac-1, Gr-1, B220, CD3ε, CD4 and CD8 lineage markers) and the expression of Sca1, c-kit, Thy1.1 and CD34 (Berman and Basch, 1985; Ikuta and Weissman, 1992; Osawa et al., 1996; Spangrude et al., 1988). An LTR-HSC enrichment of 1 in 5 cells can be achieved by fluorescent assisted cell sorting (FACS) of $Lin^-Sca1^+c\text{-}kit^+Thy1.1^{lo}$ or

[2] Property to give rise to multiple, yet limited, number of cell lineages. For example, haematopoietic stem cells can differentiate into blood cells but not into brain cells.

$Lin^{-}Sca1^{+}c\text{-}kit^{+}CD34^{lo/-}$ cell fractions (Osawa et al., 1996; Wagers et al., 2002). A more recent study has achieved very high levels of LTR-HSC purity using a simple combination of antibodies against the signalling lymphocyte activation molecule (SLAM) family markers CD48 and CD150 (frequency of 1 in 5 in $CD48^{-}CD150^{+}$ cells and 1 in 2 in $CD48^{-}CD150^{+}CD41^{-}$ cells)(Kiel et al., 2005).

Four weeks after birth, postnatal HSCs switch from a predominantly proliferating state to a more quiescent state (Bowie et al., 2007b; Bowie et al., 2006). In the adult bone marrow, elegant experiments combining flow cytometry with bromodeoxyuridine (BrdU) label-retaining assay have identified a rarely dividing (once every 36 days) HSC population and a highly dormant HSC population (once every 145 days) containing the majority of the LTR-HSC activity (Wilson et al., 2008). It is thought that quiescence prevents HSC exhaustion and limits the occurrence of mutations that could lead to transformation into cancer stem cells (Orford and Scadden, 2008; Warner et al., 2004). Even if the majority of LTR-HSC are in a quiescent state in the bone marrow, they are readily capable of reversibly switching from dormancy to self-renewal under conditions of injury and stress (Wilson et al., 2008).

1.2.1.2. The bone marrow HSC niche

The majority of adult LTR-HSC are located in the trabecular zone of the bone marrow but can also be found in much smaller numbers in the liver and the spleen (Calvi et al., 2003; Kiel and Morrison, 2008; Kiel et al., 2005; Taniguchi et al., 1996; Wolber et al., 2002; Zhang et al., 2003). Understanding the nature of the HSC niche[3] is almost as important as understanding the HSC intrinsic properties because niche elements can regulate HSC migration, quiescence and differentiation (Arai et al., 2004; Calvi et al., 2003; Nilsson et al., 2001; Orford and Scadden, 2008; Warner et al., 2004; Zhang et al., 2003). Genetic studies have shown that factors secreted by

[3] Specialized microenvironment made of supporting cells influencing HSC behaviour.

endosteal cells (osteoblasts and osteoclasts) can promote HSC maintenance (Kiel and Morrison, 2008). However, further characterisation of the endosteum as well as conditional inactivation of factors of interest, in particular endosteal cell types, remain to be performed to elucidate major niche-mediated mechanisms involved in HSC biology (Kiel and Morrison, 2008). Additionally, a growing body of evidence highlights the possible roles of sinusoid vascular cells and the wider perivascular environment (Kiel and Morrison, 2008). Possible mechanisms by which niche components can influence HSCs are complex and are likely to involve a wide range of surrounding cells (Figure 1.3).

1.2.2. The colony-forming unit spleen

Downstream of the HSC compartment in the definitive haematopoietic hierarchy are the colony-forming unit spleen (CFU-S) which are defined as cells capable of homing to the spleen and forming macroscopic colonies (Till and Mc, 1961). CFU-S can be divided into early CFU-S that can generate colonies 7-9 days after transplantations (and recede by day 10) and late CFU-S that generate colonies after 9-12 days post transplantation and remain until day 14 (Magli et al., 1982). These two CFU-S types have accordingly been named CFU-S_8 and CFU-S_{12}. CFU-S_{12} are more primitive progenitors than CFU-S_8 because of their capacity for self-renewal (Magli et al., 1982; Siminovitch et al., 1963).

CFU-S_{12} were considered to be HSCs for a long time because cell separation techniques based on expression of cell surface markers failed to separate CFU-S from HSCs. Evidence against this hypothesis came much later by allowing the separation of CFU-S and HSCs using counterflow centrifugal elutriation, a technique that separates cells according to their size and density (Jones et al., 1990).

1.2.3. Common myeloid and common lymphoid progenitors

Downstream of the CFU-S are the lineage-committed progenitors, the common lymphoid progenitor (CLP) and the common myeloid progenitor (CMP).

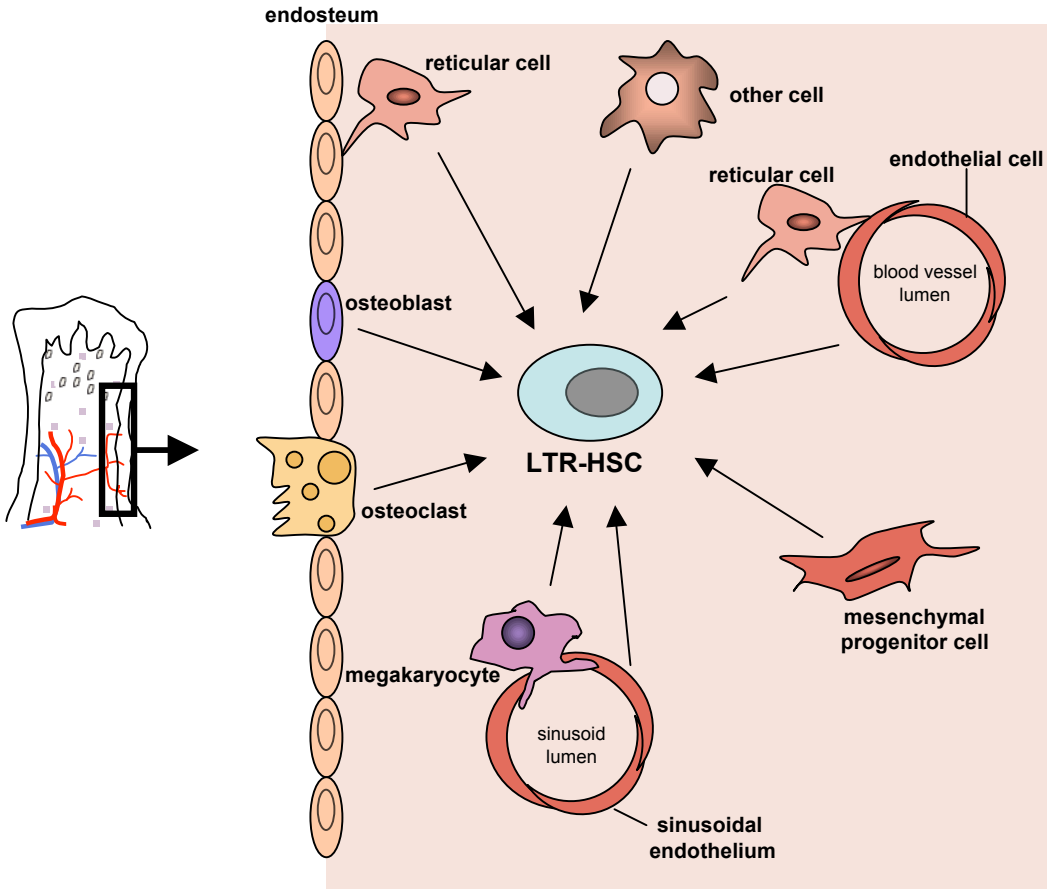

Figure 1.3: Diversity and complexity of the bone marrow LTR-HSC niche.
Contributions of cells near the endosteum (osteoblasts and osteoclasts) and at perivascular sites (vessels endothelial cells and associated reticular cells, megakaryocytes and mesenchymal progenitors). LTR-HSCs in the niche can be regulated either by cell-cell contacts, soluble factors, or by intermediate cells.
(Reviewed and adapted from Kiel and Morrison, 2008)

Similarly to HSCs, CLP and CMP are Lin^- but express low levels of Sca1 and c-kit (Akashi et al., 2000; Kondo et al., 1997). They can be isolated based on their differential expression of interleukin 7 receptor α-chain (IL7-R), CLP being $Lin^-Thy1.1^{lo}Sca1^{lo}c\text{-}kit^{lo}IL\text{-}7R\alpha^+$ and CMP being $Lin^-Thy1.1^{lo}Sca1^-c\text{-}kit^+IL\text{-}7R\alpha^-$ (Akashi et al., 2000; Kondo et al., 1997).

CLP differentiation potential is limited to lymphoid lineages. The CLPs are capable of transient *in vivo* reconstitution of the lymphoid compartment (B cells, T cells, and natural killer cells) and can only give rise to B lymphoid colonies *in vitro* even when exposed to cytokines used for myeloid differentiation (Kondo et al., 1997).

CMP differentiation potential is limited to myeloid lineages and can also provide transient *in vivo* reconstitution of the myeloid compartment (Akashi et al., 2000). The CMP population can be further divided by flow cytometry based on the differential expression of Fcγ receptor II-III (FcγR) and CD34; three functionally distinct populations with different differentiation potential can be identified. First, the CMP ($Fc\gamma R^{lo}CD34^+$) can give rise to all types of myeloid colony forming unit-culture (CFU-Cs), the progenitors to fully differentiated lineages (Akashi et al., 2000). Myeloid CFU-Cs include Burst Forming Unit-Erythroid (BFU-E), CFU-Mast, CFU-Macrophage (CFU-mac), CFU-Megakaryocyte (CFU-Meg), CFU-Granulocyte/Macrophage (CFU-GM), and CFU-Granulocyte/Erythrocyte/Macrophage/Megakaryocyte (CFU-GEMM). Second, the granulocyte macrophage lineage-restricted progenitor (GMP)($Fc\gamma R^{hi}CD34^+$) can only give rise to both CFU-mac and CFU-GM (Akashi et al., 2000). Finally; the megakaryocyte erythrocyte lineage-restricted progenitor (MEP)($Fc\gamma R^{lo}CD34^-$) can only give rise to CFU-Meg, BFU-E (Akashi et al., 2000). Experiments in which CMP were serially cultured in methylcellulose determined that the CMP gave rise to the more committed lineage restricted progenitors GMP and MEP (Akashi et al., 2000).

1.2.4. Terminally differentiated haematopoietic lineages

All cells from the leucocytic[4] lineages express the plasma membrane protein CD45 (Lagasse et al., 2000; Ledbetter and Herzenberg, 1979; Thomas, 1989). As previously mentioned, fully differentiated lineages can be divided into myeloid lineages (granulocytes, monocytes/macrophages, mast cells, magakaryocytes/platelets, erythrocytes) and lymphoid lineages (B cells, T cells, and natural killer cells).

Erythrocytes function to facilitate gaseous exchange in tissues of the organism; enucleation occurs as part of their terminal differentiation, a process that can be followed by the differential expression of the plasma membrane proteins CD71 and Ter119 (Kina et al., 2000).

Apart from having a very different array of functions (which will not be discussed here), fully differentiated haematopoietic cell lineages express different plasma membrane proteins. Development of monoclonal antibodies against these proteins has allowed the identification of these cell types by fluorescent microscopy and flow cytometry. The most commonly used lineage specific markers were summarised in Table 1.1.

1.3. The development of the haematopoietic system

Understanding the emergence of LTR-HSCs during embryonic development is of major interest because it is believed to be the only time during the mammalian organism life when LTR-HSCs can arise *de novo*. Haematopoiesis during development is very different to the steady state haematopoiesis happening in the adult and is far more complex as it occurs in various organs at various developmental times.

---

[4] Nucleated cells belonging to the immune system (also called white blood cells). Main types include neutrophils, eosinophils, basophils, lymphocytes (B cells, T cells, and natural killer cells), monocytes, macrophages and dendritic cells.

Table 1.1: Erythroid, lymphoid and myeloid lineage specific cell surface markers expressed on fully differentiated cells
(taken from Taoudi, 2006)

Haematopoietic lineage	Plasma membrane protein	References
Leucocyte	CD45/Ly-5	Ledbetter and Herzenberg, 1979; Thomas, 1989; Lagasse *et al*, 2000
Erythroid	Ter119	Kina *et al*, 2000; Zhang *et al*, 2003
	CD71	Kemp *et al*, 1987; Zhang *et al*, 2003
Lymphoid		
B-cell	B220	Hardy *et al*, 1991; Allman *et al*, 1992; Rolink *et al*, 1996
	CD19	Krop *et al*, 1996; Tedder *et al*, 1994
	CD43	Hardy et al, 1991
T-cell	CD3å	Leo *et al*, 1987; Nakano *et al*, 1996
	CD4	Pierres *et al*, 1984
	CD8á	Ledbetter *et al*, 1980; van Ewijk *et al*, 1981
Natural killer	NK1.1	Koo and Peppard, 1984; Yokoyama and Seaman, 1993
Myeloid		
Mast cell	CD34	Drew *et al*, 2002
	c-Kit/CD117	Drew *et al*, 2002
	Sca-1	Drew *et al*, 2002
	FcåRI	Ishizaka and Ishizaka, 1984; Dombrowicz *et al*, 1993; Turner *et al*, 1999
Megakaryocyte/platelet	CD41	Nieswandt *et al*, 1999; Phillips *et al*, 1991
Monocyte/Macrophage	Mac-1/CD11b	Springer *et al*, 1979; Leenen *et al*, 1994; Lagasse and Weissman, 1996
	Gr-1	Hestdal *et al*, 1991; Fleming *et al*, 1993; Lagasse and Weissman, 1996
Neutrophil	Mac-1/CD11b	Lagasse and Weissman, 1996
	Gr-1	Hestdal *et al*, 1991; Fleming *et al*, 1993; Lagasse and Weissman, 1996

During development, the dynamics of LTR-HSC emergence, migration and expansion have been linked to four major haematopoietic organs: the aorta-gonad mesonephros (AGM region), the yolk sac (YS), the fetal liver and the placenta (Gekas et al., 2005; Kumaravelu et al., 2002; Muller et al., 1994; Ottersbach and Dzierzak, 2005; Yoder et al., 1997b).

1.3.1. The embryonic origin of LTR-HSCs: the beginnings of a controversy

The first haematopoietic cells to appear in the developing embryo are observed in the YS blood islands from embryonic day (E) 7.5, approximately two days before the onset of blood circulation[5] (Moore and Metcalf, 1970). Blood islands first produce nucleated erythrocytes cells that express embryonic globins in a process called primitive erythropoiesis. The detection of CFU-S and CFU-C in early YS explants (Moore and Metcalf, 1970; Palis et al., 1999) led to the hypothesis that LTR-HSCs originate *in situ* in the early YS before migrating via peripheral circulation and colonising to the fetal liver (Moore and Metcalf, 1970). Such hypothesis was supported by experiments in avian models (Moore and Owen, 1965; Moore and Owen, 1967). Two studies in the mouse reported repopulation activity in the YS prior to E11 when donor cells were microinjected *in utero* into recipient embryos. Contribution to the adult haematopoietic system was either limited to the erythroid lineage (Toles et al., 1989) or to almost undetectable lymphoid lineages (Weissman IL, 1978).

The extra-embryonic source of LTR-HSC hypothesis was challenged when a series of elegant experiments with chicken-quail chimeras (quail embryos and haematopoietic organs were grafted onto chick YS) revealed that all blood cell types were of quail origin, thus proving the intra-embryonic origin for the adult

[5] which begins at E8.5 with the completion of the omphalomesenteric artery and is completed at E10.5 with a beating heart that drives haematopoietic circulation (McGrath et al, 2003).

haematopoietic system (Dieterlen-Lievre, 1975). Further experiments by the same group showed that while the YS was capable of generating a transient wave of erythroid cells, the site of HSC generation was predominantly intra-embryonic (Lassila et al., 1978; Lassila et al., 1982).

1.3.2. Primitive erythropoiesis in the early yolk sac

Defining primitive and definitive haematopoiesis has been subject to a long debate among scientists and is discussed further in Section 1.3.6. Here, primitive haematopoiesis will be defined as the process by which mature erythroid cells and some macrophages are formed by the early YS. After their initial formation in the E7.5 YS, the outer layer of the blood islands differentiate into endothelial cells while the inner cells loose their intercellular attachments and differentiate into primitive erythroblasts (McGrath and Palis, 2005). After their formation, primitive erythroblasts enter the embryonic vasculature where they proliferate, hence providing the embryo with an immediate supply of oxygen carrying cells necessary to fill in the gap between maternal passive oxygen diffusion and the start of erythrocytes production by E11 fetal liver. Contrary to adult type erythrocytes (as formed by the E11 fetal liver), primitive erythroblasts (also called megaloblasts due to their size) are nucleated and express the embryonic forms of hemoglobin (βH1 and ε)(McGrath and Palis, 2005; Palis et al., 1999). YS derived primitive erythroid cells are no longer found in the bloodstream after E16 (McGrath and Palis, 2005).

1.3.3. Identifying the intra-embryonic source of LTR-HSCs

The presence of CFU-S_8 and CFU-S_{11} in the E10.0 AGM region but not YS provided the first evidence of an intra-embryonic source of multilineage progenitors (Medvinsky et al., 1993). Because this activity reaches a maximum in the AGM region at E11.0, shortly before similar haematopoietic activity can be found in the fetal liver, it was speculated that the AGM region was the source of hepatic multilineage progenitors (Medvinsky et al., 1993). Proper assessment of LTR-HSC

content in the E10 embryo by serial long-term multilineage engraftment into irradiated adult recipients confirmed the AGM region as the first site in the embryo to harbour LTR-HSC activity (Muller et al., 1994). While these results indicated that the AGM region was the most potent pre-liver site of definitive haematopoiesis, this did not address the issue of the site of origin of the LTR-HSCs because of the active interchange of cells via circulation and interstitial migration that could have happened prior to E10.5 (Medvinsky and Dzierzak, 1996). The development of an *ex vivo* organ culture system, preventing possible cellular interchanges and thus revealing the autonomous and intrinsic capacity of the haematopoietic organs to generate LTR-HSCs, finally confirmed the E10.0 AGM as the first site of LTR-HSC emergence and expansion (from 1 to 12 LTR-HSCs) in the murine embryo (Kumaravelu et al., 2002; Medvinsky and Dzierzak, 1996). This was further supported by studies performed before the onset of circulation showing that E8 para-aortic spanchnopleura (P-Sp)[6], but not the YS, contained multipotent lymphomyeloid progenitors, although they were not capable of high level reconstitution of adult recipients (Cumano et al., 1996; Cumano et al., 2001).

1.3.4. The extra-embryonic sources of LTR-HSCs

1.3.4.1. The controversial role of the early yolk sac

A controversial body of evidence has indicated that the E8.0 YS was capable of generating LTR-HSCs when cells were transplanted *in utero* (Toles et al., 1989; Weissman IL, 1978). However, various studies failed to detect early YS cells with the capacity to engraft adult irradiated recipients or display multilineage differentiation prior to E11.0 (Cumano et al., 1996; Cumano et al., 2001; Medvinsky and Dzierzak, 1996; Medvinsky et al., 1993; Muller et al., 1994).

[6] Region including the splanchnic mesoderm surrounding the endoderm of the developing gut and the endothelium of arteries, it is a transient structure which develops into the AGM region at late E9 (Cumano et al, 1996).

It was hypothesised by Yoder and colleagues that the failure of ≤E11.0 YS cells to demonstrate LTR-HSC activity was a result of the failure of these cells either to home to haematopoietic microenvironments or to respond appropriately to such microenvironments (Yoder and Hiatt, 1997). Intravenous and intrahepatic injections into conditioned newborn pups confirmed this idea and showed that intrahepatic injections of E9-10 YS could give rise to high level long-term multilineage reconstitution in the adult haematopoietic system (Yoder and Hiatt, 1997; Yoder et al., 1997a; Yoder et al., 1997b).

1.3.4.2. The placenta as a haematopoietic organ

Recent studies have revived the idea that the placenta is a significant embryonic haematopoietic organ because it harbours high frequencies of committed lymphoid (pre-B cells) and myeloid progenitors (CFU-GM, CFU-GEMM, and BFU-E) from E8.5 onwards (Alvarez-Silva et al., 2003; Melchers, 1979). More recently, two research groups independently confirmed that the placenta is a reservoir for a large pool of LTR-HSCs from E11 until E13.5 when it dramatically reduces, concomitantly with the extensive hepatic pool expansion (Gekas et al., 2005; Ottersbach and Dzierzak, 2005). Placental LTR-HSCs can be enriched in the $CD34^{+}$c-$kit^{+}Sca1^{+}$ fraction, similarly to LTR-HSCs isolated in the AGM region and YS (Gekas et al., 2005; Ottersbach and Dzierzak, 2005; Sanchez et al., 1996; Yoder et al., 1997a), and are located within the endothelial layer of embryonic vessels in chorionic and labyrinth regions (Ottersbach and Dzierzak, 2005; Rhodes et al., 2008). However, the actual number of LTR-HSCs in the E12.5 placenta is still unclear because Gekas and colleagues counted approximately 50 LTR-HSCs per placenta while Ottersbach and colleagues counted approximately 12 (Gekas et al., 2005; Ottersbach and Dzierzak, 2005).

Unlike the E10.5 AGM, the E10.5 placenta is not able to autonomously initiate LTR-HSC formation when cultured as organ explant (Ottersbach and Dzierzak, 2005). The presence of haematopoietic progenitors in the allantois and the

chorion (whose fusion forms the placenta) in the early headfold embryo suggests an autonomous potential of the placenta (Zeigler et al., 2006). Additional experiments with embryos lacking a heartbeat, thus having no peripheral circulation (*Ncx1*$^{-/-}$ embryos[7]), also suggest that the placenta contains multipotent haematopoietic cells as early as E8.5, prior to the onset of circulation (Rhodes et al., 2008). However, the lack of transplantation experiments did not provide evidence in favour of autonomous LTR-HSC generation in the placenta, leaving this question unanswered.

1.3.5. Quantitative analysis of LTR-HSCs during embryonic development: a model for haematopoietic hepatic colonisation

Studies that quantified LTR-HSCs in the murine embryo from E10.5, at the onset of LTR-HSC emergence, have proven that LTR-HSCs are detected in the fetal liver by E11.5 and that this pool undergoes massive expansion (from 3.3 LTR-HSCs at early E11 up to 250 at E13)(Ema and Nakauchi, 2000; Gekas et al., 2005; Kumaravelu et al., 2002; Morrison et al., 1995). Such rapid expansion within the fetal liver cannot possibly be explained by mitotic divisions of a small number of LTR-HSCs that had previously colonised the fetal liver (Kumaravelu et al., 2002). Proper quantification of the LTR-HSCs within the haematopoietic organs from the onset of their emergence until their expansion in the liver have suggested that the fetal liver is seeded by consecutive waves of LTR-HSCs migrating from the AGM region first and subsequently from the YS and the placenta (Gekas et al., 2005; Kumaravelu et al., 2002; Moore and Metcalf, 1970). Such model is based on the following evidence and summarised in Figure 1.4:

[7] *Ncx1*$^{-/-}$ embryos lack heartbeat due to a defect in the sodium-calcium exchange pump 1 and thus do not survive beyond E10.5 (Koushik et al, 2001).

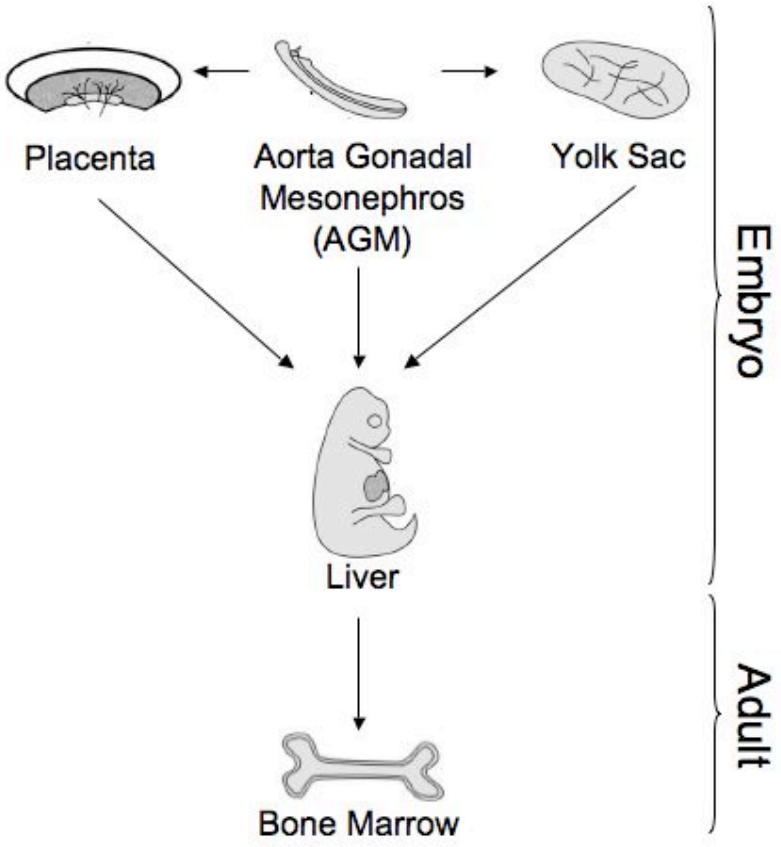

Figure 1.4: Embryonic haematopoietic sites and LTR-HSCs journey during development.

LTR-HSCs in the developing mouse embryo can be isolated first from the AGM region, the YS, and the placenta. The site where LTR-HSCs emerge is still controversial and their trafficking between these 3 embryonic sites is still unclear. After they emerge, LTR-HSC are thought to migrate to the fetal liver where they expand and migrate to the bone marrow post-natally. They reside in the bone marrow throughout life.

- The expansion of LTR-HSCs in the liver occurs concomitantly with increasing numbers of LTR-HSCs in the circulation (Kumaravelu et al., 2002).
- Although the AGM is capable of significant LTR-HSC expansion *ex vivo* (Kumaravelu et al., 2002; Medvinsky and Dzierzak, 1996), the numbers of progenitors and LTR-HSCs found *in situ* in the AGM are low at all times (between 1 and 2 LTR-HSCs)(Gekas et al., 2005; Kumaravelu et al., 2002; Muller et al., 1994).
- The YS contains similar numbers of LTR-HSCs as the AGM from E11 onwards but becomes competent to generate LTR-HSCs at E12 (7 LTR-HSCs)(Kumaravelu et al., 2002).
- The placenta contains large amount of LTR-HSCs from E10.5 but placental LTR-HSCs number dramatically decreases after E13.5 (Gekas et al., 2005; Ottersbach and Dzierzak, 2005).
- The lineage tracing of vascular endothelial (VE) cadherin positive cells suggests that haematopoietic cells in the fetal liver originate from endothelial cells in the AGM region (Zovein et al., 2008)(see Section 1.4.2.3 for more details).

Mapping LTR-HSCs numbers in developing embryos has given fundamental information about the origins of LTR-HSCs seeding the fetal liver, but one must keep in mind that the precise sites of LTR-HSC emergence are still subject to extensive debate as LTR-HSCs are first detected after the onset of circulation. Specific genetic marking of YS, AGM, and placental cells would empirically determine the extent by which each organ contributes to the LTR-HSC pool as well as whether fetal liver LTR-HSCs even originate from these sites.

1.3.6. Primitive and definitive haematopoiesis and their ontogenetical connections

1.3.6.1. Defining primitive and definitive haematopoiesis

Distinguishing between primitive (embryonic) and definitive (adult) haematopoiesis has been another great subject of debate in the HSC field. If definitive haematopoiesis was defined as adult haematopoiesis, with a hierarchy sequentially evolving from the LTR-HSCs and giving rise to CFU-S, CLP and CMP, the presence of such progenitors in the embryo prior to E10.5 would indicate that LTR-HSCs have already developed by this stage (Jaffredo et al., 2005). This would mean that LTR-HSCs are present in extra-embryonic tissues but the niche in which they reside limits their properties and differentiation potential to erythroid and macrophage lineages (Taoudi, 2006; Yoder and Hiatt, 1997). Evidently, this argues against the hypothesis of an independent mid-gestation emergence of LTR-HSCs in the AGM region.

Another possibility is that haematopoiesis during embryogenesis occurs in two waves: the first transitory wave is initiated in the E7.5 YS and generates nucleated erythrocytes and macrophages to meet the organism's immediate need for oxygen (discussed in Section 1.3.2). The second definitive wave is initiated perhaps in the E10.5 AGM region with the emergence of the first detectable LTR-HSCs and from then on it is possible that haematopoiesis occurs in an adult-like manner (ie: restricted progeny arise from LTR-HSCs)(Medvinsky and Dzierzak, 1996; Muller et al., 1994; Taoudi, 2006). In the context of this discussion, primitive haematopoiesis will refer to primitive erythropoiesis and the emergence of early progenitors, and definitive haematopoiesis will refer to the emergence and differentiation of the first LTR-HSCs in the E10.5 AGM region (Godin and Cumano, 2002).

1.3.6.2. The distinct origin of primitive and definitive haematopoiesis

1.3.6.2.1. CD41 expression as a candidate marker of definitive haematopoiesis

The platelet glycoprotein receptor IIb/IIIa (CD41) is a protein composed of two subunits that interact with CD61 to form a functional adhesive protein receptor in the presence of calcium (Phillips et al., 1988). It has long been used as a phenotypic marker for megakaryocyte-platelet lineage and is required for its normal function (Phillips et al., 1988). Additionally, CD41 expression has been reported in E10.5 AGM progenitors and in E9.5 primitive and definitive haematopoietic progenitors (Ferkowicz et al., 2003; Mikkola et al., 2003a; Mitjavila-Garcia et al., 2002). Because haematopoietic activity of YS $CD45^-$ cells could be enriched on the basis of CD41, it was hypothesized that CD41 may be an early marker for the initiation of definitive haematopoiesis (Mikkola et al., 2003a). Later during ontogeny, definitive progenitors in the E12.5-13.5 fetal liver become heterogeneous for CD41 expression (Ferkowicz et al., 2003; Mitjavila-Garcia et al., 2002). Interestingly, most E12.5 fetal and adult bone marrow LTR-HSCs are $CD41^-$, which might indicate that CD41 expression is lost upon "pre-HSC" maturation (Ferkowicz et al., 2003). The crossing of CD41 promoter driven Cre recombinase mice with a reporter mouse strain showed that CD41 is expressed in progenitors in the YS, AGM region and fetal liver *in vivo* (Emambokus and Frampton, 2003). However, the limited expression of β-galactosidase in adult bone marrow suggested that two waves of progenitors arise in the fetus and that the majority of bone marrow HSC might not emerge from a $CD41^+$ precursor (Emambokus and Frampton, 2003).

The evidence presented so far indicate that CD41 expression is the earliest haematopoietic marker (pre-CD45) as CD41 cells are committed to haematopoietic differentiation (Mikkola et al., 2003a) but fail to prove that CD41 is expressed in founder cells of the adult haematopoietic hierarchy.

1.3.6.2.2. Insights from amphibian studies

A clear model for the *in vivo* dissection of the origins of primitive and definitive haematopoiesis came from amphibian models. The ability to perform orthotopical transplantations with differentially marked cells have allowed the reliable tracing of cells that contribute to primitive and definitive haematopoiesis (Chen and Turpen, 1995; Ciau-Uitz et al., 2000; Turpen et al., 1997). In *Xenopus*

laevis, the ventral blood island (VBI), a region analogous to the mammalian YS, generates the primitive haematopoietic supply and also contributes to definitive haematopoiesis but at a later stage (Chen and Turpen, 1995; Turpen et al., 1997). The dorso-lateral plate (DLP), the region analogous to the mammalian AGM region, is only capable of definitive haematopoiesis and contributes to the majority of the hepatic haematopoietic pool and the earliest stage of liver colonization (Chen and Turpen, 1995). While this study was consistent with the hypothesis of a dual intra and extra-embryonic contribution to the hepatic LTR-HSCs pool, fate tracing experiments performed by the same group, in which the ventral marginal zone (VMZ) was differentially labelled, indicated a common origin of both primitive and definitive haematopoietic cells within the VBI and the DLP (Chen and Turpen, 1995). However, improved resolution of individual blastomeres within the VMZ and the dorsal marginal zone (DMZ) demonstrated that primitive and definitive haematopoietic lineages originate from different regions within the 32 blastomeres stage (Ciau-Uitz et al., 2000). Intriguingly, the same study by Ciau Uitz et al confirmed that the VBI is able to produce both primitive and definitive blood cells but is derived from two independent blastomeres, suggesting that primitive and definitive haematopoietic activity might be ontogenetically independent (Ciau-Uitz et al., 2000).

1.3.6.3. Molecular resolution of primitive and definitive haematopoiesis

The clearest functional resolution of primitive and definitive haematopoiesis in the murine embryo has come from gene inactivation studies. Inactivation of certain genes such as stem cell leukemia (SCL) gene, LIM domain only 2 (lmo2) or the GATA factors has been shown to disrupt both primitive and definitive haematopoiesis. Another set of genes, including notch, c-kit, c-myb, Runx1, and core-binding factor β (CBFβ), when inactivated have been shown to disrupt definitive haematopoietic specifically. A third set of genes, including β1-, α4-integrins, and CXCR4, has been shown to affect HSC migration and homing to the fetal haematopoieitic organs. As discussing the roles of each gene in detail is beyond the scope of this introduction, Table 1.2 summarises a list of the major genes

involved in governing the processes of primitive and definitive haematopoiesis (Godin and Cumano, 2002). A more detailed discussion about a few relevant genes of interest is provided.

1.3.6.3.1. The role of stem cell leukaemia (SCL) gene

The SCL gene is a member of the basic-helix-loop-helix (bHLH) class of transcription factors, and has been termed a master regulator of haematopoiesis because of the dramatic haematopoietic phenotype observed in $SCL^{-/-}$ murine model (Porcher et al., 1996; Robb et al., 1995; Shivdasani et al., 1995). SCL null embryos, which die *in utero* between E8.5 and E10.5, fail to initiate both primitive and definitive haematopoiesis as evidenced by the absence of YS blood islands and primitive nucleated erythrocytes, the absence of CFU-Cs, and the failure of $SCL^{-/-}$ ES cells to contribute to adult haematopoiesis in chimaeric mice (Porcher et al., 1996; Robb et al., 1995; Shivdasani et al., 1995).

Conditional inactivation of SCL in the adult organism revealed that SCL was dispensable for maintenance, engraftment, self-renewal and multilineage differentiation of LTR-HSCs (Mikkola et al., 2003b). Interestingly however, a recent study by Souroullas and colleagues has shown that adult "HSCs" in lyl1/SCL-conditional double knockout fail to repopulate irradiated recipients and undergo rapid apoptosis, indicating that lyl1 is essential for HSC function in the absence of SCL. Lyl1 is a bHLH transcription factor that is highly related (80%) to SCL with a similar expression pattern (Giroux et al., 2007). Despite the inability of lyl1 to rescue SCL deficient phenotype during development (Chan et al., 2007), these results indicate a functional overlap between these two proteins in the adult LTR-HSC compartment (Souroullas et al., 2009). This example illustrates functional redundancy between related proteins and brings to attention the care with which single gene inactivation studies should be interpreted.

Table 1.2: Genes involved in the ontogenesis of the haematopoietic system.
(adapted from Godin and Cumano, 2002).

Gene product	Time of death	YS haematopoiesis	FL haematopoiesis	references
Genes affecting both primitive and definitive haematopoiesis				
Tal1/SCL	9-10.5	markedly reduced	absent	Robb et al., 1995; Shivdasani et al., 1995
Lmo-2	9-10.5	markedly reduced	absent	Warren et al., 1994; Yamada et al., 1998
GATA-1	10.5-11.5	markedly reduced	absent	Pevny et al., 1991
Flk-1	8.5-9.5	markedly reduced	absent	Shalaby et al., 1997; Shalaby et al., 1995
Tie-2	8.5-9.5	markedly reduced	absent	Takakura et al., 1998
CBP	8.5-10.5	reduced	absent	Oike et al., 1999
Genes affecting definitive haematopoiesis only				
AML1/Runx1	11.5-12.5	normal	blocked	North et al., 1999; Okuda et al., 1996; Wang et al., 1996
CBFβ	11.5-14	normal	blocked	Wang et al., 1996b
GATA-2	10.5-11.5	reduced	markedly reduced	Tsai et al., 1994
c-myb	15	normal	decreased	Mucenski et al., 1991
c-kit	at birth	decreased erythropoiesis	blocked erythropoiesis	Bernex et al., 1996; Ogawa et al., 1993
Pu.1	18.5	normal	reduced	Scott et al., 1997
Ikaros	viable	normal	reduced	Georgopoulos et al., 1994; Nichogiannopoulou et al., 1999

1.3.6.3.2. The role of LIM domain only 2 (lmo2)

Lmo2/Rbtn2 encodes a LIM-domain nuclear protein that directly interacts with SCL and GATA-1 as a bridging molecule and is largely expressed in primitive and definitive erythroid cells during development (Warren et al., 1994). Lmo2 null embryos die *in utero* between E10.5 and E11.5 with a failure to develop YS blood islands and a complete absence of primitive erythrocytes (Warren et al., 1994). However, the ability of $Lmo2^{-/-}$ ES cells and E9.5 YS cells to form macrophages colonies *in vitro* indicate that haematopoiesis is not completely ablated (Warren et al., 1994), a similar phenotype as GATA-1 null embryos (see Section1.3.6.3.3). The generation of chimeric mice, in which $Lmo2^{-/-}$ ES cells were microinjected into wild type (WT) blastocysts, revealed that Lmo2 deficient cells do not contribute to adult haematopoiesis (Yamada et al., 1998). This study indicated that Lmo2 was essential for the development of the definitive haematopoietic system but the stage at which Lmo2 plays a role is yet to be determined. The only circumstantial evidence of a role for Lmo2 at the stage of LTR-HSC emergence came from the *in situ* hybridisation detection of Lmo2 in midgestation aortic endothelium, intra-aortic haematopoietic clusters (IAHC), and possibly sub-aortic patches (SAP)(Bertrand et al., 2005; Manaia et al., 2000)(see Section 1.4).

1.3.6.3.3. The roles of GATA transcription factors

The GATA family of transcription factors is composed of 6 members of zinc finger proteins that recognize a GATA consensus motif, and can be divided into two groups: *GATA-4*, *GATA-5*, and *GATA-6* which are mainly expressed in cardiac cells and lineages derived from the endoderm (Peterkin et al., 2005), and *GATA-1*, *GATA-2*, and *GATA-3* which are mainly expressed in the central nervous system and various ectodermal lineages as well as haematopoietic lineages (Evans and Felsenfeld, 1989; Pandolfi et al., 1995; Pevny et al., 1991; Tsai et al., 1994; Yu et al., 2002).

GATA-1 target sites are found in the regulatory elements of virtually all genes expressed by erythroid cells and is also expressed in mast, megakaryocyte and eosinophil lineages (Evans and Felsenfeld, 1989; Tsai et al., 1989; Yu et al., 2002).

Insights into the differential role of GATA-1 in primitive and definitive haematopoiesis have come from embryoid bodies (EB) differentiation models in which temporal appearance of precursors resembles that in the early embryo[8]. GATA-1 loss and gain of function studies have revealed the essential requirement of GATA-1 for normal definitive erythroid development both *in vitro* and *in vivo* (Fujiwara et al., 1996; Pevny et al., 1991; Simon et al., 1992). The loss of functional GATA-1 in ES cells leads to impaired primitive erythropoiesis whereas definitive erythroid progenitors are present in normal numbers yet display a severe developmental arrest and death at the pro-erythroblast stage (Weiss et al., 1994). *In vivo* however, both primitive and definitive erythroid precursors are present but experience a developmental arrest at the pro-erythroblast stage (Fujiwara et al., 1996).

GATA-2 is expressed in various haematopoietic lineages including the adult bone marrow LTR-HSC pool (Orlic et al., 1995). GATA-$2^{-/-}$ embryos die at E11.5 and exhibit marked anaemia (Tsai et al., 1994). In the midgestation embryo, GATA-2 is expressed in the E9.5-11.5 AGM region but not in the YS as assessed by *in situ* hybridisation in a reporter mouse model (Minegishi et al., 1999; Zhou et al., 1998), suggesting a predominant role in definitive rather than primitive haematopoiesis. The presence of normal primitive erythroid cells in knockout embryos, and the failure of GATA-$2^{-/-}$ cells to contribute to definitive haematopoiesis in embryonic or adult haematopoietic organs, functionally confirms the requirement of GATA-2 for definitive haematopoiesis (Tsai et al., 1994). Interestingly, GATA-2 haploinsufficient embryos failed to facilitate the LTR-HSC expansion in the E11.5-12.5 AGM region whereas YS-derived LTR-HSCs expanded similarly to controls, suggesting that there are distinct pathways governing extra and intra embryonic haematopoiesis (Ling et al., 2004).

[8] Primitive erythroid precursors arise at 6-7 days EBs whereas definitive erythroid precursors are found in E10-14 days EBs (Weiss et al, 1994).

GATA-3 gene inactivation results in embryonic lethality around E11.75-12.5 due to extensive internal haemorrhages, growth retardation and central nervous system malformations (Pandolfi et al., 1995). The numbers of YS progenitors in null E11.5 embryos are comparable to WT animals whereas the numbers of FL progenitors are markedly decreased; leading to the conclusion that GATA-3 deficiency specifically affects definitive haematopoiesis (Pandolfi et al., 1995). However, analysis of chimaeric GATA-$3^{-/-}$/RAG-$2^{-/-}$ adult mice revealed that GATA-$3^{-/-}$ cells contribute to functional adult myeloid lineages (Mac-1^{+} and Gr-1^{+}) and B cell lineage but fail to complete T-lymphocyte differentiation (Ting et al., 1996). While this highlights an important role of GATA-3 for T-lymphocyte differentiation, it also strongly suggests that GATA-$3^{-/-}$ cells contributes to definitive adult haematopoiesis (Ting et al., 1996). Additionally, GATA-3 expression was reported in SAPs (see Section 1.4.2.5) and aortic endothelium in the E10.5-11.5 AGM region, structures hypothesised to be associated with LTR-HSC emergence in the AGM region (see Section 1.4). However, the role of GATA-3 in definitive haematopoiesis is still unclear due to the lack of direct functional evidence showing a requirement of GATA-3 in the LTR-HSC compartment and linking SAPs to LTR-HSCs.

1.3.6.3.4. The role of notch signalling

The Notch family of receptors, comprising the four members Notch-1, Notch-2, Notch-3 and Notch-4, and their ligands (Delta-like-1, -3, -4, and Jagged-1 to 2) are expressed in various haematopoietic lineages and control cell fate decisions during haematopoietic lineage differentiation (Milner and Bigas, 1999). Conditional inactivation of Notch-1 in adult animals has demonstrated that it is dispensable for the maintenance of LTR-HSCs *in vivo* (Maillard et al., 2008; Mancini et al., 2005; Radtke et al., 1999), a finding confirmed and extended to all four members of the Notch family (Maillard et al., 2008).

However, Notch-1 gene inactivation is embryonic lethal by E11.5, with null embryos showing severe vasculature defects in the dorsal aorta and the YS (Krebs et al., 2000), which may disturb LTR-HSC development. *In vivo* data have shown that

Notch-1 signalling is dispensable for normal primitive haematopoiesis (Hadland et al., 2004; Kumano et al., 2003). As Notch-1 deficient ES-cells contribute to YS derived haematopoiesis but not to adult haematopoiesis in chimaeras (Hadland et al., 2004). Notch-1 in particular, specifically via activation by Jagged-1 (Robert-Moreno et al., 2008), seems to be essential for cell-autonomous emergence of LTR-HSC in the developing embryos as such observations were not made in Notch-2 or Notch-4 deficient embryos (Kumano et al., 2003; Robert-Moreno et al., 2005).

The evidence available indicates that Notch signalling does not play a major role in primitive haematopoiesis; it acts at the step of LTR-HSC emergence but is dispensable for their expansion and maintenance in the adult (Maillard et al., 2008; Mancini et al., 2005; Radtke et al., 1999; Robert-Moreno et al., 2005; Robert-Moreno et al., 2008).

1.3.6.3.5. The role of runx1

Runx1 is a critical gene involved in human leukaemogenesis (Speck and Gilliland, 2002). Runx1 gene inactivation studies have shown that Runx1 is dispensable for primitive erythrocytes formation, although required for their final maturation and normal Ter119 and GATA-1 expression (Yokomizo et al., 2008). However, Runx1 is essential for the emergence of LTR-HSCs and the establishment of definitive haematopoiesis (Okuda et al., 1996; Wang et al., 1996a). Conditional Runx1 inactivation models, created to by-pass embryonic lethality, showed that Runx1 is essential for the normal maturation of lymphoid cells (B and T cells) and megakaryocytes (Growney et al., 2005; Ichikawa et al., 2004; Ichikawa et al., 2008; Putz et al., 2006). The role of Runx1 is extensively discussed in Section 1.5.

1.4. The ancestry of LTR-HSCs in developing embryos

1.4.1. The spatial origin of LTR-HSCs in the E11.5 AGM region

At E11.5, the AGM region comprises the dorsal aorta (Ao), the urogenital ridges (UGR) and remnants of the ventral mesentery (see Figure 5.1). Transplantations of fresh Ao and UGR have demonstrated that LTR-HSCs first emerge in the Ao at E11.5 (de Bruijn et al., 2000b; Taoudi and Medvinsky, 2007). This axio-lateral polarity is still quantitatively observed at E12.5 but at this stage some LTR-HSCs can be experimentally detected in the UGR (de Bruijn et al., 2000b). Interestingly however, the presence of LTR-HSCs in E11.5 Ao and UGR explants raises the possibilities that UGRs could autonomously induce/expand LTR-HSCs or that pre-HSCs seed the UGR prior to E11.5 (de Bruijn et al., 2000b). In addition, co-culture of Ao and UGRs does not increase LTR-HSCs output from UGR or Ao, suggesting that there are no supportive/inhibitory interactions between these two tissues (de Bruijn et al., 2000b).

The hypothesis of a dorso-ventral polarity in the Ao came from the identification of IAHCs on the ventral wall of the Ao in vertebrate species (avian, mouse, human)(Figure 1.5). IAHC are structures hypothesised to mature into LTR-HSCs. This theory relies on the expression of various haematopoietic markers in IAHCs (CD34, PECAM-1, CD45 in the 5-week old human and CD45, CD34, PECAM-1, AA4.1, Runx1, Notch1, and Lmo2 in the E10.5-11.5 Ao)(Bertrand et al., 2005; Garcia-Porrero et al., 1995; Garcia-Porrero et al., 1998; Kumano et al., 2003; Manaia et al., 2000; North et al., 1999; Robert-Moreno et al., 2008). The absence of IAHC upon inactivation of genes involved in definitive haematopoiesis and the presence IAHC concomitantly with the presence of LTR-HSCs in the AGM, have supported this model (Medvinsky and Dzierzak, 1996; North et al., 1999).

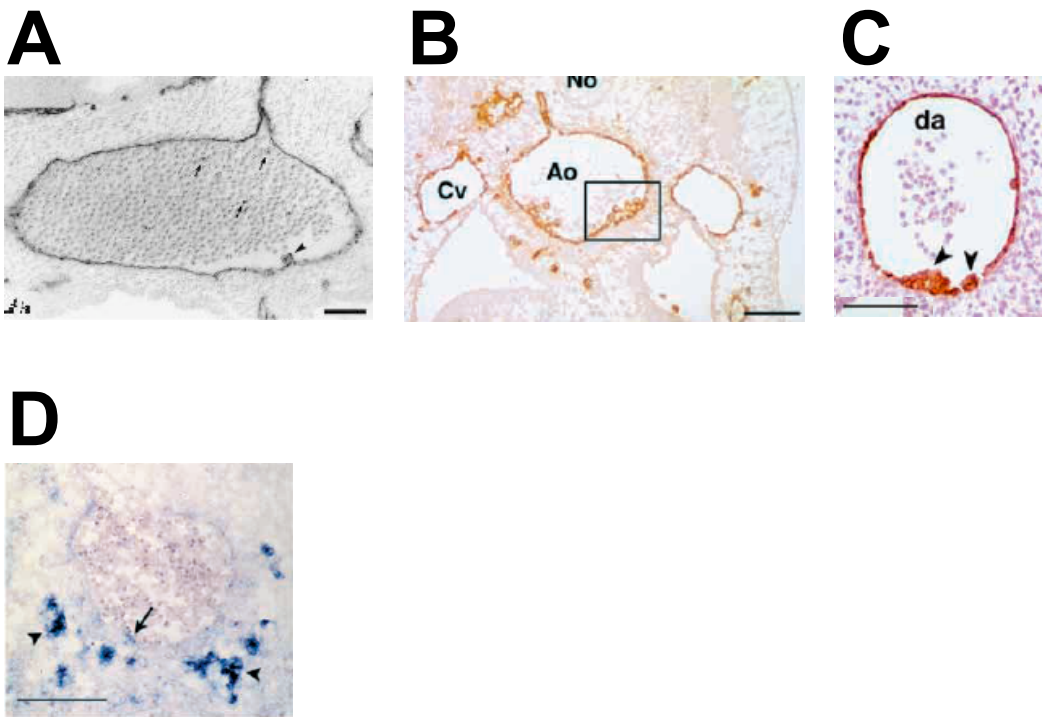

Figure 1.5: Presence of intra-aortic haematopoietic clusters on the ventral aspect of the dorsal aorta in vertebrate species of midgestation embryos.

A: transverse section through murine E11.5 AGM region, a $CD34^+$ IAHC is lying on the ventral part of the dorsal aorta (arrow head), scale bar = 57 µm (taken from Garcia-Porrero et al, 1998).

B: transverse section through avian E3 dorsal aorta, $QH1^+$ IAHC is lying on the ventral part of the dorsal aorta (square), scale bar = 75 µm (taken from Jaffredo et al, 1998) .

C: transverse section through day 32 human dorsal aorta, two $CD34^+$ IAHCs are lying on the ventral part of the dorsal aorta (arrow heads), scale bar = 100 µm (taken from Tavian et al, 1999) .

D: Transverse section through murine E11.5 AGM region, GATA-3^+ IAHC (arrow) and SAP (arrowheads) are ventrally located, scale bar = 100 µm (taken from Manaia et al, 2000).

The ventral localisation of LTR-HSC development was further hinted by the observation of SAPs in the ventral para-aortic mesenchyme, and the expression of high-levels of GATA-2, GATA-3, and Lmo2 within this region (Bertrand et al., 2005; Manaia et al., 2000).

However, to date, only one study in the mouse embryo has provided functional evidence of ventral localisation of LTR-HSCs in the E11.5 AGM region (Taoudi and Medvinsky, 2007). In this study, sub-dissection of the dorsal aorta into dorsal (AoD) and ventral (AoV) domains demonstrated that only the AoV harbours LTR-HSCs and is capable of autonomous LTR-HSC induction/expansion (Taoudi and Medvinsky, 2007). See Section 5.1 for more details.

Despite the functional evidence of dorso-ventral polarity of LTR-HSC development in the E11.5 AGM region and the large amount of circumstantial evidence linking IAHC and SAP to LTR-HSC emergence, no group to date has been able to functionally attribute LTR-HSC activity to any of these morphological structures.

1.4.2. The ancestry of LTR-HSCs in the developing embryo

As previously described, the first blood cells appear in the YS blood islands as a compact group of cells which are initially identical. As development proceeds, the cells at the exterior of the clusters adopt endothelial identity while the cells within the clusters progressively lose inter-cellular connections and differentiate into haematopoietic cells and primitive erythrocytes (McGrath and Palis, 2005). This close association of endothelial and haematopoietic cells that develop from cells that are originally identical have led to the hypothesis of a common precursor of both lineages: the haemangioblast (Sabin, 1920). The close developmental link between endothelial and haematopoietic cells is also illustrated by the close association of the IAHCs with the endothelial lining of the Ao as well as the common expression of various cell surface markers such as PECAM-1, CD34, c-kit, Tie-2, Flk-1, CD45, and VE-cadherin (Baumann et al., 2004; Bernex et al., 1996; Nishikawa et al., 1998a;

Takakura et al., 1998; Taoudi et al., 2008; Taoudi et al., 2005; Wood et al., 1997; Yoshida et al., 1998).

While there is some evidence in favour of the endothelial ancestry of LTR-HSCs, alternative theories have arisen in the past few years (schematically summarised in Figure 1.6).

1.4.2.1. The endothelial origins of LTR-HSCs

To successfully demonstrate the endothelial origin of LTR-HSCs in the embryo, it is necessary to specifically label endothelial cells and accurately trace their fate *in vivo* or evaluate their haematopoietic potential *in vitro* (Taoudi, 2006). This relies on the assumption that endothelial cells can be specifically identified based on their surface markers and/or their properties (summarized in Table 1.3). To date, the expression of VE-cadherin is the most effective single surface marker that immunophenotypically identifies endothelial cells (Breier et al., 1996; Matsuyoshi et al., 1997; Nishikawa et al., 1998b).

The only reported instance in which VE-cadherin is expressed in non-endothelial cells is in the first LTR-HSCs that reside in the E11.5 AGM region ($CD45^{+}VE\text{-}cadherin^{+}$)(North et al., 2002; Taoudi et al., 2005). Based on these results, basic immunophenotypes were defined for endothelial cells ($CD45^{-}VE\text{-}cadherin^{+}$), haematopoietic cells ($CD45^{+}VE\text{-}cadherin^{-}$), and a purified population of LTR-HSCs ($CD45^{+}VE\text{-}cadherin^{+}$)(Fraser et al., 2003; Nishikawa et al., 1998b; North et al., 2002; Taoudi et al., 2005).

1.4.2.2. Concept of the haemangioblast

The haemangioblast is defined as a precursor that is restricted to differentiate into endothelial and haematopoietic cells exclusively (Sabin, 1920). Experimentally, the isolation of Flk-1 positive precursors capable of differentiating into both endothelial and haematopoietic cells has been postulated to be putative haemangioblasts in avian and murine embryos (Eichmann et al., 1997; Huber et al.,

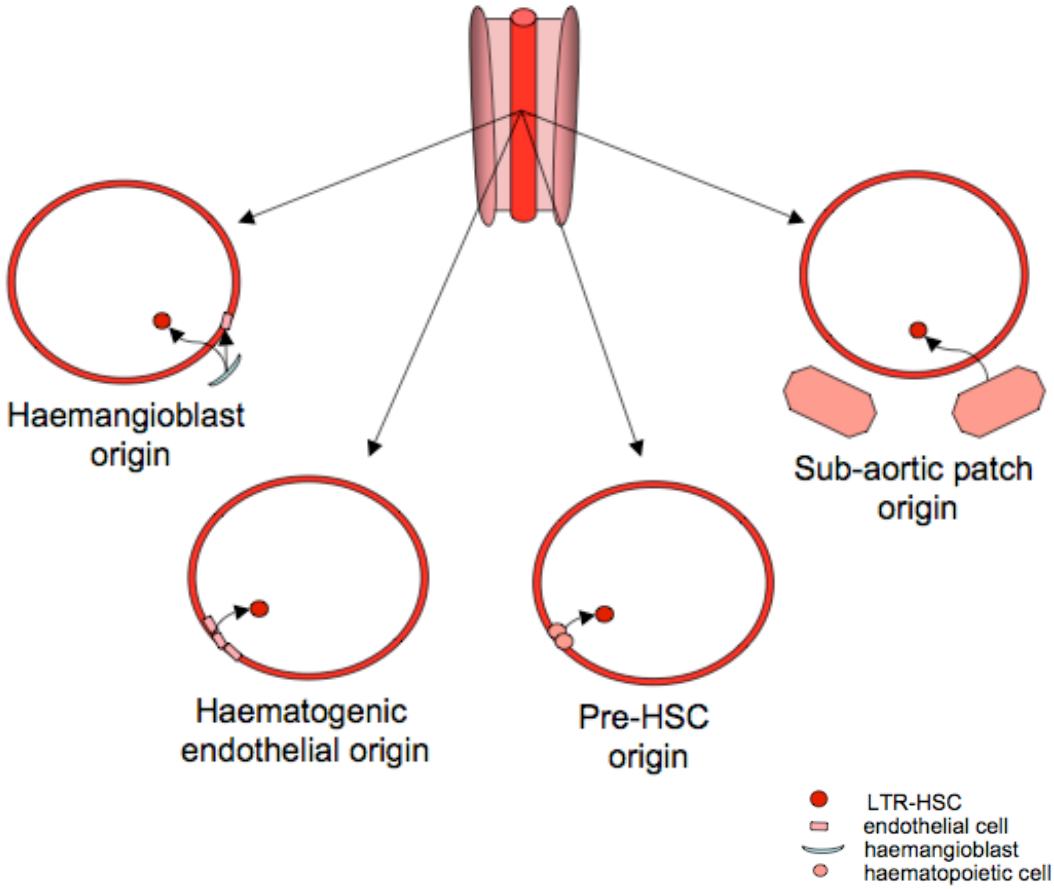

Figure 1.6: Models of candidate LTR-HSCs ancestry in the AGM region.
The haemangioblast theory implies that there is one common progenitor to endothelium and LTR-HSCs.
The haemogenic endothelium theory implies that LTR-HSCs are derived from endothelial cells that are already primed to a haematopoietic fate.
The pre-HSC theory implies that LTR-HSCs are derived from mesodermal cells that can mature into LTR-HSCs
The sub-aortic patches theory implies that LTR-HSCs are derived from mesodermal cells contained in these sub aortic structures and that subsequently migrate and mature into LTR-HSCs in IAHCs before being released into the bloodstream.
(adapted from Taoudi, 2006).

Table 1.3: Endothelial associated plasma membrane proteins
(taken from Taoudi, 2006).

Plasma membrane protein	Function/comments	References
Ac-LDL receptor	Binds Ac-LDL Expressed on macrophages	Voyta *et al*, 1984; Brown *et al*, 1979; Brown *et al*, 1980
Flk-1	VEGF receptor expressed by endothelium and mesoderm	Millauer *et al*, 1993; Quinn *et al*, 1993; Nishikawa *et al*, 1998
Tie-2	Angiopoietin-1 and Angiopoietin-2 receptor required for network formation Expressed on foetal liver and quiescent adult bone marrow LTR-dHSCs	Korhonen *et al*, 1994 Davis *et al*, 1996; Sato *et al*, 1995; Suri *et al*, 1996; Yano *et al*, 1997
PECAM-1/CD31	Involved in inter-endothelial homotypic interactions Expressed on some adult haematopoietic cells and all HSCs during ontogeny and adulthood	Vecchi *et al*, 1994; Delisser *et al*, 1994; Suri *et al*, 1996; Baumann *et al*, 2004; North *et al*, 2002
VE-cadherin/CD144	Essential for angiogenesis and preserving vascular Integrity at endothelial adherens junctions	Gotsch *et al*, 1997; Lampugnani *et al*, 1992; Breier *et al*, 1996; Carmeliet *et al*, 1999; Crosby *et al*, 2005; Gory *et al*, 1999

VE-cadherin, vascular endothelial cadherin; Flk-1, foetal liver kinase-1, PECAM-1, platelet endothelial cell adhesion molecule-1

Ac-LDL, acetylated low density lipoprotein; VEGF, vascular endothelial growth factor; HSC, haematopoietic stem cell; LTR-dHSC, long-term repopulating definitive haematopoietic stem cell

2004). Support for the haemangioblast concept was also provided by EB differentiation model: the blast colony forming cell (BL-CFC) arising within EBs after 2.5-4.0 days of differentiation has been hypothesised to be the *in vitro* equivalent of the haemangioblast (Choi et al., 1998). BL-CFCs emerge before the onset of haematopoiesis within EBs; they express the mesodermal markers Flk-1 and Brachyury, and have the potential to form colonies made of haematopoietic and endothelial cells after culture in methylcellulose containing vascular endothelial growth factor (VEGF) and transfer to liquid medium with cytokines (Choi et al., 1998; Fehling et al., 2003; Kennedy et al., 1997). An analogous *in vivo* Flk-1^{+}Brachyury^{+} population has been isolated from the posterior region of the primitive streak as a transient population in the E7-7.5 embryo (Huber et al., 2004).

The fact that BL-CFCs arise before the onset of haematopoiesis in EBs supports the idea of a common precursor for endothelial and haematopoietic cells. However, the mesodermal Flk-1^{+}Brachyury^{+} immunophenotype and the presence of smooth muscle in the differentiated colonies raised the possibility that the cells used for secondary culture were a population of uncommitted mesoderm (Choi et al., 1998; Fehling et al., 2003). Taken together, these studies do not prove the existence of the haemangioblast because it is difficult to be sure that these progenitors are not capable of differentiating into some other mesodermal lineages.

The most convincing *in vivo* proof of the haemangioblast was obtained in zebrafish through the construction of single-cell-resolution fate maps obtained by the laser activation of fluorescently labelled cells (Vogeli et al., 2006). This study demonstrated the presence of bipotential precursors arising along the ventral mesoderm and giving rise to small subsets of haematopoietic (GATA-1^{+}) and endothelial (Flk-1^{+}) cells exclusively (Vogeli et al., 2006). However, assays confirming the functionality of Flk-1^{+} as endothelial, and GATA-1^{+} as haematopoietic, would provide a stronger proof for the existence of the haemangioblast in this model system.

1.4.2.3. Concept of haemogenic endothelium

An alternative theory for the origin of haematopoiesis is that haematopoietic cells (and perhaps LTR-HSCs) are derived from endothelium that is already committed to an haematopoietic fate: the hemogenic endothelium (Jordan, 1917). Evidence in favour of this hypothesis came from studies in avian embryos in which heterotopic grafts of spanchnopleural lateral plate mesoderm, but not paraxial mesoderm, contribute to endothelial cells in the AoV as well as IAHC (Jaffredo et al., 1998; Pardanaud et al., 1996). Labelling of endothelial cells with acetylated low-density lipoprotein (a-LDL) tag or with non-replicative retroviral vector and *in vivo* tracing of their progeny, strongly suggested that the IAHCs are derived from precursors in the underlying aortic endothelium (Jaffredo et al., 2000; Jaffredo et al., 1998). However, the interpretation of these results is problematic as they rely on the following assumptions: the endothelial specificity of a-LDL uptake, the identity of endothelial cells being Flk-1^{+}CD45^{-} and all haematopoietic cells in the IAHCs being Flk-1^{-}CD45^{+} (Jaffredo et al., 1998).

The first functional evidence of a haemogenic endothelium came from an *in vitro* ES cell differentiation model showing that Flk-1^{+} could give rise to VE-cadherin^{+} that could differentiate into functional endothelium and haematopoietic cells (Nishikawa et al., 1998a). Analysis of such VE-cadherin^{+} endothelial cells (characterised as CD45^{-}, Ter119^{-}, PECAM-1^{+}, Flk-1^{+}, CD34^{+} and a-LDL^{+}) isolated from E9.5 YS and embryo proper (caudal half of the embryo) could generate lymphoid and myeloid progeny as well as fully reconstitute the haematopoietic system of conditioned newborn recipients upon intrahepatic injections (Fraser et al., 2002; Nishikawa et al., 1998b).

Recently, live cell imaging of the differentiation of ES cell derived Flk-1^{+}E-cadherin^{-} mesodermal precursors has shown that endothelial cells (defined by morphology, VE-cadherin expression, incorporation of a-LDL and claudin-5 at the cell junctions) can give rise to haematopoietic cells that express CD41 prior to CD45 (also defined by round non-adherent morphology and Mac-1 expression)(Eilken et al., 2009). These results confirm the existence of endothelial cells capable of haematopoietic commitment as well as the use of CD41 cell surface marker as the

earliest reliable marker for haematopoietic cells. Similarly, another group also using time-lapse photography showed that Tie-2^{hi}c-$kit^{+}CD41^{-}$ endothelial cell population could acquire the haematopoietic marker CD41 (Lancrin et al., 2009). Based on this transient cell population's lack of Brachyury expression and failure to generate blast colonies, they postulate that the haemogenic endothelium is downstream of the heamangioblast (Lancrin et al., 2009). Finally, labelling of VE-cadherin expressing cells during embryogenesis by crossing an inducible VE-cadherin Cre with Rosa26R-lacZ demonstrated that haematopoietic cell in the fetal liver and in the adult haematopoietic organs are the progeny of the VE-cadherin labelled cells (Zovein et al., 2008). This could be an *in vivo* proof of the endothelial origin of LTR-HSCs, but it relies on the assumption that VE-cadherin is exclusively specific to endothelial cells. In fact, VE-cadherin is expressed in the earliest population of HSCs in the AGM region (North et al., 2002; Taoudi et al., 2005).

1.4.2.4. The mesodermal theories: pre-HSCs

So far, various types of long term engrafting cells in the murine embryo have been identified using different assays: LTR-HSCs from E10.5 AGM region, neonatal repopulating cells from E9 YS and low-level adult repopulating cells in the E8 P-Sp (Cumano et al, 2001; Muller et al, 1994; Yoder et al, 1997b). However, it is not clear whether these cells are ontogenetically related. Specifically, it is reasonable to assume that early engrafting cells in the E9 YS and E8 P-Sp are pre-HSCs that require maturation before acquiring characteristics of LTR-HSCs (Medvinsky and Dzierzak, 1999). This idea is supported by a couple of circumstantial lines of evidence: first, the conserved expression of c-kit and CD34 among engrafting cells during development (ie, in the E9.5 YS and P-Sp (Yoder et al., 1997a), and LTR-HSCs in AGM region and placenta (Gekas et al., 2005; Sanchez et al., 1996)); second, the ability of the E8.25 YS cells to acquire LTR-HSC activity upon over-expression of Hoxb4 (Kyba et al., 2002) or after co-culture with the AGM-S3 cell line (Matsuoka et al., 2001b). However, the ability of E9 and P-Sp to develop LTR-HSC potential after experimental manipulation does not necessarily recapitulate the events occurring *in vivo*.

Direct evidence for pre-HSC maturation arose from kinetic analysis of the $CD45^+VE\text{-}cadherin^+$ compartment during *ex vivo* culture (Taoudi et al., 2008). Genetically labelled $CD45^+VE\text{-}cadherin^+$ isolated from the E11.5 AGM give rise to the vast majority of the 150 LTR-HSCs obtained during 4 days reaggregate culture (Taoudi et al., 2008). Carboxyfluorescein succinimidyl ester (CFSE) retention analysis demonstrated that the $CD45^+VE\text{-}cadherin^+$ cells underwent approximately 6 divisions during the 4 days culture period (Taoudi et al., 2008). Considering that the E11.5 contains 1 $CD45^+VE\text{-}cadherin^+$ LTR-HSC (Kumaravelu et al., 2002; North et al., 2002; Taoudi et al., 2005), it is virtually impossible that proliferation of this single cell could account for the 150 LTR-HSCs obtained, so it became clear that $CD45^+VE\text{-}cadherin^+$ pre-HSCs matured into LTR-HSCs during *ex vivo* culture (Taoudi et al., 2008). However, the extent to which maturation and proliferation of pre-HSCs and LTR-HSCs contribute to the final pool of LTR-HSCs after 4 days culture remains to be determined.

1.4.2.5. The mesodermal theories: sub-aortic patches

The observation of mesodermal structures, termed sub-aortic patches (SAP), located below the aortic floor in the E10.5-11.5 AGM region have been proposed to constitute a pool of pre-HSCs (Bertrand et al., 2005; Manaia et al., 2000). Immunostaining, *in situ* hybridization, and reverse transcriptase polymerase chain reaction (RT-PCR) analyses have indicated that SAPs express the haematopoietic markers Lmo-2, GATA-3, AA4.1, c-kit, PECAM-1, CD41, and low levels of CD45 (Bertrand et al., 2005; Manaia et al., 2000). As only IAHCs express similar combination of haematopoietic markers, a close developmental link between these two structures was assumed. Additionally, the concomitant disappearance of SAP and IAHC with the cessation of LTR-HSC production by the AGM region further supported the idea that the pre-HSCs or/and LTR-HSCs migrate from SAP to IAHCs from which they are released in the peripheral circulation (Bertrand et al., 2005; Manaia et al., 2000). Direct functional evidence for such a model has not been provided so far and more sophisticated lineage trace systems (such as reaggregate culture) may be useful for the accurate tracing of pre-HSCs in the SAPs.

1.4.2.6. The primordial germ cells theory

The colonisation of the genital ridges at E10.5 by germ cells with totipotent[9] potential have led scientists to hypothesise primordial germ cells (PGCs) as a source of LTR-HSCs (Rich, 1995). PGCs are ectoderm-derived, express alkaline phosphatase and emerge at the base of the allantois in E6.5 embryos (Ginsburg et al., 1990). The observation that PGCs can give rise to erythroid lineage cells and cobblestone areas indicates that these cells have haematopoietic potential, and therefore may harbour the potential for LTR-HSC formation (Rich, 1995). Functional evidence supporting this possibility remains to be published.

1.5. Runx1 as a master regulator of haematopoiesis

Runx1 (also known as AML1, PEBPα2 and CBFA2) is a transcription factor involved in many oncogenic chromosomal translocations (Speck and Gilliland, 2002). The inactivation of Runx1 in murine models has stimulated major scientific interest on Runx1 because definitive haematopoiesis is completely ablated in $Runx1^{-/-}$ embryos, whilst primitive haematopoiesis remains fairly undisturbed (Okuda et al., 1996; Wang et al., 1996a).

The Runx family of transcription factors consists of 3 members (Runx1, Runx2, and Runx3) that show a high degree of homology within their coding regions (Bae, 1993, Ogawa, 1993a). Runx2 is involved in osteogenesis *in vivo*; deficient murine embryos die neonatally, likely owing to an early arrest in osteoblast development and a malformed rib cage that prevents normal breathing (Komori et al., 1997). Runx3 is predominantly expressed in haematopoietic organs, epidermal appendages, developing bones and sensory ganglia; its inactivation *in vivo* highlights its role for the development and survival of dorsal root ganglia neurones (Levanon et al., 2002; Levanon et al., 2001a). Interestingly, Runx3 expression overlaps with

[9] Totipotency refers to the ability of a single cell to divide and produce all the cell types in an organism, including extra-embryonic tissues.

Runx1 in the developing haematopoietic system, raising the possibility that cross-regulation between them plays a role during embryogenesis (Levanon et al., 2001a; Spender et al., 2005).

1.5.1. Structure and transcriptional regulation of *Runx1* gene

1.5.1.1. Regulation of *Runx1* transcription

Mouse *Runx1* spans 224 kb gene on chromosome 16 (analogous to chromosome 21 in the human), and comprises 7 protein coding exons (Bee et al., 2009b)(Figure 1.7A). Transcriptional regulation of the human and murine Runx1 is under the control of distal (P1) and proximal (P2) promoters that are 128 kb apart and differ in their CpG contents (Bee et al., 2009b; Ghozi et al., 1996). Their alternative use directs the expression of Runx1 isoforms varying in the N-terminal region, and potentially leading to differential gene regulation (Levanon et al., 2001b). Among the upstream regulators of Runx1 expression are Runx transcription factors themselves as the P1 promoter contains Runx-binding sites (Ghozi et al., 1996; Pimanda et al., 2007). For example, Runx1 expression is repressed by Runx3 in B cells (Spender et al., 2005). Retinoic acid has also been speculated to act as an upstream regulator of Runx1 expression as an increased Runx1 expression was observed during retinoic-acid induced differentiation of human leukaemic monocyte lymphoma cell line (Tanaka et al., 1995).

Transcriptional networks regulating Runx1 expression in the development of the haematopoietic system have been under scrutiny. Recently, a 23 kb enhancer, located in the first intron of Runx1, has been identified as a cis-regulatory element, acting during early haematopoiesis and depending on upstream regulators GATA-2 and Ets proteins (Nottingham et al., 2007). BMP-4 activity, well known for facilitating haematopoietic differentiation of ES cells and HSC activity in human cord blood cells culture (Bhatia et al., 1999; Chadwick et al., 2003), can modulate Runx1 expression (Pimanda et al., 2007) (Landry et al., 2008; Nottingham et al., 2007).

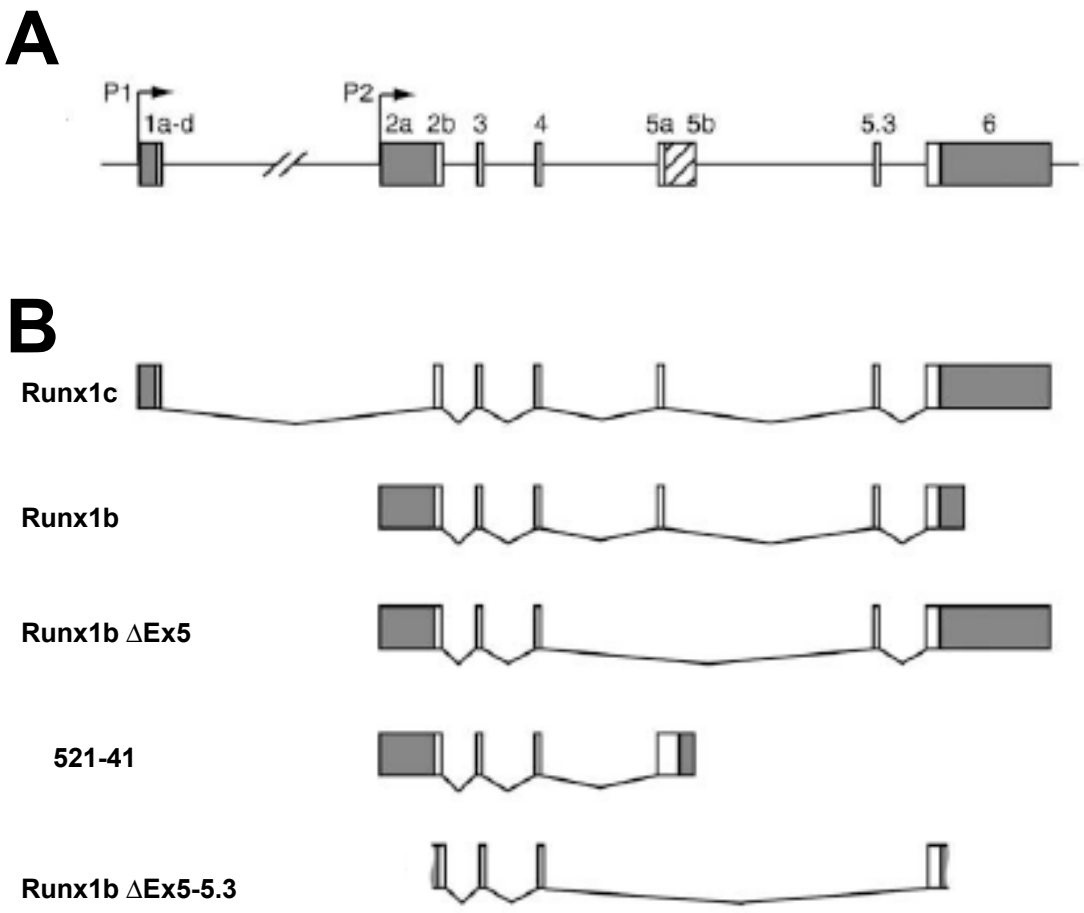

Figure 1.7: Mouse Runx1 genomic locus and alternative splice forms.
A: Runx1 genomic locus under control of distal (P1) and proximal (P2) promoters.
B: Runx1 splice forms: Runx1c, Runx1b, Runx1bΔEx5, 521-41 and Runx1bΔEx5-5.3.
Numbers correspond to exons, white boxes: coding sequences; grey: untranslated regions (UTRs); striped: predicted coding + UTR.
(adapted from Bee et al, 2009).

Finally, a recent study showed that SCL directly transactivates Runx1 in the fetal liver and YS via the binding of an SCL-Lmo2-GATA2 complex to regions flanking the conserved E-boxes of the Runx1 locus (Landry et al., 2008).

1.5.1.2. Structure of the protein and alternative splicing

The distal (P1) and proximal (P2) promoters direct primary transcripts that are alternatively spliced to give a repertoire of mRNA isoforms that are differentially expressed in various cell types at different developmental stages (Figure 1.7B). P1 encodes RUNX1c while P2 encodes RUNX1b and the short isoform RUNX1a (Miyoshi et al., 1995). Very little is known about the role of specific isoforms in the emergence, maintenance, and expansion of LTR-HSCs. The generation of mice with significantly diminished proximal promoter activity on the second allele suggested that P1 (Runx1c) activity was sufficient for primitive haematopoiesis whereas P2 activity (Runx1b) was required for adult definitive haematopoiesis (Pozner et al., 2007). Interpretations of these results are limited to the fact that a hypomorphic dose of Runx1 was available during development. A recent study focusing on P1 and P2 transcripts in the YS, AGM, placenta, fetal liver, and adult bone marrow showed that primitive erythropoiesis is largely P2 driven (Bee et al., 2009b). Both P1 and P2 act with the +23 enhancer to drive the transcription of Runx1 in the YS, AGM, and fetal liver at the time of LTR-HSC emergence (Bee et al., 2009a; Bee et al., 2009b). After haematopoietic cell migration to the liver, P1 gradually becomes the main haematopoietic promoter, as it will remain into adulthood (Bee et al., 2009b).

Runx proteins are conserved and share a runt DNA-binding domain, homologous with the Drosophila pair-rule gene runt (Kania 1990). A nuclear localisation signal (NLS) is located within the Runt domain and immunofluorescent labelling experiments have shown that Runx1 localised in the nucleus (Lu et al., 1995).

Runx1 functions as a heterodimeric transcription factor composed of Runx1 (DNA binding unit) and CBFβ, a 128 amino acids protein which allosterically enhances the DNA binding affinity of Runx1 (Yan et al., 2004). The requirement of

CBFβ for normal Runx1 function is supported by CBFβ knockout mice, which display a very similar phenotype to the Runx1 knockout animals (Niki et al., 1997; Okuda et al., 1996; Sasaki et al., 1996; Wang et al., 1996a; Wang et al., 1996b). Interestingly, CBFβ is mainly located in the cell cytoplasm, suggesting that its translocation to the nucleus is another regulatory mechanism of Runx1 function (Lu et al., 1995; Tanaka et al., 1997). Additionally, CBFβ also protects Runx1 protein from ubiquitin-proteasome-mediated degradation, thus regulating Runx1 turnover (Huang et al., 2001). A model of Runx1 cellular localisation and its regulation is summarised in Figures 1.8.

1.5.1.3. Runx1-mediated transcriptional activation

Upon DNA binding, Runx1/CBFβ acts as an organising factor by recruiting various co-factors and interacting with other transcription factors genes (Durst and Hiebert, 2004; Lutterbach et al., 2000)(summarised in Figure 1.9A). A number of haematopoietic genes are activated by Runx1, including interleukin-3 (IL-3)(Uchida et al., 1997), granulocyte-macrophage colony stimulating factor (GM-CSF), macrophage colony stimulating factor (M-CSF)(Zhang et al., 1996), CSF-1 receptor (Zhang et al., 1994), neutrophil elastase (Nuchprayoon et al., 1994), myeloperoxidase (Suzow and Friedman, 1993), or the defensin protein, NP3 (Westendorf et al., 1998) amongst many others.

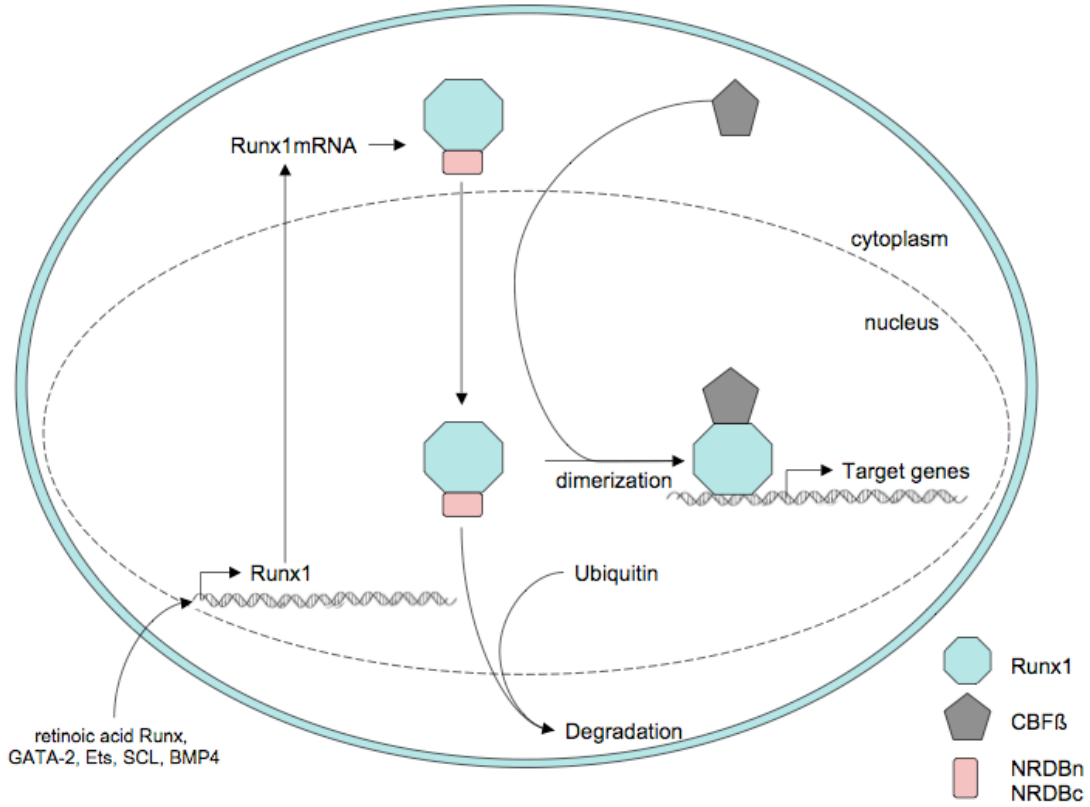

Figure 1.8: Cellular localization of Runx1 and dimerization with CBFβ.
Once synthesized, Runx1 is targeted to the nucleus but it has a poor DNA binding affinity due to negative regulatory domain for DNA binding (NRDB)n and NRDBc occupying Runx1 runt domain. CBFβ, which is stored in the cytoplasm, is targeted to the nucleus where dimerization with Runx1 happens at the runt domain, enhancing Runx1/CBFβ DNA binding affinity. Runx1/CBFβ then binds to target genes promoters and influence their transcription. If dimerization with CBFβ does not occur, Runx1 is degraded via the ubiquitin-proteasome pathway.

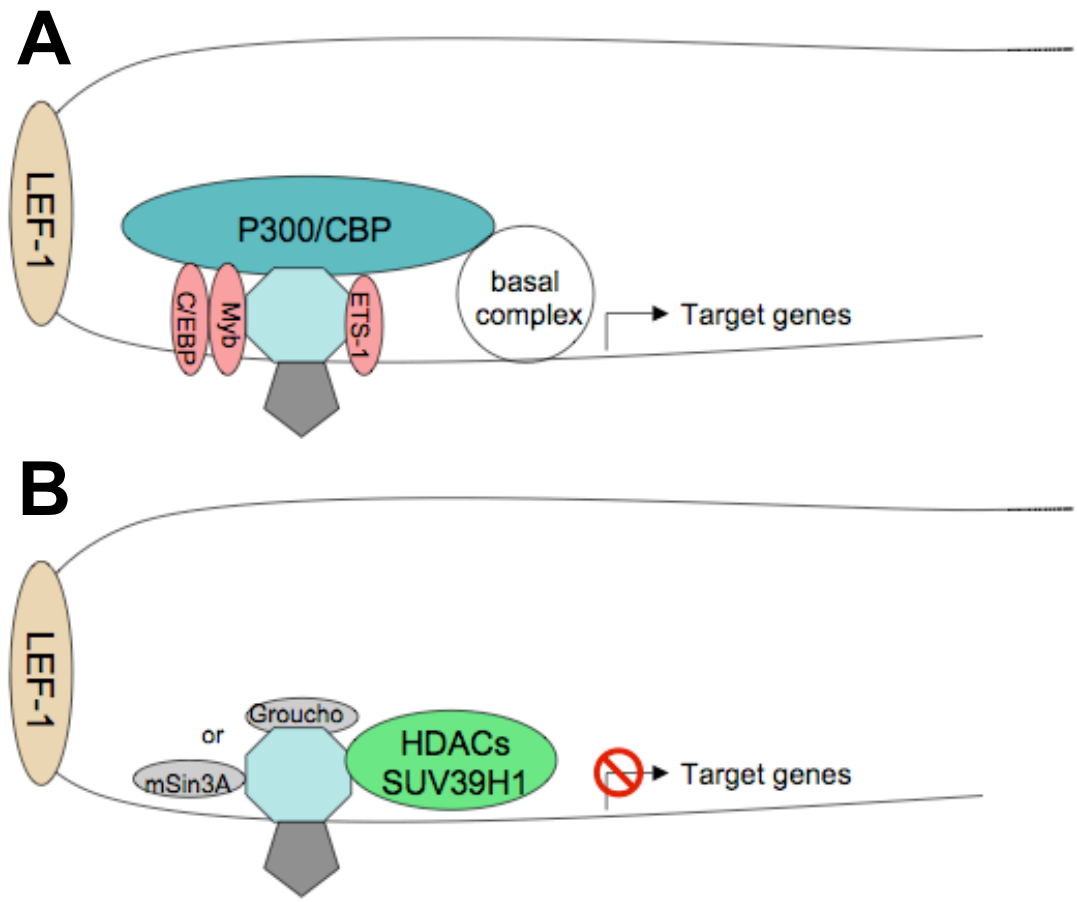

Figure 1.9: Models of Runx1-mediated transcriptional activation and repression.
A: Runx1 mediated transcriptional activation. Runx1/CBFβ binds to DNA and recruits co-activators such as ETS1, Myb, or C/EBP. LEF-1 protein induces DNA bending and P300/CBP is recruited and mediates interactions with both histone acetyltransferases and basal transcription complex proteins.
B: Runx1-mediated transcriptional repression. Upon DNA binding, Runx1/CBFβ recruits co-repressors Groucho and mSin3A and LEF-1 protein induces DNA binding. The epigenetic state is altered by histones deacetylases (HDACs) and methyltransferases (SUV39H1 for instance) when they are recruited.
These diagrams are simplified and do not take into account particular situations.

1.5.1.4. Runx1 mediated transcriptional inactivation

Even though Runx1 on its own appears to be a weak transcriptional enhancer, it is a potent transcriptional repressor (Durst and Hiebert, 2004). Interactions with Groucho, dCtBP, and histone deacetylases (Rpd3 and mSin3A) act in the maintenance of repression via three repression domains (RD1, 2, 3)(Figure 1.9B)(Aronson et al., 1997; Lutterbach et al., 2000; Wheeler et al., 2002). For example, Groucho interacts with Runt proteins at the C-terminal VWRPY amino acid sequence located in RD3 (Aronson et al., 1997) whereas recruitment of mSin3A and USV39H1, a histone methyltransferase, are via RD1 and RD2 respectively (Lutterbach et al., 2000; Reed-Inderbitzin et al., 2006). The most famous haematopoietic gene downregulated by Runx1 is the T cell marker CD4 (Durst and Hiebert, 2004).

1.5.2. The roles of Runx1 in adult haematopoiesis

The roles of Runx1 in adult haematopoiesis have been widely investigated because chromosomal translocations leading to impaired function of Runx1 in the haematopoietic system are associated with a wide range of disorders (Speck and Gilliland, 2002).

1.5.2.1. Runx1 in LTR-HSCs

The LTR-HSC enriched fraction $lin^{-}c\text{-}kit^{+}$ express high levels of Runx1 in the functional *Runx1-IRES-GFP* knock-in model, which has no observable haematopoietic phenotype (Lorsbach et al., 2004).

Although Runx1 is essential for embryonic haematopoiesis, its role during adult haematopoiesis remained unclear for a long time. To elucidate this issue, scientists generated models in which Runx1 can be deleted by Cre-mediated recombination (Growney et al., 2005; Ichikawa et al., 2004; Putz et al., 2006). Such models showed that Runx1 is not essential for adult haematopoiesis and the null

mutation ($Runx1^{\Delta/\Delta}$) leads to expansion of the LTR-HSC pool but with a possible reduced competitive repopulating activity (Growney et al., 2005; Ichikawa et al., 2004; Ichikawa et al., 2008; Putz et al., 2006).

However, the effects of different Runx1 dosages in adult mice are still unclear. While the large majority of LTR-HSCs in haploinsufficient animals express Runx1, Ichikawa and colleagues report an increase in the number of LTR-HSCs whereas Sun and Downing reports a 50% decrease in the number of LTR-HSCs (Ichikawa et al., 2008; Sun and Downing, 2004). The reason for this discrepancy is most likely due to the fact that Ichikawa's animals had two Runx1 functional alleles until poly(I:C) injection whereas Sun's animals were haploinsufficient since conception (Ichikawa et al., 2008), indicating that a full dose of Runx1 is necessary for establishing a normal LTR-HSCs pool.

1.5.2.2. Runx1 roles in lymphoid lineages

The role of Runx1 in the development of T cells is now well documented (Collins et al., 2009). In the knock-in reporter mouse, Runx1 is highly expressed in $CD4^-CD8^-$ thymocytes[10] and $CD4^+$ peripheral T cells express 2 to 3 times higher levels of Runx1 compared to $CD8^+$ T cells (Lorsbach et al., 2004). Runx1 role in mature $CD4^+$ T cells is dose-dependent, which is supported by literature documenting gene silencing of CD4 by Runx1 (Collins et al., 2009; Durst and Hiebert, 2004; Growney et al., 2005). Lineage analyses of the reconstitution obtained from $Runx1^{\Delta/\Delta}$ adults have showed a defect in lymphoid reconstitution (B and T cells)(Growney et al., 2005; Ichikawa et al., 2004; Ichikawa et al., 2008; Putz et al., 2006). The reduced size of thymi and the accumulation of $CD4^-CD8^-$ thymocytes

[10] T-cell lineage choice in the thymus progresses through a series of developmental stages: $CD4^-CD8^-$ (DN) precursors enter the thymus and begin rearranging the T-cell receptor-β chain locus and become $CD4^+CD8^+$ (DP) and then commit to $CD4^+$ or $CD8^+$ (SP) mature T cell fate (Collins et al, 2009).

indicate that Runx1 is required in the early stages of T cell differentiation (Growney et al., 2005; Putz et al., 2006).

In addition to T cells, there is a severe defect in B cell maturation in Runx1 null adults and also a defect in reconstituting the B cell compartment of recipients (Growney et al., 2005; Ichikawa et al., 2004; Putz et al., 2006). Runx1 is expressed at similar levels during stages of B cell development (North et al., 2004) but very little is known about the stage of B cell maturation at which Runx1 is important.

1.5.2.3. Roles of Runx1 in myeloid lineages

A full deletion ($Runx1^{\Delta/\Delta}$) or a haploinsufficient dose, present throughout development ($Runx1^{lz/WT}$) or induced during adulthood ($Runx1^{\Delta/WT}$), results in an increased number of committed myeloid progenitors, which can give rise to a myeloproliferative phenotype, thrombocytopaenia or splenomegaly (Ichikawa et al., 2008; Putz et al., 2006; Sun and Downing, 2004).

1.5.2.3.1. Role of Runx1 in megakaryocytes

It was shown that Runx1 is up-regulated at the early stages of megakaryocytic differentiation (Elagib et al., 2003; Lorsbach et al., 2004). Inducible Runx1 deletion ($Runx1^{\Delta/\Delta}$) results in a rapid and prolonged fivefold drop in peripheral blood platelets whereas it has minimal effects on red blood cell and neutrophil numbers (Goldfarb, 2009; Growney et al., 2005; Ichikawa et al., 2004). Histochemical analysis of $Runx1^{\Delta/\Delta}$ bone marrow with acetylcholinestase staining showed an absence of normal looking megakaryocytes but an increase in small, hypolobulated megakaryocyte-like cells showing a marked decrease in ploidy (Growney et al., 2005; Ichikawa et al., 2004).

1.5.2.3.2. Role of Runx1 in erythrocytes

Runx1 reporter models have clearly shown that Runx1 is down-regulated upon erythrocyte differentiation, which can be followed by the differential expression of cell surface markers CD71 and Ter119 (Basecke et al., 2002; Kina et al., 2000; Lorsbach et al., 2004; North et al., 2004). However, conditional deletion of Runx1 does not affect erythroid cell numbers or the potential to reconstitute the erythroid compartment (Growney et al., 2005; Putz et al., 2006; Sun and Downing, 2004), indicating Runx1 is dispensable for erythrocyte maturation.

1.5.2.3.3. Role of Runx1 in monocytes/macrophages

In WT and Runx1 haploinsufficient adult bone marrow, the large majority of myeloid blast cells, granulocytes and monocytes express Runx1 at various stages of maturation (Basecke et al., 2002; North et al., 2004). $Runx1^{\Delta/\Delta}$ animals can reconstitute the granulocytic and monocytic compartments of irradiated recipients, indicating that the effect of Runx1 deletion in these myeloid cells is milder compared to lymphoid lineages (Growney et al., 2005; Ichikawa et al., 2004). However, the increased myeloid cell numbers observed in the spleen and the bone marrow of $Runx1^{\Delta/\Delta}$ adults, together with Runx1 expression in myeloid lineages and Runx1-mediated activation of the M-CSF promoter, strongly suggest a potential role of Runx1 in myeloid development but its stage specific requirement is still to be fully investigated (Basecke et al., 2002; Growney et al., 2005; Ichikawa et al., 2004; North et al., 2004; Putz et al., 2006).

1.5.3. Roles of Runx1 during embryonic development

1.5.3.1. Runx1 expression in the developing null or haploinsufficient embryo

Runx1 expression in the knock-in LacZ reporter mouse model is first observed at E7.5, at the neural stage plate, in the endoderm and some extraembryonic mesodermal cells (North et al., 1999). At E8.5, strong LacZ expression can be

observed in the YS blood islands (both endothelial and haematopoietic cells), in the distal portion of the allantois at the junction point with the chorion, in endothelial cells of the vitelline artery and in the ventral aspect of the paired dorsal aortae (North et al., 1999). LacZ is also expressed in primitive erythrocytes but its expression diminishes and disappears by E11.5 (North et al., 1999). At E10.5, the time of LTR-HSC emergence, Runx1 expression can be observed in the vitelline and umbilical arteries, the AGM region, the fetal liver, the placental labyrinth and other sites unrelated to haematopoiesis such as the olfactory epithelium, the spinal ganglia, and the maxillary processes (North et al., 1999; Rhodes et al., 2008; Simeone et al., 1995; Zeigler et al., 2006)(Figure 1.10B). In the E10.5-11.5 AGM region, Runx1 is expressed in ventral IAHCs, and particularly endothelial, haematopoietic and mesenchymal cells (North et al., 1999; North et al., 2002)(Figure 1.10C and D). Most importantly, Runx1 marks LTR-HSCs in the Runx1 haploinsufficient embryo (North et al., 2002).

1.5.3.2. Insights from the Runx1 knockout model

Runx1 deficiency ($Runx1^{-/-}$) results in a complete block of LTR-HSC emergence with no IAHCs in the Ao and vitelline and umbilical arteries (North et al., 1999; Okada et al., 1998; Okuda et al., 1996; Wang et al., 1996b). $Runx1^{-/-}$ embryos develop extensive central nervous haemorrhages and anaemia and die between E11.5 and E12.5 (Okuda et al., 1996; Samokhvalov et al., 2006; Wang et al., 1996a)(Figure 1.10A). Extensive cellular necrosis involving endothelial cells in the nervous system capillaries has been observed (Wang et al., 1996a).

No differences in primitive erythrocyte morphology or numbers are observed between $Runx1^{-/-}$ embryos and WT age-matched controls (Okuda et al., 1996; Wang et al., 1996a). However, primitive erythrocytes in $Runx1^{-/-}$ mice display abnormal morphology and a reduced expression of Ter119 and GATA-1 (Yokomizo et al., 2008).

In contrast to primitive haematopoiesis, there is a total lack of adult-type haematopoiesis, histologically characterised by the absence of enucleated erythroid,

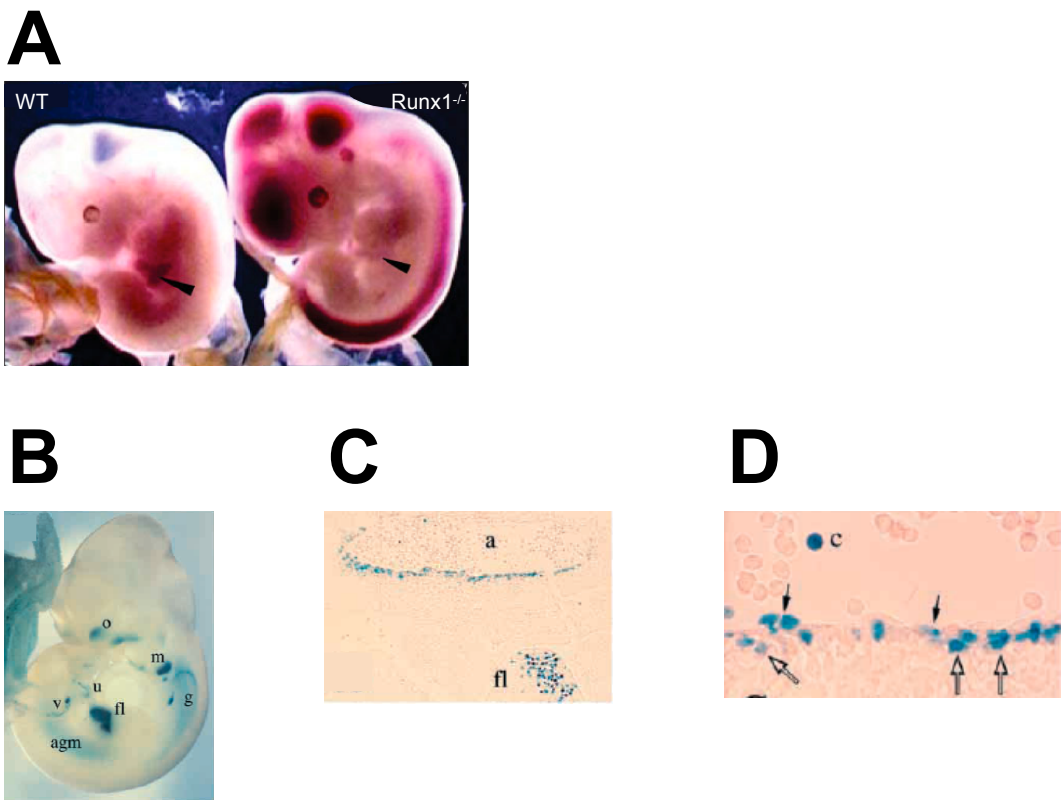

Figure 1.10: Phenotype of Runx1 deficient E11.5 embryos and Runx1 expression in embryonic organs.

A: Phenotype of E11.5 Runx1 deficient embryo ($Runx1^{-/-}$) compared to wild type (WT). $Runx1^{-/-}$ embryo displays clear central nervous system haemorrhages and liver pallor (pointed by arrows)(taken from Samokhvalov et al, 2006).

B: Runx1 expression in the E11.5 Runx1 haploinsufficient ($Runx1^{+/-}$) embryo (in LacZ knock-in reporter mouse model). Runx1 expression in observed in haematopoietic sites such as vitelline (v) and umbilical (u) arteries, the AGM (agm) region, and the fetal liver (fl) and non-haematopoietic sites such as the olfactory epithelium (o), the maxillary processes (m), spinal ganglia (g) and external genitalia (not seen from this angle)(taken from North et al, 1999).

C: Sections of E10.5 $Runx1^{+/-}$ embryo showing Runx1 expression on the ventral wall of the dorsal aorta (a) and in haematopoietic cells in the fetal liver (fl)(taken from North et al, 1999).

D: View of the ventral wall of the E10.5 $Runx1^{+/-}$ dorsal aorta showing Runx1 expression in endothelial cells (closed arrows), para-aortic mesenchyme (open arrows) and circulating haematopoietic cells (c))(taken from North et al, 1999).

myeloid, and megakaryocytic cells in the fetal liver, and functionally characterised by the absence of haematopoietic progenitors and LTR-HSCs in the E9.5-11.5 YS, P-Sp/AGM region, and fetal liver (Mukouyama et al., 2000; North et al., 1999; Okuda et al., 1996; Wang et al., 1996a). The essential requirement for Runx1 in the generation of the adult haematopoietic system was confirmed by the failure of $Runx1^{-/-}$ ES cells to contribute to adult haematopoietic system in chimaeric animals (Okuda et al., 1996). In addition, further support was obtained from experiments in which the rescue of Runx1 expression in $Runx1^{-/-}$ ES cells *in vitro*, or by conditional reactivation of a reversible knockout *in vivo* restores definitive haematopoietic potential (Goyama et al., 2004; Mukouyama et al., 2000; Okuda et al., 2000; Samokhvalov et al., 2006).

1.5.3.3. Runx1 effect on LTR-HSC emergence is dose-dependent

The study of the LacZ reporter mouse showed that haploinsufficiency results in a dramatic change in temporal and spatial distribution of LTR-HSCs (Cai et al., 2000). The emerging LTR-HSCs in the E10.5 and E11.5 AGM, vitelline and umbilical arteries in these animals all express Runx1 but have a heterogenous immunophenotype, including haematopoietic ($CD45^{+}$), endothelial ($PECAM\text{-}1^{+}$, VE-$cadherin^{+}$, and $Flk1^{+}$), and mesenchymal cells ($CD45^{-}$VE-$cadherin^{-}$); proportions in the haploinsufficient embryo varied from WT controls (North et al., 2002).

Additionally, a hemizygous dose of Runx1 results in fewer CFU-Cs in the E10.5-11.5 YS and the E9.5-11.5 P-Sp/AGM region and also CFU-S in the YS, AGM and fetal liver from E10.5 onwards (Cai et al., 2000; Mukouyama et al., 2000; Okuda et al., 1996; Robin et al., 2006; Wang et al., 1996a). Kinetics of LTR-HSCs appearance in these embryos demonstrated that LTR-HSCs emerge earlier as they are readily detectable in the E10.5 AGM region and the YS (Cai et al., 2000). Explants culture confirmed the early emergence of LTR-HSCs in the YS. However, LTR-HSC maintenance/expansion in the E10.5 AGM region requires two functional Runx1 alleles, suggesting a requirement for Runx1 in the AGM microenvironment (Cai et al., 2000). Also, both the numbers of IAHCs and LTR-HSCs in the AGM region are

Runx1 dose dependent (Cai et al., 2000; North et al., 1999; Robin et al., 2006; Yokomizo et al., 2001), providing further circumstantial evidence for a developmental link between IAHCs and LTR-HSCs.

1.5.3.4. Runx1 and the emergence of LTR-HSCs

The expression of Runx1 in an array of cell types in the E10.5 AGM region, as well as the failure of Runx1 deficient embryos to generate LTR-HSCs, has led scientists to wonder which specific cell types require Runx1 to allow LTR-HSC development. One study reported that LTR-HSCs ancestor cells are marked by Runx1 and can be traced back to the E7.5 YS (Samokhvalov et al., 2007). Apart from showing that LTR-HSCs ancestors express Runx1 at some stage, this study remains controversial because it fails to demonstrate robustly that labelling cannot occur in the embryo proper, allantois and placenta. Many other laboratories have also attempted to understand which mechanisms controlled by Runx1 are involved in the emergence of LTR-HSCs. The available data supports a model in which Runx1 is essential for the transition of haemogenic endothelial cells (see Section 1.4.2.3) to haematopoietic commitment, and more particularly LTR-HSCs (Chen et al., 2009; North et al., 2002; Yokomizo et al., 2001).

The first evidence supporting this model came from the observation that Runx1-null endothelial cells (VE-cadherin$^+$ in this case) fail to generate definitive haematopoietic lineage cells (Yokomizo et al., 2001). This was further indicated by the combined observations that Runx1-null embryos have similar numbers of VE-cadherin$^+$ compared to WT controls but have virtually no CD45$^+$VE-cadherin$^+$ cells, suggesting that there is a failure in haematopoietic commitment at this early stage (Fraser et al., 2003; Yokomizo et al., 2001). Additionally, North and colleagues reported that endothelial (PECAM-1$^+$ or VE-cadherin$^+$) and mesenchymal cell fractions in the E10.5-11.5 AGM region, vitelline and umbilical arteries had some LTR-HSC activity (North et al., 2002). However, this study involved Runx1 haploinsufficient embryos, which have impaired LTR-HSCs kinetics and immunophenotype. Additionally, their idea of a Runx1$^+$ endothelial LTR-HSC is

based on the lack of CD45 expression, indicating a non-haematopoietic phenotype (North et al., 2002). As previously discussed, CD41 is a more accurate early marker for haematopoietic cells as it is expressed earlier than CD45, suggesting that VE-cadherin^{+}CD45^{-}Runx1^{+} cells might already be haematopoietic (Eilken et al., 2009; Ferkowicz et al., 2003; Mikkola et al., 2003a). Finally, a recent study from the same lab used a conditional knockout *in vivo* approach to better define the stage at which Runx1 is essential for LTR-HSC emergence (Chen et al., 2009). Runx1 deletion in the endothelial compartment, using VE-cadherin Cre recombinase, showed that LTR-HSCs are much reduced in the E11.5 AGM region of the Runx1Δ/Δ:VE-cadherin Cre animals (Chen et al., 2009). This indicates that LTR-HSC development is impaired, but with a strong selective pressure exerted on cells that escape excision, accounting for the presence of LTR-HSCs (Chen et al., 2009). Similar experiments with Vav-Cre were carried out and showed that Runx1 excision in the Vav^{+} compartment does not affect the LTR-HSC development. Vav expression is restricted to most haematopoietic lineages *in vivo* (Ogilvy et al., 1999) so it was assumed Vav^{+} cells are already be committed haematopoietic fate. Based on this assumption, they concluded that Runx1 is essential at the endothelial cell level but is dispensable afterwards (Chen et al., 2009), pinpointing a stage at which Runx1 is no longer required. Lancrin and colleagues came to a similar conclusion using an *in vitro* ES cell model in which they could rescue Runx1 expression and showed that Runx1 is not necessary for the establishment of haemogenic endothelium (defined as Tie2^{+}c-kit^{+}CD41^{-}) but is required for definitive haematopoiesis by this population based on colony assay (Lancrin et al., 2009). Even though these studies yielded very interesting observations, the criteria by which endothelial cells are defined (Tie2 expression or VE-cadherin expression only) are not sufficiently robust; thus compromising the interpretation that Runx1 is needed for the transition from hemogenic endothelial cells to LTR-HSCs.

1.6. The *ex vivo* expansion of LTR-HSCs

The failure to generate LTR-HSCs from ES cells *in vitro* has challenged the field of haematopoiesis for years. In contrast, attempts to induce, maintain, and expand LTR-HSCs from haematopoietic tissues *ex vivo* have proven fairly successful and have provided major insights into LTR-HSC biology. HSC expansion is defined as a symmetrical self-renewal division generating two HSCs whereas HSC maintenance involves asymmetrical self-renewal division generating one HSC and a more differentiated progeny (Cellot and Sauvageau, 2006). Extensive LTR-HSC expansion occurs during ontogeny within the placenta and the fetal liver niche (Ema and Nakauchi, 2000; Gekas et al., 2005; Morrison et al., 1995). Studies aiming to achieve LTR-HSC expansion *in vitro* are briefly reviewed in the following sections.

1.6.1. Hoxb4: a potent stimulator of LTR-HSC expansion

Insights into the roles of Homeobox (Hox) genes in haematopoiesis emerged from over-expression studies. For example, over-expression of Hoxa10, Hoxb3 and Hoxb6 in bone marrow cells results in a block in differentiation of B and T cells, impaired erythropoiesis and myeloproliferative disorders (Argiropoulos and Humphries, 2007). The engineered retroviral over-expression of Hoxb4 in the bone marrow transplantation model induces LTR-HSC expansion both *in vivo* and *in vitro* (Sauvageau et al., 1995). A subsequent study using a similar approach achieved a net 41 fold *ex vivo* expansion of LTR-HSC with normal reconstitution of both the myeloid and lymphoid compartments without inducing leukaemia (Antonchuk et al., 2002), placing Hoxb4 as one of the most potent stimulator of LTR-HSC expansion. In addition, Hoxb4 over-expressing cells have enhanced regenerative potential; meaning transplantation with over-expressing Hoxb4 cells can restore the LTR-HSC pool to its normal size compared to around 25% with controls (Antonchuk et al., 2001; Antonchuk et al., 2002; Sauvageau et al., 1995; Thorsteinsdottir et al., 1999).

Intriguingly however, the effects of Hoxb4 deficiency on LTR-HSC self-renewal are fairly elusive, with no disruption of definitive haematopoiesis albeit with subtle reductions in HSC and progenitors numbers and a modest impairment of the

competitive repopulating ability (Argiropoulos and Humphries, 2007; Bijl et al., 2006; Brun et al., 2004). More recently, a near-complete Hoxb cluster knockout revealed that Hoxb genes are dispensable for normal haematopoiesis as Hoxb deficient LTR-HSCs remain competitive and retain their full differentiation potential (Bijl et al., 2006). Taken together, these studies highlight the complex network of genetic interactions between different categories of Hox genes in LTR-HSCs biology and demonstrate their potential overlapping functions (Argiropoulos and Humphries, 2007; Bijl et al., 2006).

1.6.2. Soluble growth factors as potent inducers of LTR-HSC expansion

Stem cell engineering using retroviral transduction raises the issue of safety when it comes to applying this knowledge to the clinic. Many attempts to achieve LTR-HSC expansion by modulating the growth factors present in *ex vivo* culture media have been reported. The most successful bone marrow LTR-HSC expansion achieved a 30 fold LTR-HSC expansion upon culture in serum free medium supplemented with soluble SCF, thrombopoeitin (TPO), Insulin-like growth factor 2 (IGF-2), fibroblast-growth factor 1 (FGF-1) and angiopoietin like 2 and 3 (Zhang et al., 2006). Our group also recently reported a 150-fold LTR-HSCs increase during 4 days *ex vivo* culture with SCF, IL-3 and Flt3l (Taoudi et al., 2008). However, this increase was due to pre-HSC maturation rather than expansion by symmetrical self-renewal divisions (Taoudi et al., 2008).

Cytokines are secreted proteins that regulate many aspects of LTR-HSC functions including quiescence, self-renewal, differentiation, apoptosis and mobility (Zhang and Lodish, 2008). It is believed that stromal cells in HSC niches (see Section 1.2.1.2) synthesise the appropriate HSC cytokines but little is known about which cytokine is produced by which niche stromal cell type (Zhang and Lodish, 2008). The roles of SCF, IL-3 and Flt3l in the regulation of LTR-HSC emergence/maintenance and expansion are discussed. For a more detailed summary of cytokine families involved in haematopoiesis, refer to (Zhang and Lodish, 2008).

1.6.2.1. Stem cell factor

Also known as Steel factor, SCF functions by binding to c-kit, which is expressed in LTR-HSCs throughout development (Gekas et al., 2005; Morrison et al., 1995; Sanchez et al., 1996; Yoder et al., 1997a). Almost all cytokine combinations used for the *ex vivo* culture of LTR-HSCs include SCF (Zhang and Lodish, 2008).

SCF deficiency results in reduced numbers of LTR-HSCs (assessed by numbers of $Lin^{-}Thy\text{-}1^{lo}Sca1^{+}$ cells in the E13-15 fetal liver) and CFU-S but does not affect their proliferation (Ikuta and Weissman, 1992). Interestingly, fetal liver LTR-HSCs are 6-fold more sensitive to SCF than their adult counterparts, meaning that 50 ng/mL of SCF is sufficient to maintain fetal liver LTR-HSCs *in vitro* compared to 300 ng/mL (and 20 ng/mL of IL-11) required for adult LTR-HSCs (Bowie et al., 2007a). Taken together, these studies prove that fetal LTR-HSCs are highly sensitive to exogenous SCF and that SCF/c-kit-mediated cellular responses might provide an explanation for why fetal and adult LTR-HSC display different biological properties.

1.6.2.2. Interleukin-3

The effect of IL-3 on adult LTR-HSC function remains controversial, as it has been reported both to enhance (Bryder and Jacobsen, 2000) and inhibit (Peters et al., 1996; Yonemura et al., 1996) LTR-HSC expansion *ex vivo*. These discrepancies could be due to differences in concentration, presence of other cytokines or serum (Robin et al., 2006).

Disruption of IL-3 or the IL-3 receptor genes does not affect adult steady state haematopoiesis as IL-3 deficient mice have normal blood cell counts, CFU-Cs and LTR-HSCs (Lantz et al., 1998; Mach et al., 1998). Exogenous addition of SCF to $IL\text{-}3^{-/-}$ bone marrow cultures results in fewer mast cells compared to WT cultures (Lantz et al., 1998). This defect was rescued by the addition of exogenous IL-3, highlighting the synergetic action of IL-3 and SCF (Lantz et al., 1998). Only one study to date has investigated the role of IL-3 on the emergence/expansion of LTR-HSCs during embryonic development (Robin et al., 2006). The numbers of LTR-

HSCs contained in the E11.5 AGM region, YS and placenta are decreased compared to WT controls in the IL-3 haploinsufficient embryos, and undetectable in the IL-3 knockout animals (Robin et al., 2006). Similar results were obtained in explants of IL-3 mutant haematopoietic tissues (Robin et al., 2006). Exogenous addition of IL-3 mediates proliferation and survival of phenotypically enriched LTR-HSC populations ($CD34^{+}c\text{-}kit^{+}$ (Sanchez et al., 1996) and $Sca\text{-}1^{+}c\text{-}kit^{+}$ (de Bruijn et al., 2002)) as well as their early appearances in the E10.5 AGM region and YS (Robin et al., 2006). Interestingly however, addition of exogenous IL-3 to explant medium yields an unprecedented 35-fold expansion in E11.5 AGM explants, with a similar positive effect of IL-3 observed in E11.5 YS and placenta explants (Robin et al., 2006). Taken together, this study highlights the important positive role of IL-3 in the emergence, proliferation and survival of the first LTR-HSCs (Robin et al., 2006).

1.6.2.3. Flt3-ligand

Fms-like tyrosine kinase 3 (Flt3, also known as Flk-2) is activated by its ligand (Flt3l), which can be released as a soluble homodimeric protein and is expressed in cells of the bone marrow microenvironment as well as myeloid and lymphoid heamatopoietic cell lines (Gilliland and Griffin, 2002). When soluble Flt3-l is administered to mice, haematopoietic progenitors in the bone marrow and the spleen expand and HSCs are mobilised into the peripheral blood (Brasel et al., 1996). Flt3l deficient animals do not display any overt phenotype, they have normal numbers of LTR-HSCs but display reduced numbers of B cell progenitors, dendritic cells and natural killer cells *in vivo* (McKenna et al., 2000; Sitnicka et al., 2002).

A recent study focusing on E14.5 fetal liver of Flt3 deficient embryos has shown that Flt3 receptor and ligand are dispensable for normal LTR-HSC function, both in steady state, and during fetal or posttransplantation expansion (Buza-Vidas et al., 2009). While this study implies that fetal liver LTR-HSC expansion is not impaired in Flt3l deficient embryos *in vivo*, no current study has addressed a potential role of Flt3l in the emergence of LTR-HSCs at earlier developmental stages

(E10.5 at the onset of LTR-HSC emergence) or in other embryonic haematopoietic organs (AGM region, YS and placenta).

However, the engraftability of bone marrow LTR-HSCs after *ex vivo* culture, and the enhancement of LTR-HSC expansion by the concerted effects of SCF and Flt3l, confirm previous studies reporting that Flt3l strongly synergises with other haematopoietic growth factors and interleukins (Buza-Vidas et al., 2009; Diehl et al., 2007; Gilliland and Griffin, 2002).

Despite a great progress in the past decade, identification and functional study of HSC cytokines are still at the primitive stage and many secreted or cell surface proteins that affect HSC function remain to be discovered (Zhang and Lodish, 2008).

1.7. Summary and project goals

While various sites such as the AGM region, the YS, the fetal liver and the placenta harbour LTR-HSCs during embryogenesis, the question of the site of the first LTR-HSC emergence remains controversial. Functional evidence to date has indicated that the E10.5 AGM region is the earliest site with detectable LTR-HSC activity and with the capacity to autonomously initiate LTR-HSC expansion (Medvinsky and Dzierzak, 1996; Muller et al., 1994). The unique properties of the AGM region to autonomously expand LTR-HSCs have generated a large interest in the field of haematopoiesis. However, dissection of mechanisms underlying this process has been complicated by the lack of a culture system in which individual cells could be manipulated and yet maintain the capacity of the organ to expand LTR-HSCs. Recently, the reaggregate culture system was developed in our lab (Taoudi et al., 2008). This system enables the dissociation of the E11.5 AGM region prior to culture whilst maintaining its ability to expand LTR-HSCs. The project presented here is based on this system and follows three major lines of investigation:

1. The E11.5 AGM reaggregate system is capable of *ex vivo* expanding LTR-HSCs from 1 (Kumaravelu et al., 2002) to 150 (Taoudi et al., 2008), a range similar to what is observed *in vivo* (Gekas et al., 2005). Such expansion is achieved in the presence of the cytokines IL-3, SCF and Flt3l.

a) The first goal of this project was to phenotypically characterise the LTR-HSCs obtained in reaggregates.

b) The second goal was to investigate the role of individual cytokines in the LTR-HSC expansion.

2. The second part of this project was to understand the role of Runx1 in the emergence and expansion of LTR-HSCs in the E11.5 AGM region using the reaggregate system. In order to address this question, our *Runx1*^{EGFP} reporter mouse model was used.

a) The first goal was to characterise Runx1 expression in cell populations in the adult and the E11.5 embryo to establish whether the transgenic Runx1^{EGFP} allele was functional.

b) The second goal was to identify non-haematopoietic cell populations expressing Runx1 and assess their potential to develop into LTR-HSCs using the reaggregate culture system.

3. The third part aimed to localise pre-HSCs within the E11.5 AGM region using the reaggregate culture system. De Bruijn et al have previously shown that the Ao is the site where the first LTR-HSC appear in the E11.5 AGM region (de Bruijn et al., 2000b). Within the Ao, the majority of LTR-HSCs emerge and are localised to the AoV (Taoudi and Medvinsky, 2007).

a) The first goal was to investigate the possible axio-lateral polarity of LTR-HSC development in reaggregates and whether close proximity of Ao and UGR cells affected their haematopoietic potential.

b) The second goal was to assess the presence of cells in the AoD that might be competent to mature into LTR-HSCs when exposed to the AGM microenvironment (ie, the AoV and UGR).

2. Materials and Methods

Most of the methods described in this section are routinely used in our laboratory and were previously described in (Taoudi, 2006).

2.1. General solutions

Dissection solution: room temperature (RT) Dulbecco's phosphate buffered saline (PBS) solution (with Mg^{2+} and Ca^{2+} ions; Sigma) containing 7% fetal calf serum (FCS) (Gibco, PAA, or Biosera) and 50 units/ml penicillin and streptomycin (P/S; Gibco).

Flow Cytometry buffer solution: Dulbecco's PBS (without Mg^{2+} and $Ca^{2+)}$ containing 7% FCS and 50 units/ml P/S.

2.2. Animals

2.2.1. Animal husbandry

C57BL6, CBA, aEGFP (termed GFP) and *Runx1*^{EGFP} animals were housed and bred within the University of Edinburgh animal houses and according to the regulations of the Animals Scientific Procedures Act, UK, 1986. Animals were provided with a constant supply of water and chow food, and were housed in a constant environment with a 14 hours light/10 hours dark cycle (midpoint 12am and 12pm, and midpoint 7am and 7pm for recipient animals).

Litters obtained were left with parents for three weeks postnatally before weaning by separating parents and offsprings. Only mice older than 6 weeks were used for matings.

2.2.2. Timed matings

For embryonic tissue collection, time matings were organised to obtain embryos at specific stages of gestation. Overnight matings were set up and the females were examined for the presence of vaginal plugs the following morning. Vaginal plug discovery day was assumed to correspond to E0.5.

2.2.3. Mouse lines

Tissues termed wild type (WT) were obtained from C57BL6 animals. For lineage tracing experiments, embryos were generated from the pairing of C57BL6 stud males with C57BL6/aEGFP females. Resulting WT and GFP embryos were genotyped under fluorescent light. aEGFP animals (termed GFP) constitutively express EGFP (Gilchrist et al., 2003).

2.3. *Runx1*^{EGFP} line genotyping and backcrossing

2.3.1. *Runx1*^{EGFP} mouse line genotyping

Animal ear samples were taken at weaning by the animal unit staff. To obtain DNA, samples were treated with 100µl of lysis buffer containing 10% Tween 20, NP40, and 10 mg/ml proteinase K in PCR buffer (Qiagen); and incubated at 55^{o}C overnight. Samples were vortexed and proteins denaturated at 95^{o}C for 5 minutes. Samples were either used immediately or stored at -20^{o}C.

Presence of *Runx1*^{EGFP} allele in genomic DNA was determined by polymerase chain reaction (PCR). Mastermix was prepared in clean water (Sigma) containing PCR buffer, 10mM dNTPs, 5 units/µl Taq polymerase, 3 primers at 0.1ρM/µl final concentration, and finally genomic DNA obtained from ear samples lysis. Oligonucleotide primers (Table 2.1) were designed by H. Inoue and obtained from Eurogentec. All other reagents used for PCR were obtained from Qiagen (cat #201207).

Table 2.1: *Runx1*^{EGFP} PCR genotyping primer sequences and genomic locations. H. Inoue designed oligonucleotide sequences. Transgenic allele PCR product size is 304 base pairs and wild type allele PCR product size is 367 base pairs. Refer to Figure 5.2. EGFP: enhanced green fluorescent protein, UTR: untranslated region.

primer name	genomic location	sequence
Runx1 forward	Runx1 exon 6	5'-CATCGGCATGTCAGCCATGAG-3'
EGFP forward	EGFP	5'-CGGCATCAAGGTGAACTTCAAGAT-3'
Runx1 reverse	Runx1 3'UTR	5'-TCGATGGCGATGGCGCTCAG-3'

Samples were run in a T3 thermocycler machine (Biometra) using the follwing steps: 1) denaturation at 95°C for 3 minutes, 2) followed by 35 cycles of: denaturation at 94°C for 30 seconds, annealing at 60°C for 40 seconds, extension at 72°C for 3 minutes. Samples were kept at 4°C until examination with a 2% agarose gel electrophoresis (30V for 2 hours). DNA was labelled with ethidium bromide and pictures were taken with a Geneflash camera (Syngene Bio Imaging).

2.3.2. *Runx1*^{EGFP} mouse line backcrossing

In order to transfer *Runx1*^{EGFP} animals on C57Bl6 genetic background, *Runx1*$^{EGFP/WT}$ males were mated with C57Bl6 females. Offspring were genotyped by PCR according to the procedure described in Section 2.3.1 and appropriate *Runx1*$^{EGFP/WT}$ males were subsequently mated with C57Bl6 females 8 times before the line was assumed to be of C57Bl6 background.

2.4. Embryonic tissue isolation and preparation

2.4.1. Isolation of embryonic tissue

Pregnant females were sacrificed according to schedule 1 method of cervical dissociation. The uterus was dissected and embryos were extracted into dissection solution. The embryos were then carefully separated from extra-embryonic tissues such as YS when appropriate. Developmental stage was scored according to Thelier criteria (http://genex.hgu.mrc.ac.uk/intro.html). E11.5 corresponds to stage 19, and main morphological characteristics being 41-47 somites pairs, round limb buds and not entirely completed eye pigmentation (Figure 3.1A). Embryonic organs of interest were dissected in dissection medium using sharpened tungsten needles under dissecting microscope (LEICA MZ8 microscope). When required, embryonic peripheral blood was placed on ice immediately after isolation.

For the lateral sub-dissection of the E11.5 AGM region, UGRs were gently cut along the ridges, leaving most para-aortic mesenchymal tissue attached to the Ao (Figure 5.1).

For the dorso-ventral subdissection of the E11.5 AGM region, remnants of the mesentery (ventral), somites and notochord (dorsal) were left on the AGM to easily distingusish AoV and AoD in the dissection dish. When appropriate, these extra aortic tissues were subsequently removed and AoV immediately placed into separate dishes (Figure 5.12).

2.4.2. Cellular preparation of embryonic tissues

To obtain single cell suspensions, embryonic organs were transferred to a 5ml polystyrene tube (BD Falcon) containing 450μl of dissection solution supplemented with 50μl of 10mg/ml collagenase dispase (Roche). Organs were digested in a 37^{o}C gently shaking water bath for 40 minutes. Immediately after, 1ml of dissection medium was added and then centrifuged at 1500rpm (GS-6R centrifuge, Beckman) for 5 minutes at RT. Cells were gently resuspended in flow cytometry buffer solution at RT and immediately placed on ice.

2.5. Adult tissue isolation and preparation

2.5.1. Isolation of adult tissue

Adult animals were all sacrificed according to schedule 1 method of cervical dissociation. Spleen and thymus were dissected free of connective tissue and fat and immediately placed in flow cytometry buffer solution. Peripheral blood was obtained by bleeding from lateral tail vein, and immediately collected into 1ml PBS/EDTA (200μg/ml). Bone marrow was obtained by flushing femurs in flow cytometry buffer solution with a 26-gauge syringe needle (BD Microlance).

2.5.2. Cellular preparation of adult tissues

Single cell suspensions from adult spleen and thymus were obtained by pressing grossly cut organs with a 1ml syringe plunger (BD Plastipak) into round-bottom 96 well plate (Bibby Sterilin) in the presence of flow cytometry buffer

solution. After that, tissues were filtered through a 40μm cell strainer (BD Falcon) to get rid of cell clumps. Bone marrow was mechanically dispersed in flow cytometry buffer solution using the 26-gauge syringe needle after flushing. Cells were immediately placed on ice.

2.5.3. Erythrocyte depletion in adult tissues

Adult blood samples (when appropriate, other haematopoietic cell suspensions) were centrifuged at 2000rpm (Biofuge pico from Heraeus Instruments) for 3 minutes at RT and pellets were resuspended, well mixed and incubated in dark at RT for 15 minutes in 1ml of PharM Lyse solution (BD Bioscience).

For recipient's peripheral blood reconstitution analysis, samples were then centrifuged at 2000rpm (Biofuge pico from Heraeus Instruments) for 4 minutes at RT before being resuspended in 1ml of flow cytometry buffer solution and being processed for flow cytometry analysis.

For other tissues and/or analysis, 1ml of flow cytometry buffer was added to samples, and then centrifuged at 1500rpm (Labofuge 400R from Heraeus Instruments) for 5 minutes at 4^{o}C, resuspended in 1ml of flow cytometry buffer solution and stored on ice.

2.6. Flow cytometry

2.6.1. Staining and flow cytometric analysis of adult and embryonic cellular suspensions

Cell suspensions were obtained as previously described in Sections 2.4.2 and 2.5.2. Cell numbers were determined using a haemocytometer. Staining procedures were performed in 5ml polystyrene tubes (BD Falcon). Samples were centrifuged at 1500rpm (Labofuge 400R from Heraeus Instruments) for 5 minutes at 4^{o}C and resuspended in 100μl of CD16/32 (Table 2.2). After 10 minutes incubation on ice, 100μl of antibody solution at the appropriate final concentration (Table 2.2) was

Table 2.2: Primary antibodies used for flow cytometry and confocal microscopy.

APC denotes Allophycocyanin; BIO, biotin; FITC, fluorescein isothiocyanate; PE, phycoerythrin; PerCP: peridinin chlorophyll protein; none, non-conjugated.

Antigen	Clone	Isotype	Working concentration	Conjugate	Supplier
B220	RA3-6B2	Rat IgG2α, κ	2.0 µg/ml	PE, BIO, FITC	Pharmingen
c-kit	2B8	Rat IgG2β, κ	2.0 µg/ml	PE, BIO	Pharmingen
CD3ε	145-2C11	Hamster IgG1	2.0 µg/ml	PE, FITC	eBioscience
CD4	GK1.5	Rat IgG2β, κ	2.0 µg/ml	PE, BIO	Pharmingen
CD8α	53-6.7	Rat IgG2α, κ	2.0 µg/ml	PE, FITC	eBioscience
CD16/32	93	Rat IgG2β, κ	2.0 µg/ml	none	eBioscience
CD19	1D3	Rat IgG2α, κ	2.0 µg/ml	PE	Pharmingen
CD34	RAM34	Rat IgG2α, κ	2.0 µg/ml	PE, FITC	eBioscience
CD41	MWReg30	Rat IgG1, κ	2.0 µg/ml	PE, FITC	eBioscience
CD43	eBioR2/60	Rat IgM	2.0 µg/ml	PE	eBioscience
CD45	30-F11	Rat IgG2β, κ	2.0 µg/ml	PE, FITC,APC,PerCP	Pharmingen
CD71	R17217	Rat IgG2α, κ	2.0 µg/ml	FITC	eBioscience
Gr-1	RB6-8C5	Rat IgG2β, κ	2.0 µg/ml	PE, BIO	eBioscience
Ly-5.1	A20	Mouse IgG2α, κ	2.0 µg/ml	PE, APC	Pharmingen
Ly-5.2	104	Mouse IgG2α, κ	2.0 µg/ml	FITC, APC	eBioscience
Mac-1	M1/70	Rat IgG2β, κ	2.0 µg/ml	PE, FITC	eBioscience
PECAM-1	MEC 13.3	Rat IgG2α, κ	2.0 µg/ml	PE	Pharmingen
Sca-1	D7	Rat IgG2α, κ	2.0 µg/ml	PE	Pharmingen
Ter-119	TER-119	Rat IgG2β, κ	2.0 µg/ml	PE	Pharmingen
VE-cadherin	11D4.1	Rat IgG2α, κ	8.0 µg/ml	none	Pharmingen

added to each tube. Cells were then incubated in the dark on ice for 20 to 45 minutes. After incubation, 1ml of ice-cold flow cytometry buffer solution was added to each sample and cells were centrifuged at 1500rpm (Labofuge 400R from Heraeus Instruments) for 5 minutes at 4^{o}C. When appropriate, supernatant was removed and cells were resuspended in 100µl of fluorochrome conjugated streptavidin solution (diluted at the appropriate concentration, Table 2.3). Cells were incubated for 15 minutes in the dark on ice. 1ml of ice-cold flow cytometry buffer solution was added and samples were centrifuged at 1500rpm (Labofuge 400R from Heraeus Instruments) for 5 minutes at 4^{o}C. Supernatant was gently removed and cells were resuspended in 100 to 200µl of 0.25-0.5µg/ml 7-aminoactinomycin D (7-AAD).

Flow cytometric analysis was performed using a dual laser FACScalibur (BD Bioscience). Fluorescence levels were detected by FL-1, FL-2 and Fl-4 channels (Table 2.4). Compensation adjustments were made based on appropriate isotype controls and single stains. Viable cells were selected according to their low 7-AAD intakes and detected in the FL-3 channel. Cell size and granularity were assessed by forward and side scatter profiles respectively. Data acquisition was performed using BD CellQuest^{TM} software (BD Bioscience). Data analysis and flow cytometric statistical analysis was performed using FlowJo software (Tree Star, Inc).

2.6.2. Fluorescence Activated Cell Sorting of embryonic tissues

Cell sorting was performed with the help of J.Vrana and S. Monard using a MoFlo (DakoCytomation) flow cytometer. Cells were processed and stained as described in Section 2.6.1. After processing, samples were resuspended at a concentration no higher than 1x10^{6} cells/ml in 0.25µg/ml 7-AAD. In order to avoid cell losses during collection, 5ml polystyrene tubes (BD Falcon) were wetted with ice-cold flow cytometry buffer solution and filled with buffer (2.5ml). Throughout the cell sorting procedure, cells were maintained at 4^{o}C and the conditions were maintained as aseptic as possible. When cell numbers allowed, a purity check of collected cell populations was performed.

Table 2.3: Secondary reagents and isotype controls antibodies used for flow cytometry. 7-AAD denotes 7-amino-actinomycin; APC denotes Allophycocyanin; BIO, biotin; FITC, fluorescein isothiocyanate; PE, phycoerythrin; n/a, non-applicable.

Reagent	Clone	Working concentration	Conjugate	Supplier
7-AAD	n/a	0.25-0.5 μg/ml	n/a	eBioscience
Hamster IgG1	A19-3	as appropriate	PE, FITC	Pharmingen
Mouse IgG2α, κ	G155-178	as appropriate	PE, FITC, APC	Pharmingen
Rat IgG1, κ	R3-34	as appropriate	PE, FITC	eBioscience
Rat IgG2α, κ	R35-95	as appropriate	PE, BIO, FITC, APC	Pharmingen
Rat IgG2β, κ	A95-1	as appropriate	PE, BIO, FITC, APC	Pharmingen
Rat IgM	G35-238	as appropriate	PE	Pharmingen
Streptavidin	n/a	0.2 μg/ml	PE, APC	Pharmingen
TOPRO-3	n/a	1 μM	n/a	Invitrogen

Table 2.4: FACScalibur channels and their corresponding fluorochromes.

Fluorochromes indicated here were used for flow cytometric analysis and appropriate controls were run with each fluorochrome to compensate for fluorescent leakage from one channel to another. FITC: fluorescein isothiocyanate, GFP: green fluorescent protein, eGFP: enhanced green fluorescent protein, PE: phycoerythrin, 7-AAD: 7-aminoactinomycin D, PerCP: peridinin chlorophyll protein; PE-Cy5: phycoerythrin-cyanine5, APC: allophycocyanin

channel	fluorochromes detected
FL-1	FITC, Alexa fluor-488, GFP, EGFP
FL-2	PE
Fl-3	7-AAD, PerCP, PE-Cy5.5
Fl-4	APC, TOPRO®-3

2.7. Tissue culture

Tissue culture procedures were carried out in class 2 laminar flow hoods (Envair and Nuaire) using aseptic technique by treating all surface areas and items in the hood with 70% industrial methylated spirits. Chemicals were prepared in sterile conditions.

Cells were cultured in 5% CO_2 at 37^{o}C in humidified incubators (Heraeus Instruments). Solutions were stored at +4^{o}C. Supplementary reagents were prepared by the tissue culture core-facility staff and stored at -20^{o}C (except β-mercaptoethanol which was stored at +4^{o}C). All solutions and reagents were allowed to warm-up to RT prior to use and all media were prepared freshly.

Unless otherwise stated Gibco supplied all media and supplementary reagents; PeproTech supplied all growth factors.

2.7.1. E11.5 AGM region reaggregation

The E11.5 AGM reaggregation technique was carried out as previously described (Sheridan et al., 2009; Taoudi et al., 2008); AGM suspensions were obtained from pooled embryos, centrifuged at 1500rpm for 5 minutes at 4^{o}C (GS-6R centrifuge, Beckman), and resuspended at a concentration of 1 embryo-equivalent (e.e) in 15-20μl of culture medium. 200μl pipette tip were then filled with 15-20μl of cell suspension and carefully sealed with Parafilm (VWR International). Tips were then placed in 25ml tubes (Corning) and centrifuged at 1500rpm (GS-6R centrifuge, Beckman) for 5 minutes at 4^{o}C. Cell pellets were then carefully expelled from the tip and placed onto Durapore 0.65μm membrane filters (Millipore) at the gas-liquid interface of 5ml of culture medium per well in 6 well plates. No more than 4 pellets were placed on each membrane filter.

Reaggregates were cultured in IMDM^{+} medium (Iscove's Modified Dulbecco's Medium (IMDM) containing 10-20% FCS; 4mM glutamine; 0.1mM β-mercaptoethanol; 50 units/ml P/S; 100ng/ml IL-3; 100ng/ml SCF; and 100ng/ml

Flt3l). In some cases IL-3, SCF, and Flt3l were not added to the medium (referred as $IMDM^-$ medium).

When appropriate, Durapore 0.65μm membrane filters were rinsed 3 times and incubated overnight at 37°C, 5% CO_2 in tissue culture grade with P/S. Membranes were rinsed again 3 times before being completely dried prior to use.

Following 4 to 5 days culture at 37°C, 5% CO_2, membrane filters were submersed into the culture medium, and reaggregates were collected by gentle pipetting. Reaggregates single cell suspensions were used for analysis (see section 2.4).

2.7.2. E11.5 AGM tissues explant cultures.

E11.5 AGM tissues were dissected as described in section 2.4.1. Explant cultures were slightly modified from protocols previously described (Kumaravelu et al., 2002; Medvinsky and Dzierzak, 1996). E11.5 AGM tissues were submersed in the appropriate culture medium and gently put onto Durapore 0.65μm membrane filters (sometimes washed, see Section 2.7.1). Membrane filters were placed at the liquid gas interface of 5 ml of appropriate medium and cultured for 4 days at 37°C, 5% CO_2. A maximum of 4 AGM explants were put onto each membrane. Explants were cultured in Myelo-cult medium (M5300, Stem Cell Technologies) supplemented with $1x10^{-6}$M hydrocortisone 21-hemisuccinate sodium salt and 50 units/ml P/S. On occasions, explant cultures were carried out in $IMDM^-$ medium.

After culture, explants were taken off the membranes and made into single cell suspensions (see sections 2.4 and 2.7.1).

2.8. *In vitro* haematopoietic assay: methylcellulose based differentiation

Prior to use, methylcellulose based MethoCult medium containing erythropoietin, IL-3, IL-6, and SCF (M3434, Stem Cell Technologies) was thawed at

RT and 50 units/ml P/S was added. After cell suspensions were added to MethoCult at 1/10 dilution, cultures were processed and plated according to manufacturer's instructions (www.stemcell.com). Haematopoietic colonies were counted and scored after 9-11 days of differentiation. The colonies were scored according to described standard criteria (Medvinsky et al., 2008; Taoudi, 2006)

2.9. *In vivo* haematopoietic stem cell assay: competitive long-term repopulation assay

2.9.1. *In vivo* transplantation

Cells for the long-term repopulation assay were obtained from either fresh or cultured embryonic organs from *Ly-5.2/5.2* mice. Appropriate doses of cells were resuspended in ice cold 1% FCS/PBS and co-injected along with $2x10^4$ adult carrier bone marrow cells from *Ly-5.1/5.2* animals. Prior to transplantation, *Ly-5.1/5.1* animals were irradiated. A total dose of 9.5 Gy was split into two doses separated by at least 3 hours and delivered by sealed Cs source at a rate of 21.6 rad/min. No more than 300μl of cell suspension were injected into each recipient mouse using a 30-gauge syringe needle (BD Plastipak). All injections were performed in the lateral tail vein according to the procedures described by project licence 603715 and the regulations of the Animals Scientific Procedures Act, UK, 1986.

Experiments described in Chapter 3 were performed with F1 (CBA X C57Bl6) animals. All other experiments were performed with pure C57Bl6 animals.

2.9.2. Assessment of haematopoietic reconstitution

Recipients' peripheral blood chimerism (PBC) was first assessed 6 weeks post-transplantation for short-term repopulation and at least 12 weeks post-transplantation for long-term repopulation. Blood samples were processed as described in Sections 2.5.3 and 2.6.1. Only animals with donor chimerism higher than 5% were considered reconstituted.

Multilineage analysis was performed on animals reconstituted for at least 16 weeks post-transplantation. Bone marrow, spleen, and thymus were isolated, processed and depleted of erythrocytes (see Sections 2.5.2 and 2.5.3) and myeloid and lymphoid donor contribution was assessed by flow cytometry (see Section 2.6.1).

2.10. Confocal microscopy

2.10.1. Staining for cell surface markers

2.10.1.1. Embedding and Sectioning

Fresh or cultured organs were snap-frozen in O.C.T compound (BDH Gurr) on dry ice. 10μm thick frozen sections were produced using a LEICA CM1900 cryostat (Leica) and directly put onto polysine-coated slides (VWR International). Sections were air-dried and stored at -20^{o}C. Sections were warmed up at RT and fixed with -20^{o}C cold 100% acetone for 2.5 minutes. Sections were air-dried before further processing.

2.10.1.2. Immunofluorescent staining

Sections were first encircled with a PAP pen and rehydrated with PBS (containing MgCl and CaCl) for 2 minutes. Dissection solution (no P/S) was used to block non-specific antibody binding for 15 minutes at RT. Sections were then washed once with PBS before adding fluorochrome-conjugated antibodies appropriately diluted in PBS (Table 2.2) and incubated in dark at RT for at least 30 minutes. After removal of the staining solution, sections were washed 3 times for 5 minutes with PBS. Cell nuclei were stained with 0.2% 4-6-Diamidino-2-phenylindole (DAPI)(Molecular Probes) in the dark at RT for 10 minutes, followed by quick 3 times washing with PBS and a very quick rinse with distilled H_2O before air-drying. Finally sections were mounted using a small drop of VECTORSHIELD hard-set medium (Vector Laboratories) and left to harden overnight at +4^{o}C

according to the manufacturer's instructions. Stained sections were studied and pictures were taken using an inverted confocal microscope (Leica DM IRE2). Images were then processed and prepared using Adobe Photoshop.

2.11. Cytological analysis

2.11.1. Cytospin preparation

Single cytospin chambers were loaded with a polysine-coated slide, and a filter card (Thermo), followed by filling with 100µl of the cell suspension. At RT, samples were centrifuged at 1000rpm for 5 minutes (Cytospin 3, Shandon), air-dried and fixed 100% methanol for 2.5 minutes. Methanol was removed and slides were air-dried.

2.11.2. May-Grünwald-Giemsa staining

May-Grünwald and Giemsa were freshly prepared in PBS as a 50% solution and a 10% solution respectively and filtered through number 1 Whatman filter paper (Whatman International Ltd).

Slides fixed in methanol were stained first with May-Grünwald solution for 15 minutes, followed by replacement of primary stain with Giemsa stain for 12 minutes, all in the dark at RT. Finally, slides were rinsed 3 times briefly, washed for 5 minutes with distilled H_2O, and were air-dried and stored in the dark at RT until analysis. Pictures were taken using an upright Vanox AHBT3 microscope (Olympus) and Openlab software (Improvision).

2.12. Statistical analysis

Where treatments comprised 3 or more replicates, differences in mean cell numbers, percentages, and CFU-Cs counts between treatments were calculated.

Parametric tests were used where possible to assess statistical significance. Groups were compared using either 2-sample t-tests, or paired t-tests for paired data. In each case, the assumption of similar variances between groups was also tested using an F-test, and the data inspected for normality. If these assumptions were not met, or the number of replicates was low (<4), non-parametric tests were used instead. Unmatched groups were compared using a Mann-Whitney test, while in the case of paired data; the Wilcoxon Signed Rank test was used.

Significance was calculated at the 5% significance level. All statistical analyses were performed using Minitab v15 (www.minitab.com).

In the case of the efficacy of haematopoietic reconstitution in the long-term repopulation assay, statistical significance was calculated using 2 x 2 contingency tables and the Fisher exact test (www.exactoid.com).

3. The reaggregate culture system: characterisation and insights into cytokine-mediated LTR-HSC expansion

3.1. Introduction

Studies have demonstrated that culturing the E10.5-12.5 AGM region and the E12.5 YS as explants at the liquid gas interphase can facilitate LTR-HSC expansion (Kumaravelu et al., 2002; Medvinsky and Dzierzak, 1996). An advantage of the explant culture system is that it maintains the structural integrity and preserves cell interactions that *in vivo* may be essential for LTR-HSC development. It also enables the investigation of the autonomous potential of the organ, independent of surrounding tissues. However, the need to culture an intact organ also limits the accessibility to specific cell populations, and restricts the manipulation of a potentially powerful LTR-HSC niche.

The reaggregate system (Taoudi et al., 2008), however, enables the identification of specific cell populations that play key roles in LTR-HSC development from the AGM region; including key niche components. The reaggregate culture conditions described in Section 2.7.1 were schematically represented in Figure 3.1A and will be referred as standard conditions. After culture, single cell suspensions are obtained from reaggregates and used for functional assays and flow cytometric analysis (Figure 3.1B). The methylcellulose-based assay is used to determine the number of haematopoietic progenitors (CFU-C) and the competitive repopulation assay to determine the presence of LTR-HSCs.

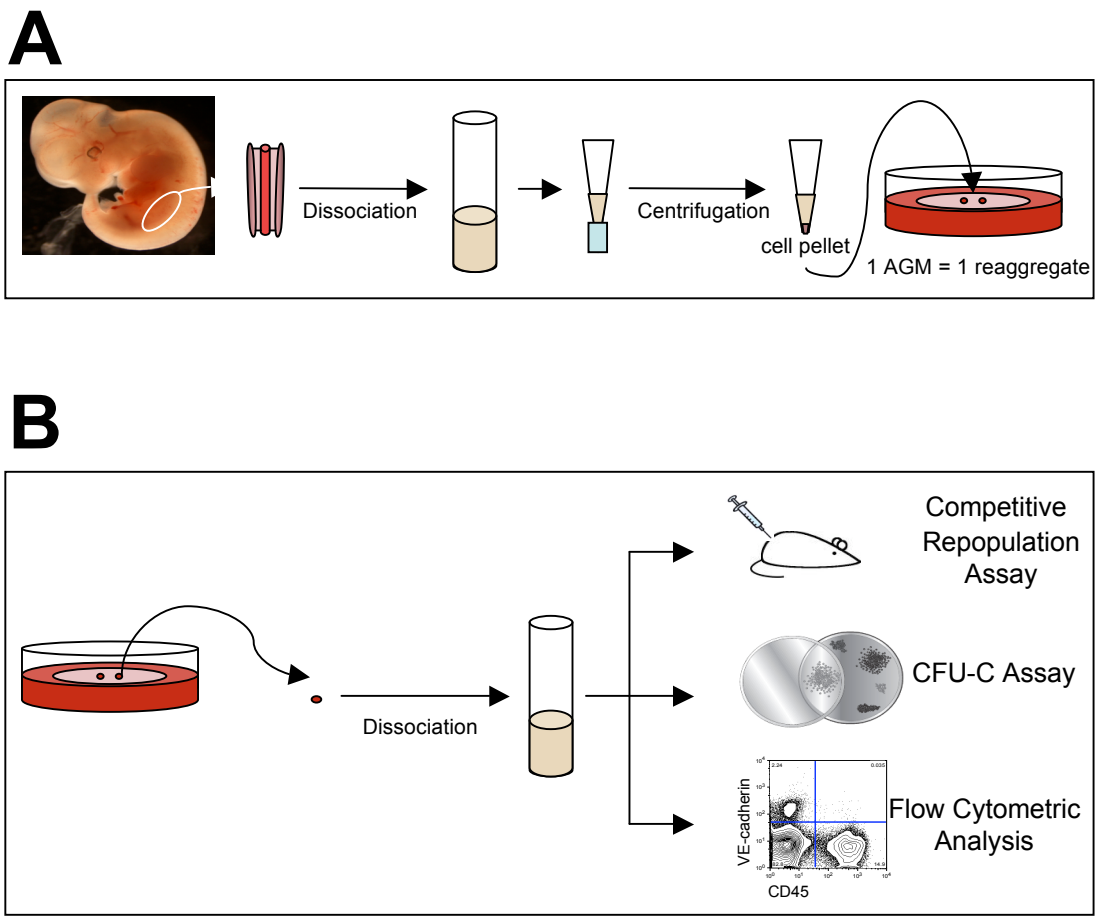

Figure 3.1: Standardised experimental procedures to generate and analyse reaggregates.

A: Standard procedure for reaggregate set-up. E11.5 AGM regions are dissected and dissociated by collagenase dispase treatment. One embryo equivalent of the cell suspension obtained is centrifuged in a sealed tip. The pellet is placed on a membrane filter at the liquid-gas interface and cultured at 37°C, 5% CO_2 for 4 days in $IMDM^{+}$.

B: Standard analysis of reaggregates. After culture, reaggregates are collected and dissociated by collagenase dispase treatment with mechanical disruption. The cell suspension obtained is used to perform competitive repopulation assays, colony forming unit culture (CFU-C) assays, and flow cytometric analysis.

3.2. Characterisation of the reaggregate culture system using standard conditions

3.2.1. Basic characterisation of the E11.5 AGM region

Standard cultures were set up to validate the reproducibility of the system (Taoudi, 2006). Flow cytometric analysis in fresh and cultured E11.5 AGM tissue was performed (Figure 3.2A). Pan-leucocyte marker CD45 was chosen to mark haematopoietic cells, and vascular-endothelial cadherin (VE-cadherin) was chosen to mark endothelial cells. The fresh E11.5 AGM contained 222100±64530 total cells of which 73060±3700 were viable (Table 3.1). The majority of the tissue (68120±610 cells) was composed of stromal (non haematopoietic, non endothelial) $CD45^{-}$VE-$cadherin^{-}$ cells. The E11.5 AGM region contained 63±22 $CD45^{+}$VE-$cadherin^{+}$ cells, a population highly enriched for LTR-HSCs (North et al., 2002; Taoudi et al., 2005). Finally, 2600±750 cells were $CD45^{+}$VE-$cadherin^{-}$ (haematopoietic, CD45 single-positive/$CD45^{SP}$) and 2420±820 cells were $CD45^{-}$VE-$cadherin^{+}$ (endothelial)(Table 3.1 and Figure 3.2A).

3.2.2. Basic characterisation of haematopoietic populations in reaggregates

After 4 days in culture, reaggregates typically adopt a circular morphology (roughly 1mm diameter) with cellular protrusions at the periphery (Figure 3.2B). Also, some red blood cells can sometimes be observed (Figure 3.2B). Flow cytometric analysis showed that a single reaggregate contained 188000±34120 cells of which 124380±18620 cells were viable (Table 3.1). Both the stromal and $CD45^{-}$ VE-$cadherin^{+}$ (endothelial) compartments were maintained as a single reaggregate contained 110650±14650 cells and 2400±1060 cells respectively (Table 3.1 and Figure 3.2A). The DP population was also maintained as there were 100±75 cells but with high variation among cultures. Finally, the $CD45^{SP}$ population underwent extensive expansion as single reaggregates contained 22070±6080 $CD45^{SP}$ cells,

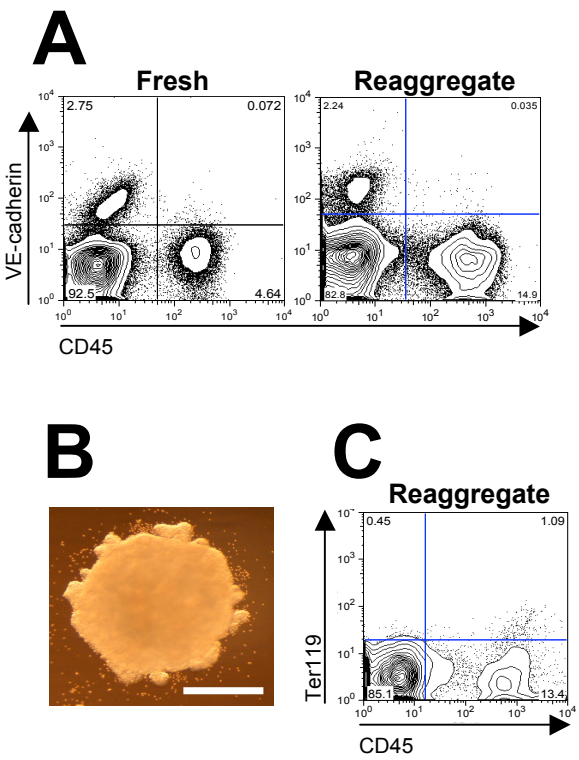

Figure 3.2: Anatomy of reaggregates and haematopoietic expansion during culture in IMDM^{+}.

A: Flow cytometric analysis of both endothelial (VE-cadherin^{+}) and haematopoietic (CD45^{+}) cell populations in fresh E11.5 AGM compared to reaggregates. Plots are representative of 7 and 8 experiments respectively.

B: Representative image of a reaggregate after 4 days culture. Typically, the gross morphology is circular with a diameter of approximately 1mm and protrusions are observed at the pheriphery. (scale bar: approximately 0.5 mm)

C: Flow cytometric analysis of erythroid (Ter119) cell population in reaggregates. Quadrants are based on appropriate isotype control (Appendix 3.1) and values indicate the percentage of cells.

Table 3.1: Cell composition of fresh E11.5 AGM region compared to reaggregates cultured in IMDM$^+$.

Results obtained by flow cytometry (viability determined by 7-AAD exclusion). Data is representative of 7 independent experiments in fresh tissue and 8 independent experiments in reaggregates.
absolute numbers ± standard deviation; DP: CD45$^+$VE-cadherin$^+$; DN: CD45$^-$VE-cadherin$^-$

	fresh	reaggregate	fold increase
total cells	222100 ± 64530	188000 ± 34120	0.8
total live cells	73060 ± 3700	124380 ± 18620	1.7
total CD45$^+$ cells	2600 ± 750	22070 ± 6080	8.5
total VE-cadherin$^+$ cells	2420 ± 820	2400 ± 1060	1.0
total DP cells	63 ± 22	100 ± 75	1.6
total DN cells	68120 ± 610	110650 ± 14650	1.6

which constitutes an 8.5 fold expansion compared to the fresh tissue (Table 3.1 and Figure 3.2A).

As the haematopoietic compartment underwent considerable expansion, the nature of the $CD45^+$ cells was further investigated. Although red blood cells could be observed under the microscope (Figure 3.2B), the absence of mature erythrocytes was indicated by the absence of $CD45^-Ter119^+$ cells (Figure 3.2C; Figure 3.3A). However, the presence of few $CD45^+CD71^+Ter119^+$ suggested that erythropoiesis was initiated (Figure 3.3A). The CD71 expression in 46.8±3.9% of $CD45^+$ cells also indicated that these haematopoietic cells were still cycling at the end of the culture period (Figure 3.3A).

The expression of LTR-HSC markers such as Sca1, c-kit and CD34 was investigated (Figure 3.3A). 43±0.2% of $CD45^+$ cells co-expressed Sca1 and c-kit, a classic LTR-HSC immunophenotype (Figure 3.3A). Interestingly, only a very small fraction of $CD45^+$ cells expressed CD34 (less than 1%), an embryonic LTR-HSC marker (Figure 3.3A)(Ema and Nakauchi, 2000; Sanchez et al., 1996; Yoder et al., 1997a).

Cytospin preparations were performed to investigate cell morphology and confirm the presence of specific haematopoietic cell types within reaggregates. Massive cell clusters were observed in high numbers but without a haematopoietic appearance (Figure 3.3B). Cells resembling macrophages and erythroid cells could be observed, confirming the flow cytometric observations (Figure 3.2C, Figure 3.3A,B). In addition, given the high frequency of cells with erythroid characteristics (blue cytoplasm and purple nucleus), the majority of these cells could also be blasts cells.

3.2.3. The expansion of haematopoietic progenitors during reaggregate culture

As $CD45^{SP}$ haematopoietic cells underwent massive expansion during culture, the expansion of haematopoietic progenitors was investigated. To this end, CFU-Cs assays were performed in the fresh E11.5 AGM region and following 4 days

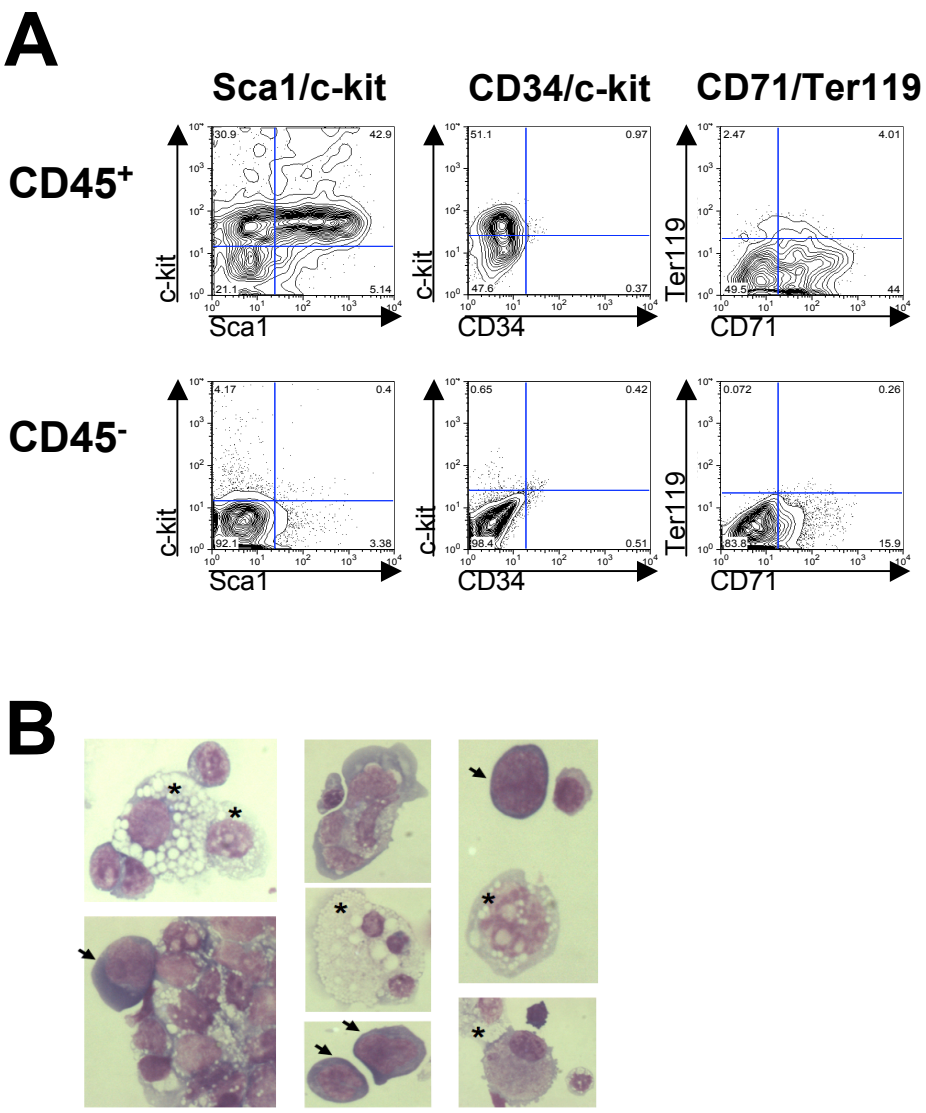

Figure 3.3: Characterisation of haematopoietic and non-haematopoietic cell populations in E11.5 AGM reaggregates cultured in IMDM^{+}.

A: Flow cytometric analysis of haematopoietic (CD45^{+}) and non-haematopoietic (CD45^{-}) cell populations. Plots are representative of two independent experiments. Quadrants are based on appropriate isotype control (Appendix 3.1); and values indicate the percentage of cells.

B: Cytospin preparations from whole reaggregates. Asterix indicate cells with macrophage like morphology (white globules inside cytoplasm and purple nuclei). Arrows indicate erythrocyte like cells or blast cells (dark blue cytoplasms and purple nuclei). Other unidentified cell types are also present in high numbers and example of cell cluster in low left panel.

reaggregate culture. Haematopoietic colonies were counted after 9 days in methylcellulose culture. Colony type was assessed according to gross morphology (initially confirmed with cytopsin until comfortable with gross scoring, (Medvinsky et al., 2008; Taoudi, 2006).

The fresh E11.5 AGM region contained 144±42 CFU-Cs made of 42±19 CFU-mast, 26±24 BFU-E, 8±7.5 CFU-GM, 60±22 CFU-mac, and 9±6 CFU-GEMM (Figure 3.4A). After culture in standard conditions, reaggregates contained 4425±1025 CFU-Cs made of 1095±700 CFU-mast, 735±380 BFU-E, 410±230 CFU-GM, 1825±970 CFU-mac, and 360±90 CFU-GEMM (Figure 3.4B). This represents a 31-fold expansion.

3.2.4. The expansion of LTR-HSCs during reaggregate culture

It was previously demonstrated that the fresh E11.5 AGM contains around 1 LTR-HSCs (Gekas et al., 2005; Kumaravelu et al., 2002). Using the explant culture on α-MEM based medium, it is possible to generate 12 LTR-HSCs after 72 hours (Medvinsky and Dzierzak, 1996). To date, a maximum of 34 LTR-HSCs can be obtained per explant AGM region by supplementing the culture medium with IL-3 (Robin et al., 2006).

To investigate the expansion of the LTR-HSC compartment during reeaggregate culture, the *in vivo* long-term repopulation assay was used (Figure 3.5A). Limiting dilution analysis was performed to functionally quantify the absolute number of LTR-HSC by the end of the culture. To this end, 0.1 dose of reaggregate (rd), 0.01rd and 0.005rd were injected into individual adult irradiated recipients and peripheral blood chimerism (PBC) was determined at least 12 weeks after transplantation. I found that 8 out of 8 mice transplanted with 0.1rd were successfully repopulated (78.6% mean PBC); 13 out of 14 mice transplanted with 0.01rd were repopulated (23.7% mean PBC) and 9 out of 10 mice transplanted with 0.005rd were repopulated (12.3% mean PBC)(Figure 3.5B). As 0.005rd was sufficient to repopulate most of the transplanted mice, this suggests the presence of at least 200

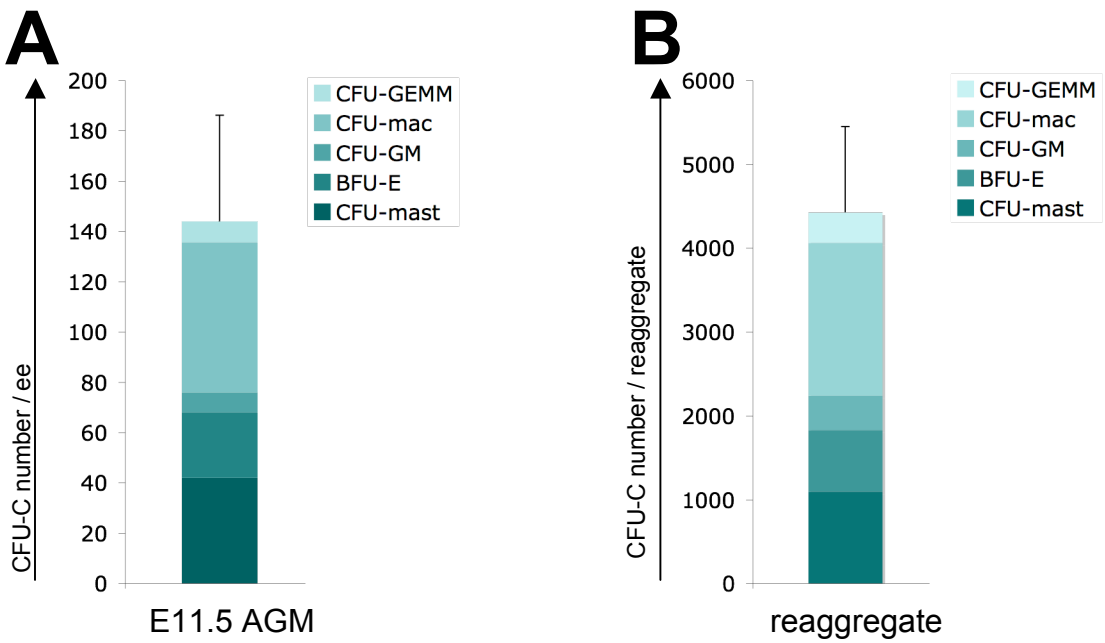

Figure 3.4: Haematopoietic progenitors expansion during reaggregate culture in IMDM^{+}.

A: Number of CFU-Cs per fresh E11.5 AGM region. Bars indicate standard deviation of three independent experiments.

B: Number of CFU-Cs per reaggregate cultured in standard conditions. Bars indicate standard deviation of ten independent experiments (from controls run throughout Chapter 3 experiments).

BFU-E: burst forming unit-erythroid; CFU: colony forming unit; Mast: mast; Mac: macrophage; GM: granulocyte/macrophage; GEMM: granulocyte/erythroid/macrophage/ megakaryocyte ; ee: embryo equivalent

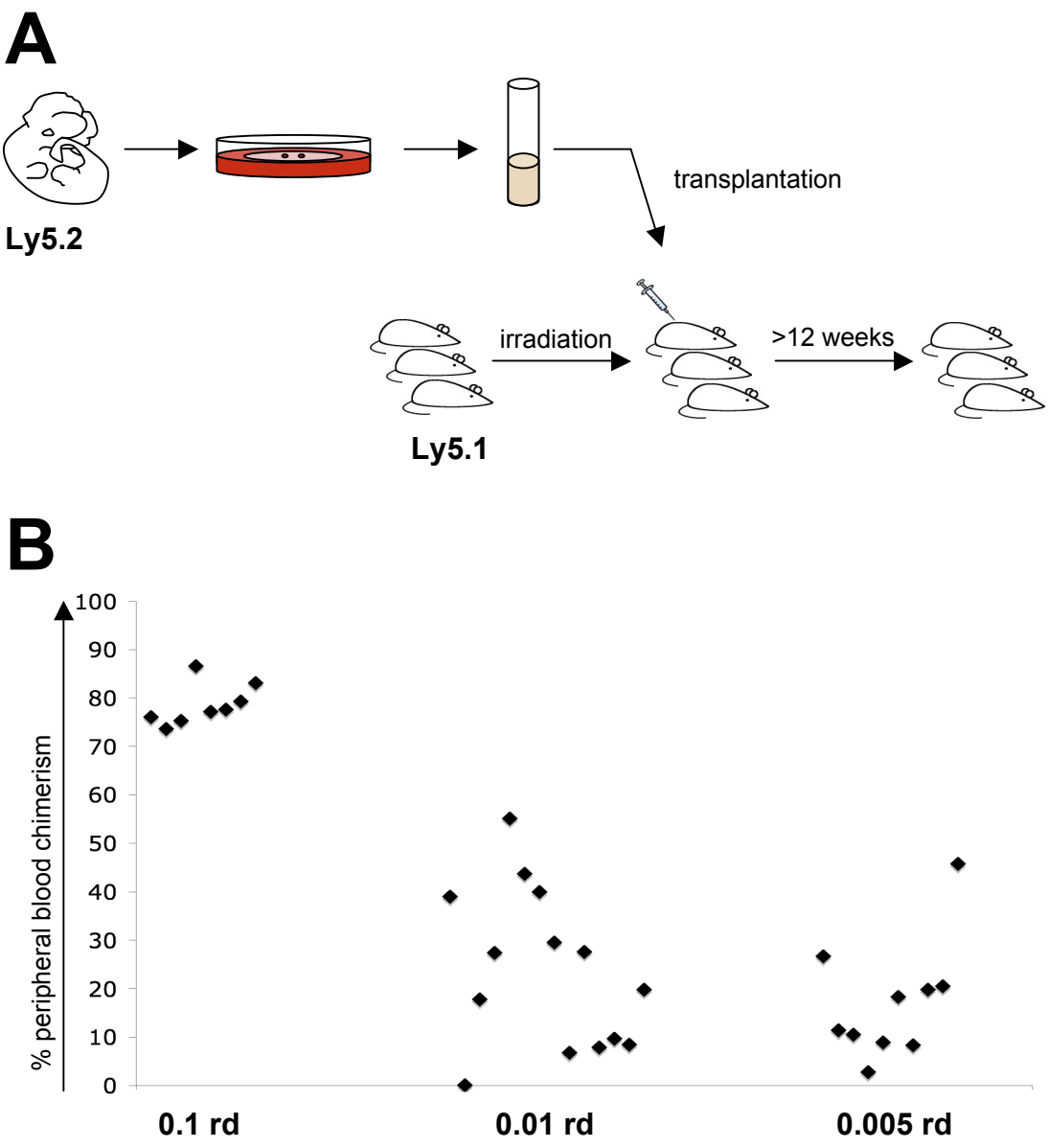

Figure 3.5: Assessment of LTR-HSC numbers in E11.5 AGM reaggregates cultured in IMDM^{+}.

A: *In-vivo* competitive long term repopulation assay. Donor cells from Ly5.2 embryos are cultured and transplanted into irradiated Ly5.1 adult recipients. LTR-HSCs are detected by peripheral blood chimerism assessed by flow cytometry using anti Ly5.1 and Ly5.2 antibodies, at least 12 weeks post-transplantation .

B: LTR-HSC limiting dilution analysis in reaggregates. Each point represents a single recipient mouse. Recipients were considered reconstituted when their peripheral blood chimerism exceeded 5% at least 12 weeks after transplantation. Cumulative result from two independent experiments. rd: reaggregate dose

LTR-HSCs in a single reaggregate, even if limiting dilution was not reached. This is consistent with data previously published, revealing that LTR-HSC numbers ranged from 98 to 150 in single reaggregates (Taoudi et al., 2008).

3.2.5. Normal LTR-HSC function: multilineage reconstitution and secondary transplantation

Contribution of donor cells into haematopoietic tissues (peripheral blood, spleen, bone marrow, and thymus) of recipients reconstituted with 0.01rd was checked by flow cytometry. All tissues contained CD45.2 donor cells in high proportions (81.7±5.1% in peripheral blood, 67.6±9.2% in spleen, 77.1±4.6% in bone marrow, and 84.6±1.2% in thymus)(Figure 3.6A). Blood, spleen and bone marrow contained both myeloid cells, marked by Mac1 and Gr1, and lymphoid cells marked by B220, CD3 and CD43 (Figure 3.6B). The majority of donor cells in the thymus were $CD4^{+}CD8^{+}$ (65.1±19.1%), an immunophenotype that corresponds to the immature T cell population (Figure 3.6B).

The AGM-derived LTR-HSCs were subject to secondary transplantations. Two reconstituted primary recipients were sacrificed and 1/10 of their whole bone marrow (paired femurs and tibias) was transplanted into each secondary recipients. Secondary recipient PBC was analysed at least 12 weeks post-transplant and multilineage analysis was performed (Figure 3.7). The primary recipients chosen for the experiment had PBC of 82.5% and 30.2% on the day of the secondary transplantation (Figure3.7A). At least 16 weeks post-transplantation, individual secondary recipients displayed 74% and 64.8% and 16.7% PBC (Figure 3.7A). The blood of secondary recipients demonstrated successful serial reconstitution of the lymphoid (CD3/B220) and myeloid (Mac1/Gr1) compartments (Figure 3.7B).

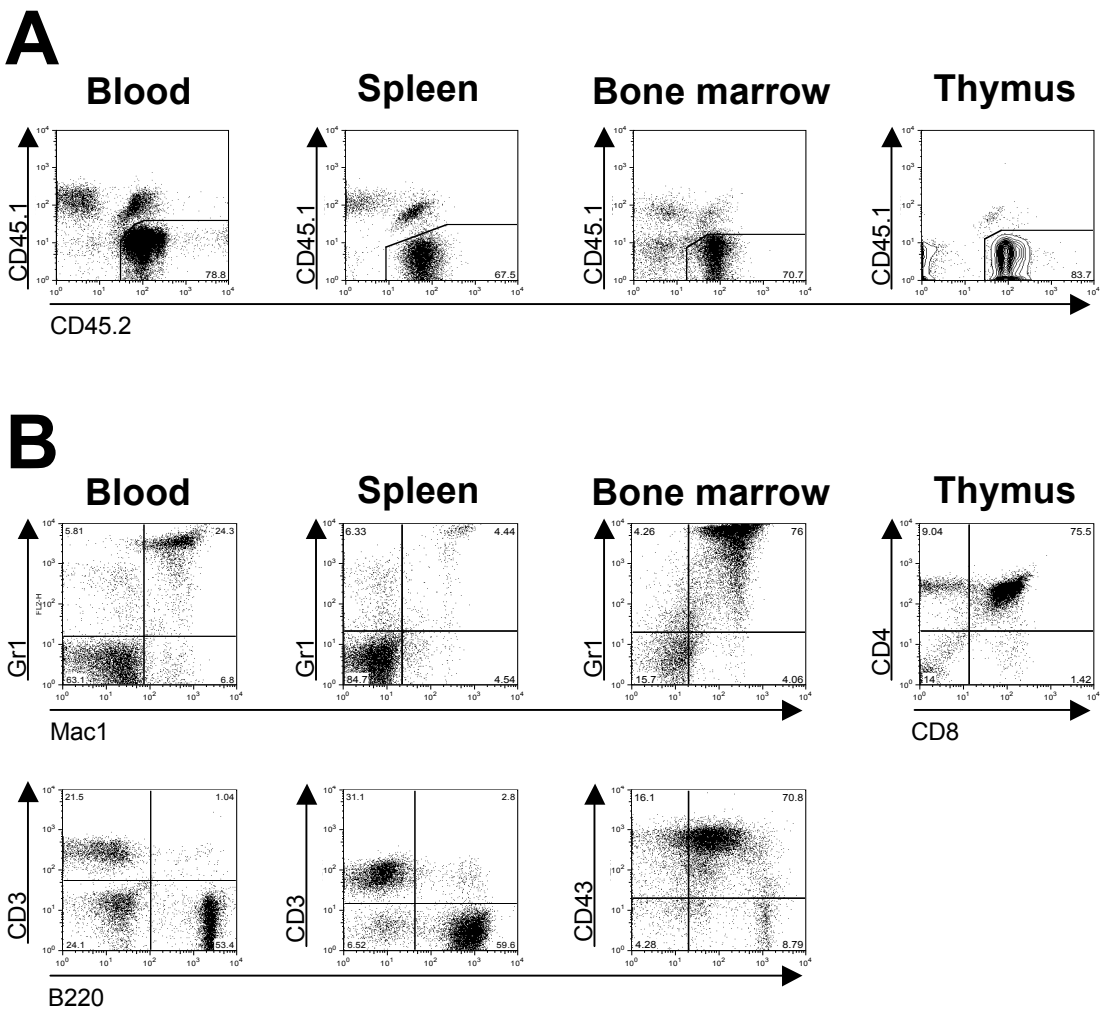

Figure 3.6: Multilineage haematopoietic reconstitution by E11.5 AGM reaggregates cultured in IMDM^{+}

A: Long term donor-derived reconstitution in major haematopoietic organs (peripheral blood, spleen, bone marrow, and thymus).

B: Long-term multilineage (myelo-lymphoid) analysis of donor derived cells in all major haematopoietic organs (peripheral blood, spleen, bone marrow, and thymus). Events gated on donor derived cells.

Representative example of analysis performed on six mice reconstituted by reaggregates. Quadrants are based on appropriate isotype control (Appendix 3.2) and values indicate percentages of cells. Cell viability was determined by 7-AAD uptake.

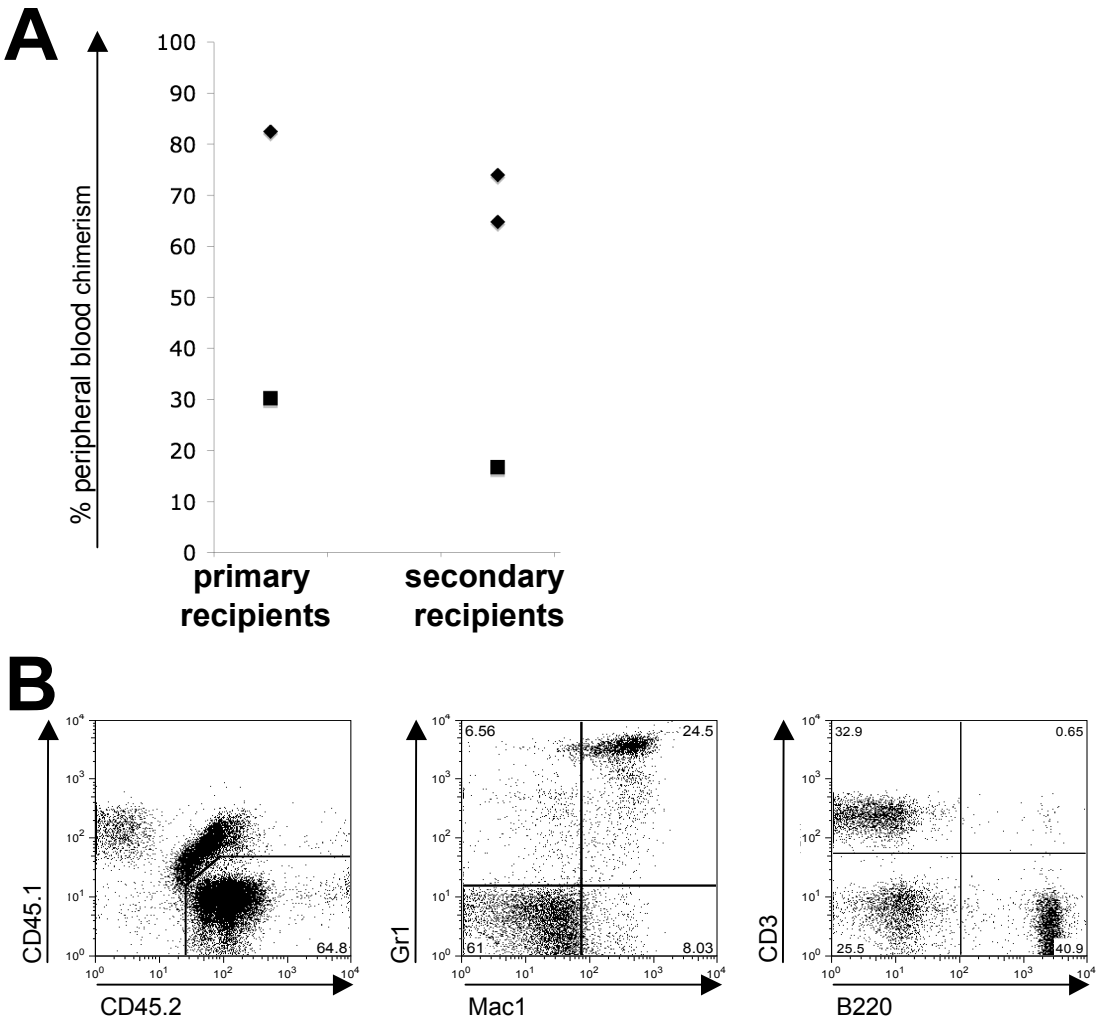

Figure 3.7: Secondary transplantations and multilineage haematopoietic reconstitution of secondary recipients.

A: Secondary transplantation of bone marrow cells from reconstituted primary recipients. 1/10 of whole bone marrow (paired femurs and tibias) from each of two primary recipients (reconstituted by reaggregates cultured in IMDM^{+}) was transplanted individually into irradiated secondary recipients. Peripheral blood chimerism in secondary recipients was analyzed at least 12 weeks after transplantation; matching symbols represent secondary recipients and their corresponding primary recipients.

B: Long term multilineage (myelo-lymphoid) analysis of donor derived cells in the peripheral blood of secondary recipients. Representative example of analysis of three secondary recipients. Quadrants are based on appropriate isotype control (Appendix 3.2); values indicate percentages of cells. Events gated on donor derived cells.

3.2.6. LTR-HSC phenotype in reaggregates

To determine the immunophenotype of LTR-HSCs generated in reaggregates, FACS was performed and cell populations of interest were transplanted into recipient mice.

Previous experiments demonstrated that all LTR-HSCs are contained in the $CD45^+$ compartment (Taoudi et al., 2008). The endothelial marker CD31 (also known as PECAM-1), the early haematopoietic marker CD41, the haematopoietic progenitor marker CD48, and the LTR-HSC markers Sca1 and c-kit were used to further characterise the LTR-HSCs population.

Analysis of CD31 expression showed that 1.66% of viable cells were $CD45^+CD31^{high}$, 18.5% were $CD45^+CD31^{medium}$, and 3.54% were $CD45^+PECAM^{low}$ (Figure 3.8A). When, 0.05rd of these three populations were transplanted into recipient mice, only $CD45^+CD31^{medium}$ cells successfully reconstituted mice (3 out of 5, mean PBC: 23%)(Figure 3.8A'), indicating that LTR-HSCs are contained in the $CD45^+CD31^{medium}$ cell population. Previous data looking at the co-expression of the endothelial markers VE-cadherin and CD31 revealed that the endothelial cells reside in the $CD31^{high}$ population (Taoudi et al., 2008; Taoudi and Medvinsky, 2007), demonstrating that reaggregate LTR-HSCs differ from the endothelium.

The $CD45^+$ cell population was then further divided using a LTR-HSC marker c-kit and an early haematopoietic marker CD41: 31.2% of the $CD45^+$ population was $c\text{-}kit^+CD41^-$, 1.65% was $c\text{-}kit^+CD41^+$, 0.35% was $c\text{-}kit^-CD41^+$, and 60% was $c\text{-}kit^-CD41^-$ (Figure 3.8B). When 0.05rd of each of these four populations were transplanted into recipient mice, the majority of LTR-HSC activity was found within $c\text{-}kit^+CD41^+$ and $c\text{-}kit^+CD41^-$ populations: 1 out of 5 mice was reconstituted at low level with $c\text{-}kit^+CD41^+$ cells (9.77% PBC), and 5 out of 8 mice were reconstituted with $c\text{-}kit^+CD41^-$ cells (mean PBC: 35.2%)(Figure 3.8B'), indicating that most HSCs in reaggregates are $c\text{-}kit^+CD41^-$. FACS purity analysis of $c\text{-}kit^+CD41^+$ population (84.6% purity with little contamination from $c\text{-}kit^-CD41^-$ cells) indicated that cell contamination was unlikely, thus a few LTR-HSCs might express CD41.

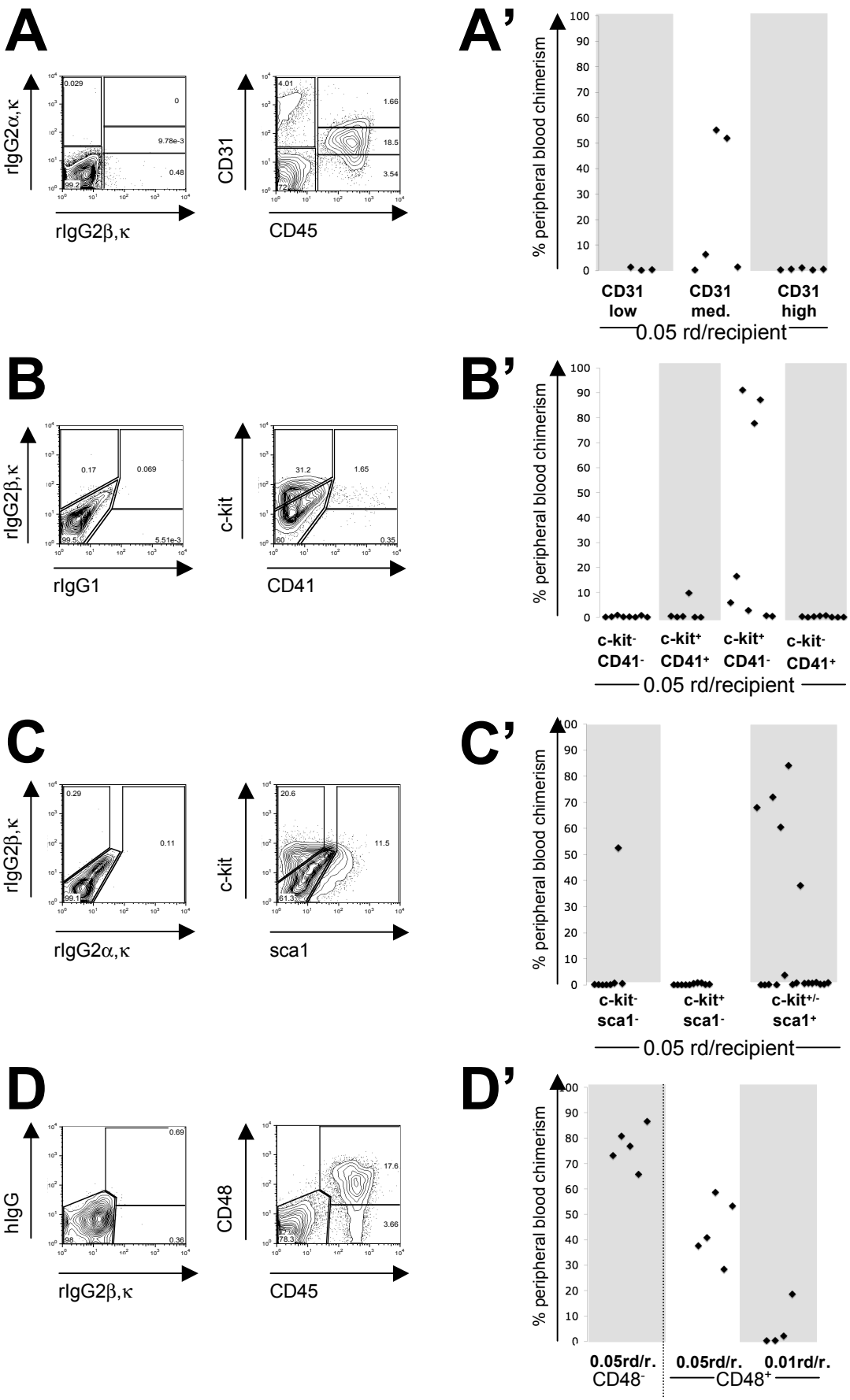
A
rIgG2α,κ
rIgG2β,κ
0.029
0
9.78e-3
0.48
99.2
CD31
CD45
4.01
1.66
18.5
3.54
72
A'
% peripheral blood chimerism
CD31 low
CD31 med.
CD31 high
0.05 rd/recipient
B
rIgG2β,κ
rIgG1
0.17
0.069
99.5
5.51e-3
c-kit
CD41
31.2
1.65
60
0.35
B'
% peripheral blood chimerism
c-kit- CD41-
c-kit+ CD41+
c-kit+ CD41-
c-kit- CD41+
0.05 rd/recipient
C
rIgG2β,κ
rIgG2α,κ
0.29
0.11
99.1
c-kit
sca1
20.6
11.5
61.3
C'
% peripheral blood chimerism
c-kit- sca1-
c-kit+ sca1-
c-kit+/- sca1+
0.05 rd/recipient
D
hIgG
rIgG2β,κ
0.69
98
0.36
CD48
CD45
17.6
3.66
78.3
D'
% peripheral blood chimerism
0.05rd/r. CD48-
0.05rd/r. CD48+
0.01rd/r. CD48+

Figure 3.8: LTR-HSC phenotyping in E11.5 AGM reaggregates cultured in IMDM$^+$.
A, A': LTR-HSC phenotyping using CD31 marker. A: isotype control (left) and representative staining pattern of reaggregates (right). A': peripheral blood chimerism of recipients transplanted with CD45$^+$ cells sorted on the basis of different CD31 expression levels. Result from 1 experiment.
B, B': LTR-HSC phenotyping using c-kit and CD41 markers. B: isotype control (left) and representative staining pattern of reaggregates CD45$^+$ population (right). B': peripherall blood chimerism of recipients transplanted with CD45$^+$ cells sorted on the basis of different c-kit and CD41 expression. Cumulative result of 2 experiments.
C, C': LTR-HSC phenotyping using c-kit and sca1 markers. C: isotype control (left) and representative staining pattern of reaggregates CD45$^+$ population (right). C': peripheral blood chimerism of recipients transplanted with CD45$^+$ cells sorted on the basis of different c-kit and sca1 expression. Cumulative result of 2 experiments.
D, D': LTR-HSC phenotyping using CD48 marker. D: isotype control (left) and representative staining pattern of reaggregates (right). D': peripheral blood chimerism of recipients transplanted with CD45$^+$ cells sorted on the basis of different CD48 expression levels. Result from 1 experiment.
All gates were based on displayed isotype control and values indicate percentages of cells. Recipients were considered reconstituted when their peripheral blood chimerism exceeded 5% at least 12 weeks post-transplantation. Dots represent individual recipient mice. rd: reaggregate dose; r: recipient; med.: medium

The $CD45^+$ cell population was also divided using classical LTR-HSC markers Sca1 and c-kit: 20.6% of the $CD45^+$ population were c-kit^+Sca1^-, 11.5% were $Sca1^+$ and 61.3% were either c-kit^-Sca1^- or autofluorescent (Figure 3.8C). When 0.05rd were transplanted per recipient, $Sca1^+$ cells achieved reconstitution in 5 out of 19 mice, whilst $Sca1^-$ cells only in 1 out of 8 mice, indicating that the vast majority of LTR-HSCs in reaggregates express Sca1 (Figure 3.8C'). The reconstitution of a mouse by c-kit^-Sca1^- cells could hardly be explained by FACS contamination (95.4% pure); however, the overlap of positive cells with autofluorescent ones (included in the c-kit^-Sca1^- gate in this case) cannot be excluded. Nevertheless, on the basis of previous experiments (Figure 3.8B') and additional data from S. Taoudi, the majority if not all HSCs are c-kit^+Sca1^+.

Finally, LTR-HSCs were tested for CD48 expression, a marker of both adult and fetal liver haematopoietic progenitors (Kiel et al., 2005; Kim et al., 2006). The $CD45^+$ population was subdivided into $CD48^+$ (17.6%) and $CD48^-$ (3.66%) fractions (Figure 3.8D). All recipient mice transplanted with 0.05rd of $CD48^-$ cells were reconstituted at high level (mean PBC: 76.6%)(Figure 3.8D'). When transplanted with 0.05rd and 0.01rd of $CD48^+$ cells, 5 out of 5 mice (mean PBC: 43.8%) and 1 out of 4 mice (18% PBC) were reconstituted respectively (Figure 3.8D'), indicating that reaggregate LTR-HSCs are heterogenous for CD48 expression.

Taken together, these experiments demonstrate that the majority of LTR-HSCs produced in reaggregates are $CD45^+CD31^{medium}$c-kit^+Sca1^+. Interestingly; LTR-HSCs were heterogenous for the cell surface markers CD41 and CD48.

3.2.7. Conclusions

The reaggregate culture system described above is a robust and reproducible model system that allows the dissociation of the E11.5 AGM prior to culture whilst maintaining its ability to produce LTR-HSCs. During culture, haematopoiesis is largely stimulated as 8.5-fold expansion of haematopoietic ($CD45^+$) cells is observed. Functional analysis also demonstrated an extensive expansion of haematopoietic progenitors and LTR-HSCs: around 146 LTR-HSCs are obtained

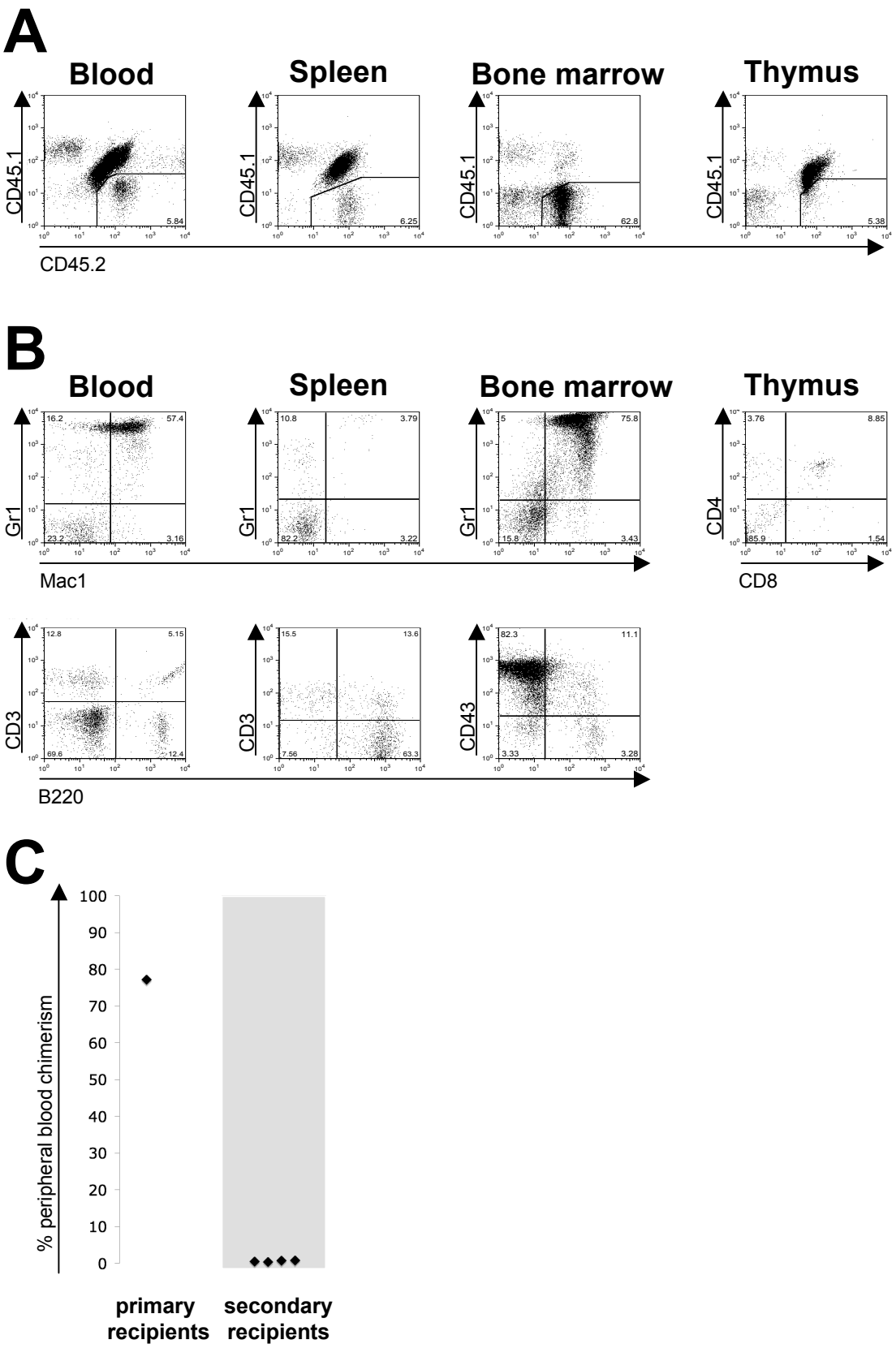
A
Blood
Spleen
Bone marrow
Thymus
CD45.1
CD45.2
5.84
6.25
62.8
5.38
B
Blood
Spleen
Bone marrow
Thymus
Gr1
Mac1
CD4
CD8
16.2
57.4
23.2
3.16
10.8
3.79
82.2
3.22
5
75.8
15.8
3.43
3.76
8.85
85.9
1.54
CD3
B220
CD43
12.8
5.15
69.6
12.4
15.5
13.6
7.56
63.3
82.3
11.1
3.33
3.28
C
% peripheral blood chimerism
100
90
80
70
60
50
40
30
20
10
0
primary recipients
secondary recipients

Figure 3.12: Multilineage haematopoietic reconstitution and secondary transplantations of LTR-HSCs generated in growth factors free conditions

A: Long-term donor derived reconstitution in major haematopoietic organs of primary recipient (peripheral blood, spleen, bone marrow, and thymus).

B: Long-term multilineage (myelo-lymphoid) analysis of donor-derived cells in major haematopoietic organs of primary recipient (peripheral blood, spleen, bone marrow, and thymus).

Representative example of analysis from two mice reconstituted with reaggregates cultured in growth factors free conditions. Quadrants are based on appropriate isotype control (Appendix 3.2); values indicate percentages of cells.

C: Secondary transplantation of bone marrow cells from a reconstituted primary recipient. 1/10 of whole bone marrow (2 femurs and 2 tibias) from the primary recipient was transplanted into each secondary recipient; peripheral blood chimerism was analysed at least 12 weeks post-transplantation.

from E11.5 AGM region while it originally contains one (Kumaravelu et al., 2002; Taoudi et al., 2008).

3.3. Refinement of culture conditions for E11.5 AGM reaggregates

3.3.1. The role of FCS in IMDM$^+$ for LTR-HSC expansion

As FCS contains some unknown and variable components between batches, an FCS-free culture medium would provide a system less susceptible to biological variations and allow more defined studies on molecular pathways involved in LTR-HSC development. IMDM$^+$ medium contains defined growth factors (IL-3, SCF, Flt3l), suggesting that FCS could be dispensable for LTR-HSC expansion. In order to investigate this hypothesis, reaggregates were set up and cultured in IMDM$^+$ and IMDM$^+$ without FCS (IMDM$^+$ - FCS).

3.3.1.1. Serum free conditions: haematopoietic progenitor expansion

The difference in expansion of haematopoietic progenitors was investigated in 2 experiments presented individually. In the presence of FCS (IMDM$^+$), there was a total of 5300 and 6450 CFU-Cs (2000 and 1850 CFU-mast, 700 and 1800 BFU-E, 100 and 800 CFU-GM, 2050 and 1500 CFU-mac, and 450 and 500 CFU-GEMM respectively)(Figure 3.9A). In the absence of FCS, there was a total of 2800 and 1900 CFU-Cs (950 and 800 CFU-mast, 650 and 200 BFU-E, 50 and 50 CFU-GM, 850 and 600 CFU-mac, 300 and 250 CFU-GEMM respectively)(Figure 3.9A). In both experiments, the presence of FCS significantly stimulated the expansion of CFU-Cs.

3.3.1.2. Serum free conditions: LTR-HSC expansion

The requirement of FCS for LTR-HSC expansion was then investigated by transplanting 0.01rd into single recipients. PBC was determined at least 12 weeks

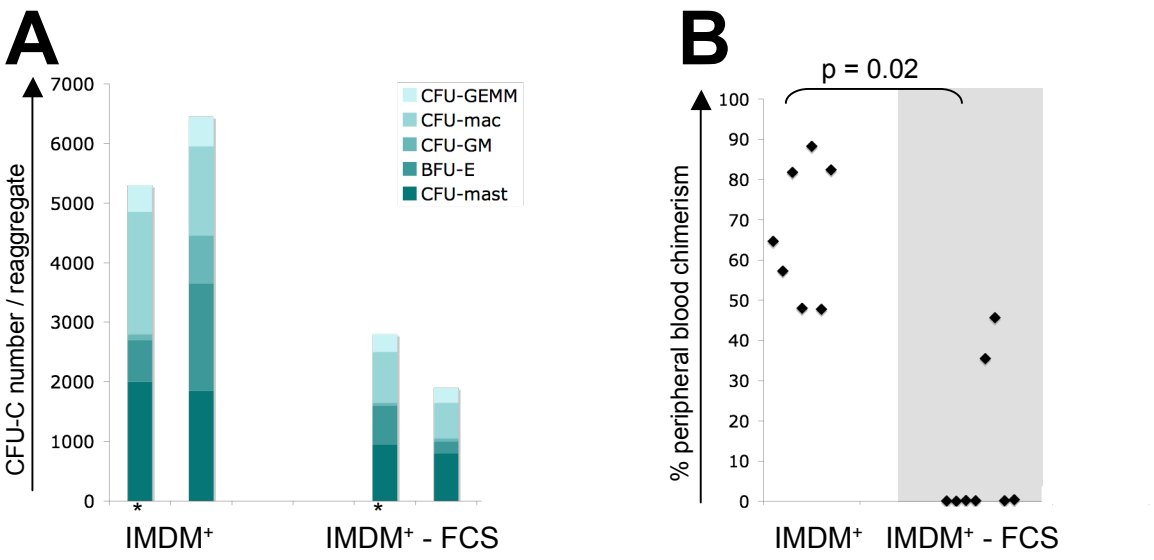

Figure 3.9: Haematopoietic progenitors and LTR-HSC expansion in reaggregates cultured in serum free conditions

A: Numbers of CFU-Cs per reaggregate cultured in the presence ($IMDM^+$) or absence ($IMDM^+$ - FCS) of fetal calf serum (FCS). Cumulative result of two independent experiments (* correspond to the values from experiment 1, others to values from experiment 2).

BFU-E: burst forming unit-erythroid; CFU: colony forming unit; Mac: macrophage; GM: granulocyte/macrophage; GEMM: granulocyte/erythroid/macrophage/ megakaryocyte

B: Peripheral blood chimerism of recipients transplanted with 0.01rd of reaggregates cultured in the presence ($IMDM^+$) or absence ($IMDM^+$ - FCS) of FCS.

Each dot represents a single recipient mouse. Recipients were considered reconstituted when their peripheral blood chimerism exceeded 5% at least 12 weeks after transplantation. Cumulative result of two independent experiments.

post transplantation by flow cytometric analysis. With IMDM$^+$, 7 out of 7 recipients were reconstituted at high level (mean PBC: 67.2%)(Figure 3.9B). In IMDM$^+$ -FCS, only 2 out of 8 recipients were reconstituted (mean PBC: 40.6%)(Figure 3.9B). Only 2 out of 8 recipients were reconstituted in serum free condition, compared to 7 out of 7 with medium containing FCS, indicating fewer LTR-HSCs in the absence of FCS. This difference was statistically significant (Fisher's exact test; p=0.02). However, the reconstitution of 2 out of 8 mice in serum free cultures suggested the presence of at least 25 LTR-HSCs. This still represents a significant LTR-HSC expansion compared to the fresh E11.5 AGM region (Gekas et al., 2005; Kumaravelu et al., 2002).

3.3.1.3. Serum free conditions: long-term multilineage contribution and secondary transplantations.

To confirm the normal function of LTR-HSCs generated in serum free conditions, long-term multilineage analysis of haematopoietic organs and secondary transplantations were performed. High donor cell reconstitution was observed in peripheral blood, spleen, and thymus (Figure 3.10A). The donor cells in peripheral blood and spleen were of both myeloid (Mac1$^+$ and Gr1$^+$) and lymphoid lineages (CD3$^+$ and B220$^+$)(Figure 3.10B). In addition, the majority of donor cells in the thymus were immature (CD4$^+$CD8$^+$) T cells (Figure 3.10B). The low reconstitution level in bone marrow (3.65%) was multilineage as both myeloid (Mac1$^+$ and Gr1$^+$) and lymphoid lineages (CD3$^+$ and B220$^+$) were present (Figure 3.10A, B). However, such low reconstitution was not observed in the other recipient analysed (62.8% PBC, both myeloid and lymphoid).

As 2 of the recipients transplanted with "serum free reaggregates" were highly reconstituted, secondary transplantations were performed. One primary recipient was sacrificed and 1/10 of its bone marrow (paired femurs and tibias) was transplanted into each secondary recipient. Secondary recipients PBC was analysed at least 12 weeks post-transplantation (Figure 3.10C). While the PBC of the primary recipient was 35.5%, none of the secondary recipient was reconstituted with donor

bone marrow cells (Figure 3.10C). This is either due to the low reconstitution level of bone marrow in the primary recipient (4.03%) or a genuine defect in LTR-HSCs; additional secondary transplantations would be required to discriminate between these two options.

3.3.2. The need for growth factors for LTR-HSC expansion

It was demonstrated that maximal LTR-HSC expansion requires FCS in $IMDM^+$. Based on this result, the requirement of the growth factors cocktail for LTR-HSC expansion was also investigated. E11.5 AGM reaggregates were cultured in $IMDM^+$ or $IMDM^-$ (containing FCS but no growth factors) to address this question.

3.3.2.1. Growth factor free conditions: haematopoietic progenitor expansion

The difference in CFU-C expansion between cultures in $IMDM^+$ and $IMDM^-$ was first quantified in 2 experiments presented individually. In $IMDM^+$, reaggregates contained a total of 6450 and 5300 CFU-Cs as previously described in section 3.3.2.1 (Figure 3.9A and Figure 3.11A). When cultured in $IMDM^-$, reaggregates contained a total of 150 and 200 CFU-Cs, consisting of 0 and 150 BFU-E, 50 and 0 CFU-mac, and 150 and 0 CFU-GEMM (Figure 3.11A). It was concluded that growth factors in the medium are strongly required for optimal CFU-C expansion in reaggregates. Interestingly, it appeared that the original numbers of CFU-Cs in the fresh E11.5 AGM region tissue (144±42 CFU-Cs, Figure 3.4) were in a similar range as reaggregates cultured in $IMDM^-$, suggesting that FCS might be enough for maintenance/survival of CFU-Cs numbers.

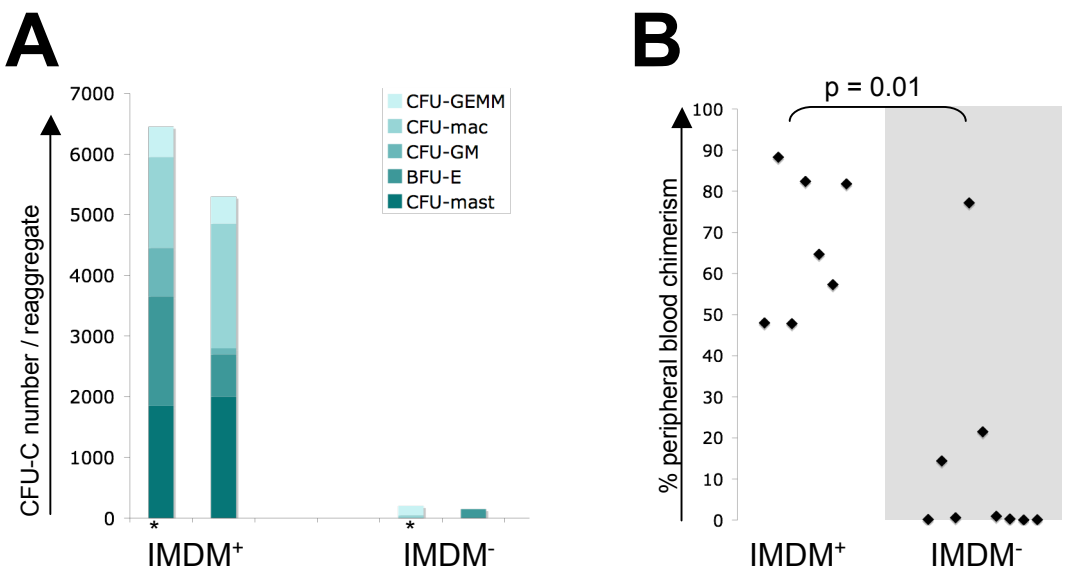

Figure 3.11: Haematopoietic progenitor and LTR-HSC content in reaggregates cultured in growth factor free conditions

A: Numbers of CFU-Cs per reaggregate cultured in the presence ($IMDM^+$) or absence of growth factors ($IMDM^-$). Cumulative result of 2 independent experiments (* correspond to the values from experiment 1, others to values from experiment 2).

BFU-E: burst forming unit-erythroid; CFU: colony forming unit; Mac: macrophage; GM: granulocyte/macrophage; GEMM: granulocyte/erythroid/macrophage/ megakaryocyte

B: Peripheral blood chimerism of recipients transplanted with 0.01rd of reaggregates cultured in the presence ($IMDM^+$) or absence of growth factors ($IMDM^-$).

Each point represents a single recipient mouse. Recipients were considered reconstituted when their peripheral blood chimerism exceeded 5% at least 12 weeks after transplantation. Cumulative result of 2 independent experiments.

3.3.2.2. Growth factor free conditions: LTR-HSC expansion

The expansion in LTR-HSCs was investigated by transplanting 0.01rd into each recipient mouse. In $IMDM^+$, 7 out of 7 mice (100%) were reconstituted at high level (mean PBC: 67.2%)(Figure 3.11B). In $IMDM^-$, only 3 out of 9 mice (33%) were reconstituted (mean PBC: 37.7%)(Figure 3.11B). Thus, "$IMDM^-$ reaggregates" contained significantly fewer LTR-HSCs than "$IMDM^+$ reaggregates" (Fisher's exact test, p=0.01).

3.3.2.3. Growth factor free conditions: long-term multilineage analysis and secondary transplantations.

The function of LTR-HSCs was then investigated by multilineage analysis of haematopoietic organs and secondary transplantations. Peripheral blood, spleen, and bone marrow were reconstituted with donor cells of myeloid ($Mac1^+$ and $Gr1^+$) and lymphoid ($CD3^+$ and $B220^+$) lineages (Figure 3.12A, B). Interestingly, the thymus was not highly reconstituted and the proportion of T cells ($CD4^+$ and $CD8^+$) derived from donor cells was very low (Figure 3.12A, B). This could hardly be explained by technical difficulty in isolating thymic tissue in aged mice (due to thymic involution) as flow cytometric analysis of the whole tissue showed it contained 71% of $CD4^+CD8^+$ cells, as expected. Instead, this observation made in both recipients analysed suggests that at least one growth factor in the culture is necessary for the generation of fully functional LTR-HSCs capable of T-cell maturation.

To assess the self-renewal potential of LTR-HSCs generated in $IMDM^-$, secondary transplantations were performed. The primary recipient, which had 77.2% PBC, was sacrificed and 1/10 of its bone marrow (paired femurs and tibias) was transplanted into each secondary recipient. None of the secondary recipients were reconstituted with donor cells, which was intringuing because the primary recipient blood was highly reconstituted (Figure 3.12C). However, the bone marrow reconstitution level of the primary recipient, testing additional primary recipients, and clonal analysis, would be required to draw any conclusion about a possible defect.

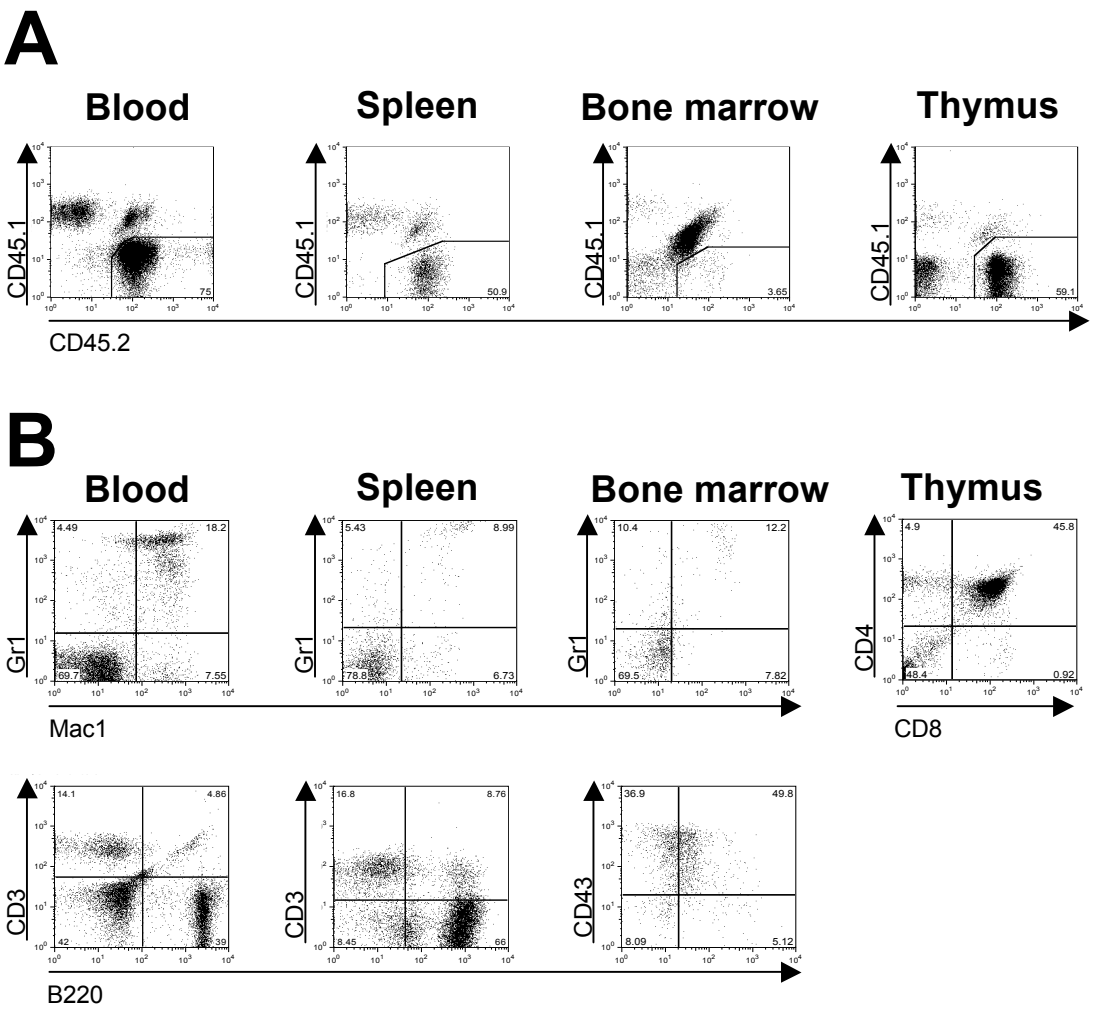
A
Blood
Spleen
Bone marrow
Thymus
CD45.1
CD45.2
75
50.9
3.65
59.1
B
Blood
Spleen
Bone marrow
Thymus
Gr1
Mac1
4.49
18.2
69.7
7.55
5.43
8.99
78.8
6.73
10.4
12.2
69.5
7.82
CD4
CD8
4.9
45.8
48.4
0.92
CD3
B220
14.1
4.86
42
39
16.8
8.76
8.45
66
CD43
36.9
49.8
8.09
5.12
C
% peripheral blood chimerism
100
90
80
70
60
50
40
30
20
10
0
primary recipients
secondary recipients

Figure 3.10: Multilineage haematopoietic reconstitution and secondary transplantations of LTR-HSCs generated in serum free conditions

A: Long-term donor derived reconstitution in major haematopoietic organs of primary recipient (peripheral blood, spleen, bone marrow, and thymus).

B: Long-term multilineage (myelo-lymphoid) analysis of donor derived cells in major haematopoietic organs of primary recipient (peripheral blood, spleen, bone marrow, and thymus).

Representative example of analysis from two mice reconstituted with reaggregates cultured in serum free conditions. Quadrants are based on appropriate isotype control (Appendix 3.2); values indicate percentages of cells.

C: Secondary transplantation of bone marrow cells from a reconstituted primary recipient. 1/10 of whole bone marrow (paired femurs and tibias) from the primary recipient was transplanted into each secondary recipient; peripheral blood chimerism was analysed at least 12 weeks post-transplantation.

3.4. Requirement of individual growth factors for optimal haematopoietic development in E11.5 AGM reaggregates

3.4.1. The impact of growth factor deprivation on E11.5 AGM reaggregates haematopoiesis

Previous studies have demonstrated that all three growth factors used in IMDM$^+$ (IL-3, SCF, and Flt3l) are involved in haematopoiesis (see Section 1.6.2). In order to investigate whether any one of these factors plays a predominant role in the extensive LTR-HSC expansion observed in E11.5 AGM reaggregates, single growth factors were omitted from the culture medium.

3.4.1.1. Descriptive analysis: morphology and haematopoietic cells

After 4 days of culture, images of reaggregates showed no obvious morphological differences among different conditions (either size or morphology)(Figure 3.13A).

In addition, cells were counted and flow cytometry was performed with anti-CD45 antibody to mark haematopoietic cells in two experiments presented individually. In IMDM$^+$, there were a total of 140000 and 140300 cells, of which 19200 and 15200 were CD45$^+$ respectively (Figure 3.13B). Without IL-3, there were 120000 and 116300 cells in total, of which 5700 and 4200 were CD45$^+$ (Figure 3.13B). Without SCF, there were 200000 and 121200 cells in total, of which 23200 and 10850 were CD45$^+$ (Figure 3.13B). Without Flt3l, there were180000 and 89600 cells in total, of which 16600 and 9500 were CD45$^+$ (Figure 3.13B). Interestingly, only the removal of IL-3 resulted in consistently lower numbers of CD45$^+$ cells compared to IMDM$^+$ controls but did not compromise the maintenance of the original CD45$^+$ compartment (Figure 3.13B; Table 3.1).

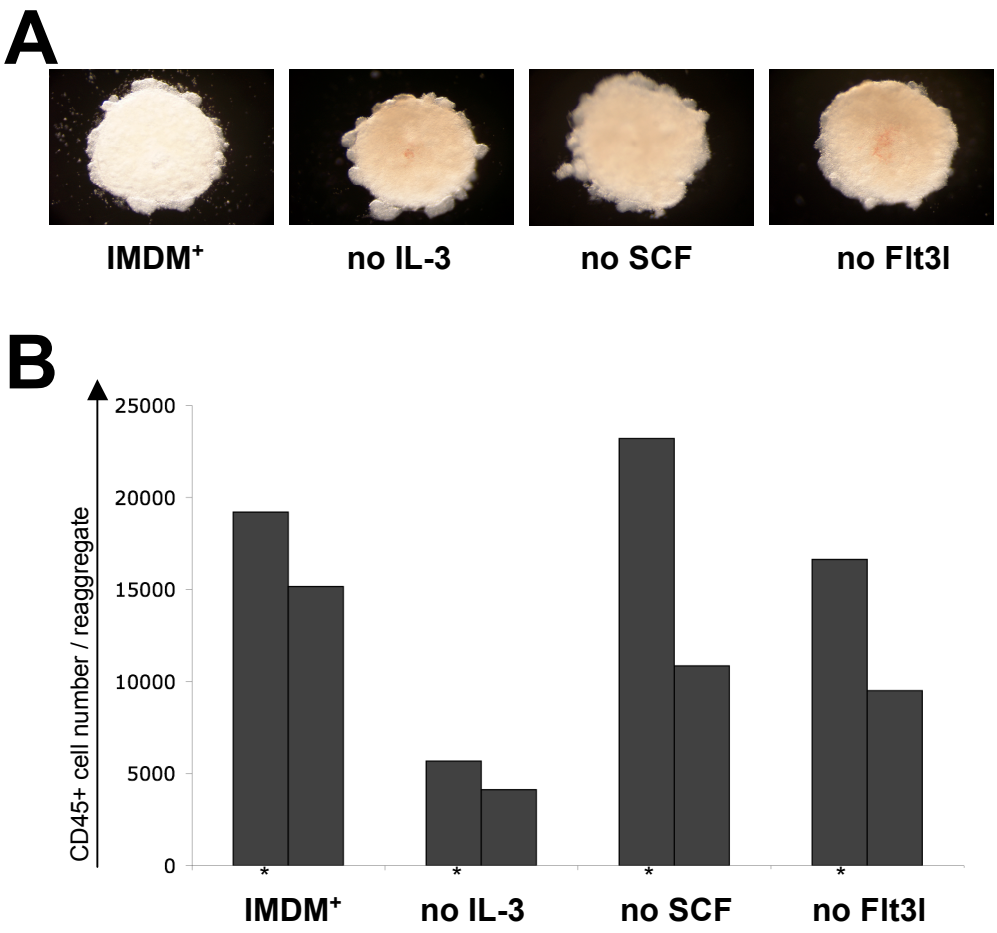

Figure 3.13: Effect of growth factor deprivation on reaggregates morphology and haematopoiesis

A: Representative images of reaggregates cultured in media deprived of single growth factors. All reaggregates had similar morphology (round with peripheral protrusions) with a rough diameter of 1mm.

B: Haematopoietic cell numbers ($CD45^+$) per reaggregate cultured in media media deprived of single growth factors. (* correspond to the values from experiment 1, others to values from experiment 2). Values obtained by flow cytometric analysis (cell viability determined by 7-AAD uptake).

3.4.1.2. Functional analysis: haematopoietic progenitors

After 4 days culture, CFU-Cs assays were set up to investigate the impact of single growth factor deprivation on the expansion of haematopoietic progenitors. In $IMDM^+$, there was a total of 4080±1333 CFU-Cs (1275±518 CFU-mast, 875±492 BFU-E, 400±318 CFU-GM, 1165±199 CFU-mac, 366±175 CFU-GEMM)(Figure 3.14A). In the absence of IL-3, there was a total of 470±60 CFU-Cs (186±29 CFU-mast, 50±86 BFU-E, no CFU-GM, 233±58 CFU-mac, and no CFU-GEMM)(Figure 3.14A). In the absence of SCF, there was a total of 3030±630 CFU-Cs (967±153 CFU-mast, 630±208 BFU-E, 400±0 CFU-GM, 800±264 CFU-mac, and 233±58 CFU-GEMM)(Figure 3.14A). In the absence of Flt3l, there was a total of 2920±320 CFU-Cs (1050±50 CFU-mast, 386±202 BFU-E, 283±144 CFU-GM, 750±450 CFU-mac, and 450±304 CFU-GEMM)(Figure 3.14A). Compared to $IMDM^+$ control, only the lack of IL-3 resulted in a significantly reduced CFU-C expansion (Paired T-test; p=0.001)(SCF deprived: p=0.23; Flt3l deprived: p=0.12).

3.4.1.3. Functional analysis: LTR-HSC expansion

Repopulation assays were performed to investigate the impact of single growth factor deprivation on LTR-HSC expansion. In each experiment, 0.01rd was transplanted into individual recipient mice and PBC was determined at least 12 weeks post-transplantation. In standard conditions ($IMDM^+$), 11 out of 11 mice (100%) were reconstituted at high level (mean PBC: 70.2%)(Figure 3.14B). In the absence of IL-3, only 8 out of 12 mice (66%) were successfully reconstituted (mean PBC: 59.5%)(Figure 3.14B). In the absence of SCF, 9 out of 11 recipient mice (82%) were reconstituted (mean PBC: 48.5%)(Figure 3.14B). In the absence of Flt3l, 5 out of 7 mice (71%) were successfully reconstituted (mean PBC: 69.7%)(Figure 3.14B). The presence of non-reconstituted mice upon removal of any single growth factor indicates fewer LTR-HSCs than in $IMDM^+$ control, suggesting that all three factors are required for maximal LTR-HSC expansion. Nevertheless, the large proportion of reconstituted animals in each condition indicates a significant LTR-HSC expansion, suggesting that the concerted action of at least 2 growth factors is sufficient for LTR-

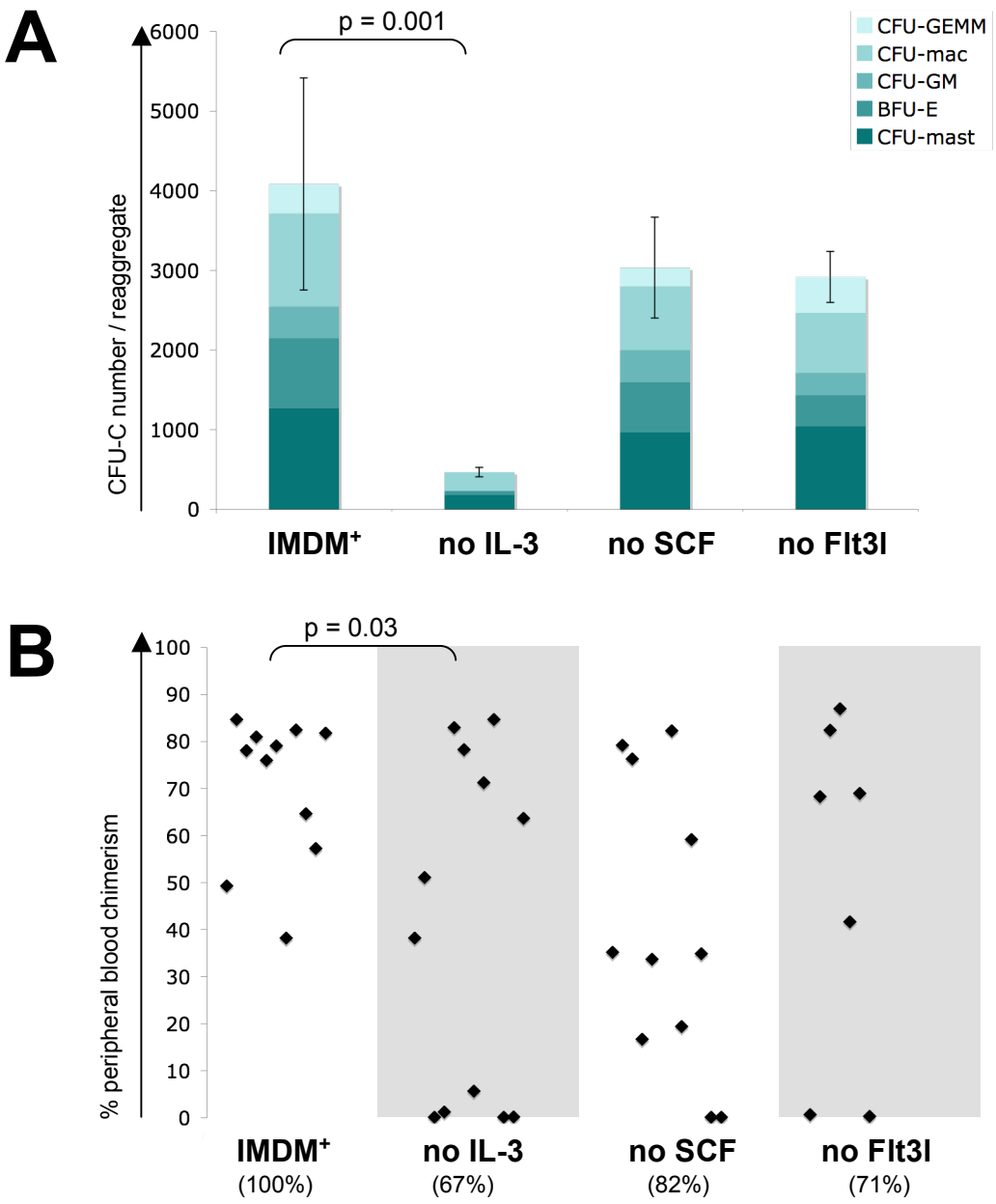

Figure 3.14: Haematopoietic progenitors and LTR-HSCs expansion in reaggregates cultured in media deprived of single growth factors.

A: Number of CFU-Cs contained per reaggregate cultured in media deprived of a single growth factor. Bars indicate standard deviation from 3 independent experiments.
BFU-E: burst forming unit-erythroid; CFU: colony forming unit; Mac: macrophage; GM: granulocyte/macrophage; GEMM: granulocyte/erythroid/macrophage/ megakaryocyte
B: Peripheral blood chimerism of recipients transplanted with 0.01dose of reaggregates cultured in media deprived of a single growth factor.
Each point represents a single recipient mouse. Recipients were considered reconstituted when their peripheral blood chimerism exceeded 5% at least 12 weeks after transplantation. Cumulative result of 3 independent experiments.

HSC expansion. Whilst only the removal of IL-3 generated significantly fewer reconstituted mice (Fisher's exact test, p=0.03) compared to $IMDM^+$ control (SCF deprived: p=0.4; Flt3l deprived: p=0.13), the removal of other growth factors resulted in similar percentages of reconstituted mice. In order to appropriately quantify the absolute number of LTR-HSCs in each condition, limiting dilution experiments would be required and increasing the numbers of recipients would strengthen the statistical analysis.

3.4.1.4. Normal function of LTR-HSCs: multilineage analysis and secondary transplantations

To confirm that LTR-HSCs generated in each condition were fully functional, multilineage analysis and secondary transplantations were performed. Previous data showed that LTR-HSCs generated in $IMDM^+$ are fully functional (Figures 3.6 and 3.7). In other conditions, the contribution of donor cells to myeloid and lymphoid lineages in haematopoietic tissues (blood, spleen, bone marrow and thymus) was assessed by flow cytometry at least 12 weeks post-transplant except for "no SCF" condition due to the lack of available animal. In the absence of IL-3 and Flt3l, peripheral blood, spleen, bone marrow and thymus were reconstituted with donor cells (Figure 3.15A, B). Donor derived lymphoid cells ($CD3^+$, $CD43^+$ and $B220^+$) were observed in blood, spleen and bone marrow in both conditions (Figure 3.15A', B'). Myeloid cells ($Mac1^+$ and $Gr1^+$) were also observed in these tissues in both conditions (Figure 3.15A', B'). Donor derived cells in the thymus contributed to T cells populations ($CD4^+$ and $CD8^+$)(Figure 3.15A', B'). Low numbers of Mac^+ cells in the spleen of mice transplanted with cells cultured without IL-3 or without Flt3l was not observed in other analysed recipients, so LTR-HSCs generated without IL-3 or without Flt3l may provide multilineage contribution to recipient haematopoietic tissues.

Secondary transplantations were performed in each condition to identify any potential LTR-HSC defect. One primary recipient from each condition was sacrificed and 1/10 of its whole bone marrow (paired femurs and tibias) was transplanted into

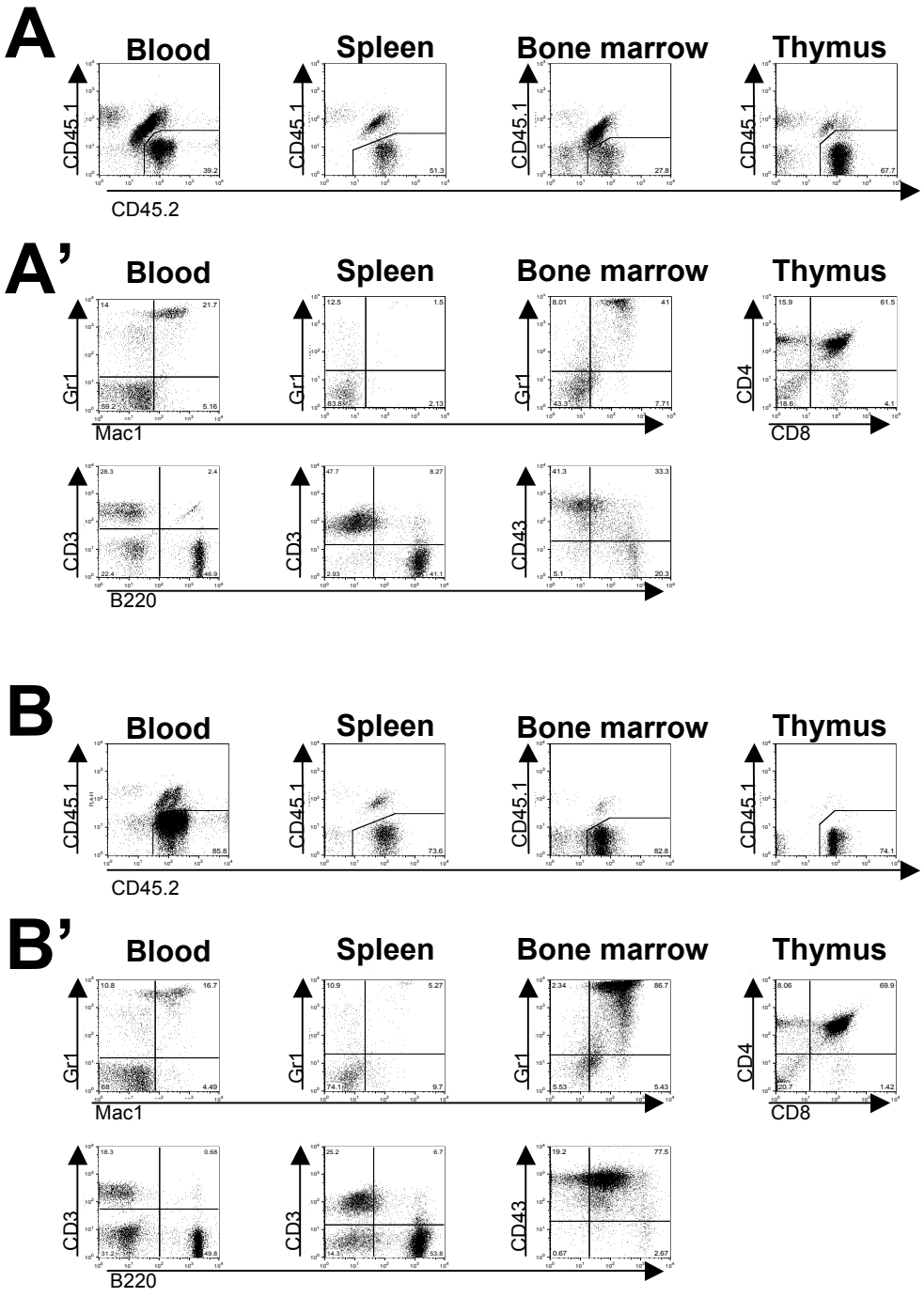
A
Blood
Spleen
Bone marrow
Thymus
CD45.1
CD45.2
A'
Gr1
Mac1
CD4
CD8
CD3
B220
CD43
B
B'

Figure 3.15: Multilineage haematopoietic reconstitution by LTR-HSCs generated in media deprived of single growth factors.

A, A': Long-term multilineage analysis of recipient mice reconstituted with reaggregatess cultured in the absence of IL-3. A: Donor derived reconstitution in major haematopoietic organs (peripheral blood, spleen, bone marrow, and thymus). A': Multilineage (myelo-lymphoid) contribution in major haematopoietic organs (peripheral blood, spleen, bone marrow, and thymus) of recipients. Events gated on donor derived cells.

B, B': Long-term multilineage analysis of recipient mice reconstituted with reaggregatess cultured in the absence of Flt3l. B: Donor derived reconstitution in major haematopoietic organs (peripheral blood, spleen, bone marrow, and thymus). B': Multilineage (myelo-lymphoid) contribution in major haematopoietic organs (peripheral blood, spleen, bone marrow, and thymus) of recipients. Events gated on donor derived cells.

Representative example of analysis from two mice reconstituted with reaggregates cultured in single growth factor deprived conditions. Quadrants are based on appropriate isotype control (Appendix 3.2); values indicate percentages of cells. Analysis of primary recipients peripheral blood was performed at least 12 weeks after transplantation.

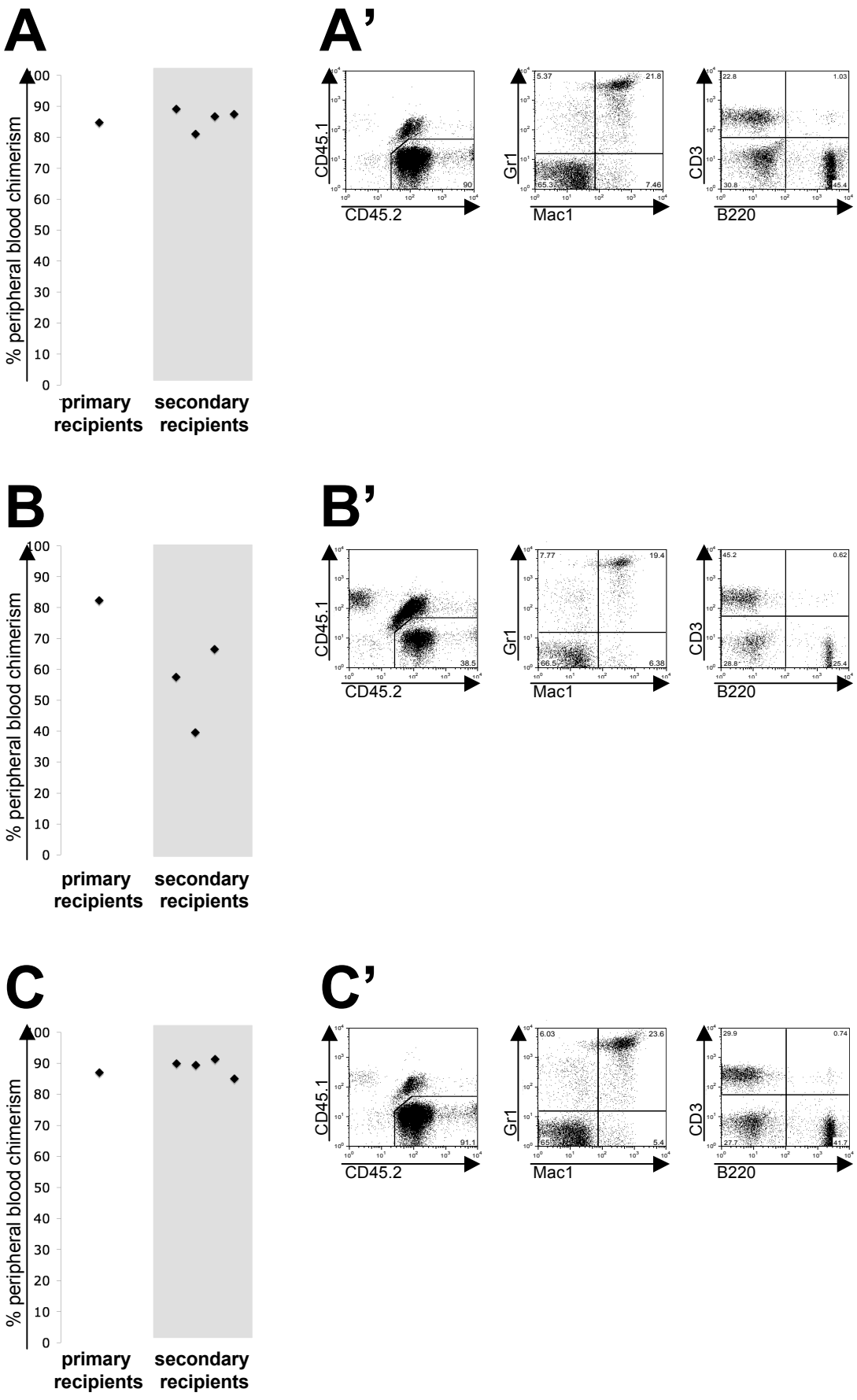
A
A'
% peripheral blood chimerism
primary recipients
secondary recipients
CD45.1
CD45.2
Gr1
Mac1
CD3
B220
B
B'
C
C'

Figure 3.16: Secondary transplantations of LTR-HSCs generated in media deprived of single growth factors

A, A': Secondary transplantation and multilineage reconstitution in peripheral blood of secondary recipients transplanted with bone marrow originally reconstituted with reaggregates cultured in the absence of IL-3. A: Secondary transplantation of bone marrow cells from reconstituted primary recipient. A': Long-term multilineage (myelo-lymphoid) contribution in secondary recipients peripheral blood.

B, B': Secondary transplantation and multilineage reconstitution in peripheral blood of secondary recipients transplanted with bone marrow originally reconstituted with reaggregates cultured in the absence of SCF. B: Secondary transplantation of bone marrow cells from reconstituted primary recipient. B': Long-term multilineage (myelo-lymphoid) contribution in secondary recipients peripheral blood.

C, C': Secondary transplantation and multilineage reconstitution in peripheral blood of secondary recipients transplanted with bone marrow originally reconstituted with reaggregates cultured in the absence of Flt3l. C: Secondary transplantation of bone marrow cells from reconstituted primary recipient. C': Long-term multilineage (myelo-lymphoid) contribution in secondary recipients peripheral blood.

A, B, C: 1/10 of whole bone marrow (2 femurs and 2 tibias) from a primary recipient was transplanted into each secondary recipient; peripheral blood chimerism was analysed at least 12 weeks post-transplantation.

A', B', C': Representative example of analysis from two reconstituted secondary recipients. Quadrants are based on appropriate isotype control (Appendix 3.2); values indicate percentages of cells. Events gated on donor derived cells.

each secondary recipients and PBC was determined at least 12 weeks post transplant. Without IL-3, the primary recipient had a PBC of 84.7% and 4 out of 4 secondary recipients were reconstituted at high level (mean PBC: 86%)(Figure 3.16A). Both myeloid ($Mac1^+$ and $Gr1^+$) and lymphoid ($CD3^+$ and $B220^+$) compartments were repopulated (Figure 3.16A'). Without SCF, the primary recipient had 82.3% PBC and 3 out of 3 secondary recipients were reconstituted at a lower level compared to the primary recipient (mean PBC: 54.5%)(Figure 3.16B). Both myeloid ($Mac1^+$ and $Gr1^+$) and lymphoid ($CD3^+$ and $B220^+$) lineages in the blood were repopulated (Figure 3.16B'). Without Flt3l, the primary recipient used had a PBC of 87% and 4 out of 4 secondary recipients were reconstituted at high level (mean PBC: 88.9%)(Figure 3.16C). Both myeloid ($Mac1^+$ and $Gr1^+$) and lymphoid ($CD3^+$ and $B220^+$) lineages in the blood were reconstituted (Figure 3.16C').

3.4.1.5. Conclusions

All growth factors (IL-3, SCF and Flt3l) are required to achieve maximal LTR-HSC expansion in reaggregate culture. However, the LTR-HSCs generated in the absence of single growth factors were capable of multilineage reconstitution in various haematopoietic organs and successfully reconstituted secondary recipients.

3.4.2. Influence of individual growth factor on haematopoiesis in E11.5 AGM reaggregates

In order to understand the roles of individual growth factors in the expansion of haematopoietic cells ($CD45^+$), progenitors (CFU-Cs) and LTR-HSCs, reaggregates were cultured with individual cytokines and analysed after 4 days reaggregate culture.

3.4.2.1. Descriptive analysis: morphology and cell numbers

Gross morphological study of reaggregates from each condition revealed no obvious differences as reaggregates were of similar size and had cell protrusions at their periphery (Figure 3.17A). In standard conditions ($IMDM^+$), one reaggregate contained 198800±33170 cells, of which 16840±4920 were $CD45^+$ (Figure 3.17B). When cultured in IL-3 only, one reaggregate contained 191820±36010 cells of which 8000±2790 were $CD45^+$ (Figure 3.17B). When cultured in SCF only, one reaggregate contained 154000±32240 cells of which 2040±760 cells $CD45^+$ (Figure 3.17B). When cultured in Flt3l only, one reaggregate contained 199210±35230 cells of which 2340±500 were $CD45^+$ (Figure 3.17B). Every condition generated a significantly lower number of $CD45^+$ cells compared to $IMDM^+$ control (Paired T-test; IL-3: p=0.008; SCF: p=0.002; Flt3l: 0.002), indicating that optimal haematopoietic cell expansion occurs from a synergetic response of at least two growth factors.

3.4.2.2. Functional analysis: expansion of haematopoietic progenitors

After 4 days, progenitor content per reaggregate was assessed by CFU-C assay. In $IMDM^+$, there were 4620±990 CFU-Cs (1620±333 CFU-mast, 550±50 BFU-E, 600±50 CFU-GM, 1517±562 CFU-mac, and 333±104 CFU-GEMM)(Figure 3.18A). In the presence of IL-3, there were 2730±310 CFU-Cs (1030±176 CFU-mast, 383±161 BFU-E, 333±58 CFU-GM, 833±29 CFU-mac, 150±132 CFU-GEMM)(Figure 3.18A). In the presence of SCF, there were a total of 670±300 CFU-Cs (333±208 CFU-mast, 100±87 BFU-E, 33±58 CFU-GM, 133±76 CFU-mac, 70±115 CFU-GEMM)(Figure 3.18A). In the presence of Flt3l, there were a total of 280±30 CFU-Cs (130±58 CFU-mast, 33±29 BFU-E and 117±29 CFU-mac)(Figure 3.18A). Statistical analysis demonstrated that significantly fewer CFU-Cs were generated in all conditions (Paired T-test, IL-3: p=0.03; SCF: p=0.002; Flt3l: p=0.01), once again indicating that optimal CFU-C expansion occurs through combined effects of at least 2 growth factors.

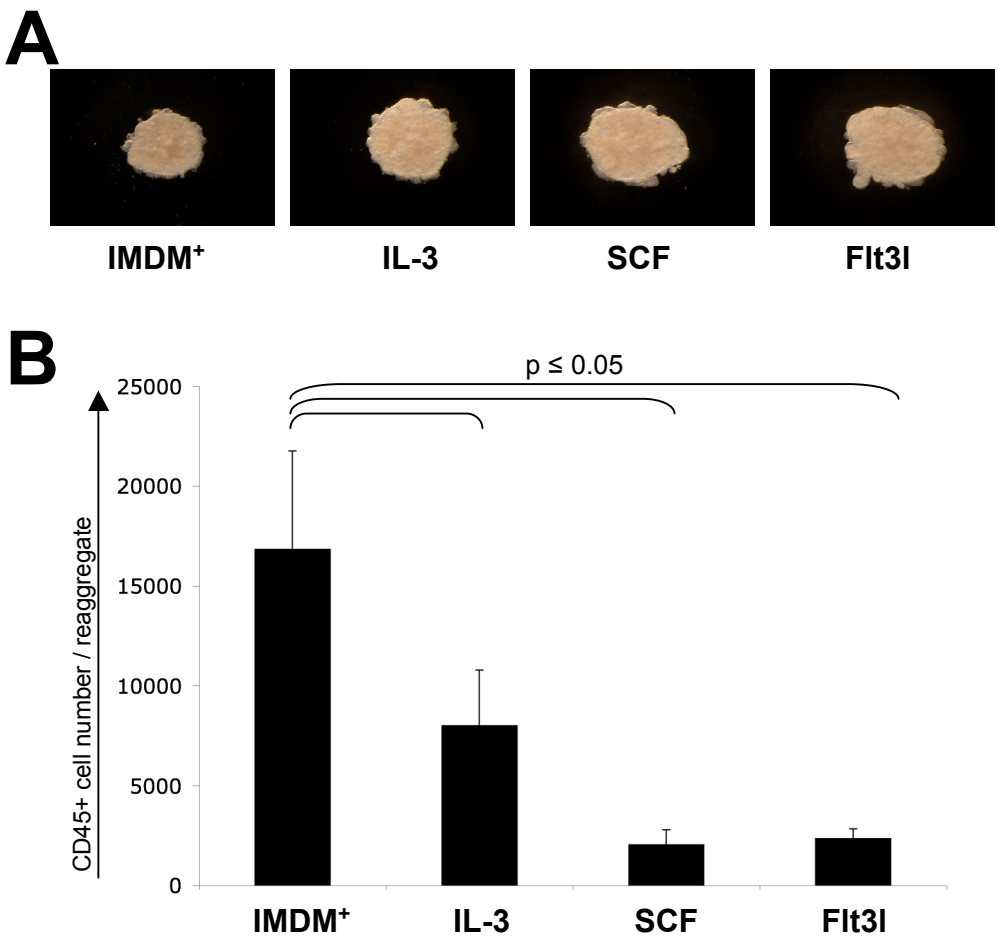

Figure 3.17: Influence of single growth factors on reaggregate morphology and haematopoiesis.

A: Morphology of reaggregates cultured in single growth factor media. All reaggregates had similar morphology (round with cell protrusions) with a diameter of approximately 1mm.
B: Haematopoietic cell numbers ($CD45^+$) contained per reaggregate cultured in single growth factor media. Bars indicate the standard deviation of 5 independent experiments.

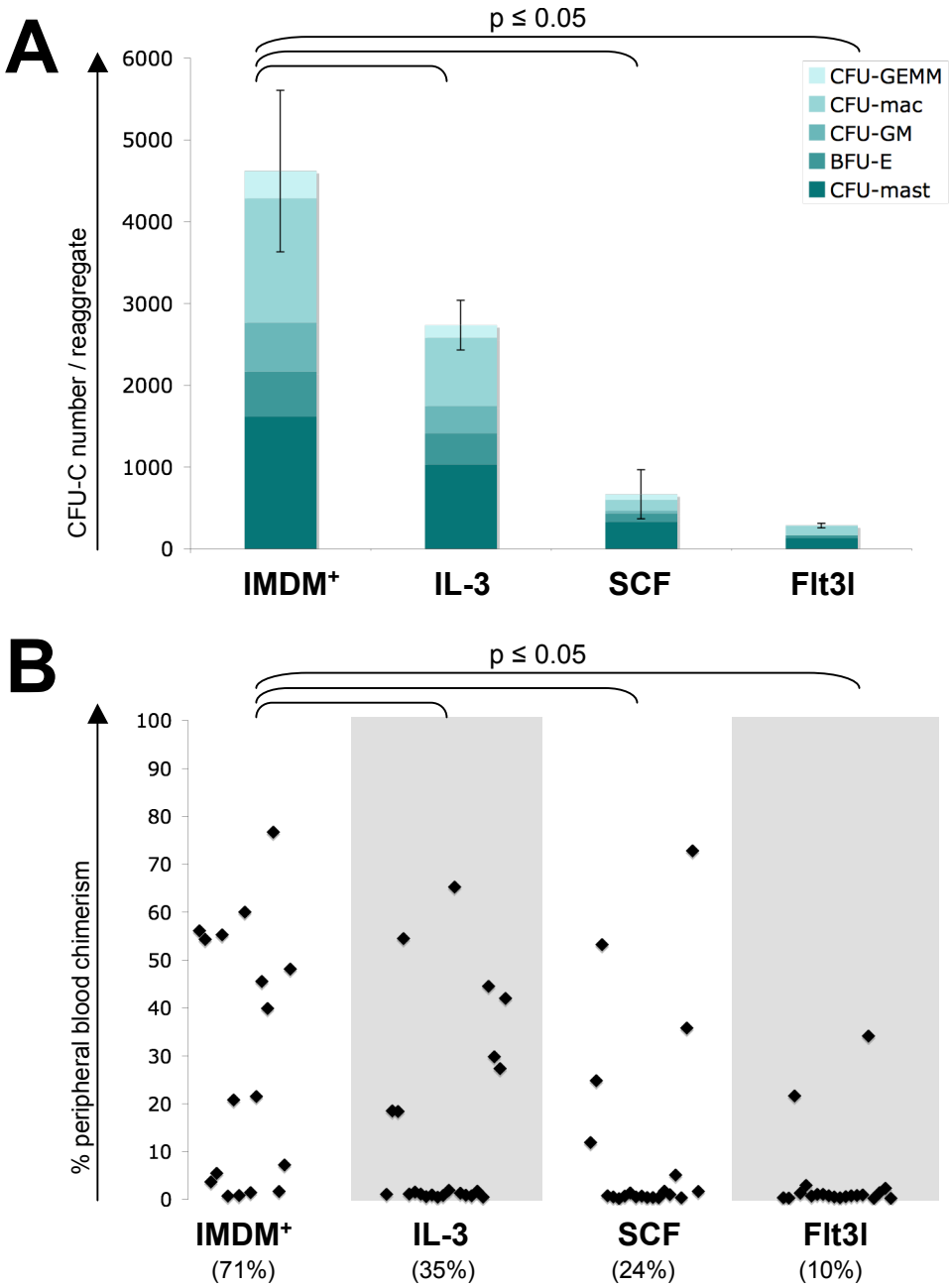

Figure 3.18: Haematopoietic progenitors and LTR-HSC expansion in reaggregates cultured in single growth factor media.

A: Numbers of CFU-Cs per reaggregate cultured in media containing a single growth factor. Bars indicate standard deviation of 3 independent experiments. BFU-E: burst forming unit-erythroid; CFU: colony forming unit; Mac: macrophage; GM:: granulocyte/macrophage; GEMM: granulocyte/erythroid/macrophage/ megakaryocyte

B: Peripheral blood chimerism of recipients transplanted with 0.01dose of reaggregates cultured in media containing a single growth factor.

Each point represents a single recipient mouse. Recipients were considered reconstituted when their peripheral blood chimerism exceeded 5% at least 12 weeks after transplantation. Cumulative result of 3 independent experiments.

3.4.2.3. Functional analysis: expansion of LTR-HSCs

Repopulation assays were performed to assess LTR-HSC expansion in each condition. In control experiments ($IMDM^+$), 12 out of 17 mice (71%) injected with 0.01 rd each were reconstituted (mean PBC: 40.9%)(Figure 3.18B). This level of repopulation was lower than expected, most probably due to biological variations. In the presence of IL-3, 8 out of 22 mice (36%) were successfully reconstituted (mean PBC: 37.5%)(Figure 3.18B). This result approximates findings previously reported (Robin et al., 2006). In the presence of SCF, 6 out of 20 mice (30%) were reconstituted (mean PBC: 33.9%) and in Flt3l, 2 out of 20 mice (10%) were reconstituted (mean PBC: 27.8%)(Figure 3.18B). Compared to $IMDM^+$ control, all conditions contained significantly lower proportion of reconstituted recipients (Fisher's exact test; IL-3: p=0.05; SCF: p=0.02; Flt3l: p=0.0004). Thus, the presence of a single growth factor cannot on its own account for the extensive LTR-HSC expansion observed in reaggregates, but rather results from a combined effect of at least two growth factors.

3.4.2.4. Normal function of LTR-HSCs: multilineage analysis and secondary transplantations

The function of LTR-HSCs from each condition was assessed by multilineage analysis and secondary transplantations. Multilineage analysis of peripheral blood, spleen, bone marrow and thymus was performed by flow cytometry on reconstituted recipients at least 12 weeks post-transplant. In all conditions, donor derived cells of myeloid ($Mac1^+$ and $Gr1^+$) and lymphoid ($CD3^+$, $B220^+$, $CD4^+$ and $CD8^+$) lineages were detected in all tissues (Figure 3.19A', B', and C').

For secondary transplantations, primary recipients were sacrificed and 1/10 of their whole bone marrow (paired femurs and tibias) was transplanted into secondary recipients. In the presence of IL-3, the primary recipient (75% PBC) bone marrow cells successfully reconstituted 4 out of 4 secondary recipients (mean PBC: 37.2%)(Figure 3.20A). In the presence of SCF only, the primary recipient (85.8% PBC) bone marrow cells successfully reconstituted 3 out of 3 secondary recipients

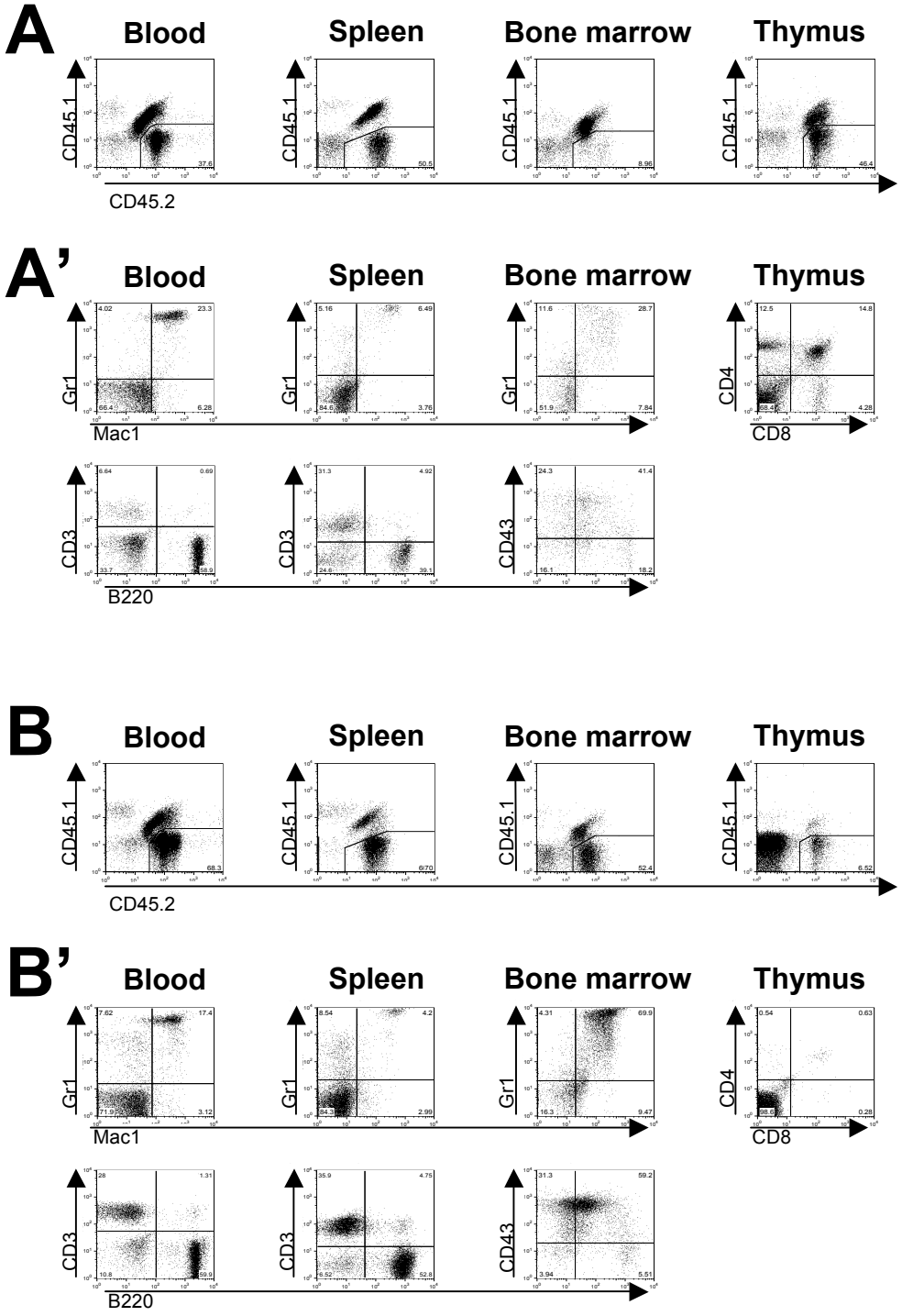
A
Blood
Spleen
Bone marrow
Thymus
CD45.1
CD45.2
A'
Gr1
Mac1
CD4
CD8
CD3
B220
CD43
B
B'

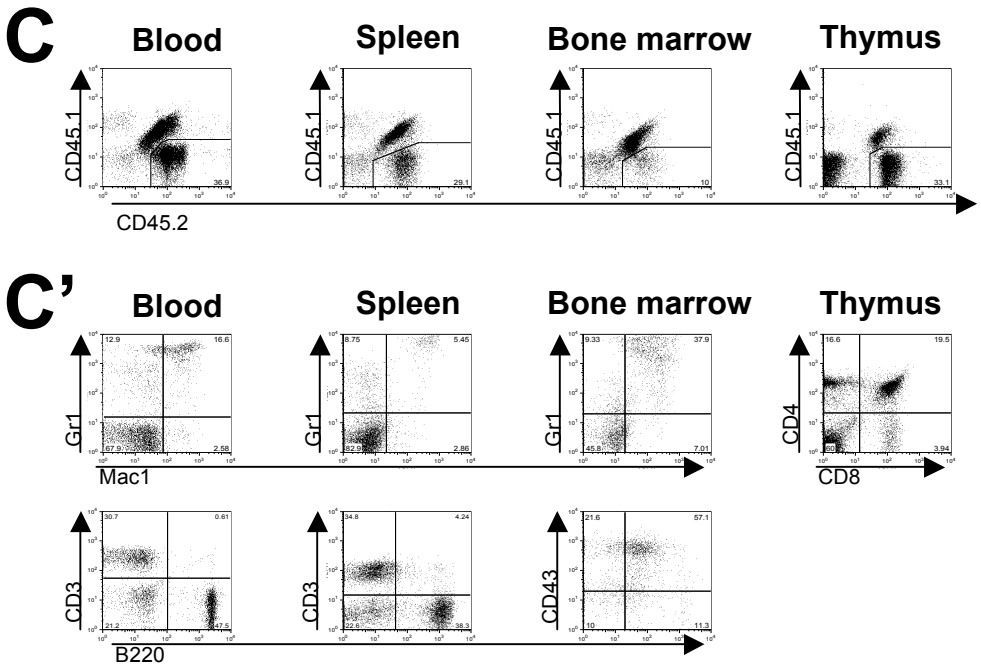

Figure 3.19: Multilineage haematopoietic reconstitution by reaggregates cultured in the presence of single growth factors.

A, A': Long-term multilineage analysis of recipient mice reconstituted with reaggregates cultured in the presence of IL-3. A: Donor derived reconstitution major haematopoietic organs (peripheral blood, spleen, bone marrow, and thymus). A': Multilineage (myelo-lymphoid) contribution in major haematopoietic organs (peripheral blood, spleen, bone marrow, and thymus) of recipients. Events gated on donor derived cells.

B, B': Long-term multilineage analysis of recipient mice reconstituted with reaggregates cultured in the presence of SCF. B: Donor derived reconstitution major haematopoietic organs (peripheral blood, spleen, bone marrow, and thymus). B': Multilineage (myelo-lymphoid) contribution in major haematopoietic organs (peripheral blood, spleen, bone marrow, and thymus) of recipients. Events gated on donor derived cells.

C, C': Long-term multilineage analysis of recipient mice reconstituted with reaggregates cultured in the presence of Flt3l. C: Donor derived reconstitution major haematopoietic organs (peripheral blood, spleen, bone marrow, and thymus). C': Multilineage (myelo-lymphoid) contribution in major haematopoietic organs (peripheral blood, spleen, bone marrow, and thymus) of recipients. Events gated on donor derived cells.

Representative example of analysis from two mice reconstituted with reaggregates cultured in single growth factor conditions. Quadrants are based on appropriate isotype control (Appendix 3.2); values indicate percentages of cells.

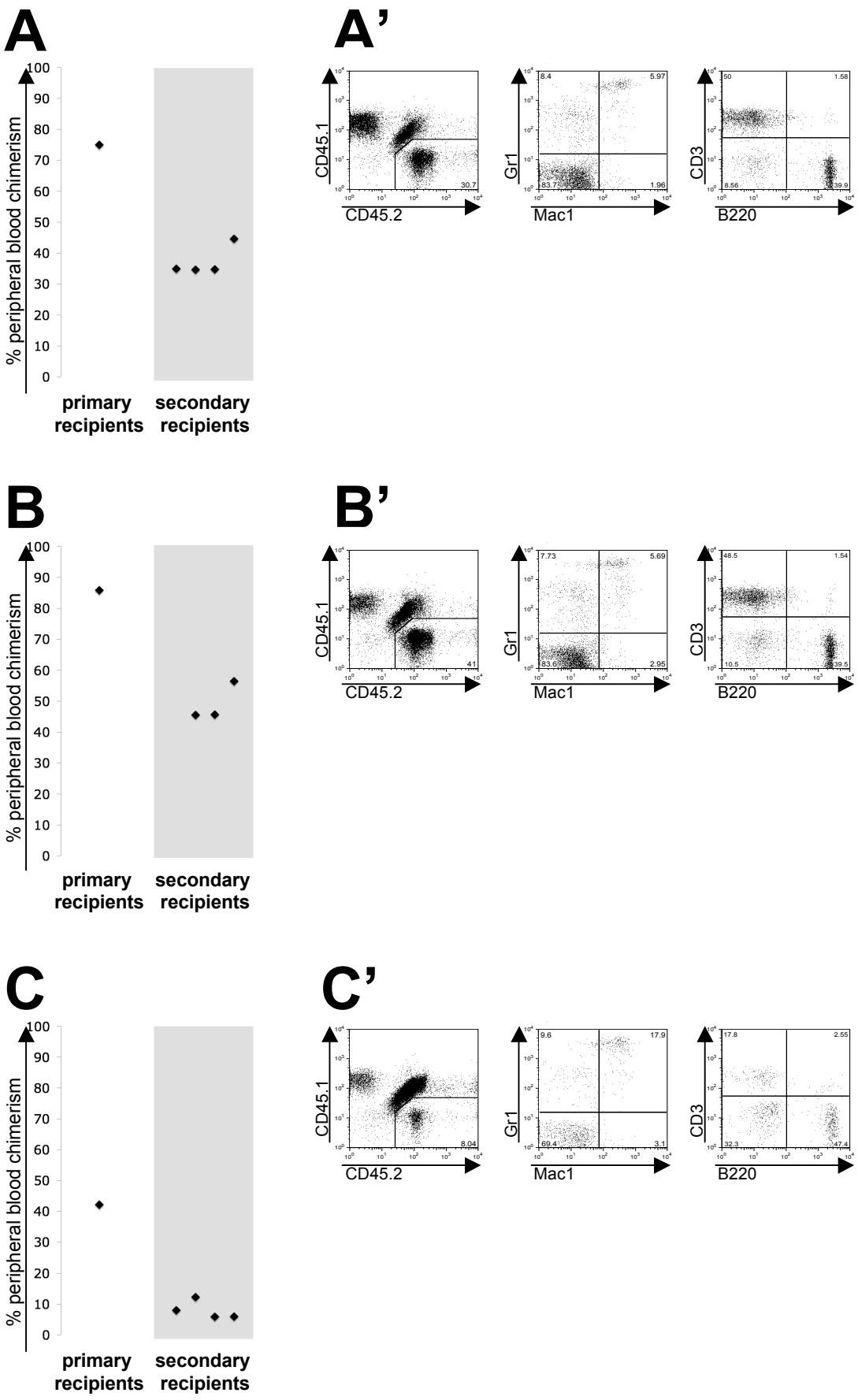
A
A'
% peripheral blood chimerism
100
90
80
70
60
50
40
30
20
10
0
primary recipients
secondary recipients
CD45.1
CD45.2
30.7
Gr1
Mac1
8.4
5.97
83.7
1.96
CD3
B220
50
1.58
8.56
39.9
B
B'
% peripheral blood chimerism
primary recipients
secondary recipients
CD45.1
CD45.2
41
Gr1
Mac1
7.73
5.69
83.6
2.95
CD3
B220
48.5
1.54
10.5
39.5
C
C'
% peripheral blood chimerism
primary recipients
secondary recipients
CD45.1
CD45.2
8.04
Gr1
Mac1
9.6
17.9
69.4
3.1
CD3
B220
17.8
2.55
32.3
47.4

Figure 3.20: Secondary transplantations of LTR-HSCs generated in the presence of single growth factor.

A, A': Secondary transplantation and multilineage reconstitution of secondary recipients transplanted with bone marrow originally reconstituted with reaggregates cultured in the presence IL-3. A: Secondary transplantation of bone marrow cells obtained from reconstituted primary recipient. A': Long-term multilineage (myelo-lymphoid) contribution in secondary recipients peripheral blood.

B, B': Secondary transplantation and multilineage reconstitution of secondary recipients transplanted with bone marrow originally reconstituted with reaggregates cultured in the presence of SCF. B: Secondary transplantation of bone marrow cells obtained from reconstituted primary recipient. B': Long-term multilineage (myelo-lymphoid) contribution in secondary recipients peripheral blood.

C, C': Secondary transplantation and multilineage reconstitution of secondary recipients transplanted with bone marrow originally reconstituted with reaggregates cultured in the presence of Flt3l. C: Secondary transplantation of bone marrow cells obtained from reconstituted primary recipient. C': Long-term multilineage (myelo-lymphoid) contribution in secondary recipients peripheral blood.

A, B, C: 1/10 of whole bone marrow (paired femurs and tibias) from the primary recipient was transplanted into each secondary recipient; peripheral blood chimerism was analysed at least 12 weeks post-transplantation.

A', B', C': Representative example of analysis from two mice reconstituted with reaggregates cultured in single growth factor conditions. Quadrants are based on appropriate isotype control (Appendix 3.2); values indicate percentages of cells. Events gated on donor derived cells.

(mean PBC: 49.2%)(Figure 3.20B). In the presence of Flt3l only, the primary recipient (42.2% PBC) bone marrow cells reconstituted 4 out of 4 secondary recipients at relatively low level (mean PBC: 7.10%)(Figure 3.20C). In all conditions, donor-derived cells of both myeloid ($Mac1^+$ and $Gr1^+$) and lymphoid ($CD3^+$ and $B220^+$) lineages were observed (Figure 3.20A', B', and C'). These results indicate that the LTR-HSCs generated in the presence of single growth factors are fully functional as they provide long-term multilineage reconstitution of secondary recipients.

3.4.2.5. Conclusions

The results presented in this section confirm that at least 2 growth factors in $IMDM^+$ are required for maximal LTR-HSC expansion. However, reaggregates cultured in IL-3 only generated higher numbers of $CD45^+$ cells, CFU-Cs and LTR-HSCs compared to other conditions, raising the possibility that IL-3 might be the most potent factor in the $IMDM^+$.

3.5. Discussion

The reaggregate culture system is a robust and reliable model for the study of LTR-HSC development in the E11.5 AGM as it allows the dissociation of the tissue prior to culture, giving access to specific cell populations, whilst maintaining the tissue's intrinsic ability to generate LTR-HSCs. Herein, culture conditions were tested and it was concluded that the extensive haematopoietic cell, precursors, and stem cell expansion during culture was due to the concerted effects of IL-3, SCF, Flt3l, and FCS.

3.5.1. The reaggregate culture system, *in vitro* model of *in vivo* LTR-HSC development?

At E11.5 the entire embryo contains from 3 to 10 LTR-HSCs, a number which rises to 70 to 150 by E12.5 (Gekas et al., 2005; Kumaravelu et al., 2002). The LTR-HSC expansion in reaggregates (approximately 146 LTR-HSCs) appears similar to the one that naturally occurs *in vivo* (Taoudi et al., 2008), implying it might recapitulate biological processes that occur during development.

An interesting aspect of the reaggregate culture is the $CD45^{+}cKit^{+}Sca1^{+}PECAM^{med}CD34^{-}$ immunophenotype of the LTR-HSCs produced, which is similar to adult LTR-HSCs rather than AGM LTR-HSCs (Baumann et al., 2004; Osawa et al., 1996; Taoudi et al., 2005; Uchida and Weissman, 1992). The lack of CD34 expression indicates that the fetal liver stage might have been by-passed (Matsuoka et al., 2001a; Taoudi et al., 2005). However, the heterogeneity for CD48 expression was intriguing. Additional experiments using a different anti-CD48 antibody clone would be required to confirm the LTR-HSC heterogeneity for CD48 expression since data previously published demonstrated that neither adult nor fetal (in E12.5 fetal liver, placenta, E9.5 YS and E11.5 AGM region) expressed CD48 (Kiel et al., 2005; Kim et al., 2006; McKinney-Freeman et al., 2009). The most likely explanation is that the *ex vivo* culture altered LTR-HSC phenotype. Such phenomenon is observed in reaggregates because, contrary to the fresh tissue, LTR-HSCs no longer express CD34 after reaggregate culture (Noda et al., 2008; Sanchez et al., 1996; Taoudi et al., 2008). Interestingly, similarly to reaggregate LTR-HSCs, HSCs obtained upon cultured of ES-cells treated with ectopic *Cdx4* and *HoxB4* do not express CD34 and are heterogenous for CD48 (McKinney-Freeman et al., 2009).

3.5.2. The requirement for growth factors in reaggregate culture

Various culture conditions were tested to identify the factors that might be of importance for LTR-HSC expansion in reaggregates.

Interestingly, some LTR-HSC expansion was retained upon removal of FCS (approximately 23 LTR-HSCs). This is promising for the future study of molecular pathways involved in LTR-HSC emergence, as they require stringent defined culture conditions. Some LTR-HSC expansion was also retained upon removal of all growth factors ($IMDM^-$)(approximately 33 LTR-HSCs), indicating that FCS is sufficient to support limited LTR-HSC expansion. However, it is important to note that FCS batch variations could potentially trigger results different to the ones reported here.

The roles of individual cytokines (IL-3, SCF, and Flt3l) in LTR-HSC expansion were investigated. These well-studied haematopoietic cytokines are commonly used for LTR-HSC culture, and their roles in various aspects of haematopoiesis have been extensively reported (see Section 1.6.2). The removal of single growth factors showed that none was dispensable for optimal LTR-HSC expansion in E11.5 AGM reaggregates.

When reaggregates were cultured in the presence of single growth factors, there were significantly fewer LTR-HSC compared to control and to numbers obtained in the presence of 2 growth factors. This indicates that the concerted action of at least growth factors enhances LTR-HSC expansion. Approximately 35 LTR-HSCs were obtained when reaggregates were cultured in IL-3, a result comparable to that observed in E11.5 AGM explants (Robin et al., 2006). Apart from cultures with IL-3 only, the numbers of LTR-HSC in other conditions are comparable to the one obtained in $IMDM^-$ (approximately between 10 and 25 LTR-HSCs). Thus, SCF and Flt3l on their own are not sufficient to support extensive LTR-HSC expansion. Altogether, these observations supported the conclusion that growth factors act in a synergistic way. This result was expected because previous studies have reported that Flt3l strongly synergises with other haematopoietic growth factors, including SCF, and interleukins (Buza-Vidas et al., 2009; Diehl et al., 2007; Gilliland and Griffin, 2002).

Although various growth factor combinations yielded different numbers of LTR-HSCs, successful multilineage contribution and secondary transplantations was achieved in each condition, demonstrating that LTR-HSCs were fully functional.

Most of LTR-HSC numbers in this study were estimated based on the proportion of reconstituted animals in each condition. Limiting dilution analyses will be required to determine the exact numbers of LTR-HSCs in each condition, thus defining more accurately the roles of each cytokine in reaggregate culture. Each cytokine might act on different processes involved in LTR-HSC development. As it has been shown that (although proliferation may also be important) the extensive LTR-HSC expansion observed in reaggregates is the result of pre-HSC maturation (Taoudi et al., 2008), future studies will aim to understand which individual cytokine promotes such process.

4. Characterisation of Runx1 expression in the *Runx1*^{EGFP} reporter mouse model

4.1. Introduction

The second part of this study focused on the role of Runx1 in the emergence of LTR-HSCs in the E11.5 AGM region and investigating Runx1 expression in pre-HSC populations.

Although current theory states that Runx1 transcription factor is required for the transition from endothelial to haematopoietic fate, its precise role remains unclear (see Section 1.5.3).

Various Runx1 reporter mouse models were generated to track Runx1 expression and better understand its roles in haematopoiesis. The Runx1-LacZ reporter mouse contains *LacZ* sequences fused to the 3' coding sequence of the *Runx1* locus and generates a non-functional allele (*Runx1*^{lz})(North et al., 1999). Haploinsufficient dose of Runx1 results in fewer CFU-Cs and CFU-S_{11} in the YS, fetal liver and AGM region (Cai et al., 2000; Mukouyama et al., 2000; Wang et al., 1996a), and in deviation of spatial and temporal LTR-HSC development (Cai et al., 2000). To avoid haploinsufficiency, another Runx1 reporter mouse model was generated by introducing *Runx1* cDNA linked to green fluorescent protein (GFP) via internal ribosome entry site (IRES) sequences within the endogenous *Runx1* locus (*Runx1*^{GFP})(Lorsbach et al., 2004). Although Runx1 protein is functional, this mouse expresses only one major Runx1 isoform, Runx1b. In addition, the presence of an active selection marker here may interfer with expression of nearby genes or Runx1 itself. Also, important regulatory elements within the Runx1 3'UTR are not active in this model.

To avoid these potential problems, A. Suleman in our laboratory produced a Runx1 mouse reporter line in which an IRES-EGFP sequence was introduced after exon 6 of the Runx1 locus (Figure 4.1A). The insertion of IRES-EGFP does not replace any genomic sequence and leaves both the Runx1 promoters and the 3'UTR regulatory sequences intact, allowing normal regulation of Runx1 expression. In addition, EGFP was chosen as the reporter protein because it is significantly brighter than WT GFP owing to a double amino-acid substitution of FL64,65ST (Yang et al., 1996). This allows more sensitive detection of Runx1 expression levels.

By introducing only a subtle modification within the targeted Runx1 locus, *Runx1*^{EGFP} reporter mice should provide an accurate model for studying the temporal and spatial expression pattern of Runx1 in the embryo and the adult. It is also useful for purification of various Runx1^{+} populations for *ex vivo* assays.

The first goal of this study was to perform extensive descriptive and functional analysis of the *Runx1*$^{EGFP/EGFP}$ line to determine if these animals display any detectable phenotype. The second goal was to identify which cell populations express Runx1 in both the adult haematopoietic system and in the E11.5 AGM.

4.2. Genotyping of the *Runx1*^{EGFP} mice

As targeting experiments were performed on the 129 genetic background, the *Runx1*^{EGFP} mouse line was backcrossed for 8 generations to transfer the line to the pure C57 Bl/6 genetic background (see Section 2.3.2) and allow *in vivo* transplantations into C57 Bl/6 recipient mice.

For genotyping animals, PCR primers were designed by H. Inoue in our laboratory and consisted of: two forward primers, one within Runx1 exon 6 and another one within the IRES-EGFP sequence, and a reverse primer located within the Runx1 3'UTR (Figure 4.1A; sequences provided in Table 2.1). Resulting PCR products were 367bp for the *Runx1*^{WT} allele and 304bp for the *Runx1*^{EGFP} allele. Sizes of PCR products were determined by agarose gel electrophoresis in comparison with migration of 1KB ladder. DNA controls (both *Runx1*^{WT} and *Runx1*^{EGFP}) and

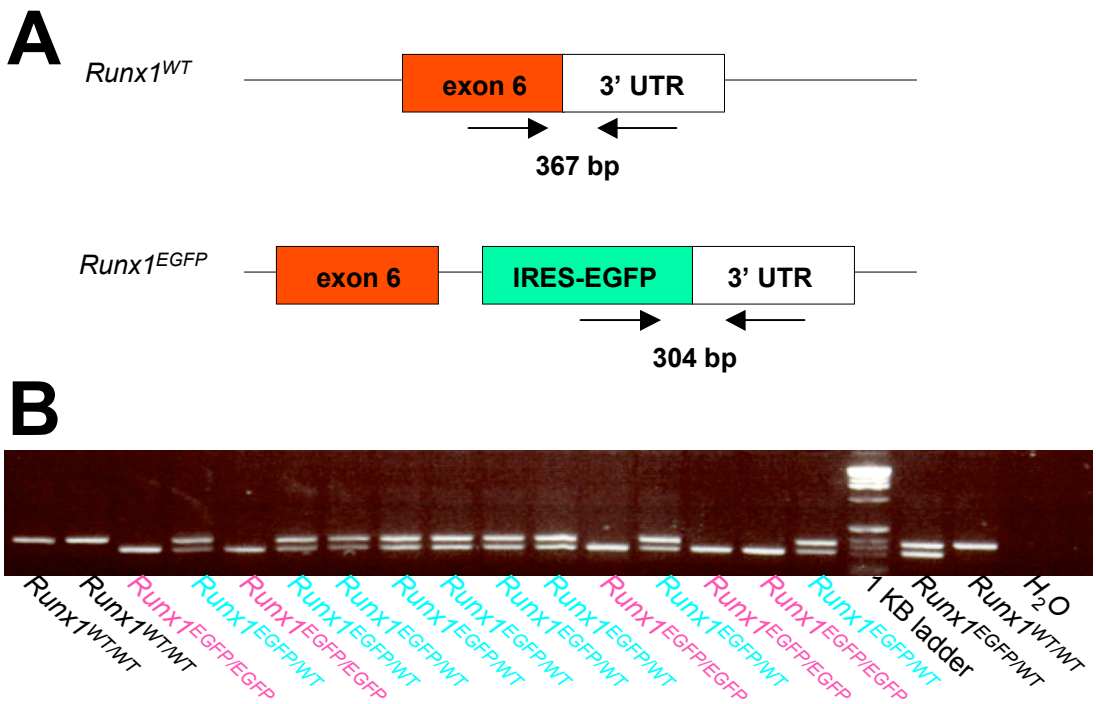

Figure 4.1: *Runx1*^{EGFP} mouse line PCR genotyping design.
A: Schematic representation of *Runx1*^{WT} and Runx1^{EGFP} alleles with primer sets (arrows) used for genotyping and sizes of the resulting PCR fragments.
B: Representative example of PCR genotyping performed on offspring from *Runx1*$^{EGFP/WT}$ X *Runx1*$^{EGFP/WT}$ cross. Each lane corresponds to an individual animal; upper fragment corresponds to *Runx1*^{WT} (367bp) and lower fragment corresponds to *Runx1*^{EGFP} (304bp). Fragment sizes were determined based on 1KB ladder migration. H_2O controls were run in every case to detect cases of contamination. Black: *Runx1*$^{WT/WT}$, Blue: *Runx1*$^{EGFP/WT}$, Pink: *Runx1*$^{EGFP/EGFP}$.

water control were run along with samples (Figure 4.1B). The black, blue, and pink genotypes in future figures refer to *Runx1*$^{WT/WT}$, *Runx1*$^{EGFP/WT}$, and *Runx1*$^{EGFP/EGFP}$ animals respectively.

All experiments in this study were performed with *Runx1*$^{WT/WT}$ age matched controls. Unless otherwise stated, all adult and embryonic Runx1 expression analyses presented here were performed on a mixed genetic background.

4.3. Mendelian inheritance pattern of the *Runx1*^{EGFP} mouse line

Runx1^{EGFP} mice were expected to have a phenotype comparable with *Runx1*^{WT} animals, due to only minor modification introduced into the Runx1 locus.

No obvious morphological defects were observed in *Runx1*$^{EGFP/EGFP}$ adults and E11.5 embryos. *Runx1*^{EGFP} mice were born in expected Mendelian ratio (Table 4.1). Crosses of *Runx1*$^{EGFP/WT}$ males and *Runx1*$^{EGFP/WT}$ females produced 25% of *Runx1*$^{WT/WT}$, 48% of *Runx1*$^{EGFP/WT}$, and 28% of *Runx1*$^{EGFP/EGFP}$ of offsprings (expected ratio is 25% of *Runx1*$^{WT/WT}$, 50% of *Runx1*$^{EGFP/WT}$, and 25% of *Runx1*$^{EGFP/EGFP}$).

To rule out the possibility that a proportion of transgenic animals preferably die before birth, E11.5 embryos from *Runx1*$^{EGFP/WT}$ x *Runx1*$^{EGFP/WT}$ crosses were analysed. Out of a total of 36 embryos, 28% were *Runx1*$^{WT/WT}$, 50% were *Runx1*$^{EGFP/WT}$, and 22% were *Runx1*$^{EGFP/EGFP}$ (Table 4.1), roughly coinciding with predicted Mendelian ratio. Slightly low percentage of *Runx1*$^{EGFP/EGFP}$ embryos (22%) can be explained by the low numbers of litters. No breeding impairment was observed when the mouse line was maintained as a homozygous *Runx1*$^{EGFP/EGFP}$ colony.

Table 4.1: *Runx1*^{EGFP} mouse line breed in Mendelian proportions.

Total numbers and the relative percentage of offspring with different genotypes (*Runx1*$^{WT/WT}$, *Runx1*$^{EGFP/WT}$, *Runx1*$^{EGFP/EGFP}$) obtained from *Runx1*$^{EGFP/WT}$ X *Runx1*$^{EGFP/WT}$ cross. Animal numbers were obtained by genotyping both adult and E11.5 animals.
Numbers in brackets correspond to Mendelian breeding ratios proportions .

		Runx1$^{WT/WT}$	*Runx1*$^{EGFP/WT}$	*Runx1*$^{EGFP/EGFP}$
adult	animals	25	48	28
	% of total	25% (25%)	48% (50%)	28% (25%)
E11.5	animals	10	18	8
embryos	% of total	28% (25%)	50% (50%)	22% (25%)

Table 4.2: Cellularity of adult haematopoietic organs of *Runx1*$^{EGFP/EGFP}$ animals compared to *Runx1*$^{WT/WT}$ animals.

Haematopoietic organs were obtained from aged-matched individual adult males. Cell counts were performed using Newbauer haemocytometer.
Absolute numbers ± standard deviation; average of 6 independent experiments.

Cell counts (x10^5)		
	Runx1$^{WT/WT}$	*Runx1*$^{EGFP/EGFP}$
bone marrow	235 ± 48	209 ± 14
spleen	992 ± 99	1076 ± 171
thymus	762 ± 204	680 ± 143

4.4. Absence of detectable phenotype in the *Runx1*^{EGFP} mice

4.4.1. Cellularity of *Runx1*$^{EGFP/EGFP}$ adult haematopoietic organs

The cellularity of major adult haematopoietic organs (bone marrow, spleen, and thymus) was compared between *Runx1*$^{WT/WT}$ and *Runx1*$^{EGFP/EGFP}$ males. Of importance, transgenic animals were all age matched and on pure C57 Bl/6 background. *Runx1*$^{WT/WT}$ and *Runx1*$^{EGFP/EGFP}$ adult bone marrows (count made from paired femurs and tibias) contained a total of 235±48 x10^5 cells and 209±14 x10^5 cells respectively (Table 4.2). Statistical analysis using a paired T-test revealed no significant difference between *Runx1*$^{WT/WT}$ and *Runx1*$^{EGFP/EGFP}$ bone marrows ($p = 0.129$).

Runx1$^{WT/WT}$ and *Runx1*$^{EGFP/EGFP}$ adult spleens contained a total of 992±99 x10^5 cells and 1076±171 x10^5 cells respectively (Table 4.2). Paired T-test revealed no significant difference between *Runx1*$^{WT/WT}$ and *Runx1*$^{EGFP/EGFP}$ spleens ($p = 0.301$).

Runx1$^{WT/WT}$ and *Runx1*$^{EGFP/EGFP}$ adult thymi contained a total of 762±204 x10^5 cells and 680±203 x10^5 cells respectively (Table 4.2). Paired T-test revealed no significant difference between *Runx1*$^{WT/WT}$ and *Runx1*$^{EGFP/EGFP}$ thymi ($p = 0.115$).

Thus, no difference was observed in the cellularity of major adult haematopoietic organs (bone marrow, spleen and thymus) between *Runx1*$^{WT/WT}$ and fully backcrossed *Runx1*$^{EGFP/EGFP}$ adults.

4.4.2. Heamatopoietic progenitors content in *Runx1*$^{EGFP/EGFP}$ adult bone marrow

To further investigate whether *Runx1*$^{EGFP/EGFP}$ mice on a C57 Bl/6 background have a haematopoietic phenotype, numbers of CFU-Cs contained in the bone marrow of *Runx1*$^{WT/WT}$ and *Runx1*$^{EGFP/EGFP}$ adult males were compared. There

were 76±5 CFU-Cs per $2x10^4$ *Runx1*$^{WT/WT}$ bone marrow cells (19±2 CFU-mast, 4±3 BFU-E, 30±9 CFU-GM, 22±3 CFU-mac, and 1±1 CFU-GEMM)(Figure 4.2). In comparison, *Runx1*$^{EGFP/EGFP}$ bone marrow contained 72±11 CFU-Cs per $2x10^4$ cells (18±4 CFU-mast, 5±4 BFU-E, 26±8 CFU-GM, 23±6 CFU-mac, and 1±1 CFU-GEMM)(Figure 4.2). Paired T-test showed no significant difference in bone marrow CFU-Cs numbers between *Runx1*$^{WT/WT}$ and *Runx1*$^{EGFP/EGFP}$ animals ($p = 0.591$).

4.4.3. Cellularity of the *Runx1*^{EGFP} E11.5 AGM region

E11.5 AGM regions from *Runx1*$^{WT/WT}$, *Runx1*$^{EGFP/WT}$, and *Runx1*$^{EGFP/EGFP}$ embryos were dissected and cell counted. These animals looked morphologically normal at E11.5, with no obvious defect. Numbers of cells in the E11.5 AGM region were summarized in Table 4.3. A paired T-test showed a significant difference between *Runx1*$^{WT/WT}$ and *Runx1*$^{EGFP/WT}$ AGM total cell numbers ($p=0.003$). Intriguingly, no difference was observed between *Runx1*$^{WT/WT}$ and *Runx1*$^{EGFP/EGFP}$ animals (paired T-test, $p=0.1$). However, Wilcoxon signed-rank test showed no significant difference between $CD45^+$ cell numbers among genotypes ($p \geq 0.2$ in each case). Such observation has various explanations. First, some human error is likely when performing haemocytometer based cell counts so additional replicates would be required for more powerful statistical analysis. Second, the fact that $CD45^+$ cell numbers were similar in *Runx1*$^{WT/WT}$, *Runx1*$^{EGFP/WT}$, and *Runx1*$^{EGFP/EGFP}$ embryos suggests that normal haematopoiesis occurs in transgenic embryos, but perhaps other stromal cell types are sensitive and preferentially die during flow cytometry processing.

4.4.4. Flow cytometric analysis of *Runx1*^{EGFP} mice

Flow cytometric analyses were performed in *Runx1*^{EGFP} mice to characterise populations expressing EGFP in the adult and embryonic haematopoietic systems. To pick possible differences and an eventual haematopoietic phenotype, percentages of cells falling into each cell population were compared between *Runx1*$^{WT/WT}$ and *Runx1*^{EGFP} animals.

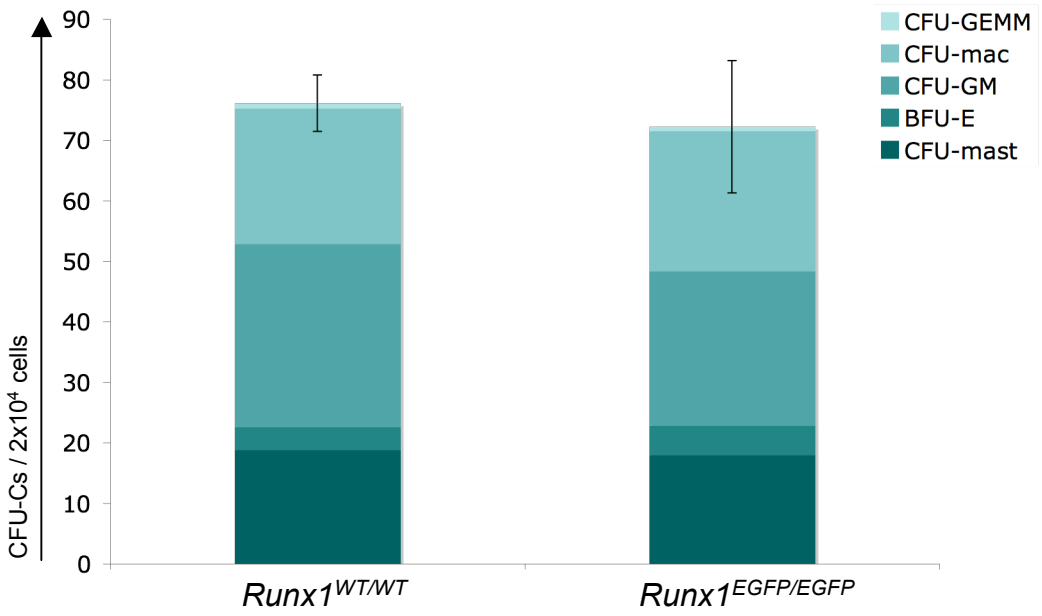

Figure 4.2: Haematopoietic progenitors contained in adult bone marrow of *Runx1*$^{EGFP/EGFP}$ animals compared to *Runx1*$^{WT/WT}$ animals.

Bars indicate the standard deviation of 4 independent experiments for total CFU-Cs.

BFU-E: burst forming unit-erythroid; CFU: colony forming unit; Mac: macrophage; GM: granulocyte/macrophage; GEMM: granulocyte/erythroid/macrophage/megakaryocyte.

Table 4.3: Comparison of the cell compositions of *Runx1*$^{WT/WT}$, *Runx1*$^{EGFP/WT}$, and *Runx1*$^{EGFP/EGFP}$ E11.5 AGM regions.

Data is representative of 7 independent experiments for *Runx1*$^{WT/WT}$ embryos, 3 independent experiments for *Runx1*$^{EGFP/WT}$ embryos, and 4 independent experiments for *Runx1*$^{EGFP/EGFP}$ embryos.

Data was acquired by flow cytometric analysis; cell viability was determined by 7-AAD uptake. Absolute numbers ± standard deviation; EGFP: enhanced green fluorescent protein; WT: wild type

	Runx1 $^{WT/WT}$	***Runx1*** $^{EGFP/WT}$	***Runx1*** $^{EGFP/EGFP}$
total cells	293530 ± 41490	239440 ± 27400	272990 ± 44900
live cells	94440 ± 25380	89780 ± 20120	86630 ± 18230
CD45$^+$ cells	3200 ± 780	3670 ± 570	3460 ± 940

In the adult haematopoietic system, Wilcoxon signed-rank test showed no significant differences in percentages of cells between *Runx1*$^{WT/WT}$ and *Runx1*$^{EGFP/WT}$ mice in any of the cell populations and tissues tested ($p \geq 0.2$ in all gates). Original flow cytometry dot plots were provided in Figures 4.4A, 4.5A B C, 4.6A B, 4.7A B, 4.8A B C D, and 4.9 and percentages of cells were summarized in Figure 4.9.

In the E11.5 AGM region, Wilcoxon signed-rank test showed no significant differences in percentages of cells between *Runx1*$^{WT/WT}$ and *Runx1*$^{EGFP/EGFP}$ embryos in any of the cell populations tested ($p \geq 0.2$ in all gates)(Figure 4.11A, 4.12A, 4.13A, and 4.14A, summarized in Figure 4.9). Although not statistically different, percentages of cells in haematopoietic cell populations were consistently higher in the *Runx1*$^{EGFP/EGFP}$ embryos compared to *Runx1*$^{WT/WT}$ embryos. Although results were collected from 4 independent experiments, this observation highlights the limitations of statistical analysis with low numbers of replicates and the need for additional experiments to detect very small but significant differences between *Runx1*$^{WT/WT}$ and *Runx1*$^{EGFP/EGFP}$ mice.

4.5. Characterisation of Runx1 expression in the *Runx1*^{EGFP} adult mouse

4.5.1. Runx1 expression in the bone marrow lin$^-$sca1$^+$c-kit$^+$ (LSK) fraction

LTR-HSCs are phenotypically characterised by the absence of expression of mature lineage markers (Weissman et al., 2001). To investigate Runx1 expression in the LTR-HSC population and non-committed progenitors of adult bone marrow, flow cytometric analysis using a cocktail of lineage specific antibodies (anti-CD3ε, anti-CD4, anti-CD8, anti-B220, anti-Gr1, anti-Mac1, anti-Ter119) permitted the exclusion of mature haematopoietic cells; and Sca1 and c-kit staining allowed detection of the LSK fraction, which is highly enriched in LTR-HSCs (Osawa et al., 1996; Wagers et al., 2002). All flow cytometric analyses within this section were

carried out using age-matched *Runx1*$^{WT/WT}$ and *Runx1*$^{EGFP/WT}$ adult males on a C57 Bl/6 background.

Adult bone marrow from *Runx1*$^{WT/WT}$ and *Runx1*$^{EGFP/WT}$ mice contained 2.62±0.7% and 2.21±0.6% of lin$^-$ cells respectively. Whole population shifts were observed in all the lin$^-$ populations except Sca1$^-$c-kit$^-$ (Figure 4.3B). Conservative gating was performed in each histogram to obtain an approximate percentage of cells expressing EGFP. The EGFP$^+$ cells represented 35.1±6.8% of the lin$^-$sca1$^-$c-kit$^-$ population, 77.3±7.1% of the lin$^-$sca1$^-$c-kit$^+$ population, 18.2±21% of the lin$^-$sca1$^+$c-kit$^-$ population, and 75.3±15% of the LSK population (Figure 4.3B).

The median fluorescence intensity (MFI) shift of the *Runx1*$^{EGFP/WT}$ mice compared to *Runx1*$^{WT/WT}$ mice was 6.5±0.4 in the lin$^-$sca1$^-$c-kit$^-$ population, 21.4±0.9 in the lin$^-$sca1$^-$c-kit$^+$ population, 6.33±0.2 in the lin$^-$sca1$^+$c-kit$^-$ population, and 11.16±0.9 in the LSK population (Figure 4.3B; Table 4.3).

Altogether, these data show that EGFP/Runx1 is expressed in all lin$^-$ cell fractions of the bone marrow. Fractions with the highest proportion of EGFP$^+$ cells as well as the highest EGFP intensity (shown by highest relative MFI) were lin$^-$Sca1$^-$c-kit$^+$ and LSK. This strongly suggests that adult bone marrow LTR-HSCs express high levels of Runx1, confirming findings of the haploinsufficient model (North et al., 2004).

4.5.2. Runx1 expression in myeloid lineages in *Runx1*$^{EGFP/WT}$ adult mouse

4.5.2.1. Runx1 expression in granulocytes and monocytes

Because Runx1 is involved in many fusion genes associated with myeloid leukaemias, it is likely that Runx1 plays a role during myeloid lineages differentiation (Speck and Gilliland, 2002). To investigate Runx1 expression in granulocytes and monocytes, haematopoietic organs (bone marrow, blood, and spleen) were dissected from *Runx1*$^{EGFP/WT}$ adult mice, stained for the granulocyte and monocyte markers Gr1 and Mac1, and analysed by flow cytometry. Contrary to other

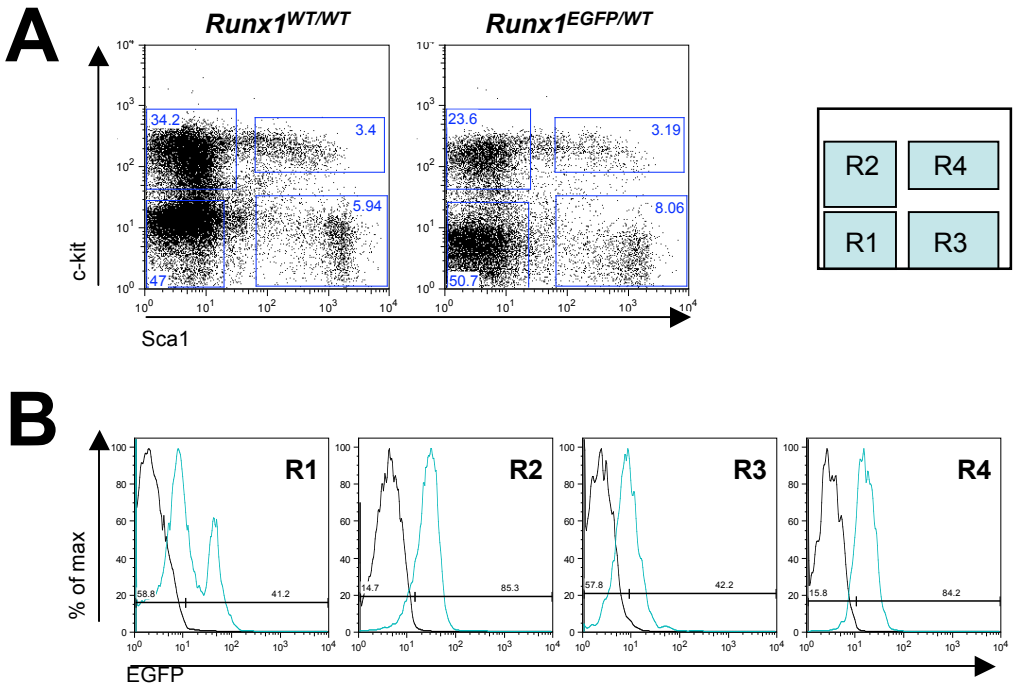

Figure 4.3: EGFP expression within adult bone marrow lin$^-$c-kit$^+$Sca1$^+$fraction.
A: Representative lin$^-$sca1$^+$c-kit$^+$ (LSK) stains in adult bone marrow of *Runx1*$^{EGFP/WT}$ animals compared to *Runx1*$^{WT/WT}$ animals. Quadrants were based on appropriate isotype controls (Appendix 4.1A) and values indicate percentages of cells
B: Histograms showing EGFP expression in sca1$^-$c-kit$^-$, sca1$^-$c-kit$^+$, sca1$^+$c-kit$^-$, and sca1$^+$c-kit$^+$ fractions. Black: *Runx1*$^{WT/WT}$ animals; Blue: *Runx1*$^{EGFP/WT}$ animals. Values indicate percentages of cells in *Runx1*$^{EGFP/WT}$ animals.
Cells were stained with a cocktail of antibodies against mature lineage markers (anti-CD3ε, anti-CD4, anti-CD8, anti-B220, anti-Gr1, anti-Mac1, anti-Ter119), positive cells for those markers were excluded along with dead cells (uptaking 7-AAD) in the Fl-3 channel.
Plots are representative examples of 3 independent experiments.

Runx1 reporter models (Lorsbach et al., 2004; North et al., 1999), analysis of the percentage of EGFP positive cells in our *Runx1*^{EGFP} mouse was problematic due to very small EGFP shifts. As a result, conservative gating was not appropriate. Instead, measures of the MFI in *Runx1*$^{EGFP/WT}$ mice compared to *Runx1*$^{WT/WT}$ mice were presented to report small, yet consistent, population shifts (summarized in Table 4.4). Finally, to prove that very small EGFP shifts in the FL-1 channel were not a false positive signal due to under-compensation from the FL-2 channel, FL-2 single stains performed in *Runx1*$^{WT/WT}$ tissues were presented in Appendix 4.1.

In the adult bone marrow, the MFI shift of the *Runx1*$^{EGFP/WT}$ mice compared to *Runx1*$^{WT/WT}$ mice was 1.66±0.5 in the Mac1^{-}Gr1^{-} population, 5.08±1.4 in the Mac1^{lo}Gr1^{-} population, 2.95±0.67 in the Mac1^{hi}Gr1^{lo} population, and 1.9±0.2 in the Mac1^{hi}Gr1^{hi} population (Figure 4.4A; Table 4.4).

In the peripheral blood, the MFI shift of the *Runx1*$^{EGFP/WT}$ mice compared to *Runx1*$^{WT/WT}$ mice was 2.09±0.15 in the Mac1^{-}Gr1^{-} population, 2.23±0.3 in the Mac1^{lo}Gr1^{-} population, 2.43±0.7 in the Mac1^{hi}Gr1^{lo} population, and 6.1±2.8 in the Mac1^{hi}Gr1^{hi} population (Figure 4.4B; Table 4.4).

In the spleen, the MFI shift of the *Runx1*$^{EGFP/WT}$ mice compared to *Runx1*$^{WT/WT}$ mice was 0.88±0.1 in the Mac1^{-}Gr1^{-} population, 1.52±0.3 in the Mac1^{lo}Gr1^{-} population, 1.7±0.5 in the Mac1^{hi}Gr1^{lo} population, and 1.1±0.3 in Mac1^{hi}Gr1^{hi} population (Figure 4.4C; Table 4.4).

Mac1^{lo}Gr1^{-} cell population, which contains monocytes, expressed the highest levels of EGFP in bone marrow, as shown by the MFI analysis. As previously reported, MFI shifts become smaller upon increasing expression of the Gr1 antigen in the bone marrow (Lorsbach et al., 2004). Because Gr1 expression increases in maturing myeloid cells, the MFI analysis here suggests that Runx1 expression decreases upon myeloid maturation (Lorsbach et al., 2004).

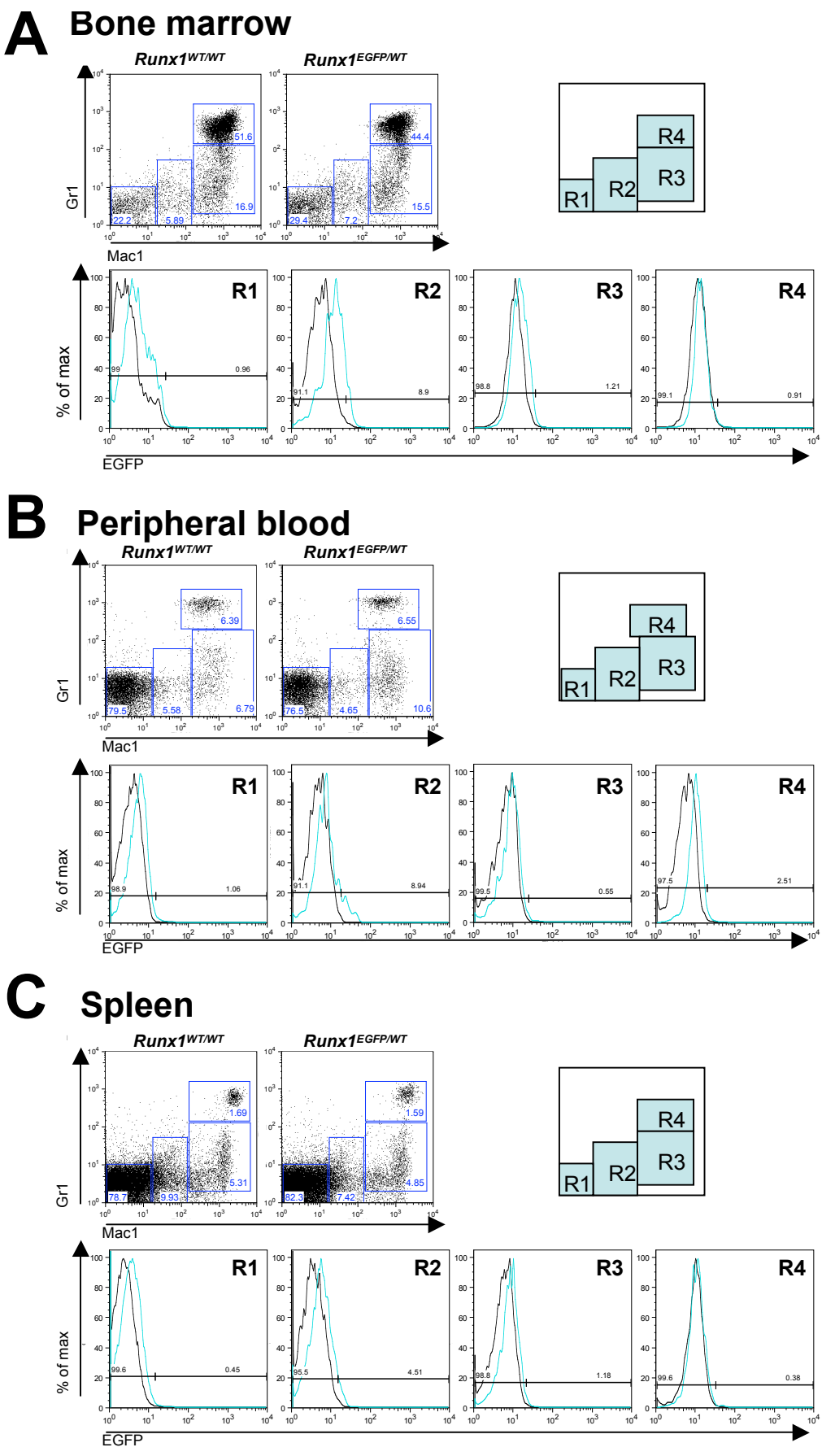
A
Bone marrow
Runx1WT/WT
Runx1EGFP/WT
Gr1
Mac1
51.6
16.9
22.2
5.89
44.4
15.5
29.4
7.2
R1
R2
R3
R4
% of max
EGFP
0.96
8.9
1.21
0.91
99
91.1
98.8
99.1
B
Peripheral blood
6.39
6.79
79.5
5.58
6.55
10.6
76.5
4.65
1.06
8.94
0.55
2.51
98.9
91.1
99.5
97.5
C
Spleen
1.69
5.31
78.7
9.93
1.59
4.85
82.3
7.42
0.45
4.51
1.18
0.38
99.6
95.5
98.8
99.6

Figure 4.4: EGFP expression in myeloid cells: granulocytes and macrophages lineages.
A: Representative Mac1 Gr1 stains in adult bone marrow of *Runx1*$^{EGFP/WT}$ animals compared to *Runx1*$^{WT/WT}$ animals and histograms showing EGFP expression in Mac1^{-}Gr1^{-}, Mac1^{lo}Gr1^{lo}, Mac1^{hi}Gr1^{lo}, and Mac1^{hi}Gr1^{hi} fractions in the bone marrow.
B: Representative Mac1 Gr1 stains in adult peripheral blood of *Runx1*$^{EGFP/WT}$ animals compared to *Runx1*$^{WT/WT}$ animals and histograms showing EGFP expression in Mac1^{-}Gr1^{-}, Mac1^{lo}Gr1^{lo}, Mac1^{hi}Gr1^{lo}, and Mac1^{hi}Gr1^{hi} fractions in the peripheral blood.
C: Representative Mac1 Gr1 stains in adult spleen of *Runx1*$^{EGFP/WT}$ animals compared to *Runx1*$^{WT/WT}$ animals and histograms showing EGFP expression in Mac1^{-}Gr1^{-}, Mac1^{lo}Gr1^{lo}, Mac1^{hi}Gr1^{lo}, and Mac1^{hi}Gr1^{hi} fractions in the spleen.
Black: *Runx1*$^{WT/WT}$ animals; Blue: *Runx1*$^{EGFP/WT}$ animals. Quadrants on dot plots were based on appropriate isotype controls (Appendix 4.1B); values indicate percentages of cells. Cell viability was determined by 7-AAD uptake. In histograms, values indicate percentages of cells in *Runx1*$^{EGFP/WT}$ animals.
All plots are representative examples of 3 independent experiments.

4.5.2.2. Runx1 expression during erythroid differentiation

To characterise Runx1 expression in the erythroid lineage, bone marrow and spleen cells from *Runx1*$^{EGFP/WT}$ adult mice were collected and analysed on the basis of co-expression of CD45 and Ter119 markers (Kina et al., 2000). Indeed, erythrocyte maturation is described by the down regulation of CD45 marker and the acquisition of Ter119 marker, and thus processes through the following immunophenotypes: CD45^{hi}Ter119^{-}, CD45^{hi}Ter119^{+}, CD45^{lo}Ter119^{+}, CD45^{-}Ter119^{+} (Kina et al., 2000).

In the adult bone marrow, the MFI shift of the *Runx1*$^{EGFP/WT}$ mice compared to *Runx1*$^{WT/WT}$ mice was 6.11±1.0 in the CD45^{hi}Ter119^{-} population, 5.54±0.8 in the CD45^{hi}Ter119^{+} population, 1.6±0.5 in the CD45^{lo}Ter119^{+} population, and 0.25±0.06 in the CD45^{-}Ter119^{+} population (Figure 4.5A; Table 4.4).

In the adult spleen, the MFI shift of the *Runx1*$^{EGFP/WT}$ mice compared to *Runx1*$^{WT/WT}$ mice was 2.04±0.3 in the CD45^{hi}Ter119^{-} population, 2.03±0.3 in the CD45^{hi}Ter119^{+} population, 0±0.1 in the CD45^{lo}Ter119^{+} population, and 0±0.04 in the CD45^{-}Ter119^{+} population (Figure 4.5B; Table 4.4).

Here, Runx1 expression is down regulated during erythrocyte development, consistent with previous reports (Lorsbach et al., 2004; North et al., 2004). However, additional Ter119 CD71 staining would be needed to describe more precisely the patterns of Runx1 expression during specific stages of erythrocyte maturation.

4.5.3. Runx1 expression in lymphoid lineages in *Runx1*$^{EGFP/WT}$ adult mouse

4.5.3.1. Runx1 expression in T cell lineages

Reports have shown that Runx1 is involved at various stages of T cell development (Collins et al., 2009). Anti-CD4 and anti-CD8 antibodies are commonly used to characterise T cell maturation stages and are also markers for mature helper T cells and cytotoxic T cells respectively (Collins et al., 2009). Both were used to stain peripheral blood and thymus from *Runx1*$^{WT/WT}$ and *Runx1*$^{EGFP/WT}$ adult males.

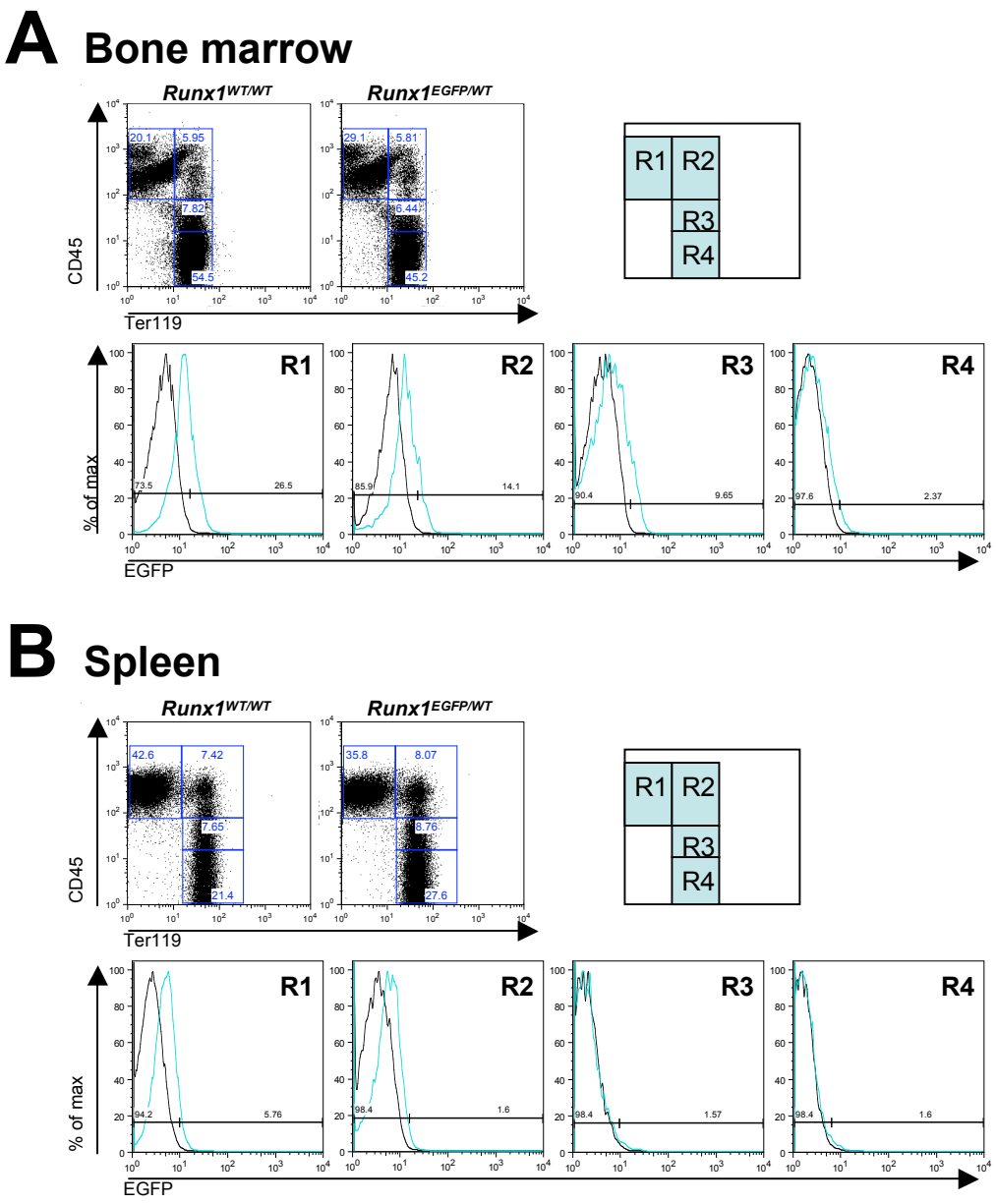

Figure 4.5: EGFP expression in myeloid cells: erythroid lineage.

A: Representative CD45 Ter119 stains in adult bone marrow of *Runx1*$^{EGFP/WT}$ animals compared to *Runx1*$^{WT/WT}$ animals and histograms showing EGFP expression in CD45^{+}Ter119^{-}, CD45^{+}Ter119^{+}, CD45^{lo}Ter119^{+}, and CD45^{-}Ter119^{+} fractions in the bone marrow.

B: Representative CD45 Ter119 stains in adult spleen of *Runx1*$^{EGFP/WT}$ animals compared to *Runx1*$^{WT/WT}$ animals and histograms showing EGFP expression in CD45^{+}Ter119^{-}, CD45^{+}Ter119^{+}, CD45^{lo}Ter119^{+}, and CD45^{-}Ter119^{+} fractions in the spleen.

Black: *Runx1*$^{WT/WT}$ animals; Blue: *Runx1*$^{EGFP/WT}$ animals. Quadrants on dot plots were based on appropriate isotype controls (Appendix 4.1C); values indicate percentages of cells. Cell viability was determined by 7-AAD uptake.

In histograms, values indicate percentages of cells for *Runx1*$^{EGFP/WT}$ animals.

All plots are representative examples of 3 independent experiments.

In the peripheral blood, the MFI shift of the *Runx1*$^{EGFP/WT}$ mice compared to *Runx1*$^{WT/WT}$ mice was 2.5±0.3 in the CD4^{-}CD8^{-} population, 1.76±0.3 in the CD4^{+}CD8^{-} population, and 0.91±0.3 in the CD4^{-}CD8^{+} population (Figure 4.6A; Table 4.4). CD4^{+}CD8^{+} population was not analysed because its percentage was insignificant (Figure 4.6A; Table 4.4). A small subset of autofluorescent cells in the CD4^{-}CD8^{+} and CD4^{+}CD8^{-} cell populations (1.06±1.2% and 1.5±1.2 respectively) could be observed (Figure 4.6A).

In the thymus, the MFI shift of the *Runx1*$^{EGFP/WT}$ mice compared to *Runx1*$^{WT/WT}$ mice was 3±0.4 in the CD4^{-}CD8^{-} population, 3.0±0.5 in the CD4^{+}CD8^{-} population, 1.6±0.1 in the CD4^{-}CD8^{+} population, and 2.93± 0.3 in the CD4^{+}CD8^{+} population (Figure 4.6B; Table 4.4).

In addition to CD4 and CD8, populations of mature T cells were analysed for EGFP expression using anti-CD3 antibody in adult haematopoietic tissues (bone marrow, peripheral blood, spleen and thymus). In the T cell CD3^{+}B220^{-} population the MFI shift of the *Runx1*$^{EGFP/WT}$ mice compared to *Runx1*$^{WT/WT}$ mice was 1.4±0.3 in the bone marrow, 1.67±0.3 in the peripheral blood, 0.62±0.17 in the spleen, and 1.68±0.1 in the thymus (Figure 4.7A, B, C, D; Table 4.4).

Altogether, there is very little expression of EGFP in T cell compartment of *Runx1*$^{EGFP/WT}$ adult mouse. As previously reported, populations of mature T cells (CD4^{+}CD8^{-}, CD4^{-}CD8^{+} and CD3^{+}B220^{-}) generally have stronger EGFP expression in the thymus compared to other organs (Lorsbach et al., 2004). Analysis also showed that the EGFP expression in the thymus was the highest in CD4^{-}CD8^{-} cells, in line with the role of Runx1 in the transition from CD4^{-}CD8^{-} to CD4^{+}CD8^{+} stages of T cell maturation (Growney et al., 2005; Putz et al., 2006). Additionally, EGFP was stronger in CD4^{+}CD8^{-} cells compared to CD4^{-}CD8^{+} cells, also consistent with published observations (Lorsbach et al., 2004).

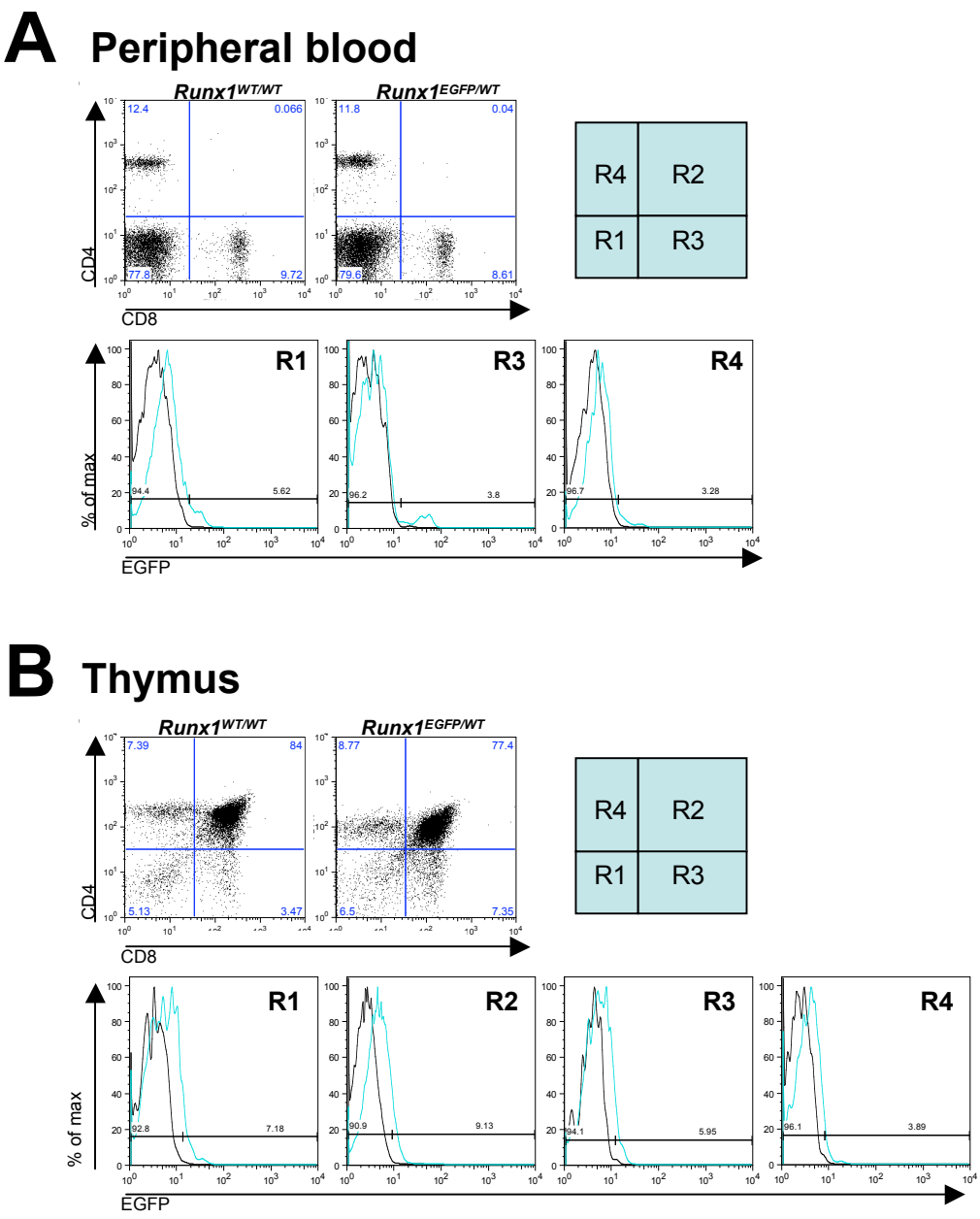

Figure 4.6: EGFP expression in lymphoid cells: T cell lineage.

A: Representative CD4 CD8 stains in adult peripheral blood of *Runx1*$^{EGFP/WT}$ animals compared to *Runx1*$^{WT/WT}$ animals and histograms showing EGFP expression in $CD4^{-}CD8^{-}$, $CD4^{-}CD8^{+}$, and $CD4^{+}CD8^{-}$ fractions in the peripheral blood.

B: Representative CD4 CD8 stains in the adult thymus of *Runx1*$^{EGFP/WT}$ animals compared to *Runx1*$^{WT/WT}$ animals and histograms showing EGFP expression in $CD4^{-}CD8^{-}$, $CD4^{-}CD8^{+}$, and $CD4^{+}CD8^{-}$ fractions in the thymus.

Black: *Runx1*$^{WT/WT}$animals; Blue: *Runx1*$^{EGFP/WT}$animals. Quadrants on dot plots were based on appropriate isotype controls (Appendix 4.1D); values indicate percentages of cells. Cell viability was determined by 7-AAD uptake.

In histograms, values indicate percentages of cells for *Runx1*$^{EGFP/WT}$ animals.

All plots are representative examples of 3 independent experiments.

A Bone marrow

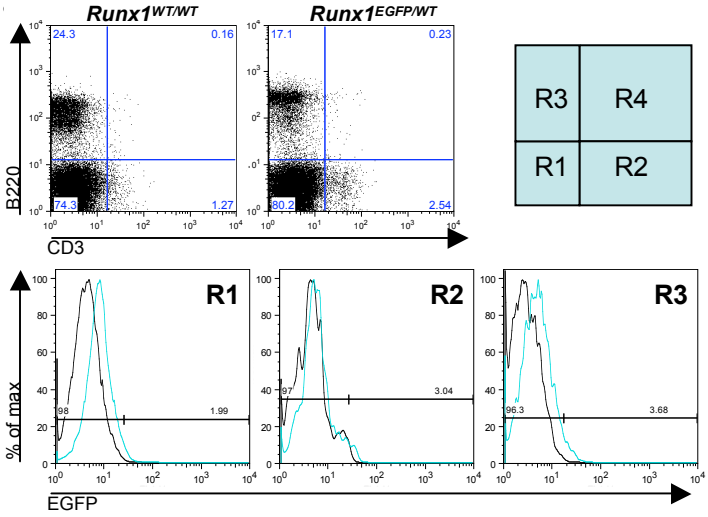

B Peripheral blood

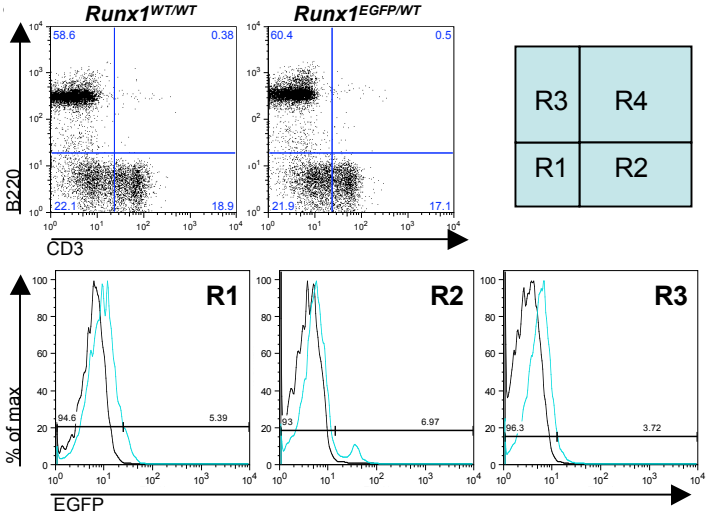

C Spleen

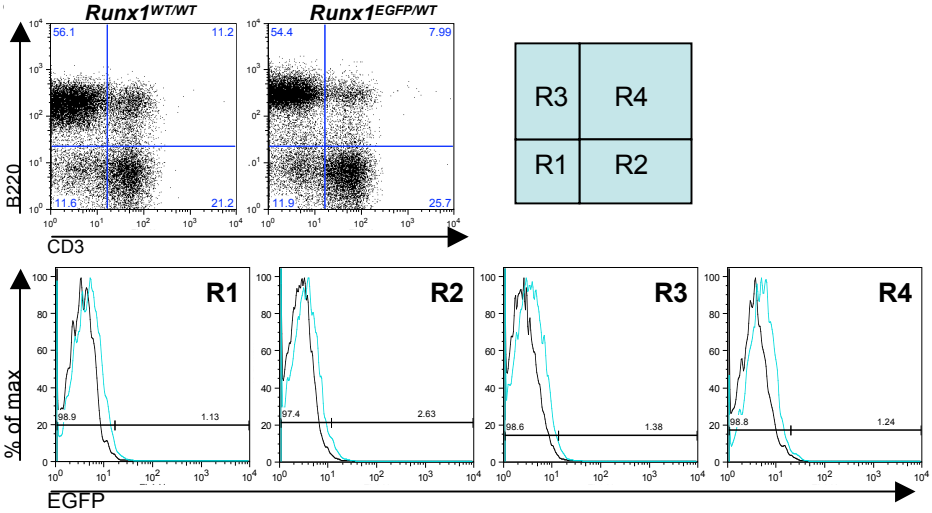

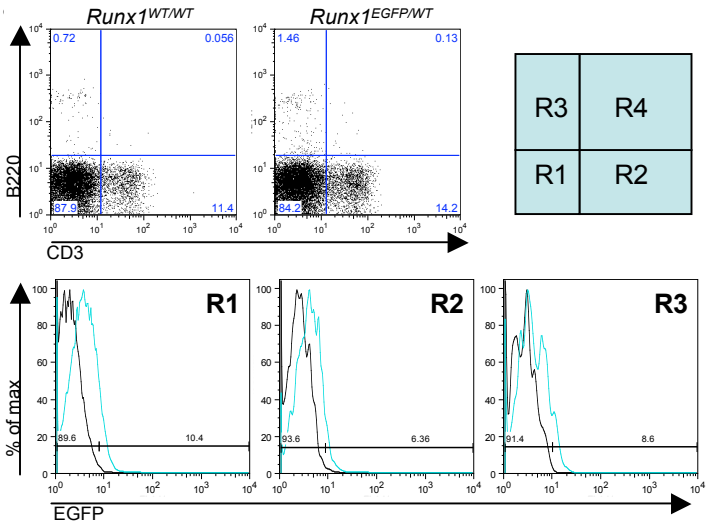

Figure 4.7: EGFP expression in lymphoid cells: T and B cell lineages.

A: Representative CD3 B220 stains in adult bone marrow of *Runx1*$^{EGFP/WT}$ animals compared to *Runx1*$^{WT/WT}$ animals and histograms showing EGFP expression in CD3^{-}B220^{-}, CD3^{+}B220^{-}, and CD3^{-}B220^{+} fractions in the bone marrow.

B: Representative CD3 B220 stains in adult peripheral blood of *Runx1*$^{EGFP/WT}$ animals compared to *Runx1*$^{WT/WT}$ animals and histograms showing EGFP expression in CD3^{-}B220^{-}, CD3^{+}B220^{-}, and CD3^{-}B220^{+} fractions in the peripheral blood.

C: Representative CD3 B220 stains in the adult spleen of *Runx1*$^{EGFP/WT}$ animals compared to *Runx1*$^{WT/WT}$ animals and histograms showing EGFP expression in CD3^{-}B220^{-}, CD3^{+}B220^{-}, CD3^{-}B220^{+}, and CD3^{+}B220^{+} fractions in the spleen.

D: Representative CD3 B220 stains in the adult thymus of *Runx1*$^{EGFP/WT}$ animals compared to *Runx1*$^{WT/WT}$ animals and histograms showing EGFP expression in CD3^{-}B220^{-}, CD3^{+}B220^{-}, CD3^{-}B220^{+} fractions in the thymus.

Black: *Runx1*$^{WT/WT}$ animals; Blue: *Runx1*$^{EGFP/Wt}$animals. Quadrants on dot plots were based on appropriate isotype controls (Appendix 4.1E) and values indicate percentages of cells. Cell viability was determined by 7-AAD uptake.

In histograms, values indicate percentages of cells for *Runx1*$^{EGFP/WT}$ animals.

All plots are representative examples of 3 independent experiments.

4.5.3.2. Runx1 expression in B cell lineages

Involvement of Runx1 in paediatric acute B-lymphocytic leukaemia suggests that an important role of Runx1 in B lymphopoiesis (Speck and Gilliland, 2002). Thus, the expression of EGFP in B cell subset was analysed in bone marrow, peripheral blood, spleen and thymus using an anti-B220 antibody, which marks most mature B cells. In addition, anti-CD19 antibody was used to detect mature B cells in the bone marrow.

In the B cell $CD3^{-}B220^{+}$ population, the MFI shift of the *Runx1*$^{EGFP/WT}$ mice compared to *Runx1*$^{WT/WT}$ mice was 1.8±0.4 in the bone marrow, 2.29±0.3 in the peripheral blood, 0.68±0.1 in the spleen, and 3.42±1.2 in the thymus (Figure 4.7A, B, C, D; Table 4.4).

As B220 expression is not completely restricted to B cells, anti-CD19 in combination with anti-B220 were used in the bone marrow, where B cell maturation takes place, to analyse EGFP expression in mature B cells ($CD19^{+}B220^{+}$). The MFI shift of the *Runx1*$^{EGFP/WT}$ mice compared to *Runx1*$^{WT/WT}$ mice was 2.45±0.5 in the $CD19^{lo}B220^{+}$ population, 2.39±0.5 in the $CD19^{-}B220^{+}$ population, and 2.08±0.4 in the $CD19^{+}B220^{+}$ population (Figure 4.8 and Table 4.4).

There was no difference in the EGFP expression between immature B cells ($CD19^{-}B220^{+}$) and mature B cells ($CD19^{+}B220^{+}$). These data compare with Runx1$^{lacZ/+}$ haploinsufficient mice that have no B cell phenotype and no obvious difference in Runx1 expression during B-cell differentiation, as appropriately assessed with anti-CD43 and anti-B220 stainings (North et al., 2004).

4.6. Characterisation of Runx1 expression in the *Runx1*^{EGFP} embryo

Runx1 deficient embryos completely lack definitive haematopoietic progenitors (CFU-Cs and CFU-S_{11}) and definitive LTR-HSCs in the YS, fetal liver, and AGM region (Cai et al., 2000; Mukouyama et al., 2000; North et al., 1999; North et al., 2002; Okada et al., 1998; Okuda et al., 1996; Wang et al., 1996a). During

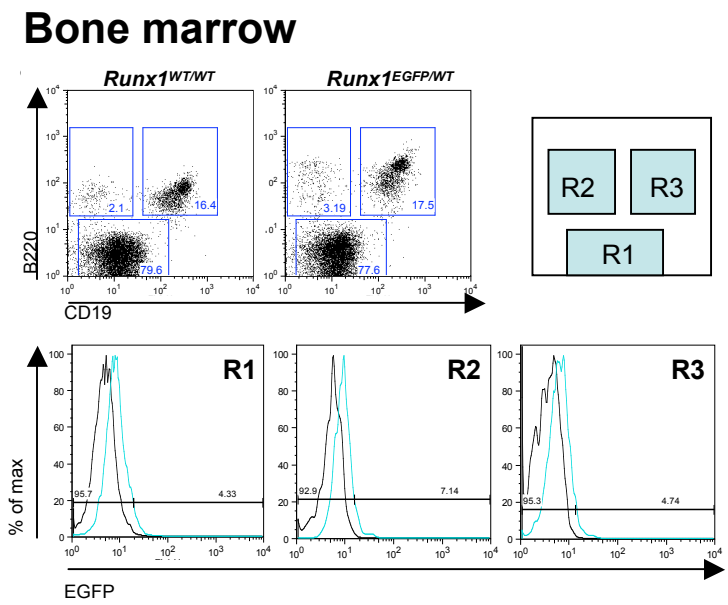

Figure 4.8: EGFP expression in lymphoid cells: B cell lineage.
Representative CD19 B220 stains in adult bone marrow of *Runx1*$^{EGFP/WT}$ animals compared to *Runx1*$^{WT/WT}$ animals and histograms showing EGFP expression in CD19^{lo}B220^{-}, CD19^{-}B220^{+}, and CD19^{+}B220^{+} fractions in the bone marrow.
Black: *Runx1*$^{WT/WT}$ animals; Blue: *Runx1*$^{EGFP/WT}$ animals. Quadrants on dot plots were based on appropriate isotype controls (Appendix 5.1F) and values indicate percentages of cells. Cell viability was determined by 7-AAD uptake. In histograms, values indicate percentages of positive cells for *Runx1*$^{EGFP/WT}$ animals.
All plots are representative examples of 3 independent experiments.

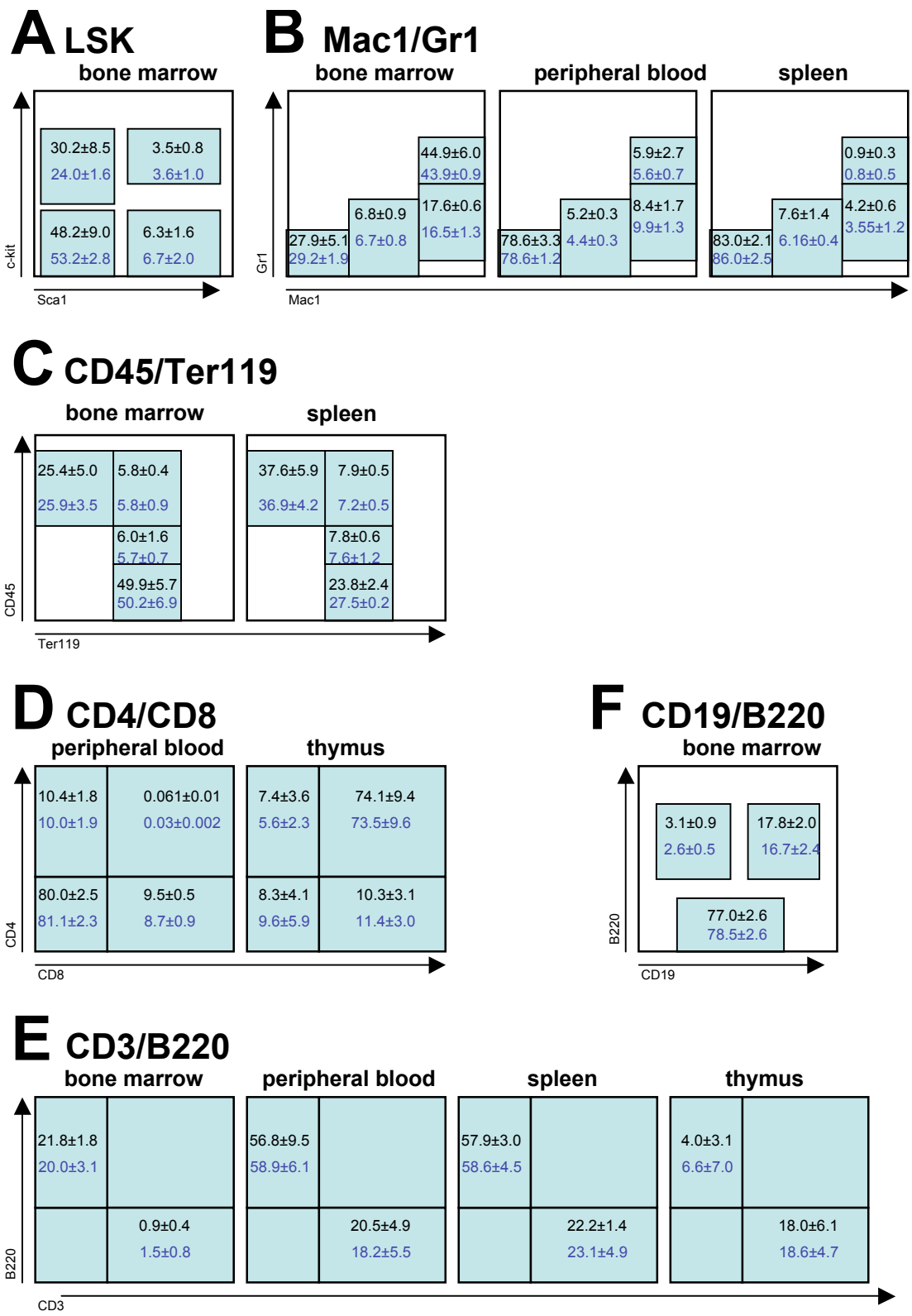

Figure 4.9: Summary of proportion of cell populations in Runx1$^{WT/WT}$ and Runx1$^{EGFP/WT}$ adult haematopoietic system .

Black: *Runx1$^{WT/WT}$* animals; Blue: *Runx1$^{EGFP/WT}$* animals. Values indicate percentages of cells (mean±standard deviation of 3 experiments). Cell viability was determined by 7-AAD uptake.

Table 4.4: Relative EGFP expression within haematopoietic cell subsets in the *Runx1*$^{EGFP/WT}$ adult mouse.

Relative median fluorescent intensity (MFI)(*Runx1*$^{EGFP/WT}$ MFI – *Runx1*$^{WT/WT}$ MFI) for each cell populations with the mentioned phenotype.

SEM: standard error of the mean. Lineage identity is associated with each phenotype and each organ is color-coded: black: bone marrow; red: peripheral blood; green: spleen; orange: thymus.

Haematopoietic lineage	Phenotype	Tissue	Relative MFI±SEM
HSC	lin$^-$sca1$^+$c-kit$^+$	bone marrow	11.16±0.9
Progenitors	lin$^-$sca1$^+$c-kit$^-$	bone marrow	6.33±0.2
Myeloid lineages			
monocytes	Mac1^{lo}Gr1^{lo}	bone marrow	5.08±1.4
		blood	2.23±0.3
		spleen	1.52±0.26
macrophages	Mac1^{hi}Gr1^{lo}	bone marrow	2.95±0.67
		blood	2.43±0.7
		spleen	1.7±0.55
neutrophils	Mac1^{hi}Gr1^{hi}	bone marrow	1.9±0.2
		blood	6.1±2.8
		spleen	1.1±0.3
non erythroid	CD45^{hi}Ter119$^-$	bone marrow	6.11±1.0
		spleen	2.04±0.3
immature erythroid	CD45^{hi}Ter119$^+$	bone marrow	5.54±0.8
		spleen	2.03±0.3
	CD45^{lo}Ter119$^+$	bone marrow	1.60±0.5
		spleen	0±0.1
mature erythroid	CD45$^-$Ter119$^+$	bone marrow	0.25±0.06
		spleen	0±0.04
Lymphoid lineages			
mature T cells	CD3$^+$B220$^-$	bone marrow	1.4±0.3
		blood	1.67±0.29
		spleen	0.62±0.17
		thymus	1.68±0.11
	CD4$^+$CD8$^-$	blood	1.76±0
		thymus	3.0±0.5
	CD4$^-$CD8$^+$	blood	0.91±0.3
		thymus	1.6±0.1
immature T cells	CD4$^+$CD8$^+$	thymus	2.93±0.3
B cells	CD3$^-$B220$^+$	bone marrow	1.8±0.4
		blood	2.29±0.27
		spleen	0.68±0.1
		thymus	3.42±1.2
pro-B cells dendritic cells	CD19$^-$B220$^+$	bone marrow	2.39±0.53
mature B cells	CD19+B220+	bone marrow	2.08±0.46

development, previous analysis performed by A. Suleman in E9.5 and E10.5 *Runx1*^{EGFP} embryos did not detect any abnormalities. Here, a more detailed analysis focusing on the E11.5 AGM region and using fully backcrossed homozygous *Runx1*$^{EGFP/EGFP}$ animals was performed.

4.6.1. EGFP expression in the E11.5 AGM region: CD34^{+} cell subsets.

EGFP expression in CD34$^{+/-}$ cell subsets was investigated as CD34 marks LTR-HSCs in the E11.5 AGM region (Sanchez et al., 1996). A whole population shift was observed in the CD45^{SP} cell fraction of the AGM region, showing that most express EGFP (92.6±6.58%)(Figure 4.10B). Values from conservative gating were presented since few cells appeared to be CD45^{+}EGFP^{-}. They were gated out although it is not possible to rule out that they express very low levels of EGFP; due to major overlap between *Runx1*$^{WT/WT}$ and *Runx1*$^{EGFP/EGFP}$ plots (Figure 4.10B). The MFI shift of the *Runx1*$^{EGFP/EGFP}$ mice compared to *Runx1*$^{WT/WT}$ mice was 12.69±1.9 in the CD45^{SP} population. Similar gating strategy to the CD45^{SP} population was adopted for the CD45^{+}CD34^{+} population and showed that 71.95±21.6% of cells were EGFP^{+} (Figure 4.10B). The MFI shift of the *Runx1*$^{EGFP/WT}$ mice compared to *Runx1*$^{WT/WT}$ mice was 25.06±4.1 in the CD45^{+}CD34^{+} population.

Histograms were not used for the analysis of CD45^{-} cell populations as no detectable EGFP shift was observed, showing that the majority of CD45^{-} cells do not express EGFP. However, overlaying of *Runx1*$^{WT/WT}$ and *Runx1*$^{EGFP/EGFP}$ dot plots revealed the existence of few EGFP^{+} cells in CD45^{-} populations (Figure 4.10B). Two distinct populations expressing EGFP were observed in the CD45^{-}CD34^{-} cell fraction: a EGFP^{lo} fraction that overlaid with WT cells but with higher density (suggesting a very low EGFP expression) and a EGFP^{+} fraction (0.47±0.1%), distinctive from WT cells (Figure 4.10B). By using conservative gating, there were 1.75±0.4% of EGFP^{+} cells in the CD45^{-}CD34^{+} population (Figure 4.10B). Of note, the majority of these cells appeared to be CD45^{lo} (Figure 4.10B).

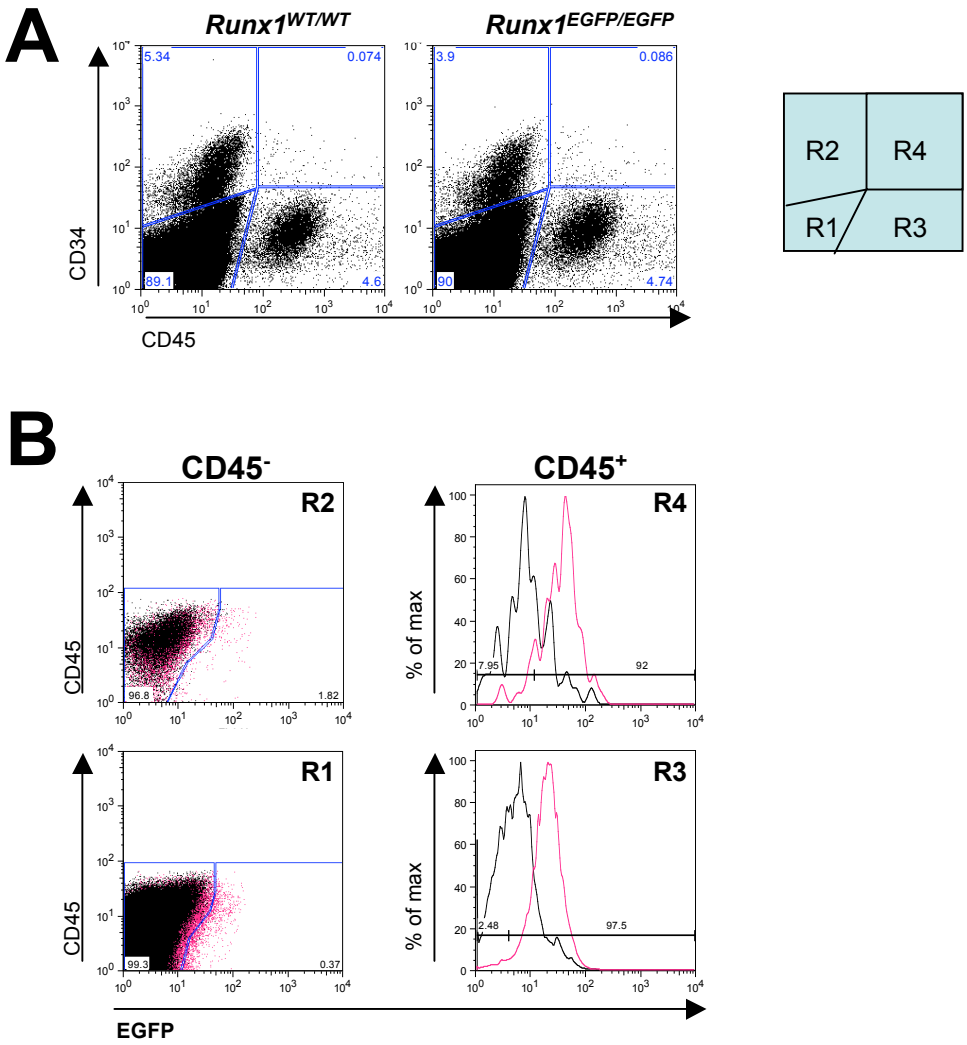

Figure 4.10: EGFP expression in E11.5 AGM region haematopoietic stem cells ($CD45^+CD34^+$ fraction).

A: Representative CD45 CD34 stains in E11.5 AGM region of *Runx1*$^{EGFP/EGFP}$ animals compared to *Runx1*$^{WT/WT}$ animals. Quadrants on dot plots were based on appropriate isotype controls (Appendix 4.2A).

B: Histograms and dot plots showing analysis EGFP expression in $CD45^-CD34^-$, $CD45^-CD34^+$, $CD45^+CD34^-$, and $CD45^+CD34^+$ cell fractions in the E11.5 AGM region. Values indicate percentages of cells for *Runx1*$^{EGFP/EGFP}$ animals.

Black: *Runx1*$^{WT/WT}$ embryos; Pink: *Runx1*$^{EGFP/EGFP}$ embryos. All plots display live cells only (determined by 7-AAD uptake).

All plots are representative examples of 4 independent experiments.

EGFP: enhanced green fluorescent protein; WT: wild type

4.6.2. EGFP expression in the E11.5 AGM region: c-kit^{+} cell subsets.

EGFP expression in c-kit$^{+/-}$ cell subsets was investigated as c-kit also marks LTR-HSCs in the E11.5 AGM region (Sanchez et al., 1996). For the reasons previously described, histograms were used to present CD45^{+} cell fractions and dot plots used to describe CD45^{-} cell fractions. EGFP was expressed in 96.67±0.3% of CD45^{SP} cells and 83.4±24.9% of CD45^{+}c-kit^{+} cells (Figure 4.11B). The MFI shift of the *Runx1*$^{EGFP/EGFP}$ embryos compared to *Runx1*$^{WT/WT}$ embryos was 12.85±1.1 in the CD45^{SP} population and was not calculated for the CD45^{+}c-kit^{+} (Figure 4.11B). Indeed, the *Runx1*$^{WT/WT}$ curve was pushed against the axis, probably due to slight over-compensation in this channel.

In the CD45^{-}c-kit^{-} cell fraction, 0.24±0.1% of cells were EGFP^{+} (Figure 4.11B). In the CD45^{-}c-kit^{+} cell fraction, 0.98±0.2% of cells were EGFP^{+} (Figure 4.11B). No population shifts were observed in these two populations when histograms of *Runx1*$^{WT/WT}$ and *Runx1*$^{EGFP/EGFP}$ were plotted, together indicating that only very few non-haematopoietic cells express EGFP.

4.6.3. EGFP expression in the E11.5 AGM region: VE-cadherin cell subsets

Because LTR-HSCs in the E11.5 AGM region also have a CD45^{+}VE-cadherin^{+} immunophenotype (North et al., 2002; Taoudi et al., 2005), EGFP expression was investigated in this cell compartment. The gating strategy was similar to that previously described. In the CD45^{SP} cells, 98.20±1.0% of cells were EGFP^{+} and in the CD45^{+}VE-cadherin^{+} cells, 96.76±1.0 were EGFP^{+} (Figure 4.12B). The MFI shift of the *Runx1*$^{EGFP/EGFP}$ embryos compared to *Runx1*$^{WT/WT}$ embryos was 9.8±2.0 in the CD45^{SP} population and 16.33±8.3 in the CD45^{+}VE-cadherin^{+} population (Figure 4.12B).

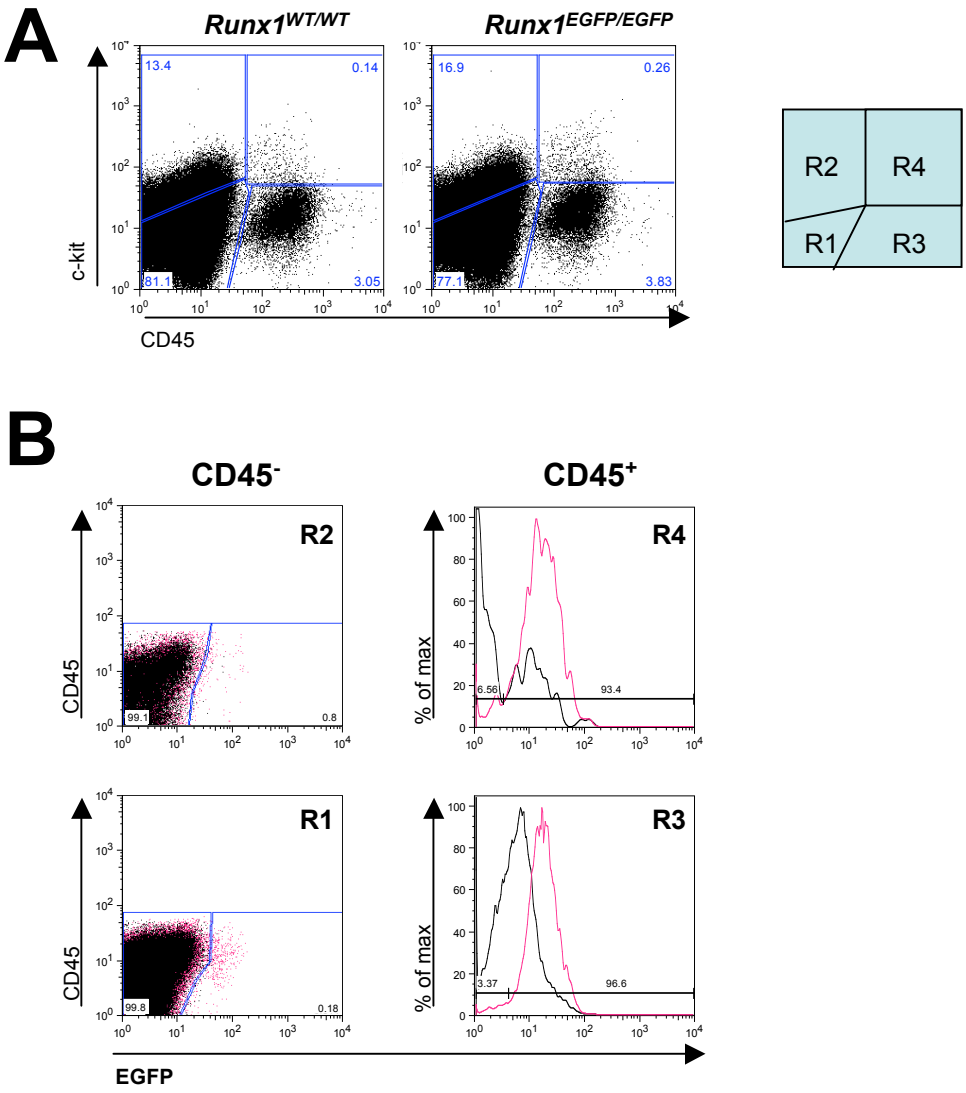

Figure 4.11: EGFP expression in E11.5 AGM region haematopoietic stem cells ($CD45^+c\text{-}kit^+$ fraction).

A: Representative CD45 c-kit stains in E11.5 AGM region of *Runx1*$^{EGFP/EGFP}$ animals compared to *Runx1*$^{WT/WT}$ animals. Quadrants on dot plots were based on appropriate isotype controls (Appendix 4.2B)

B: Histograms and dot plots showing analysis EGFP expression in $CD45^-c\text{-}kit^-$, $CD45^-c\text{-}kit^+$, $CD45^+c\text{-}kit^-$, and $CD45^+c\text{-}kit^+$ cell fractions in the E11.5 AGM region. Values indicate percentages of cells for *Runx1*$^{EGFP/EGFP}$ animals.

Black: *Runx1*$^{WT/WT}$ embryos; Pink: *Runx1*$^{EGFP/EGFP}$ embryos. All plots display live cells only (determined by 7-AAD uptake).

All plots are representative examples of 4 independent experiments.

EGFP: enhanced green fluorescent protein; WT: wild type

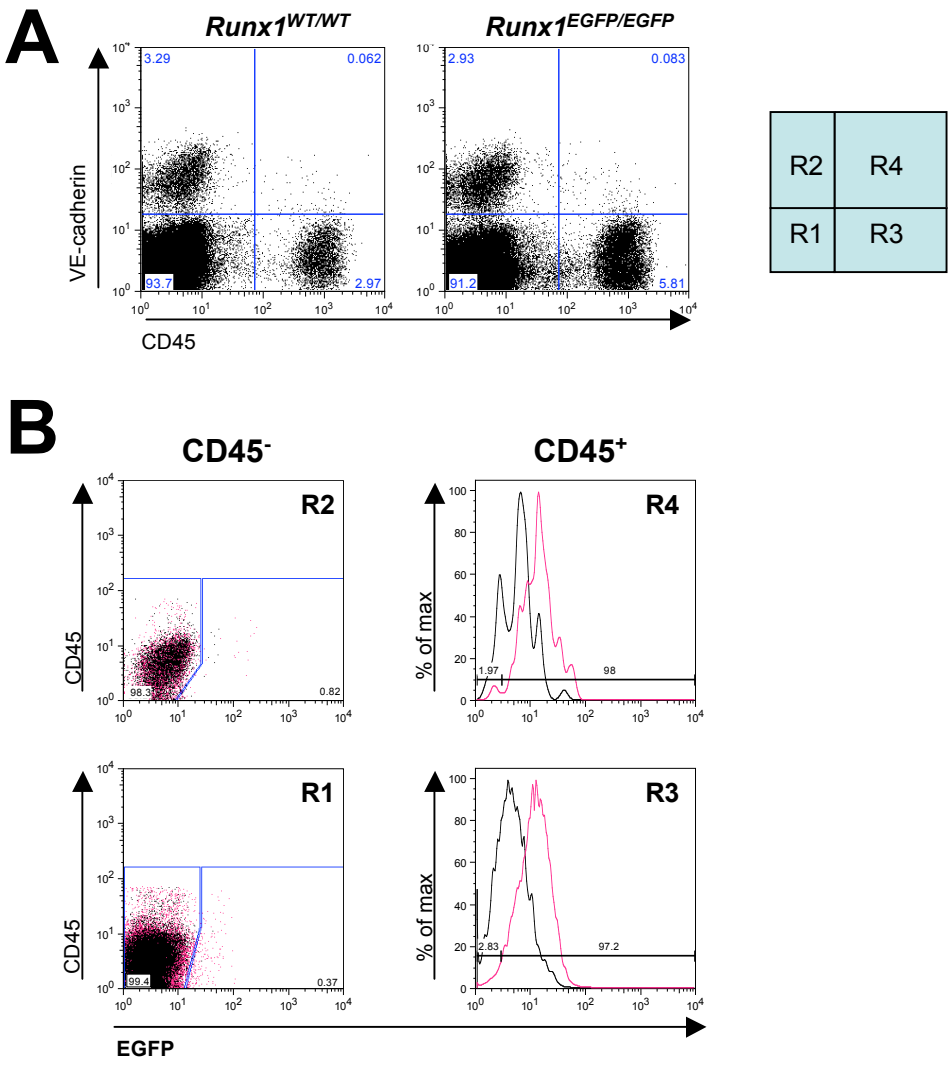

Figure 4.12: EGFP expression in E11.5 AGM region haematopoietic stem cells (CD45$^+$VE-cadherin$^+$).

A: Representative CD45 VE-cadherin stains in E11.5 AGM region of *Runx1*$^{EGFP/EGFP}$ animals compared to *Runx1*$^{WT/WT}$ animals. Quadrants on dot plots were based on appropriate isotype controls (Appendix 4.3A)

B: Histograms and dot plots showing analysis EGFP expression in CD45$^-$VE-cadherin$^-$, CD45$^-$VE-cadherin$^-$, CD45$^-$VE-cadherin$^+$, CD45$^+$VE-cadherin$^+$cell fractions in the E11.5 AGM region. Values indicate percentages of cells for *Runx1*$^{EGFP/EGFP}$ animals.

Black: *Runx1*$^{WT/WT}$ embryos; Pink: *Runx1*$^{EGFP/EGFP}$ embryos. All plots display live cells only (determined by 7-AAD uptake). EGFP: enhanced green fluorescent protein; WT: wild type

All plots are representative examples of 4 independent experiments.

In the non-haematopoietic fractions, 0.43±0.1% of cells expressed EGFP in the $CD45^{-}VE\text{-}cadherin^{-}$ fraction, and 0.82±0.05% of cells in the $CD45^{-}VE\text{-}cadherin^{+}$ (Figure 4.12B).

4.6.4. EGFP expression in the E11.5 AGM region: pre-LTR-HSCs type I ($CD45^{+}VE\text{-}cadherin^{+}CD41^{lo}$)

Here, the aim was to further characterise non-haematopoietic cell subsets expressing Runx1. $CD45^{+}$ cells were excluded using an anti-CD45 PerCP antibody (Appendix 4.2C), and anti-VE-cadherin (endothelial) and anti-CD41 (pre-haematopoietic) antibodies were used. Such population is of interest to our laboratory as it has been shown that $CD45^{-}VE\text{-}cadherin^{+}CD41^{lo}$ can develop into LTR-HSCs (S. Rybstov, unpublished data). These cells were termed pre-LTR-HSCs type I because their phenotype is more primitive (ie: do not express CD45) than the pre-LTR-HSCs type II ($CD45^{+}VE\text{-}cadherin^{+}$), which already have a haematopoietic phenotype. Analysis below addressed whether pre-HSCs type-I cell population express Runx1.

Because analysis involves $CD45^{-}$ cells only, dot plots were used. As previously, histograms were checked and there was no readily noticeable EGFP shift in cell populations. The percentage of $EGFP^{+}$ cells increased as the level of CD41 expression increased: 1.0±0.4% in $CD45^{-}VE\text{-}cadherin^{-}CD41^{-}$ cells, 13.8±3.2% in $CD45^{-}VE\text{-}cadherin^{-}CD41^{med}$ cells and 38.9±16.9% in $CD45^{-}VE\text{-}cadherin^{-}CD41^{hi}$ cells (Figure 4.13B). A similar observation was made in the endothelial cell population ($VE\text{-}cadherin^{+}$), with $EGFP^{+}$ cells representing: 0.26±0.1% in $CD45^{-}VE\text{-}cadherin^{+}CD41^{-}$ population, 13.27±4.1% in $CD45^{-}VE\text{-}cadherin^{+}CD41^{med}$ population, and 41.2±7.5% in $CD45^{+}VE\text{-}cadherin^{+}CD41^{hi}$ population (Figure 4.13B).

4.6.5. EGFP expression in E11.5 AGM reaggregates

Future experiments with the $Runx1^{EGFP}$ mice will involve sorting of $CD45^{-}EGFP^{+}$ cells prior to *ex vivo* culture to assess whether such cells are enriched for pre-HSCs. $Runx1^{EGFP/EGFP}$ E11.5 AGM reaggregates were set up to confirm that

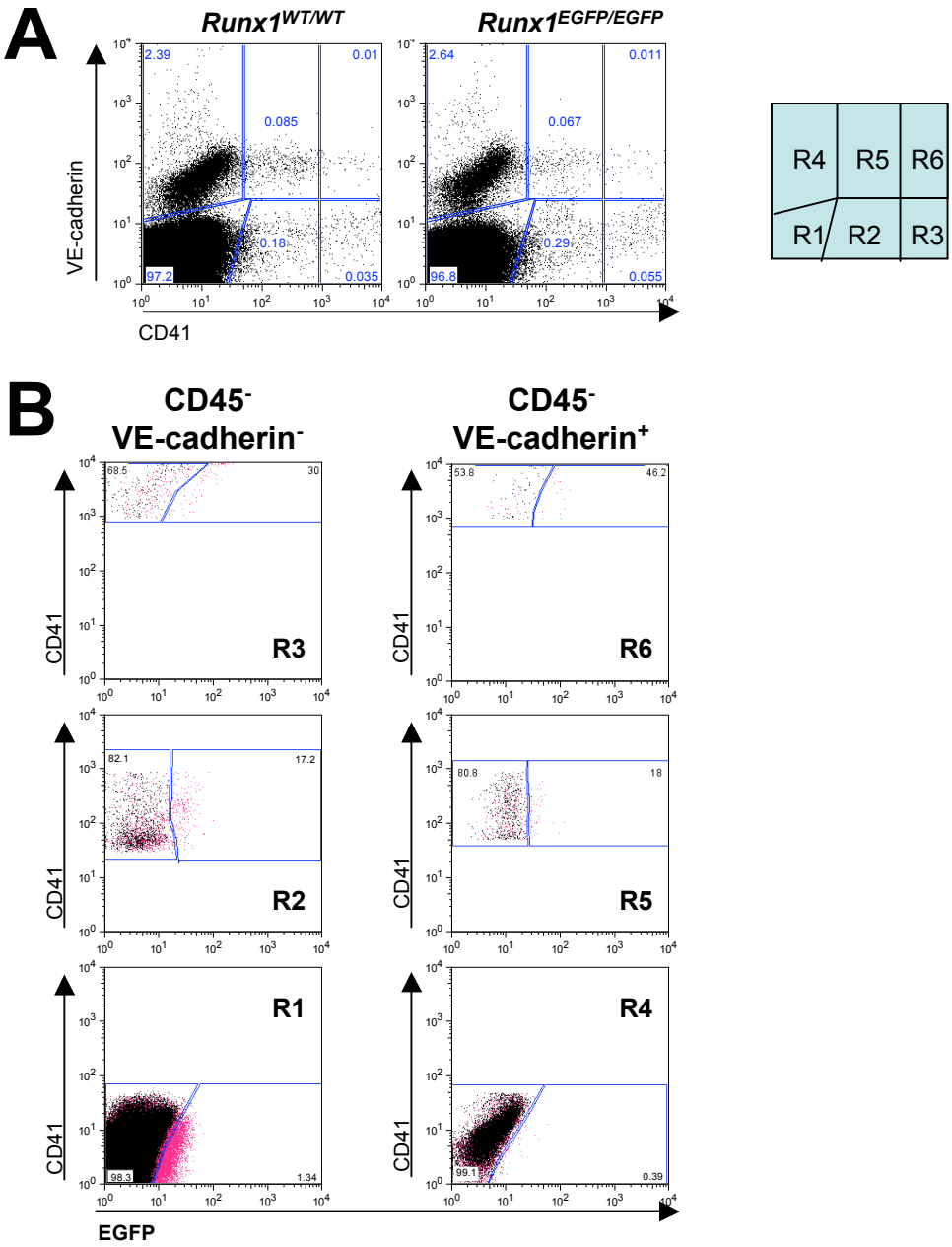

Figure 4.13: EGFP expression in E11.5 AGM region in pre haematopoietic stem cells type I (CD45$^-$VEcadherin$^+$CD41^{med} fraction).

A: Representative VE-cadherin CD41 stains in the non-haematopoietic cells (CD45$^-$) in the E11.5 AGM region of *Runx1*$^{EGFP/EGFP}$ animals compared to *Runx1*$^{WT/WT}$ animals. Quadrants on dot plots were based on appropriate isotype controls (Appendix 4.2C)

B: Dot plots showing analysis EGFP expression in CD45$^-$VE-cahderin-CD41$^-$, CD45$^-$VE-cadherin$^-$CD41^{med}, CD45$^-$VE-cadherin$^-$CD41^{hi}, CD45$^-$VE-cadherin$^+$CD41$^-$, CD45$^-$VE-cadherin$^+$CD41^{med}, and CD45$^-$VE-cadherin$^+$CD41^{hi} cell fractions in the E11.5 AGM region. Values indicate percentages of positive cells for *Runx1*$^{EGFP/EGFP}$ animals.

Black: *Runx1*$^{WT/WT}$ embryos; Pink: *Runx1*$^{EGFP/EGFP}$ embryos. All plots display live cells only (determined by 7-AAD uptake). EGFP: enhanced green fluorescent protein; WT: wild type. All plots are representative examples of 4 independent experiments.

Runx1$^{EGFP/EGFP}$ E11.5 AGM region performs similarly as *Runx1*$^{WT/WT}$ embryos and also to characterise EGFP$^+$ populations in reaggregates. Wilcoxon signed-rank test showed no significant difference cells percentages between *Runx1*$^{WT/WT}$ and *Runx1*$^{EGFP/EGFP}$ reaggregates ($p \geq 0.1$ in all gates). Similarly to the fresh E11.5 AGM region however, the percentage of CD45^{SP} cells was consistently higher in *Runx1*$^{EGFP/EGFP}$ reaggregates (Figure 4.14A).

When conservative gating was applied, 98.2±1.3% of CD45^{SP} cells were EGFP$^+$ (Figure 4.14B). The MFI shift of the *Runx1*$^{EGFP/EGFP}$ reaggregates compared to *Runx1*$^{WT/WT}$ reaggregates was 10.15±5.8 in the CD45^{SP} population (Figure 4.14B). Only 3.01±0.5% of the CD45$^+$VE-cadherin$^+$ population was EGFP$^+$ (Figure 4.14B). The collection of more events would allow detection of a possible population shift in this population.

In the non-haematopoietic populations, 0.34±0.07% of CD45$^-$VE-cadherin$^+$ cells were EGFP$^+$ (Figure 4.14B). Interestingly, only 0.08±0.04% of CD45$^-$VE-cadherin$^-$ population was EGFP$^+$, which represents a 5 fold decrease compared to the fresh tissue (0.43±0.1%, Figure 4.13B, Figure 4.14B). This observation raises the question of the fate of these EGFP$^+$ stromal cells, and further experiments will determine whether these cells matured into LTR-HSCs during reaggregate culture.

The strategy will consist of FACS sorting of CD45$^-$EGFP$^+$ cells, and reaggregating them with other AGM cell populations to assess their potential for developing into LTR-HSCs. Such chimeric reaggregate set-up, however, would be limited by the fact that EGFP is restricted to Runx1$^+$ cells, and thus cannot be used as a genetic marker to lineage trace cells in culture. To overcome this technical limitation, a lineage-trace system taking advantage of the Ly-5.1 and Ly-5.2 system was set up. Briefly, as *Runx1*$^{EGFP/EGFP}$ animals have a Ly-5.2/5.2 genotype, *Runx1*^{EGFP} cells could be reaggregated with Ly-5.2/5.1 or Ly-5.1/5.1 cells and thus still be discriminated by flow cytometry. The fact that only CD45$^+$ cells could be identified using this system should not be a problem because all reaggregate LTR-HSCs express CD45 (Taoudi et al., 2008). The normal behaviour of Ly-5.2/5.1 and Ly-5.1/5.1 cells when cultured as reaggregates was tested and proved the validity of Ly5.2/5.1 cells for this system (Appendix 4.4). Fully backcrossed *Runx1*^{EGFP} animals

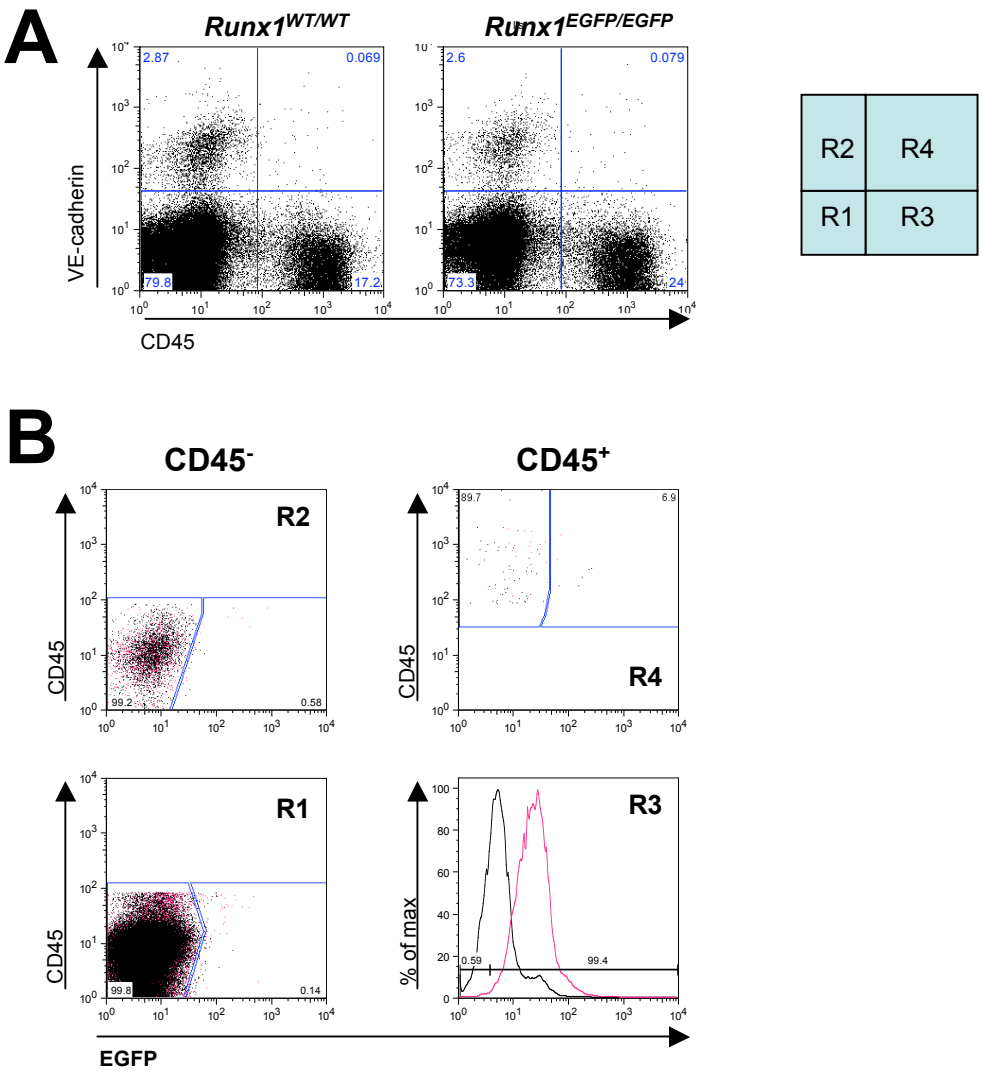

Figure 4.14: EGFP expression in haematopoietic and endothelial compartments of *Runx1*$^{EGFP/EGFP}$ E11.5 AGM reaggregates.

A: Representative CD45 VE-cadherin stains in *Runx1*$^{EGFP/EGFP}$ and *Runx1*$^{WT/WT}$ E11.5 AGM reaggregates of *Runx1*$^{EGFP/EGFP}$ animals. Quadrants on dot plots were based on appropriate isotype controls (Appendix 4.3C).

B: Analysis of EGFP in CD45^{-}VE-cadherin^{-}, CD45^{-}VEcadherin^{+}, CD45^{+}VE-cadherin^{-}, CD45^{+}VE-cadherin^{+} cell fractions. Values indicate percentages of cells in *Runx1*$^{EGFP/EGFP}$ reaggregates.

Black: *Runx1*$^{WT/WT}$ reaggregates; Pink: *Runx1*$^{EGFP/EGFP}$ reaggregates. All plots display live cells only (determined by 7-AAD uptake). EGFP: enhanced green fluorescent protein; WT: wild type. All plots are representative examples of 4 independent experiments.

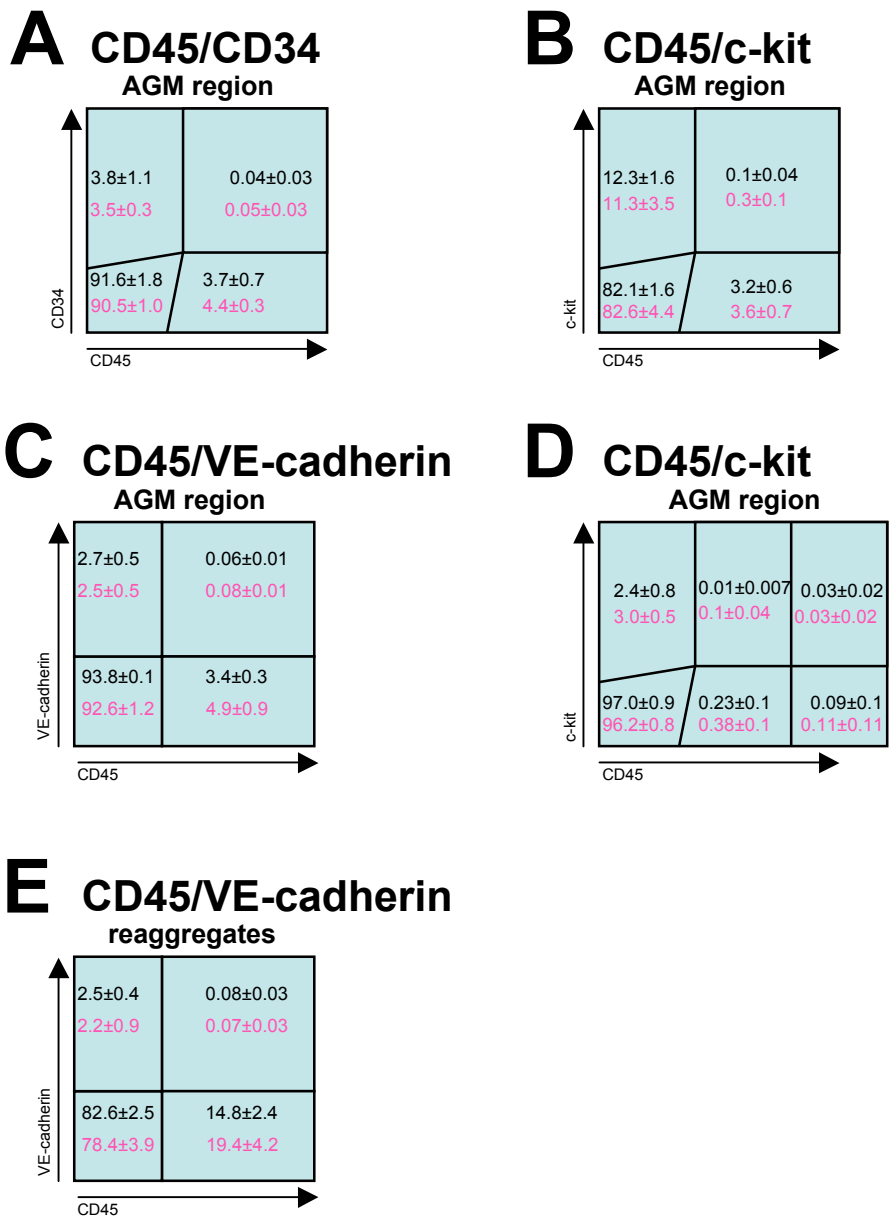

Figure 4.15: Summary of proportion of cell populations in Runx1$^{WT/WT}$ and Runx1$^{EGFP/EGFP}$ E11.5 AGM region .

Black: *Runx1$^{WT/WT}$* animals; Pink: *Runx1$^{EGFP/EGFP}$* animals. Values indicate percentages of cells (mean±standard deviation of 4 experiments). Cell viability was determined by 7-AAD uptake.

were obtained only recently so functional experiments using this lineage-trace system for $EGFP^+$ cells are still pending.

4.7. LTR-HSC numbers in the *Runx1^{EGFP}* E11.5 AGM region

After backcrossing, functional analysis of the *Runx1^{EGFP}* mice could be started. Fresh E11.5 AGM transplantation was carried out to assess whether LTR-HSC numbers were similar in *Runx1^{EGFP}* and *Runx1^{WT}* E11.5 embryos. This experiment was important to functionally prove that the *Runx1^{EGFP}* allele was functional, as it was clearly shown that Runx1 dosage had an impact on LTR-HSC development (Cai et al., 2000; North et al., 2002).

4.7.1. Functional analysis of LTR-HSCs in *Runx1^{EGFP}* mice: LTR-HSCs numbers

Upon transplantation of 2 *Runx1$^{WT/WT}$* E11.5 AGM regions into each recipient mouse, 7 out of 10 recipients were reconstituted by donor cells, 6 of which had a PBC higher than 20% (Figure 4.16). When *Runx1$^{EGFP/WT}$* AGM regions were transplanted, 3 out of 11 recipients were reconstituted and 2 of them had a PBC higher than 20% (Figure 4.16). Although the proportions of reconstituted animals were 70% and 27% with *Runx1$^{WT/WT}$* and *Runx1$^{EGFP/WT}$* donor cells respectively (Figure 4.16), there was no statistical difference between the two conditions (Fisher's exact test, p=0.08). Limiting dilution experiments will be required to accurately determine the numbers of LTR-HSCs in *Runx1$^{EGFP/WT}$* embryos. Also, mutlilineage characterisation will be required to demonstrate their normal function.

Additionally, as preliminary experiments indicated that *Runx1$^{EGFP/WT}$* E11.5 AGM contains fewer LTR-HSCs than *Runx1$^{WT/WT}$* embryos based on the proportions of reconstituted animals, transplantations using *Runx1$^{EGFP/EGFP}$* embryos will be performed to investigate any effect of *Runx1^{EGFP}* allele dosage on LTR-HSC numbers and so conclude whether this allele is fully functional.

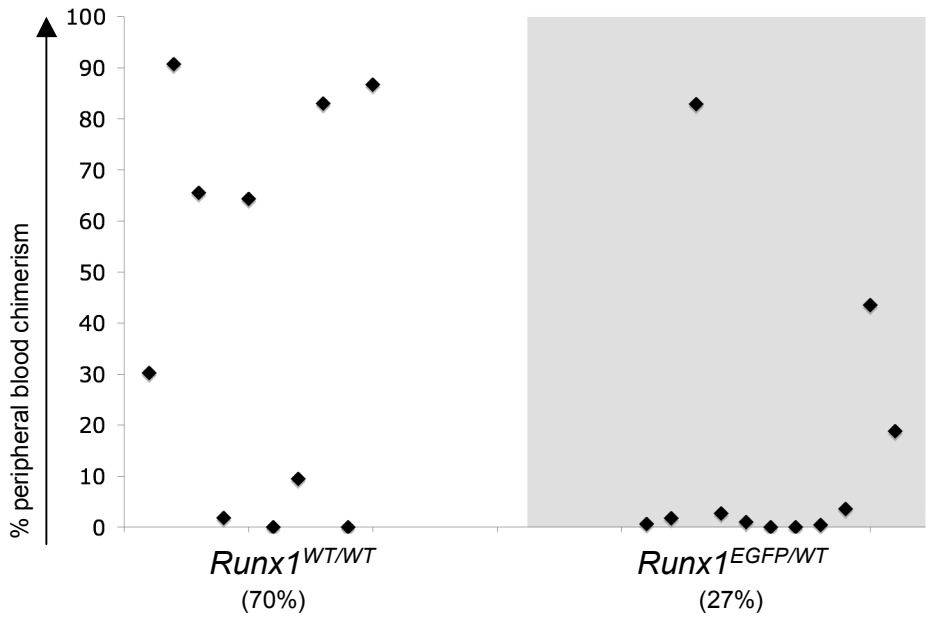

Figure 4.16: Functional assessment of LTR-HSCs content in *Runx1*$^{WT/WT}$ and *Runx1*$^{EGFP/WT}$ E11.5 AGM region.

Peripheral blood chimerism of recipients each transplanted with 2 embryos equivalent of E11.5 AGM cells.

Each point represents a single recipient mouse. Recipients were considered reconstituted when their peripheral blood chimerism exceeded 5% at least 12 weeks after transplantation. Percentages show the proportion of reconstituted recipients. Data is cumulative of 4 independent experiments.

4.8. Discussion

Flow cytometry and functional assays presented here describe the pattern of Runx1 expression in *Runx1*^{EGFP} adult and E11.5 embryos. Although allowing detection of small EGFP expression by flow cytometry, our reporter, as others, has technical limitations. Firstly, insertion of the reporter gene after *Runx1* exon 6 results in EGFP expression only when Runx1b and Runx1c isoforms are expressed. Secondly, although EGFP is much brighter than GFP, it also has a longer half-life than GFP (over 24 hours compared to 9 hours for GFP)(Choi et al., 2005; Li et al., 1998; Verkhusha et al., 2003). Since the half-life of the Runx1 protein is 3.3 hours (Huang et al., 2001), EGFP is detectable in cells that no longer express Runx1. Thus, future experiments require the evaluation of the fidelity of the EGFP reporter to Runx1 by checking the overlapping expression of EGFP and Runx1 with more sensitive techniques such as quantitative PCR. Despite these points, EGFP expression reported here coincides with Runx1 expression patterns reported in other models so the *Runx1*$^{EGFP/EGFP}$ mouse should provide an accurate Runx1 reporter, correlating closely to the WT situation (Ichikawa et al., 2004; Lorsbach et al., 2004; North et al., 1999; North et al., 2002; North et al., 2004). Statistical analysis presented here must also be interpreted carefully as few independent experiments limit the power of any statistical test. Additional replicates should be performed in order to obtain more robust statistical analysis and detect potential subtle differences.

4.8.1. EGFP expression in the *Runx1*^{EGFP} adult mouse

Both descriptive (cellularity, flow cytometry) and functional (CFU-Cs) analyses in *Runx1*$^{WT/WT}$ and *Runx1*$^{EGFP/WT}$ mice showed no detectable phenotype in adult animals. However, *in vivo* transplantations performed at limiting dilution would be required to conclude about any adult LTR-HSC phenotype.

EGFP was highly expressed in LSK cells, which are enriched for LTR-HSCs (Osawa et al., 1996; Wagers et al., 2002). In addition, EGFP was expressed in the lin$^-$ Sca1$^-$c-kit$^-$cell fraction, which contains common lymphoid progenitors (lin$^-$sca1^{lo}c-

kit^{lo}Thy-1^{-}IL7R^{-} immunophenotype)(Kondo et al., 1997) and in the lin^{-}Sca1^{+}c-kit^{-}, which contains common myeloid progenitors (Akashi et al., 2000).

Very small EGFP shifts were observed in mature lymphoid and myeloid lineages. As a result, conservative gating was not appropriate for analysis and measures of MFI were reported as an indication of small population shifts. The MFI values were consistent between experiments and compensation plots of FL-2 single stains were provided in Appendix 4.1 in order to rule out any false positive signals. The patterns of EGFP expression in the adult haematopoietic system were consistent with observations in other mice reporter models (Lorsbach et al., 2004; North et al., 2004).

In myeloid lineages, EGFP expression was decreased upon granulocyte differentiation as the MFI decreased with increasing levels of Gr1, suggesting a down-regulation of Runx1 upon myeloid differentiation (Lorsbach et al., 2004). This contrasts with the Runx1 LacZ reporter in which a high proportion of bone marrow and peripheral blood Mac1^{+} and Gr1^{+} cells express LacZ; but the relevance of such observation in our context is limited because myeloid cells numbers are significantly increased in *Runx1^{lz}* mice (North et al., 2004). Also, EGFP was expressed in erythroid progenitors but rapidly downregulated upon erythroid differentiation, which processes through the following phenotypes: CD45^{hi}Ter119^{-}, CD45^{hi}Ter119^{+}, CD45^{lo}Ter119^{+}, CD45^{-}Ter119^{+} (Kina et al., 2000). Other groups observed the same Runx1 down-regulation upon erythrocyte maturation (Lorsbach et al., 2004; North et al., 2004). Additional Ter119 CD71 staining would be needed to precisely describe the patterns Runx1 expression during specific stages of erythrocyte maturation.

In lymphoid lineages, populations of mature T cells (CD4^{+}CD8^{-}, CD4^{-}CD8^{+} and CD3^{+}B220^{-}) displayed a stronger EGFP expression in the thymus, the site of T cells maturation, also consistent with previous observations (Lorsbach et al., 2004). In the thymus, EGFP expression was the highest in CD4^{-}CD8^{-} cells, which corresponds to the early thymocyte (CD4^{-}CD8^{-}) population. This observation was not surprising as previous reports using conditional inactivation of Runx1 in adult mice showed a reduction in thymus size and an accumulation of CD4^{-}CD8^{-} thymocytes, suggesting that Runx1 plays a role in early T-cell differentiation (Growney et al.,

2005; Putz et al., 2006). Finally, also consistent with previous observations, EGFP was stronger in $CD4^+CD8^-$ cells compared to $CD4^-CD8^+$ cells (Lorsbach et al., 2004).

EGFP was expressed at similar levels in immature B cells ($CD19^-B220^+$) and mature B cells ($CD19^+B220^+$). These data compare with $Runx1^{lacZ/+}$ haploinsufficient mice where Runx1 expression is maintained during B-cell differentiation (North et al., 2004). Additional staining with anti-CD43 and anti-B220 antibodies would be required to assess accurately Runx1 expression during B cell differentiation. Interestingly, B cell development is severely impaired in conditionally inactivated Runx1 adult mice and LTR-HSC *in vivo* transplantations fail to reconstitute peripheral B and T cells (Ichikawa et al., 2004). The observation that $Runx1^{EGFP/WT}$ mice compared with $Runx1^{WT/WT}$ animals indicates that the $Runx1^{EGFP}$ allele is most probably functional in the lymphoid compartments.

4.8.2. EGFP expression in the $Runx1^{EGFP}$ E11.5 embryo

The second part of this study focused on the E11.5 AGM region because a focus of the lab is to investigate the role of Runx1 in the emerging LTR-HSCs in the E11.5 AGM region. $Runx1^{EGFP/EGFP}$ embryos were used for most analyses because adult analyses had shown that EGFP shifts were very small in the $Runx1^{EGFP/WT}$ animals.

It was shown that most $CD45^+$ cells in the E11.5 AGM region express EGFP, consistent with other reporter models (North et al., 1999; North et al., 2002). The relative EGFP MFI of cell populations that are enriched for LTR-HSCs ($CD45^+$ c-kit^+ $CD34^+$ VE-$cadherin^+$)(North et al., 2002; Sanchez et al., 1996; Taoudi et al., 2005) were higher than in other haematopoietic cell populations. Interestingly, a small sub-population of $CD45^-$ cells expressed EGFP. Further characterisation of this cell population showed that most of these cells did not have an endothelial phenotype based on VE-cadherin expression. Also, some of them express the pre-haematopoietic marker CD41 at high levels. This is of interest because CD41 is expressed at the onset of definitive haematopoiesis (Ferkowicz et al., 2003; Mikkola et al., 2003a; North et al., 2002; Sanchez et al., 1996; Taoudi et al., 2005) and a

recent report has demonstrated that CD41 is expressed prior to CD45 on haematogenic endothelial cells (Eilken et al., 2009). Additionally, this cell population ($CD45^{-}VE\text{-}cadherin^{-}EGFP^{+}$) decreased by 6 fold during reaggregate culture. Cell sorting of such $EGFP^{+}$ cells and their reaggregation with complementary AGM cell fractions will assess the potential of these cells to develop into LTR-HSCs. Because the EGFP marker is only restricted to cells expressing Runx1, a lineage trace system that consists in setting up Ly-5.2/5.2 and Ly-5.2/5.1 chimeric reaggregates has been established and should provide a useful system to answer whether $CD45^{-}VE\text{-}cadherin^{-}Runx1^{+}$ are pre-LTR-HSC or are an important element of the LTR-HSC niche in the AGM microenvironment.

4.8.3. LTR-HSCs numbers in the *Runx1^{EGFP}* E11.5 AGM region

Transplantations of fresh E11.5 AGM region were performed to confirm the absence of LTR-HSC phenotype in *Runx1^{EGFP}* embryos. Surprisingly, the *Runx1$^{EGFP/WT}$* AGM region appeared to contain fewer LTR-HSCs compared with WT animals. If this result is confirmed by limiting dilution experiments, it could have two major implications: *Runx1^{EGFP}* embryos are developmentally retarded and LTR-HSCs appear slightly later; or *Runx1^{EGFP}* allele is hypomorphic and there are fewer LTR-HSCs with potential functional defects. Future experiments will need to investigate if there is any dose-dependent effect of the *Runx1^{EGFP}* allele by transplanting *Runx1$^{EGFP/EGFP}$* embryos and will help discriminating between these hypotheses. This is important because an abnormal LTR-HSC phenotype during development could severely affect the outcome of reaggregate lineage trace experiments.

5. The spatial localisation of pre-HSC in the E11.5 AGM region

5.1. Introduction

The third part of this study focused on localising pre-HSCs in the AGM region and identifying potential interactions between sub-compartments of the AGM region. I focused on: 1) the axio-lateral polarity of LTR-HSC development and 2) the dorso-ventral polarity of LTR-HSC development and the hypothesis that cells in the AoD might be competent to become LTR-HSCs when exposed to the appropriate microenvironment.

The E11.5 AGM region harbours and can autonomously expand the first LTR-HSCs of the embryo (Medvinsky and Dzierzak, 1996; Muller et al., 1994). However, the question of the origin of LTR-HSCs within the AGM region and identification of key niche components remains of importance.

Previous studies have addressed the axio-lateral repartition of haematopoietic progenitors (CFU-S_8 and CFU-S_{11}) and LTR-HSCs in the E11.5 AGM region (de Bruijn et al., 2000a; de Bruijn et al., 2000b; Medvinsky et al., 1996; Taoudi and Medvinsky, 2007). Although their numbers are slightly higher in the dorsal aorta (Ao), both Ao and the urogenital ridges (UGRs) contain CFU-S_8 and CFU-S_{11} at E10.5 (de Bruijn et al., 2000a; Medvinsky et al., 1996). Absolute numbers of CFU-S increased at E11.5 and E12.5 in both regions (de Bruijn et al., 2000a; Medvinsky et al., 1996). In contrast, LTR-HSCs were exclusively located in the Ao (including surrounding mesenchyme) at E11.5 (de Bruijn et al., 2000b; Taoudi and Medvinsky, 2007). At E12.5 however, LTR-HSCs are still preferentially located in the Ao but can be functionally detected in the UGRs, and more precisely in the mesonephroi (de Bruijn et al., 2000b). Small numbers of LTR-HSCs can be obtained from E11.5 UGRs when they are cultured as explants showing either their capacity to autonomously initiate LTR-HSC induction/expansion or that they were populated by

pre-HSCs from the Ao prior to E11.5 (de Bruijn et al., 2000b). Co-culture of Ao and UGRs as explants failed to show any stimulatory or inhibitory action from either tissue on each other (de Bruijn et al., 2000b).

Since reaggregation, in contrast to explant culture, ensures close intercellular contacts, this part of my study addressed whether culturing the E11.5 AGM as reaggregates would reveal potential enhancing/inhibiting interactions between Ao and UGR in LTR-HSC development. In addition, the presence of IL-3, SCF, and Flt3l and longer culture period could possibly influence the outcome of such experiments.

This part of my study also was to understand cellular mechanisms underlying dorso-ventral polarization in LTR-HSC development. The ventral domain of the E10.5-11.5 Ao (AoV) contains the majority of LTR-HSCs in the fresh tissue and is capable of autonomous LTR-HSCs generation (Taoudi and Medvinsky, 2007). I tested, using the reaggregate culture system, whether the dorsal domain of the Ao (AoD) contains cells capable of developing into LTR-HSCs under the influence of the competent AoV microenvironment.

5.2. Axio-lateral polarity of LTR-HSC expansion within E11.5 AGM region

E11.5 embryos were selected as described in Section 2.4.1, and the AGM regions were sub-dissected into UGR and Ao (Figure 5.1). Importantly, UGRs were dissected along the ridges so that the para-aortic mesenchyme was left with the Ao. The blood within the Ao was not removed (Figure 5.1).

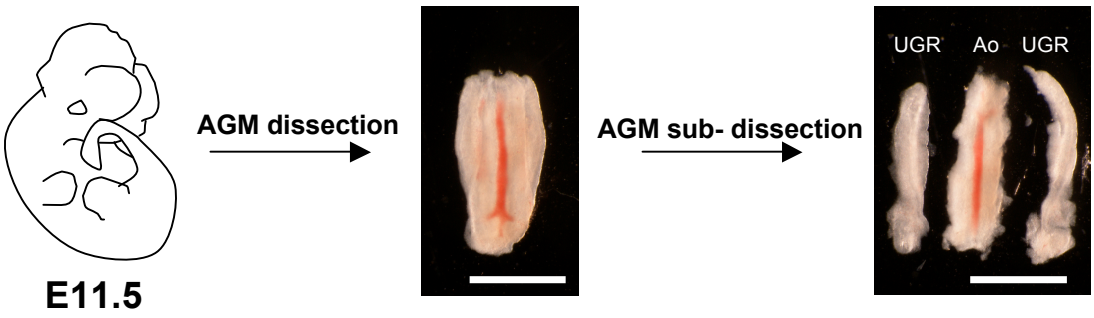

Figure 5.1: Scheme of E11.5 AGM region lateral sub-dissection into dorsal aorta and urogenital reidges.
Sub-dissection of the E11.5 AGM region into the dorsal aorta and its surrounding mesenchyme (Ao), and the two urogenital ridges (UGR)(scale bar: 1mm).

Table 5.1: Lateral repartition of cells in the E11.5 AGM region (Ao and UGR).
Data was acquired by flow cytometric analysis; viability determined by 7-AAD uptake. Absolute numbers ± standard deviation; mean of 4 independent experiments.
DP: $CD45^{+}VE\text{-}cadherin^{+}$; DN: $CE45^{-}VE\text{-}cadherin^{-}$

	AGM	Ao	UGR
total cells	232500 ± 24660	77460 ± 19170	134300 ± 36210
total live cells	113400 ± 28610	47660 ± 10140	59440 ± 11500
total CD45+ cells	3360 ± 780	1270 ± 400	1800 ± 260
total VE cadherin+ cells	1410 ± 440	470 ± 160	970 ± 340
total DP cells	63 ± 38	20 ± 22	15 ± 9
total DN cells	108600 ± 27570	45900 ± 9690	56650 ± 11150

5.2.1. Axio-lateral characterisation of the fresh E11.5 AGM region

5.2.1.1. Cellular composition of the Ao and UGR

The lateral repartition of haematopoietic ($CD45^+$) cells and LTR-HSCs ($CD45^+$VE-$cadherin^+$) between Ao and UGR were analysed by flow cytometry. The Ao contained 77460±19170 cells, of which 47660±10140 were viable (Table 5.1). The UGR contained 134300±36210 cells, of which 59440±11500 were viable (Table 5.1). There was no polarised repartition of haematopoietic cells between Ao and UGR, which contained 1270±400 and 1800±260 $CD45^{SP}$ cells respectively (paired T-test, p≥0.2)(Table 5.1). There was also no polarised repartition of the $CD45^+$VE-$cadherin^+$ cells between Ao and UGR, which contained 20±22 and 15±9 $CD45^+$VE-$cadherin^+$ cells respectively (paired T-test, p≥0.2)(Table 5.1). Finally, the Ao and UGR respectively contained 470±160 and 970±340 $CD45^-$VE-$cadherin^+$ cells and 45910±9690 and 56650±11150 $CD45^-$VE-$cadherin^-$ cells (Table 5.1).

Of note, the sum of Ao and UGR cells reached the range of the numbers found in the whole AGM (Table 5.1) indicating that there was no preferential cell death in either the Ao and UGR during flow cytometry processing.

5.2.1.2. Axio-lateral repartition of haematopoietic progenitors in the E11.5 AGM region

There was no significant difference in haematopoietic progenitors (CFU-Cs) between fresh E11.5 Ao and UGR (paired T-test, p=0.09)(Figure 5.2). Ao contained 84±11 CFU-Cs (17±9 CFU-mast, 10±7 BFU-E, 8±6 CFU-GM, 46±15 CFU-mac, and 3±1 CFU-GEMM) and the UGR contained 47±24 CFU-Cs (10±7 CFU-mast, 6±6 BFU-E, 4±4 CFU-GM, 17±27 CFU-mac, and 0 CFU-GEMM)(Figure 5.2). Although there were considerable variations within types and numbers of CFU-Cs in the UGR, there were consistently more CFU-Cs in the Ao compared to UGR. Interestingly, no CFU-GEMM was observed in the UGRs in any of the experiments (Figure 5.2).

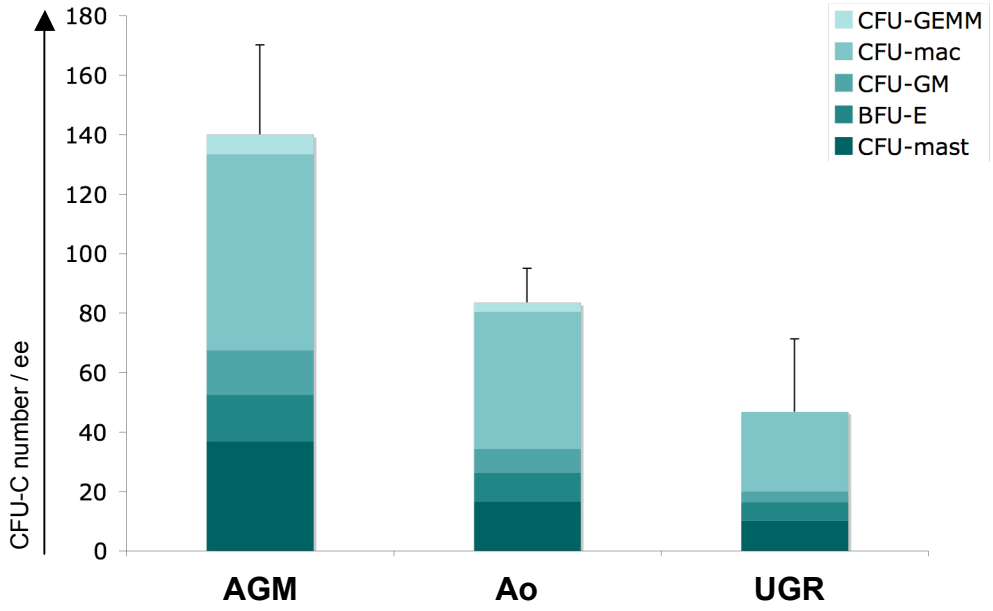

Figure 5.2: Lateral repartition of haematopoietic progenitors in the E11.5 AGM (Ao and UGR).

Bars indicate the standard deviation of 4 independent experiments.

BFU-E: burst forming unit-erythroid; CFU: colony forming unit; Mac: macrophage; GM: granulocyte/macrophage; GEMM: granulocyte/erythroid/macrophage/megakaryocyte; ee: embryo equivalent.

Cumulative numbers of CFU-Cs in Ao and UGRs roughly corresponded to the range of CFU-C numbers in the whole AGM (140±30 CFU-Cs: 37±22 CFU-mast, 15±3 BFU-E, 15±13 CFU-GM, 66±13 CFU-mac, and 7±2 CFU-GEMM)(Figure 5.2) suggesting that sub-dissection of the AGM does not influence development of haematopoietic colonies in culture.

5.2.2. Autonomous haematopoietic potential of E11.5 Ao and UGRs in reaggregate cultures

As described in Chapter 3, the reaggregate culture system enables efficient expansion of LTR-HSCs from 1 to around 150 within 4 days (Kumaravelu et al., 2002; Taoudi et al., 2008). Ao and UGR reaggregates were set up in IMDM^{+} to examine their autonomous haematopoietic potential.

5.2.2.1. Expansion of haematopoeitc (CD45^{+}) cells in E11.5 Ao and UGR reaggregates

Ao and UGR reaggregates were similar by size but UGR reaggregates lacked peripheral cell protrusions characteristic of AGM reaggregates (Figure 5.3A). There was no statistical difference between cell numbers in Ao and UGR reaggregates which respectively contained 98840±31170 and 143170±49860 cells (paired T-test, p=0.1)(Figure 5.3B). Ao and UGR reaggregates contained 16070±7130 and 7880±3860 CD45^{+} cells respectively (Figure 5.3B). Although CD45^{+} cells were not statistically different in Ao and UGR cultures (paired T-test, p≥0.2), Ao reaggregates contained more CD45^{+} cells than UGR reaggregates in 3 out of 4 experiments. Cumulatively, haematopoietic cell numbers in Ao and UGR reaggregates in each experiment were similar to those in entire AGM reaggregates (Figure 5.3B), suggesting no inhibiting or enhancing interactions between Ao and UGR.

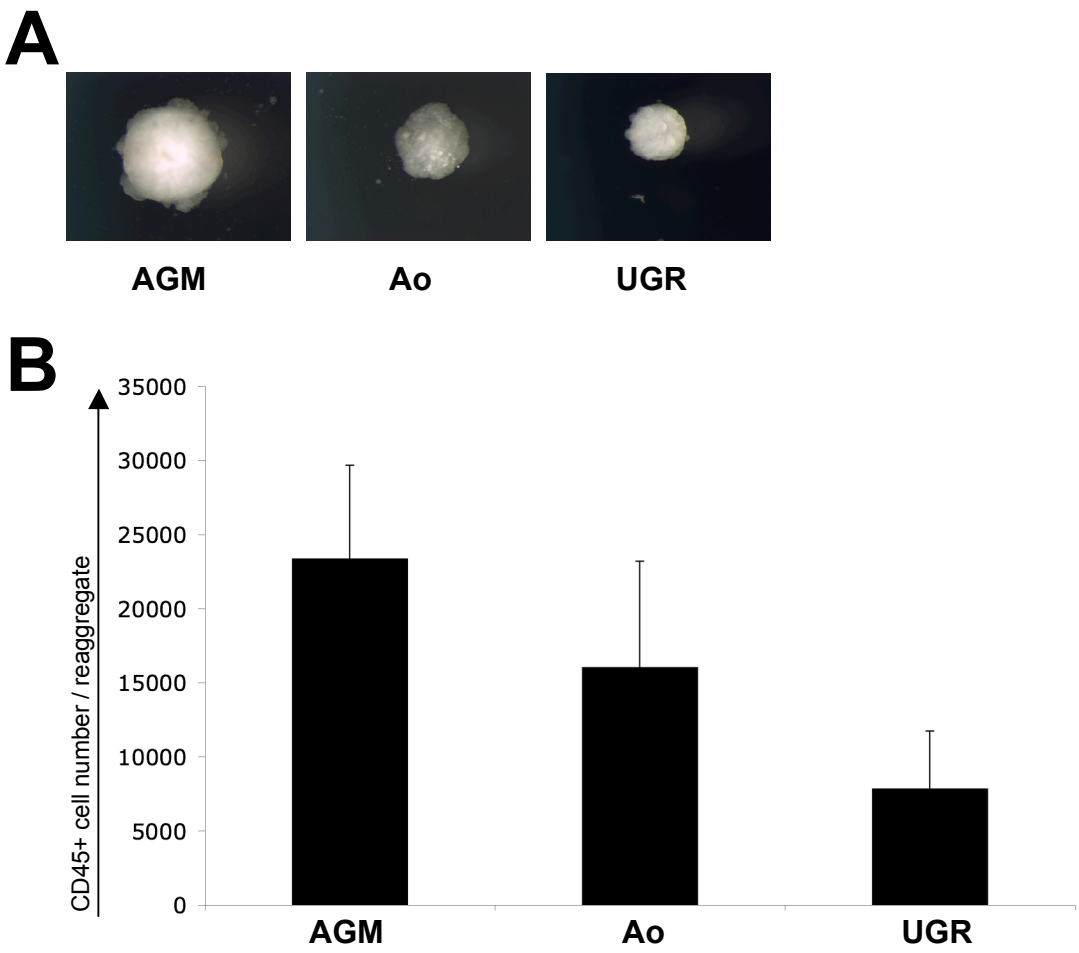

Figure 5.3: Haematopoietic potential of Ao and UGR reaggregates.
A: Representative images of AGM, Ao and UGR reaggregates. Ao and UGR reaggregates had similar morphology and were smaller than their AGM controls counterparts.
B: Haematopoietic cell numbers ($CD45^+$) in AGM, Ao, and UGR reaggregates. Bars indicate standard deviation of 6 experiments in AGM and Ao reaggregates, and 4 experiments in UGR reaggregates.
Data was acquired by flow cytometric analysis; cell viability was determined by 7-AAD uptake.

5.2.2.2. Expansion of haematopoietic progenitors in E11.5 Ao and UGR reaggregates

The expansion of haematopoietic progenitors in Ao and UGR reaggregates was assessed by the CFU-C assay. The Ao reaggregates contained 1780±1350 CFU-Cs (780±568 CFU-mast, 163±213 BFU-E, 25±29 CFU-GM, 725±527 CFU-mac, and 88±118 CFU-GEMM) while the UGR reaggregates contained 540±540 CFU-Cs (300±280 CFU-mast, 25±50 BFU-E, 15±25 CFU-GM, 191±200 CFU-mac, and 0 CFU-GEMM)(Figure 5.4). Even though Ao reaggregates consistently contained more CFU-Cs than UGR reaggregates (n=4), the difference was not significant (paired T-test; p=0.216). Interestingly, similar to the fresh tissue, UGR reaggregates did not contain CFU-GEMM.

AGM reaggregates controls for each of these experiments contained 4190±1280 CFU-Cs (1725±674 CFU-mast, 450±311 BFU-E, 275±263 CFU-GM, 1500±734 CFU-mac, and 240±165 CFU-GEMM)(Figure 5.4). In each of the four experimental replicates, CFU-C number in AGM reaggregates was significantly higher than the cumulative numbers obtained from Ao and UGR reaggregates; suggesting a stimulatory interaction between Ao and UGR.

5.2.2.3. Expansion of LTR-HSC in E11.5 Ao and UGR reaggregates

In vivo transplantations experiments were set up to answer the following questions: 1) do Ao and UGR have the autonomous potential to expand LTR-HSCs when cultured as reaggregates in $IMDM^{+}$? 2) If so, is number of LTR-HSCs generated in Ao and UGR reaggregates cumulatively similar to those generated in AGM reaggregates?

Transplantation of AGM reaggregates (0.01rd/recipient) resulted in repopulation of 23 out of 27 recipients (85%)(mean PBC: 58.4±27 %)(Figure 5.5A). The same dose of Ao reaggregates resulted in repopulation of only 10 out 22 recipient mice (45%)(mean PBC: 32.3±17 %)(Figure 5.5A). A higher dose of Ao reaggregate (0.05rd/recipient) resulted in repopulation of 5 out of 11 recipients

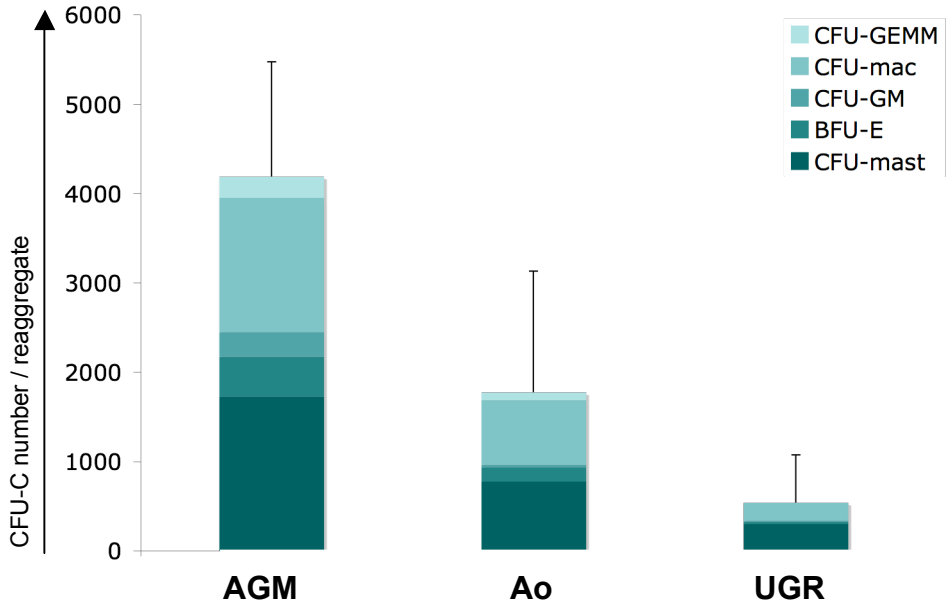

Figure 5.4: Haematopoietic progenitor expansion in Ao and UGR reaggregates.
Bars indicate the standard deviation of 4 independent experiments.
BFU-E: burst forming unit-erythroid; CFU: colony forming unit; Mac: macrophage; GM: granulocyte/macrophage; GEMM: granulocyte/erythroid/macrophage/megakaryocyte; ee: embryo equivalent.

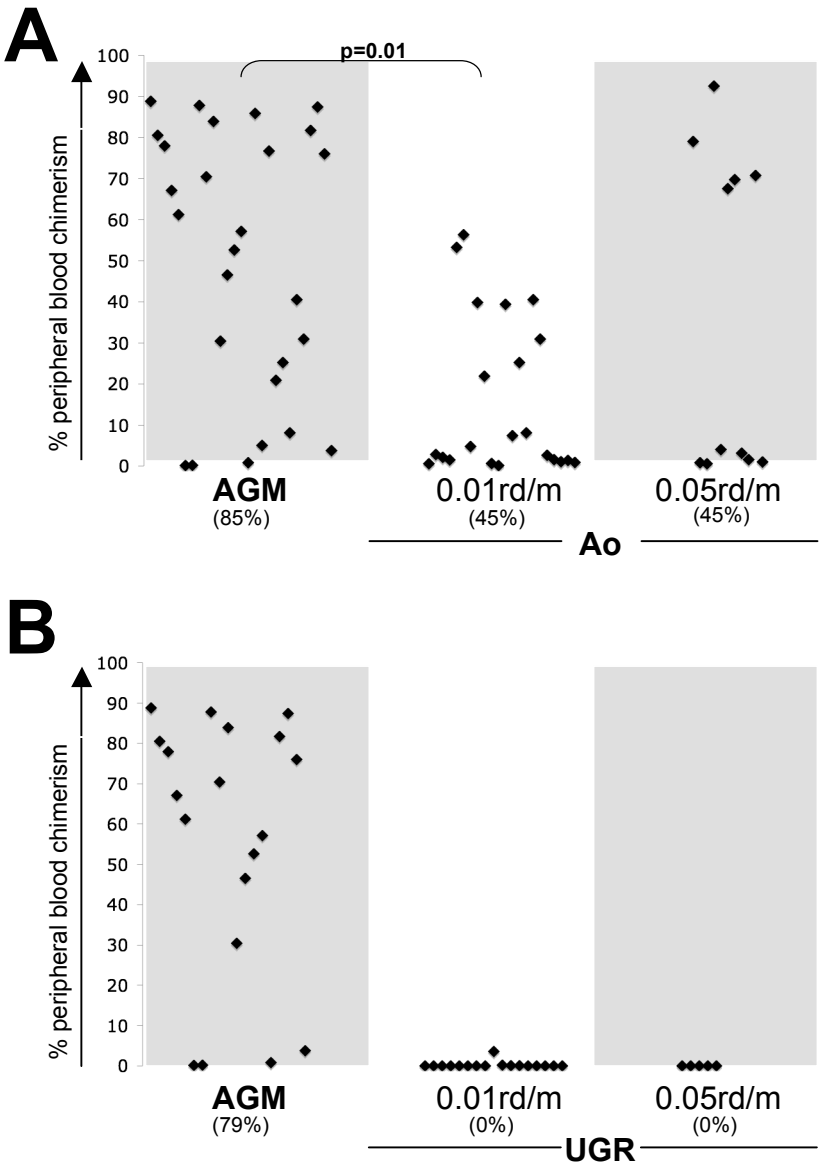

Figure 5.5: Autonomous LTR-HSCs expansion potential of the Ao and UGR as reaggregates.

A: Peripheral blood chimerism of recipients transplanted with Ao reaggregates. Data is cumulative of 6 independent experiments.

B: Peripheral blood chimerism of recipients transplanted with UGR reaggregates. Data is cumulative of 4 independent experiments. Each point represents a single recipient mouse. Recipients were considered reconstituted when their peripheral blood chimerism exceeded 5% at least 12 weeks after transplantation. (rd: dose of reaggregate injected per recipient mouse)

(45%)(mean PBC: 75.9±10 %)(Figure 5.5A). The mean PBC in this case was higher than with a lower dose, suggesting a higher number of LTR-HSCs. Statistical analysis showed that there was a significant difference in reconstitution levels between AGM reaggregates and Ao reaggregates (Fisher's exact test, p=0.01).

Similar experiments were set up with UGR reaggregates. Control AGM reaggregates (0.01rd/recipient) gave repopulation of 15 out of 19 recipients (79%)(mean PBC: 69.9±17.2 %)(Figure 5.5B). The same dose of UGR reaggregates gave no repopulation (0 out of 17 recipients) except one recipient with low-level reconstitution (3.58%)(Figure 5.5B). A higher dose (0.05rd/recipient) was transplanted to potentially detect low numbers of LTR-HSCs. No recipient mice were reconstituted (Figure 5.5B), suggesting that the UGR cannot autonomously generate detectable LTR-HSCs even in the presence of growth factors.

Taken together, these data indicate that only the Ao can autonomously generate detectable numbers of LTR-HSCs. However, the data show that AGM reaggregates can generate more LTR-HSCs (approximately 85) than the Ao on its own (approximately 45). In addition, the mean PBC of recipients transplanted with AGM reaggregates was higher than those of recipients transplanted with Ao reaggregates. This further indicates that AGM reaggregates produce more LTR-HSCs than Ao reaggregates. Thus, although UGR reaggregates cannot independently facilitate LTR-HSC formation, UGRs could enhance optimal LTR-HSC formation in the Ao. Alternatively, Ao could induce formation of LTR-HSCs from the UGRs.

5.2.2.4. Multilineage reconstitution by LTR-HSCs derived from Ao reaggregates

Multilineage analysis of mice transplanted with Ao reaggregates cells was performed by flow cytometry. The presence of donor cells in primary recipients was checked 16 weeks post-transplantation in haematopoietic tissues (peripheral blood, spleen, bone marrow, and thymus). All tissues contained CD45.2 donor cells in high proportions (ranging from 40 to 73% in peripheral blood, 7 to 70% in bone marrow, 44 to 76% in the spleen, and 90 to 95% in the thymus)(Figure 5.6A). Peripheral

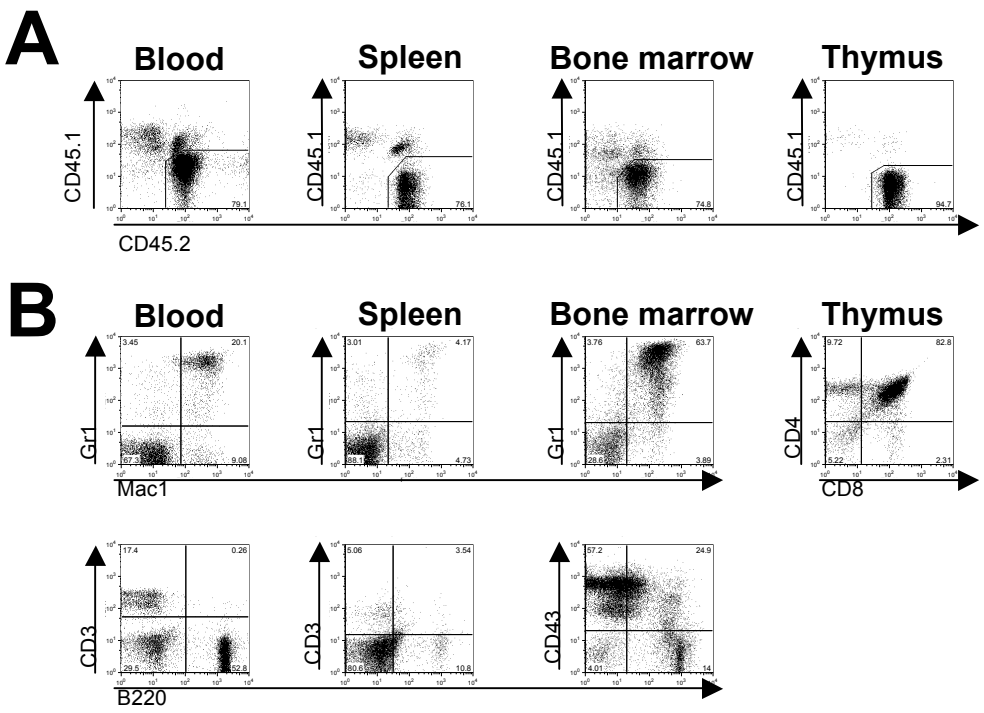

Figure 5.6: Multilineage haematopoietic reconstitution by LTR-HSCs generated in Ao reaggregates.

A: Long-term donor derived reconstitution in major haematopoietic organs (peripheral blood, spleen, bone marrow, and thymus).

B: Long-term multilineage (myelo-lymphoid) contribution in major haematopoietic organs (peripheral blood, spleen, bone marrow, and thymus) of recipients. Events were gated on donor cells exclusively.

Representative example of analysis performed on 2 recipients transplanted with 0.05rd showing high-level reconstitution.

Quadrants are based on appropriate isotype control (Appendix 3.2) and values indicate percentages of cells. Cell viability was determined by 7-AAD uptake.

blood, spleen and bone marrow contained myeloid cells ($Mac1^+$ and $Gr1^+$) and lymphoid cells ($CD3^+$ T cells, and $B220^+$ and $CD43^+$ B cells)(Figure 5.6B). The majority of donor cells in the thymus were immature $CD4^+CD8^+$ T cells and mature single-positive T cells ($CD4^+CD8^-$ and $CD4^-CD8^+$)(Figure 5.6B). Thus, HSCs generated by Ao reaggregates are true multilineage LTR-HSCs.

5.2.3. Spatial origin of LTR-HSCs in E11.5 AGM reaggregates: axio-lateral polarity

The fact that AGM reaggregates produce more LTR-HSCs than Ao reaggregates has two possible explanations: UGRs could generate high level reconstituting LTR-HSCs when induced by Ao cells; or that UGRs could enhance LTR-HSCs production from the Ao. Chimeric reaggregates combining WT and GFP cells were set up to distinguish between these two possibilities. The experimental strategy was to produce Ao^{GFP} with UGR^{WT} chimeric reaggregates to trace Ao and UGR cells during culture (Figure 5.7A). To exclude a potential influence of constitutive GFP expression, reciprocal experiments in which chimeric Ao^{WT} and UGR^{GFP} reaggregates were produced (Figure 5.7A). In addition, basic characterisation of E11.5 AGM^{GFP} was performed to confirm constitutive GFP expression in the tissue (Appendix 5.1; Gilchrist et al., 2003). No significant difference in cell numbers between GFP and WT E11.5 AGM regions were observed (Appendix 5.1A). Interestingly, 1.44±0.4 % of viable cells were GFP^- (Appendix 5.1A). GFP reaggregates were also set up. Although 1.34% of cells in GFP reaggregates were GFP^-, all $CD45^+$ cells were GFP^+ (Appendix 5.1B). Analysis of a reconstituted recipient showed that more than 98% of leucocytes in the peripheral blood were GFP^+. This analysis confirmed the validity of using GFP mice in cell fate tracing experiments.

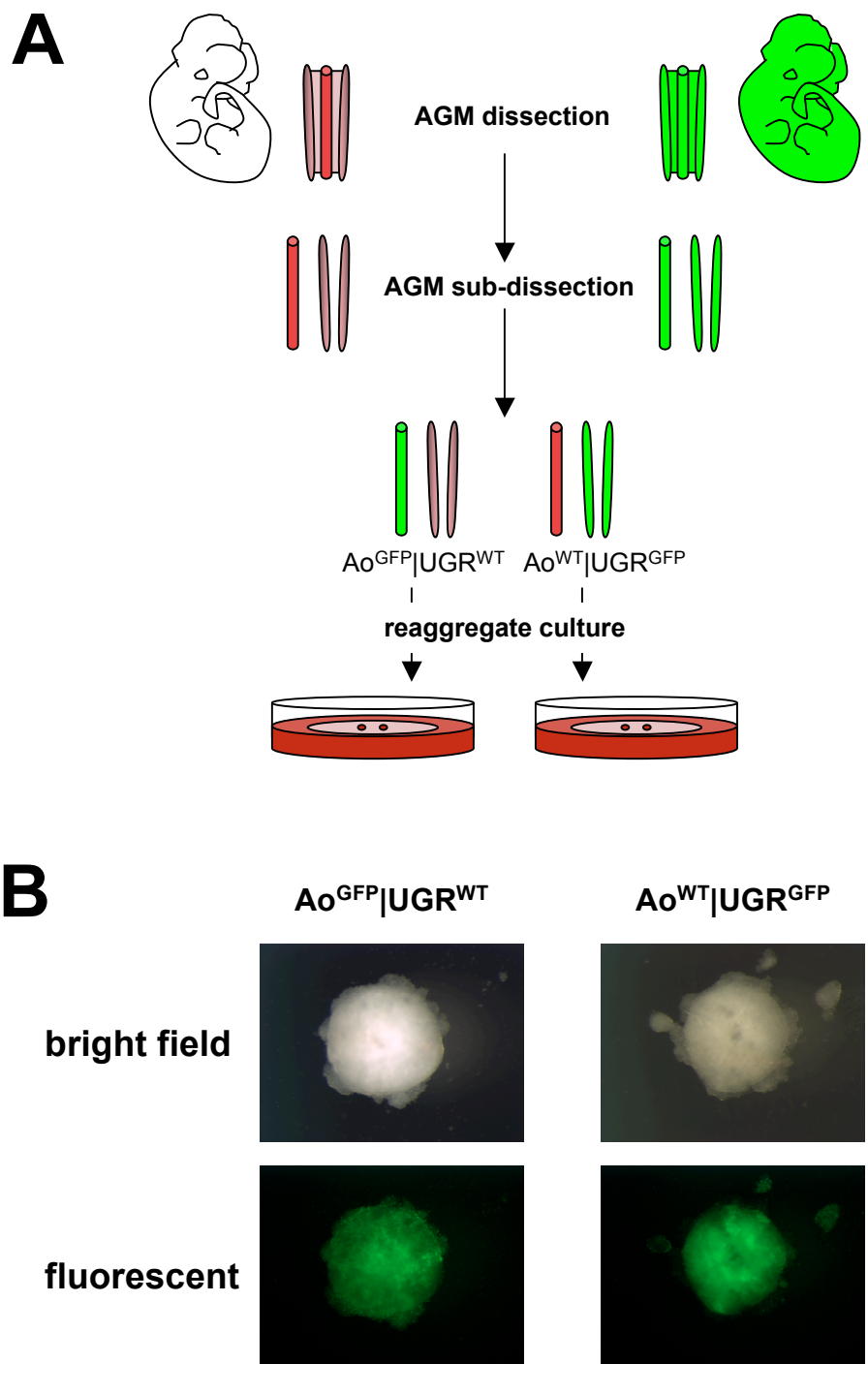

Figure 5.7: Experimental design to trace the origin of LTR-HSCs in the E11.5 AGM region.

A: Generation of chimeric reaggregates to trace pre-HSCs in the E11.5 AGM region: organs are laterally sub-dissected in both WT and GFP embryos and chimeric reaggregates are produced with Ao and UGR from the 2 genotypes. After 4 days in culture, LTR-HSCs are assessed by competitive repopulation assay.

B: Representative images of AGM chimeric reaggregates showing no morphological difference between reciprocal set-ups.

5.2.3.1. Expansion of haematopoietic ($CD45^+$) cells in chimeric (Ao/UGR) E11.5 AGM reaggregates

There were no obvious morphological or size differences between $Ao^{WT}|UGR^{GFP}$ and $Ao^{GFP}|UGR^{WT}$ reaggregates (Figure 5.7B). Fluorescent images of these reaggregates showed preferable concentration of Ao cells in the centre of the reaggregates (Figure 5.7B). More accurate analysis by confocal microscopy is required to investigate the spatial segregation of Ao and UGR derived cells.

There was no statistical difference in cell numbers between reciprocal reaggregate set-ups ($Ao^{WT}|UGR^{GFP}$: 199500±51030 cells and $Ao^{GFP}|UGR^{WT}$: 194330±19120 cells)(Wilcoxon signed rank test, $p \geq 0.2$). Respective contribution of Ao and UGR to the viable cell population was assessed by flow cytometry. Wilcoxon signed rank test showed no significant differences between reciprocate set ups ($p \geq 0.2$ for both Ao and UGR): in $Ao^{WT}|UGR^{GFP}$ and $Ao^{GFP}|UGR^{WT}$ set ups, UGR generated 78200±15480 and 82670±14810 cells respectively; and Ao generated 58850±17980 and 53570±12200 cells respectively (Figure 5.8A).

Wilcoxon signed rank test showed no significant difference between the numbers of haematopoietic ($CD45^+$) cells in reciprocate set-ups ($p \geq 0.2$): $Ao^{WT}|UGR^{GFP}$ and $Ao^{GFP}|UGR^{WT}$ reaggregates contained 21700±5300 and 20000±5510 $CD45^+$ cells respectively (Figure 5.8B). In $Ao^{WT}|UGR^{GFP}$ and $Ao^{GFP}|UGR^{WT}$ reaggregates, Ao generated 15370±3390 cells and 13800±4290 $CD45^+$ cells respectively (Figure 5.8B). In $Ao^{WT}|UGR^{GFP}$ and $Ao^{GFP}|UGR^{WT}$ reaggregates, UGRs generated 6340±2540 and 6170±1260 $CD45^+$ cells respectively (Figure 5.8B). Respective contributions of Ao and UGRs to $CD45^+$ cells were not significantly different between reciprocate set-ups (Wilcoxon signed rank test, $p= 0.58$ for UGR, and $p=0.85$ for Ao).

Taken together, these data indicate that similar cell contributions from Ao and UGR are obtained in $Ao^{WT}|UGR^{GFP}$ and $Ao^{GFP}|UGR^{WT}$ reaggregates. In both cases, the majority (around 70%) of $CD45^+$ cells in reaggregates are Ao-derived and only around 30% of $CD45^+$ are derived from UGR.

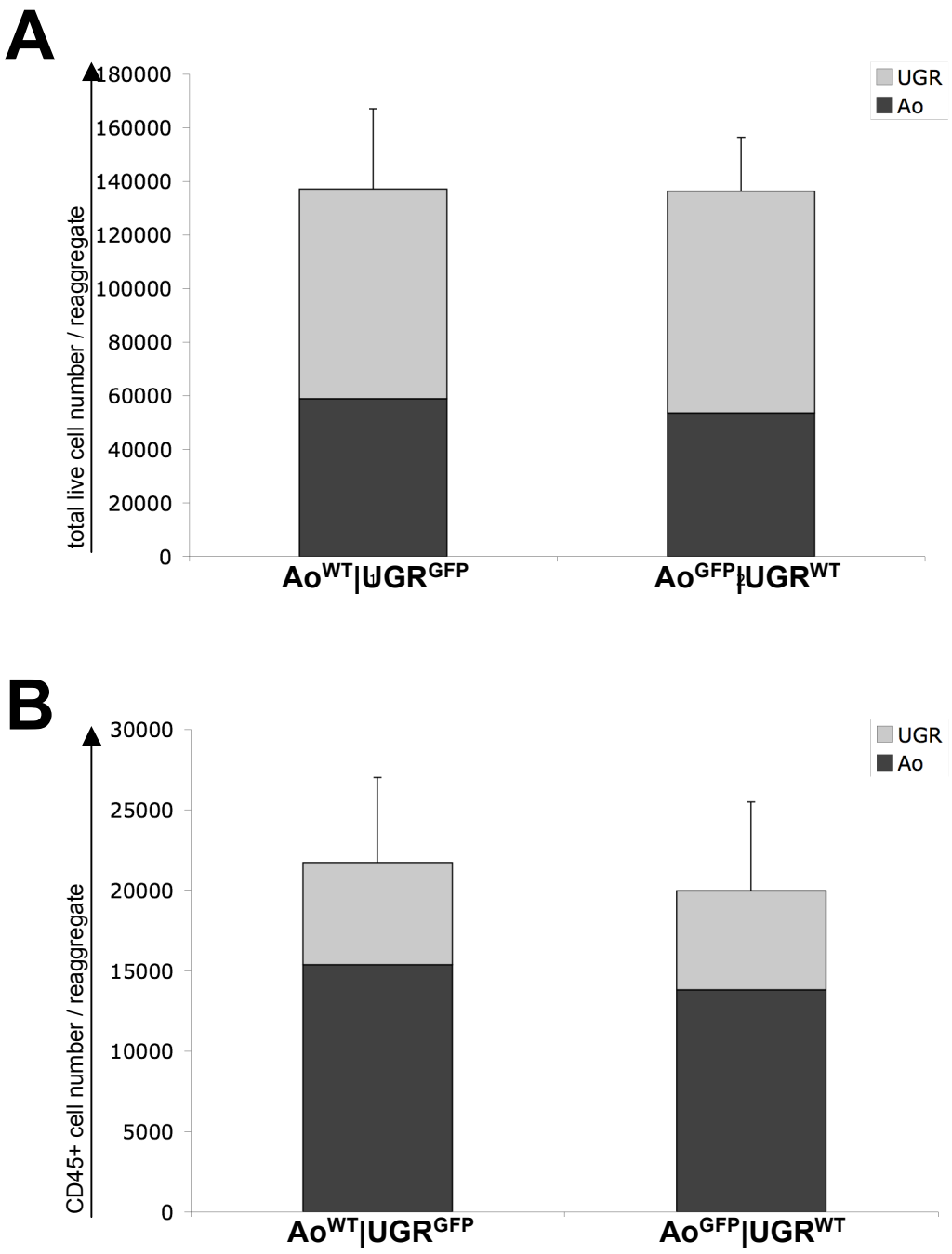

Figure 5.8: Respective contribution of Ao and UGR to the haematopoietic cell compartment of E11.5 AGM chimeric reaggregates.

A: Live cells numbers and respective contribution of Ao and UGR.

B: Haematopoietic cell ($CD45^+$) numbers and respective contribution of Ao and UGR.

Bars indicate the standard deviation of 4 independent experiments.

Data was acquired by flow cytometric analysis; cell viability was determined by 7-AAD uptake.

When compared with the fresh tissue, Ao and UGR cells respectively underwent between 1.2 and 1.3 fold expansion during reaggregate culture. However, $CD45^+$ cells from Ao underwent 12-fold expansion while $CD45^+$ cells from UGR underwent 3-fold expansion. Thus, the haematopoietic potential of the Ao, judged by the number of $CD45^+$ cells produced, is significantly greater than the UGR.

5.2.3.2. CFU-C expansion potential of chimeric (Ao/UGR) E11.5 AGM reaggregates

There was no difference in CFU-Cs numbers between $Ao^{WT}|UGR^{GFP}$ and $Ao^{GFP}|UGR^{WT}$ set-ups (Wilcoxon signed rank test, p=0.85)(Figure 5.9). $Ao^{WT}|UGR^{GFP}$ and $Ao^{GFP}|UGR^{WT}$ reaggregates respectively contained 4190±1280 CFU-Cs (1725±674 CFU-mast, 450±311 BFU-E, 275±263 CFU-GM, 1500±734 CFU-mac, and 240±165 CFU-GEMM) and 3940±840 CFU-Cs (1775±685 CFU-mast, 312±165 BFU-E, 265±209 CFU-GM, 1387±522 CFU-mac, and 200±168 CFU-GEMM)(Figure 5.9).

Unfortunately, the respective contribution of the Ao and UGR to CFU-Cs could not be reliably assessed for several reasons. First, there was a high amount of autofluorescence background in methylcellulose colonies (based on WT colonies controls), making the evaluation unreliable. In addition, some mature haematopoietic cells express low levels of GFP (own observation and S. Gordon-Keylock, personal communication), which are hard to detect by microscopy. To overcome this problem, FACS could be attempted but the very low numbers of cells in some individual colonies (around 100 in some cases) was unsuitable for flow cytometry processing. As a result, several attempts to determine the origin of individual CFU-C colonies based on GFP expression were unsuccessful.

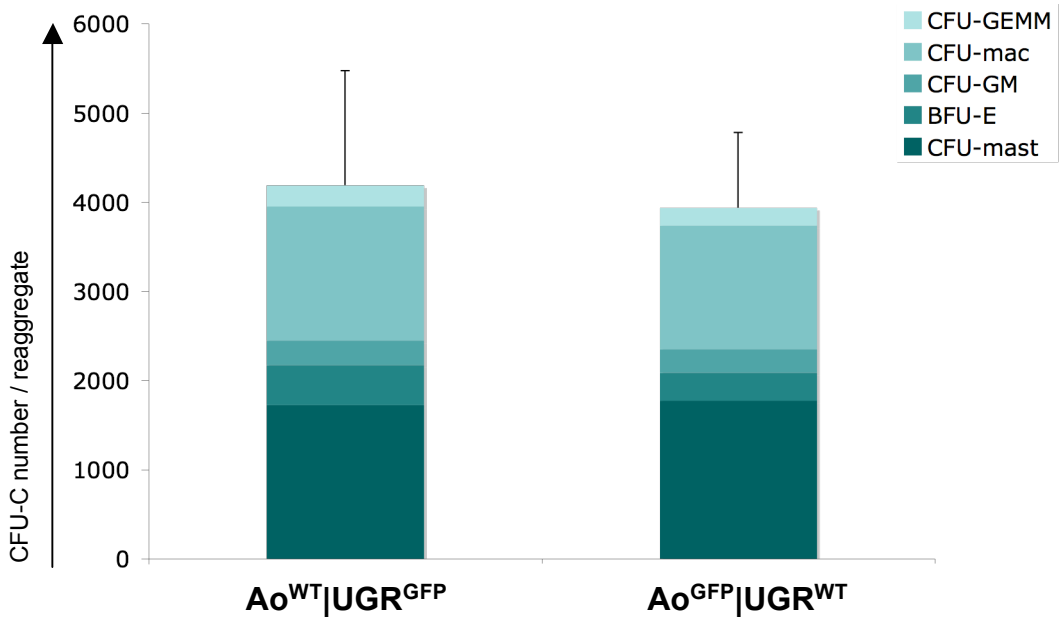

Figure 5.9: Haematopoietic progenitors expansion in E11.5 AGM chimeric reaggregates.

Bars indicate the standard deviation of 4 independent experiments.

BFU-E: burst forming unit-erythroid; CFU: colony forming unit; Mac: macrophage; GM: granulocyte/macrophage; GEMM: granulocyte/erythroid/macrophage/megakaryocyte; ee: embryo equivalent

5.2.3.3. The axio-lateral polarity of LTR-HSC development

The respective contribution of Ao and UGR into the chimeric reaggregates LTR-HSCs compartment was assessed using GFP expression. Transplantation of 0.01dose of chimeric $Ao^{WT}|UGR^{GFP}$ reaggregates resulted in reconstitution of 19 out of 27 recipients (70%)(mean PBC: 62±22 %)(Figure 5.10). Transplantation of 0.01dose of $Ao^{GFP}|UGR^{WT}$ reaggregates resulted in reconstitution of 8 out of 15 recipients (54%)(mean PBC: 53±37 %)(Figure 5.10). Although it appeared that $Ao^{WT}|UGR^{GFP}$ contained more LTR-HSCs than $Ao^{GFP}|UGR^{WT}$ based on the proportion of reconstituted recipients, this was not statistically significant (Fisher's exact test, p=0.3).

Respective contribution of Ao and UGR to recipient's peripheral blood was analysed based on GFP expression. The large majority of high level of blood chimerism was derived from Ao, both in $Ao^{WT}|UGR^{GFP}$ and $Ao^{GFP}|UGR^{WT}$ set-ups (Figure 5.10). In contrast, UGR only contributed to low level chimerism in 2 out of 19 recipients (9% and 3.7%) tranplanted $Ao^{WT}|UGR^{GFP}$ reaggregates (Figure 5.10). However, most recipients reconstituted with $Ao^{GFP}|UGR^{WT}$ reaggregates cells had low (between 0.9 and 4.7%) but yet detectable contribution by UGR-derived cells (Figure 5.10). It is conceivable that some low WT donor contribution was due to down-regulating GFP in Ao-derived blood cells. Quantitative PCR would be required to properly establish this. However, given that LTR-HSCs are considered to be high level repopulating cells, we can safely conclude that in AGM reaggregates, LTR-HSCs originate from the Ao. Combined with the conclusion that higher numbers of LTR-HSCs are produced in AGM reaggregates compared to Ao reaggregates, these data demonstrate that LTR-HSCs production from the Ao is significantly enhanced by the presence of UGRs in the reaggregates.

5.2.4. Supportive effect of the UGR on LTR-HSC expansion

The better LTR-HSC production in AGM reaggregates could either be due to the presence of the UGRs providing a positive effect on Ao or to the size of the reaggregate (called here "community effect"). In order to test this possibility,

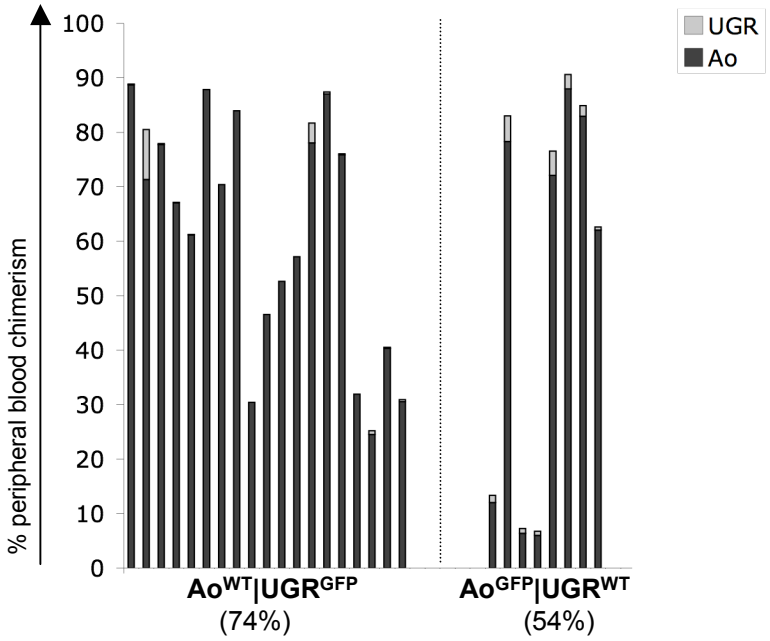

Figure 5.10: Lateral polarity of LTR-HSC expansion in E11.5 AGM chimeric reaggregates.

Peripheral blood chimerism of recipients transplanted with 0.01 dose of E11.5 AGM chimeric reaggregates.

Data is cumulative of 6 independent experiments for $Ao^{WT}|UGR^{GFP}$, and 4 independent experiments for $Ao^{GFP}|UGR^{WT}$.

Only reconstituted mice are displayed; percentages correspond to the proportion of reconstituted recipients. Each bar represents a single recipient mouse. Recipients were considered reconstituted when their peripheral blood chimerism exceeded 5% at least 12 weeks after transplantation.

reaggregates made with 2 Ao (Ao|Ao) were set up along with AGM controls and Ao reaggregates.

Only LTR-HSC data were analysed for these experiments. When 0.01 dose of AGM reaggregate was transplanted into single recipient mice, 8 out of 8 mice (100%) were reconstituted (mean PBC: 36.3%)(Figure 5.11). In similar conditions, only 3 out of 5 mice (60%) were reconstituted when transplanted with Ao reaggregate cells (mean PBC: 37.1%); and 3 out of 6 mice (50%) were reconstituted when transplanted with Ao|Ao reaggregates (mean PBC: 21%)(Figure 5.11). When transplanted with 0.05 doses of reaggregates, 3 out of 6 mice (50%) were reconstituted with Ao reaggregate cells (mean PBC of 79.6%) and 4 out of 6 mice (67%) were reconstituted with Ao|Ao reaggregates (mean PBC: 34.6%)(Figure 5.11). These data show that doubling of the numbers of Ao cells in reaggregates generates approximately the same LTR-HSCs numbers (≈60 in both Ao and Ao|Ao reaggregates in contrast to at least 100 in AGM reaggregates).

Furthermore, because comparable numbers of LTR-HSCs were obtained from a single Ao and two Ao, suggests the performance of a single Ao is decreased when exposed to additional Ao cells. Altogether, these results confirm that co-culture with UGR cells specifically enhances LTR-HSCs formation from Ao. Additional experiments would be required in order to obtain more accurate numbers of LTR-HSCs generated by the Ao.

5.3. Dorso-ventral polarity of LTR-HSC development within E11.5 AGM region

Our laboratory has demonstrated that LTR-HSCs in the E11.5 AGM region are almost exclusively located in the AoV and that only this site has the autonomous potential of expanding LTR-HSCs when cultured as explants (Taoudi and Medvinsky, 2007).

Here, I focused on the haematopoietic potential of the AoD and aimed to establish whether it harbours cells that are competent to develop into LTR-HSCs.

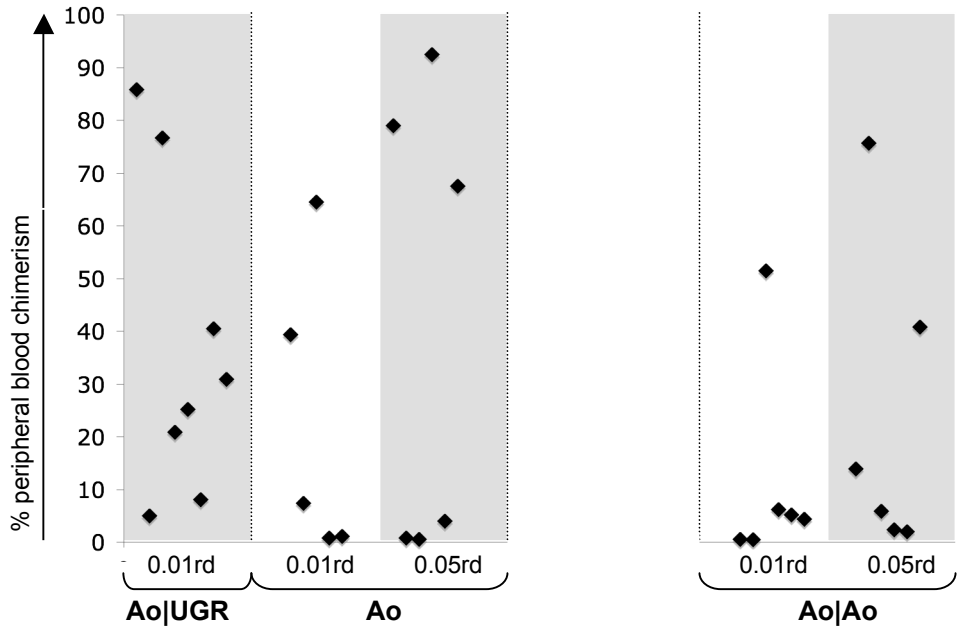

Figure 5.11: Supportive effect of the UGR on LTR-HSCs expansion from the Ao.
Reaggregation of large numbers of Ao cells (Ao|Ao, 2 embryo equivalent per reaggregate) compared to E11.5 AGM region (Ao|UGR) reaggregates.
Data are cumulative of 2 independent experiments.
Each point represents a single recipient mouse. Recipients were considered reconstituted when their peripheral blood chimerism exceeded 5% at least 12 weeks after transplantation.
(rd: dose of reaggregate injected per recipient mouse)

Two major approaches were undertaken to address this issue: 1) does the pesence of the notochord and adjoining somites inhibit LTR-HSCs formation in the AoD? 2) Can LTR-HSCs be induced from AoD when exposed to AoV/UGR and the combination of IL-3, SCF, and Flt3l?

5.3.1. Dorso-ventral dissections of the E11.5 AGM region

Previously, the dorsal tissue (DT)(containing notochord and partly somites) was left attached to the AoD in order to facilitate the dissections and to keep a landmark for the dorso-ventral orientation of the Ao. To test whether DT influences the AoD haematopoietic potential, DT was dissected from the AGM region prior to AoD-AoV sub-dissection.

Figure 5.12 shows dorso-ventral dissections and highlights that DT can be removed from the AGM prior to sub-dissection of the Ao (Figure 5.12A and B). Confocal microscopy confirmed that the endothelial lining of the AoD and AoV, marked by CD31 staining, was not disrupted during sub-dissections (Figure 5.12C). Note that the confocal pictures shown in this figure were taken prior to DT dissections.

5.3.2. Dorso-ventral distribution of cell populations in the fresh E11.5 AGM region

5.3.2.1. Dorso-ventral distribution of haematopoietic ($CD45^+$) and endothelial ($VE\text{-}cadherin^+$) cells

E11.5 AGM regions were sub-dissected and analysed by flow cytometry. DT was also isolated and analysed. Wilcoxon singed rank test showed no significant difference in cell numbers between AoD and AoV, containing 49330±11010 and 66330±8000 total cells respectively, and 35570±8250 and 38750±3110 viable cells respectively ($p=0.18$)(Table 5.2). No obvious dorso-ventral polarity of

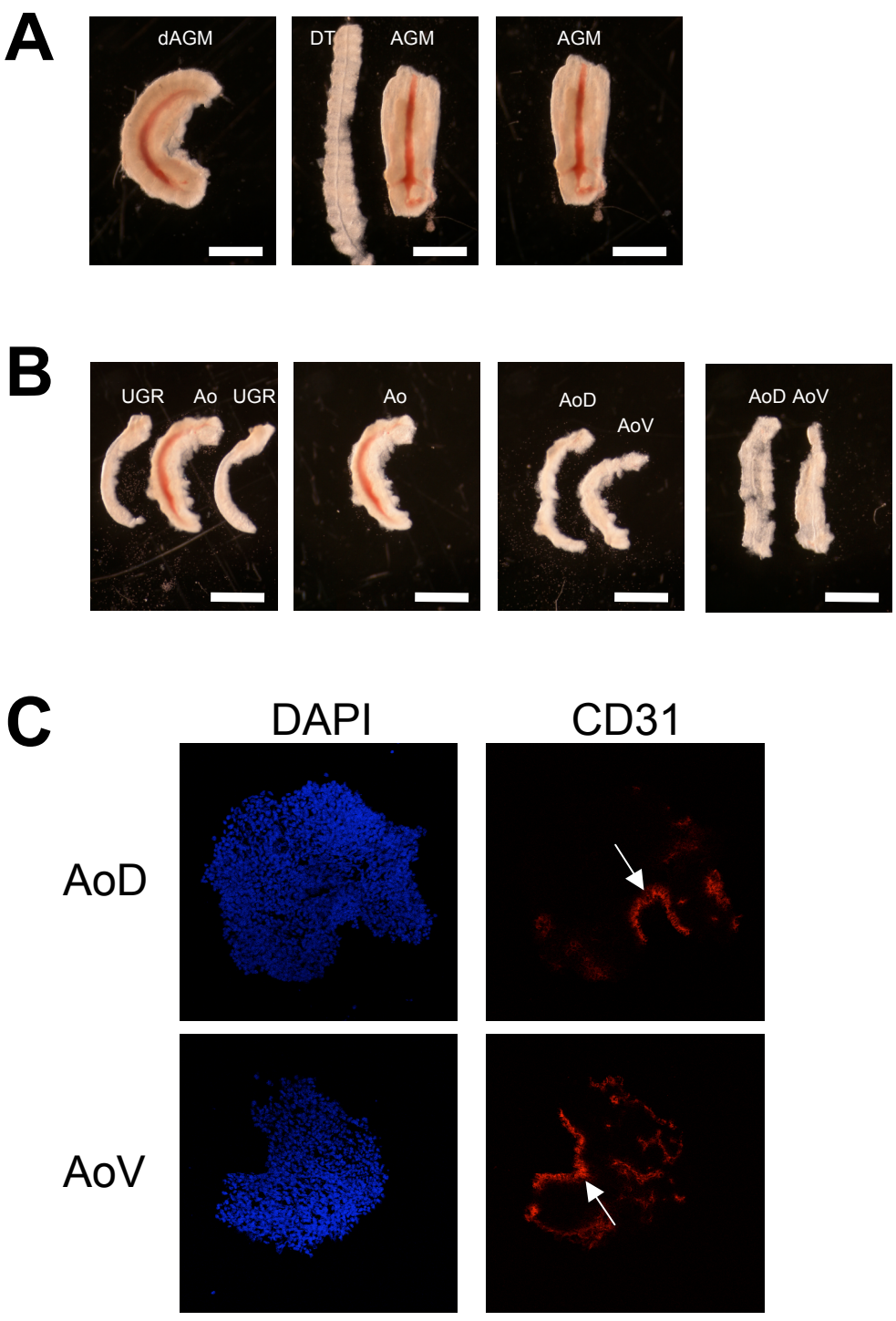

Figure 5.12: Scheme of E11.5 AGM region dorso-ventral subdissection into dorsal and ventral aspects of the dorsal aorta

A: Dissection of the E11.5 AGM region and removal of the dorsal tissue (DT) containing notochord and somite remnants. Bars: 1mm

B: Sub-dissection of the AGM region into urogenital ridges (UGR) and dorsal (AoD) and ventral (AoV) domains of the dorsal aorta. Bars: 1mm

C: Confocal miscroscopy of AoD and AoD shows intact endothelial lining of the dorsal aorta (Ao) after dissection (arrows). Blue: DAPI, Red: CD31

Table 5.2: Cell composition of the fresh E11.5 AGM region and their dorso-ventral repartition in AoV, AoD, and dorsal tissue.
Data was acquired by flow cytometry; cell viability was determined by 7-AAD uptake.
Mean absolute numbers ± standard deviation of 4 independent experiments.
DP: $CD45^{+}VE\text{-}cadherin^{+}$; DN: $CD45^{-}VE\text{-}cadherin^{-}$

	AGM	AoD	AoV	UGR	DT
total cells	229000 ± 47880	49330 ± 11010	66330 ± 8000	151400 ± 45230	123670 ± 9500
total live cells	120200 ± 8830	35570 ± 8250	38750 ± 3110	58740 ± 12900	93700 ± 13340
total $CD45^{+}$ cells	3400 ± 1110	880 ± 260	1380 ± 190	1560 ± 300	1600 ± 200
total VE $cadherin^{+}$ cells	3030 ± 540	340 ± 110	660 ± 140	1450 ± 230	290 ± 30
total DP cells	76 ± 37	22 ± 11	35 ± 11	26 ± 11	8 ± 2
total DN cells	113140 ± 7120	34150 ± 7990	36680 ± 2990	55680 ± 12410	91800 ± 13160

haematopoietic ($CD45^+$) cells was observed: AoD and AoV contained 880±260 and 1380±190 $CD45^+$ cells respectively (Wilcoxon signed rank test, p=0.18)(Table 5.2). Although not significantly different, numbers of $CD45^+$VE-$cadherin^+$ cells (enriched for LTR-HSCs) were consistently higher in the AoV compared to AoD (AoD: 22±11 $CD45^+$VE-$cadherin^+$ cells, AoV: 35±11 $CD45^+$VE-$cadherin^+$ cells; Table 5.2) (Wilcoxon signed rank test, p=0.18). Interestingly, DT contained 1600±190 of $CD45^+$ cells, comparable to what is obtained in the AoD and AoV (Table 5.2). There were 8±2 $CD45^+$VE-$cadherin^+$ cells in DT (Table 5.2).

Altogether, these data confirm published data that there is no significant dorso-ventral polarisation of haematopoietic cells in the E11.5 AGM region (Taoudi et al., 2008). Furthermore, the DT did not differ in this respect to the AoV and AoD. This raises the question of the haematopoietic potential of the DT and its potential to influence haematopoiesis from the AoD.

5.3.2.2. Dorso-ventral distribution of $EGFP^+$ cells in $Runx1^{EGFP/WT}$ embryos

In Runx1 haploinsufficient mice, Runx1 expression is restricted to the AoV (North et al., 1999). This observation was based on histological sections and the dorso-ventral polarity of Runx1 expression in the E11.5 AGM region has yet to be quantified and characterised. $Runx1^{WT/WT}$ and $Runx1^{EGFP/WT}$ E11.5 AGM regions were sub-dissected into AoV, AoD, and UGRs, and analysed by flow cytometry according to the strategy described in Chapter 4.

In the UGRs, 96.9±1.7% of $CD45^{SP}$ cells were $EGFP^+$ and 89.3±1.7 of $CD45^+$VE-$cadherin^+$ cells were $EGFP^+$ (Figure 5.13B). The MFI shift of the $Runx1^{EGFP/WT}$ embryos compared to $Runx1^{WT/WT}$ embryos was 11.1±0.7 in the $CD45^{SP}$ population and 13.9±0.8 in the $CD45^+$VE-$cadherin^+$ population (Figure 5.13B). In the non-haematopoietic fractions, 0.60±0.1% of cells expressed EGFP in the $CD45^-$ VE-$cadherin^-$ fraction, and 0.80±0.2% of cells in the $CD45^-$VE-$cadherin^+$ (Figure 5.13B).

In the AoD, 93.5±2.3% of $CD45^{SP}$ cells were $EGFP^{+}$ and 97.6±2.3% of $CD45^{+}$VE-$cadherin^{+}$ cells were $EGFP^{+}$ (Figure 5.13B). The MFI shift of the $Runx1^{EGFP/WT}$ embryos compared to $Runx1^{WT/WT}$ embryos was 9.6±0.8 in the $CD45^{SP}$ population and 21.0±4.8 in the $CD45^{+}$VE-$cadherin^{+}$ population (Figure 5.13B). In the non-haematopoietic fractions, 0.19±0.06% of cells expressed EGFP in the $CD45^{-}$ VE-$cadherin^{-}$ fraction, and 1.37±0.1% of cells in the $CD45^{-}$VE-$cadherin^{+}$ (Figure 5.13B).

In the AoV, 96.7±0.4% of $CD45^{SP}$ cells were $EGFP^{+}$ and 98.0±1.5 of $CD45^{+}$VE-$cadherin^{+}$ cells were $EGFP^{+}$ (Figure 5.13B). The MFI shift of the $Runx1^{EGFP/WT}$ embryos compared to $Runx1^{WT/WT}$ embryos was 11.3±1.1 in the $CD45^{SP}$ population and 23.2±1.8 in the $CD45^{+}$VE-$cadherin^{+}$ population (Figure 5.13B). In the non-haematopoietic fractions, 1.22±0.2% of cells expressed EGFP in the $CD45^{-}$ VE-$cadherin^{-}$ fraction, and 0.71±0.2% of cells in the $CD45^{-}$VE-$cadherin^{+}$ (Figure 5.13B).

The MFI shift of the $Runx1^{EGFP/WT}$ embryos compared to $Runx1^{WT/WT}$ embryos was lower in the UGR than in aortic region (AoD and AoV). The presence of few $CD45^{-}EGFP^{+}$ cells in UGRs, AoD, and AoV indicates that such cells are not segregated to a particular location. Interestingly however, a larger proportion of these $CD45^{-}EGFP^{+}$ cells were located in the AoV, giving additional incentive to investigate the fate of such cells. These results also confirm that most $CD45^{+}$ cells express EGFP/Runx1 (Sections 4.5.1, 4.5.3, 4.5.4, 4.5.5), independently of their location in the AGM region. Combining cell numbers with flow cytometric analysis indicates that Runx1 positive cells are equally distributed in the AoV and AoD. This contradicts previous report in which Runx1 expression was concentrated in the AoV in haploinsufficient $Runx1^{lz/+}$ mice (de Bruijn et al., 2002; North et al., 1999). Such discrepancy is likely due to the Runx1 haploinsufficiency in $Runx1^{lz/+}$ mice.

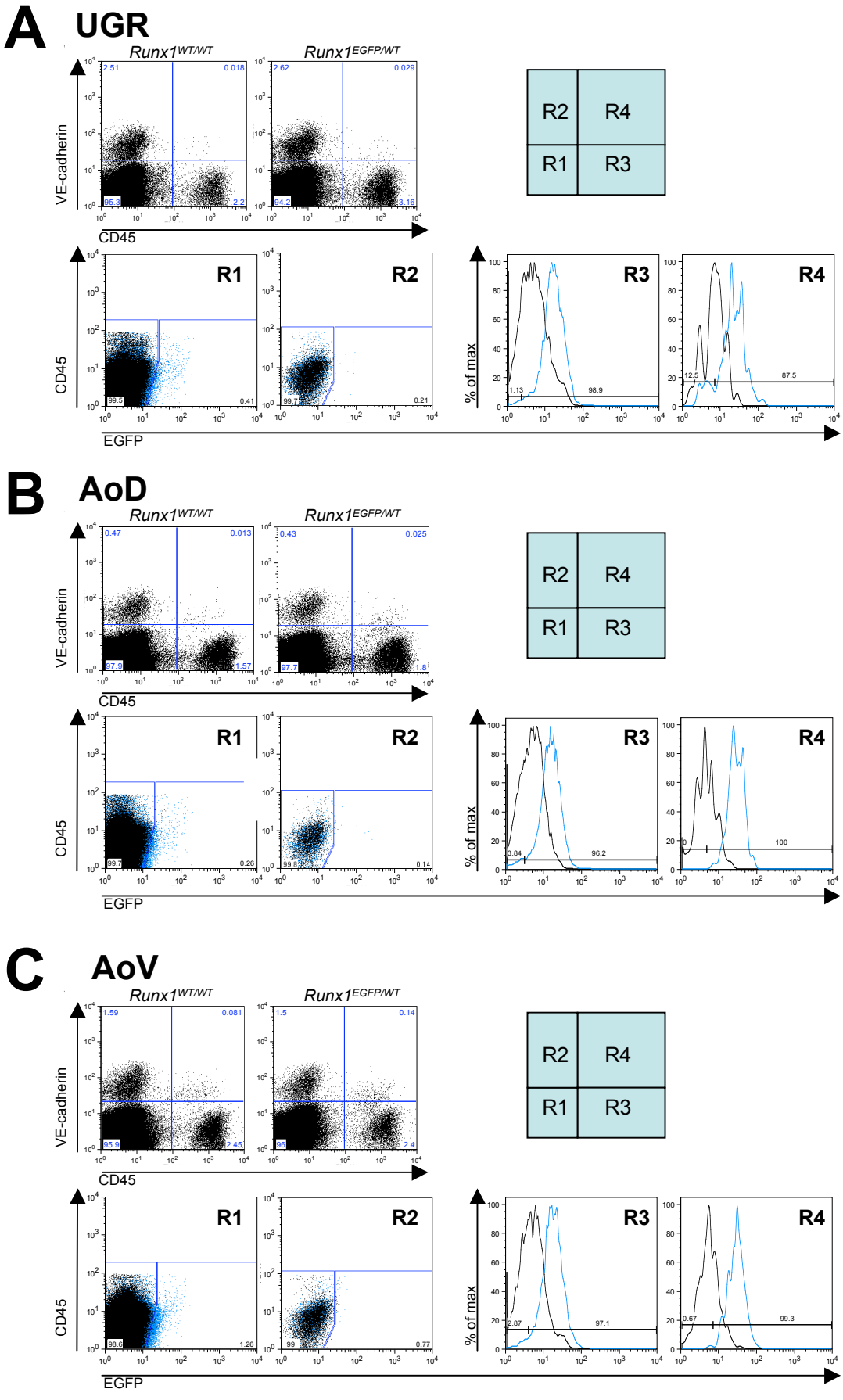
A
UGR
Runx1WT/WT
Runx1EGFP/WT
VE-cadherin
CD45
R2
R4
R1
R3
R1
R2
R3
R4
CD45
EGFP
% of max
B
AoD
Runx1WT/WT
Runx1EGFP/WT
VE-cadherin
CD45
R2
R4
R1
R3
R1
R2
R3
R4
CD45
EGFP
% of max
C
AoV
Runx1WT/WT
Runx1EGFP/WT
VE-cadherin
CD45
R2
R4
R1
R3
R1
R2
R3
R4
CD45
EGFP
% of max

Figure 5.13: EGFP expression in haematopoietic and endothelial compartments of *Runx1*$^{EGFP/WT}$ E11.5 UGR, AoD, and AoV.

A: Representative CD45 VE-cadherin stains in E11.5 UGRs of *Runx1*$^{EGFP/WT}$ animals compared to *Runx1*$^{WT/WT}$ animals and analysis of EGFP in CD45^{-}VE-cadherin^{-}, CD45^{-} VEcadherin^{+}, CD45^{+}VE-cadherin^{-}, CD45^{+}VE-cadherin^{+} cell fractions. Quadrants on dot plots were based on appropriate isotype controls (Appendix 4.3B).

B: Representative CD45 VE-cadherin stains in E11.5 AoD of *Runx1*$^{EGFP/WT}$ animals compared to *Runx1*$^{WT/WT}$ animals and analysis of EGFP in CD45^{-}VE-cadherin^{-}, CD45^{-} VEcadherin^{+}, CD45^{+}VE-cadherin^{-}, CD45^{+}VE-cadherin^{+} cell fractions.

C: Representative CD45 VE-cadherin stains in E11.5 AoV of *Runx1*$^{EGFP/WT}$ animals compared to *Runx1*$^{WT/WT}$ animals and analysis of EGFP in CD45^{-}VE-cadherin^{-}, CD45^{-} VEcadherin^{+}, CD45^{+}VE-cadherin^{-}, CD45^{+}VE-cadherin^{+} cell fractions.

EGFP: enhanced green fluorescent protein; WT: wild type; UGR: urogenital ridges; AoD: dorsal domain of the dorsal aorta; AoV: ventral domain of the dorsal aorta.

Black: *Runx1*$^{WT/WT}$ animals; Blue: *Runx1*$^{EGFP/Wt}$animals. Quadrants on dot plots were based on appropriate isotype controls (Appendix 4.3B) and values indicate percentages of cells. Cell viability was determined by 7-AAD uptake.

In histograms, values indicate percentages of cells for *Runx1*$^{EGFP/WT}$ animals.

All plots are representative examples of 3 independent experiments.

5.3.3. Dorso-ventral distribution of haematopoietic progenitors (CFU-Cs) in the fresh E11.5 AGM region.

The fresh AoD contained 20±7.0 CFU-Cs (4±3.0 CFU-mast, 4±1.5 BFU-E, 1±0.7 CFU-GM, 10±3.4 CFU-mac, and 1±0.5 CFU-GEMM) and AoV contained 42±11.8 CFU-Cs (14±2.5 CFU-mast, 6±2.5 BFU-E, 4±2.6 CFU-GM, 17±5.0 CFU-mac, and 2±1.5 CFU-GEMM), suggesting that there was a dorso-ventral gradient of CFU-Cs (Wilcoxon signed rank test, p=0.18)(Figure 5.14). Similarly to AoD, DT contained 22±11 CFU-Cs (7±4.5 CFU-mast, 2±0.3 BFU-E, 1±2.2 CFU-GM, 12±5.1 CFU-mac, and 0 CFU-GEMM)(Figure 5.14). When DT and AoD were not separated (DAoD), there were a total of 50±17.2 CFU-Cs (17±4.8 CFU-mast, 7±4.5 BFU-E, 4±2.5 CFU-GM, 21±9.7 CFU-mac, and 1±0.8 CFU-GEMM). This corresponded approximately to the sum of AoD and DT CFU-Cs, indicating that the presence of DT had no influence on haematopoietic colony formation during methylcellulose culture (Figure 5.14).

Similarly, the sum of fresh AGM (138±29.3 CFU-Cs in this case) and DT CFU-Cs roughly corresponded to DAGM CFU-C number (159±20 CFU-Cs: 51±7.4 CFU-mast, 30±7.6 BFU-E, 21±17.7 CFU-GM, 51±4.6 CFU-mac, and 6±3 CFU-GEMM), confirming that DT does not influence colony formation in methylcellulose cultures (Figure 5.14).

5.3.4. The influence of dorsal tissue on AoD haematopoiesis

5.3.4.1. Influence of dorsal tissue on AoD haematopoietic cells outcome during explant culture.

To test whether DT influences AoD haematopoiesis during *ex vivo* culture, explants of AGM, DAGM, AoD and DAoD were set up in IMDM$^-$ (IMDM based medium with 20% serum but without IL-3, SCF, or Flt3l) and Myelocult medium (M5300, Stem Cell Technologies).

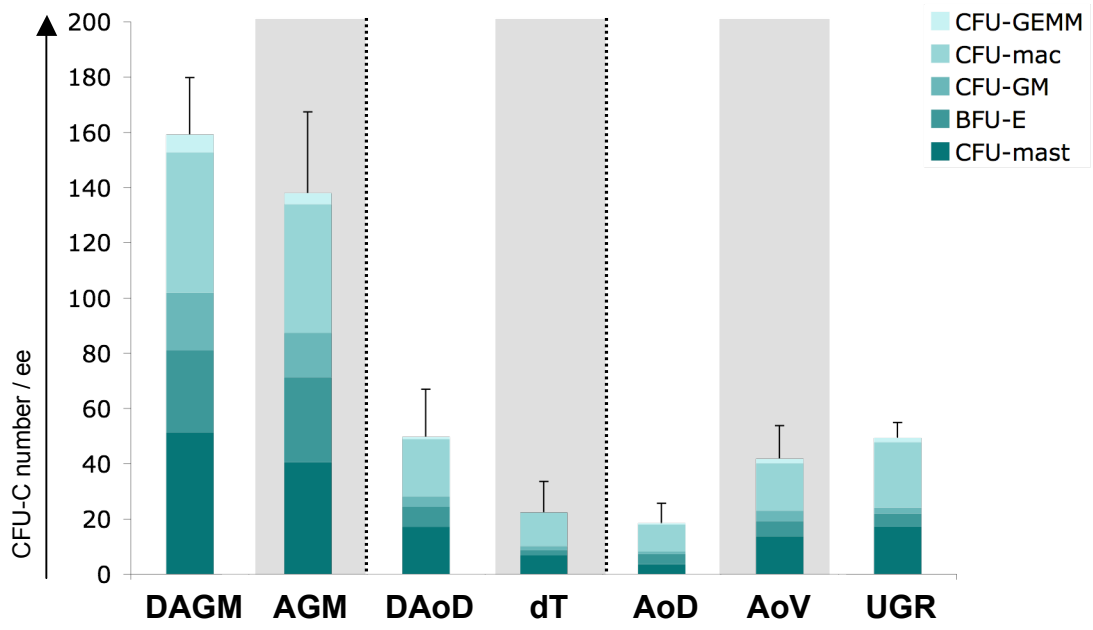

Figure 5.14: Dorso-ventral segregation of haematopoietic progenitors in fresh E11.5 AoV, AoD, and dorsal tissue.

Bars indicate the standard deviation of 3 independent experiments.

BFU-E: burst forming unit-erythroid; CFU: colony forming unit; Mac: macrophage; GM: granulocyte/macrophage; GEMM: granulocyte/erythroid/macrophage/megakaryocyte; ee: embryo equivalent.

After 4 days in IMDM$^-$ medium, DAGM and AGM explants contained 7990±2095 and 6610±1820 CD45$^+$ cells respectively (Figure 5.15A). DAoD and AoD explants contained 1830±840 and 970±570 CD45$^+$ cells respectively, which was not significantly different (Wilcoxon signed rank test, p=0.18)(Figure 5.15A). AoV explants contained 1700±555 CD45$^+$ cells (Figure 5.15A). There was no significant difference in CD45$^+$ cell numbers between AoD and AoV explants (Wilcoxon signed rank test, p=0.18).

After 4 days in Myelocult medium, AGM explants contained 5770±1840 CD45$^+$ cells (Figure 5.15B). DAoD and AoD explants contained 900±300 and 310±120 CD45$^+$ cells respectively (Figure 5.15A' and B'). AoV explants contained 840±360 CD45$^+$ cells (Figure 5.15B). Similarly to IMDM$^-$ medium explants, there were no significant differences in CD45$^+$ cell numbers between AoD and DAoD explants and between AoD and AoV explants (Wilcoxon signed rank test, p=0.18 in both cases).

When compared to the fresh tissue, there was no expansion of CD45$^+$ cells during culture in IMDM$^-$ (x1.0 fold expansion for AoD, and x1.2 fold expansion for AoV). Interestingly, there were consistently more CD45$^+$ cells in DAoD explants compared to AoD explants, indicating that DT does not have inhibitory influence of AoD haematopoietic cells. However, DT explants are required to understand its autonomous haematopoietic potential.

5.3.4.2. The influence of dorsal tissue on AoD haematopoietic progenitors.

The expansion of CFU-Cs in explant cultures was also assessed. When cultured in IMDM$^-$, DAGM and AGM explants contained similar numbers of CFU-Cs: 250±30 and 290±80 CFU-Cs respectively (Wilcoxon signed rank test, p=0.79)(Figure 5.16A). There was also no statistical difference between DAoD and AoD explants which contained 39±14 and 50±33 CFU-Cs respectively (Wilcoxon signed rank test, p=0.78)(Figure 5.16A). AoV explants contained 64±39 CFU-Cs (Figure 5.16A). Although not significantly different, CFU-Cs numbers in AoV

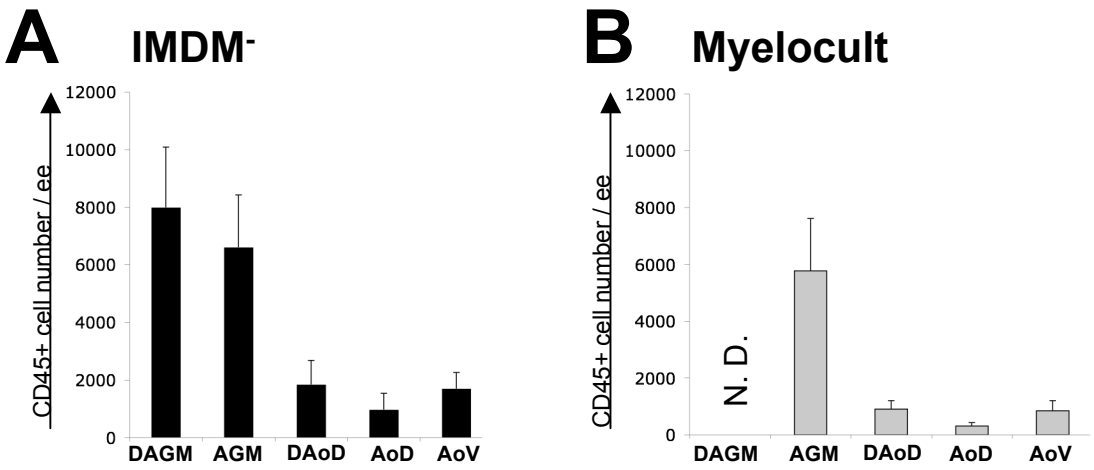

Figure 5.15: Influence of dorsal tissue on autonomous haematopoietic cell expansion in E11.5 AGM, AoV, and AoD explants.

A: Haematopoietic cell numbers in explants cultured in IMDM$^-$ for 4 days.

B: Haematopoietic cell numbers in explants cultured in Myelocult for 4 days.

Bars indicate the standard deviation of 3 independent experiments

Black: cultures in IMDM$^-$; Grey: cultures in Myelocult

N.D.: not done; ee: embryo equivalent

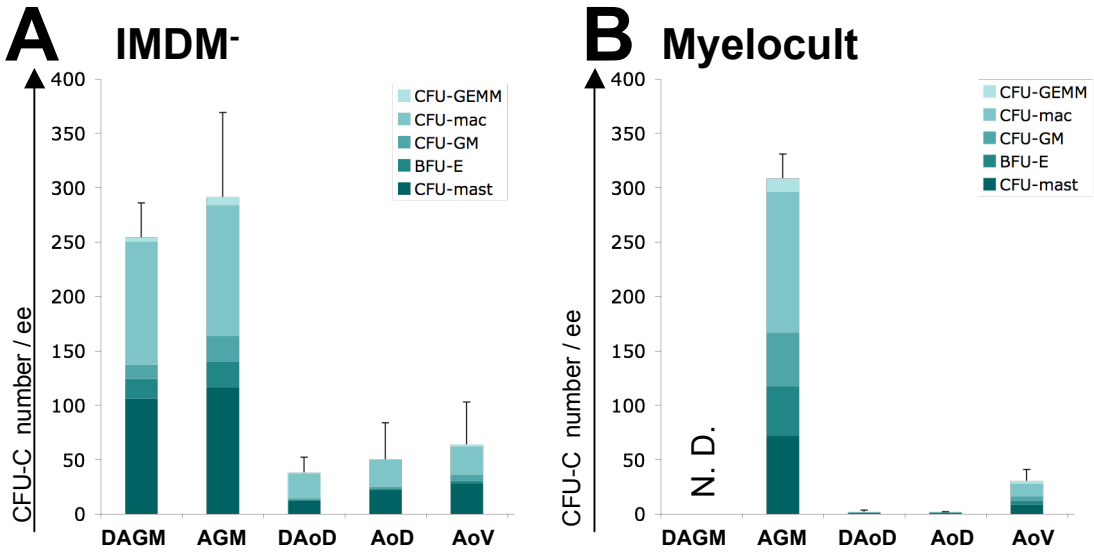

Figure 5.16: Influence of dorsal tissue on autonomous haematopoietic progenitors expansion in E11.5 AGM, AoV, and AoD explants.

A: CFU-C numbers contained in E11.5 DAGM, AGM, DAoD, AoD, and AoV explants cultured in IMDM$^-$ for 4 days.

B: CFU-C numbers contained in E11.5 AGM, DAoD, AoD, and AoV explants cultured in Myelocult medium for 4 days.

Bars indicate the standard deviation of 3 independent experiments.

BFU-E: burst forming unit-erythroid; CFU: colony forming unit; Mac: macrophage; GM: granulocyte/macrophage; GEMM: granulocyte/erythroid/macrophage/megakaryocyte; ee: embryo equivalent. N.D.: not done.

explants were consistently higher than those in DAoD and AoD explants (Wilcoxon signed rank test, p=0.18).

However, when Myelocult medium was used, a clear dorso-ventral repartition of CFU-Cs was observed as DAoD and AoD explants both contained 2 CFU-Cs whereas AoV explants contained 31±10 CFU-Cs (Figure 5.16B). AGM explants contained 310±22 CFU-Cs (Figure 5.16B). These observations were in line with previous data (Taoudi and Medvinsky, 2007).

AoD explants have a tendency to give lower numbers of CFU-Cs than AoV explants in both IMDM$^-$ and Myelocult media. Such tendency was accentuated in Myelocult medium, which might be likely to have inhibitory effects on the production of CFU-Cs by AoD.

5.3.4.3. Influence of dorsal tissue on LTR-HSC expansion using explant cultures

LTR-HSC content in explants was assessed by competitive long-term *in vivo* repopulation assay. When E11.5 AGM explants cultured in IMDM$^-$ medium for 4 days were transplanted (0.3 ee/recipient), 7 out of 13 recipients (54%) were reconstituted (mean PBC: 56.9%)(Figure 5.17A). However, DAGM in the same conditions showed significantly reduced LTR-HSC activity: only 1 out 9 recipient mice (11%) was reconstituted at high level (87.4%)(Fisher's exact test, p=0.03)(Figure 5.17). Although control AGM explants showed slightly lower LTR-HSC activity than expected (S. Taoudi, personal communication), there was a clear indication that the presence of DT inhibited LTR-HSC development in the AGM.

When cultured in Myelocult medium, AGM explants (0.3 ee/recipient) reconstituted 8 out of 9 recipients to similar levels as previously reported in this tissue (Figure 5.17B)(Taoudi and Medvinsky, 2007).

Unfortunately, none of the mice transplanted with AoV or AoD explants (0.3 ee/recipient) were reconstituted. These experiments were performed when organ/reaggregate cultures worked suboptimally for all members of the lab, which

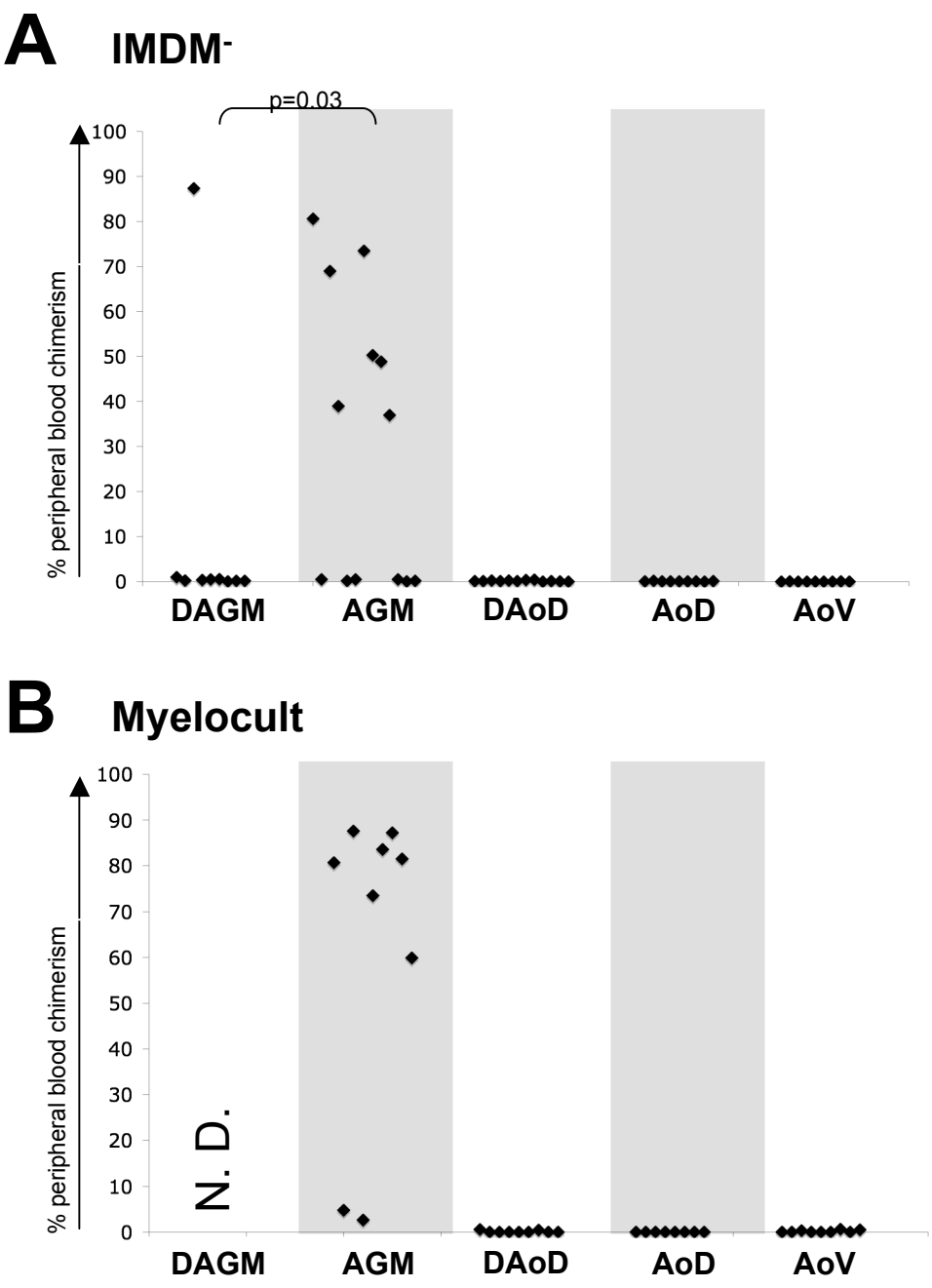

Figure 5.17: Influence of dorsal tissue on LTR-HSCs expansion in E11.5 AGM, AoV, and AoD explants.

Peripheral blood chimerism of recipients transplanted with 0.3 embryo equivalents of explant cells.

A: LTR-HSCs expansion in explants cultured in IMDM$^-$ for 4 days.

B: LTR-HSCs expansion in explants cultured in Myelocult for 4 days.

Each point represents a single recipient mouse. Recipients were considered reconstituted when their peripheral blood chimerism exceeded 5% at least 12 weeks after transplantation. Percentage represents the proportion of reconstituted animals. Cumulative result of 3 independent experiments.

N.D.: not done.

could explain this intriguing result. Alternatively, this could be due to the longer culture period. Thus, these experiments should be repeated and higher doses of cells should be transplanted to ensure LTR-HSC detection.

5.3.4.4. Analysis of multilineage reconstitution of mice transplanted with IMDM$^-$ AGM explant cultures

Multilineage analysis of LTR-HSCs was performed at least 16 weeks post-transplantation (Figure 5.18). Peripheral blood, spleen, bone marrow, and thymus were analysed. All tissues contained CD45.2 donor cells in high proportions (ranging from 76 to 81% in peripheral blood, 44 to 72% in the bone marrow, 62 to 71% in the spleen, and 96 to 99% in the thymus)(Figure 5.18A). Peripheral blood, spleen and bone marrow contained both myeloid (Mac1$^+$ and Gr1$^+$) and lymphoid populations (CD3$^+$ T cells, and B220$^+$ and CD43$^+$ B cells)(Figure 5.18B). The majority of donor cells in the thymus were immature double positive (CD4$^+$CD8$^+$) T cells and mature single positive (CD4$^+$CD8$^-$ and CD4$^-$CD8$^+$) T cells (Figure 5.18B). Thus, LTR-HSCs produced in IMDM$^-$ were functional. Multilineage reconstitution from E11.5 AGM explants cultured in Myelocult was previously published (Medvinsky and Dzierzak, 1996).

5.3.5. Dorso-ventral polarity in generation of LTR-HSCs in the E11.5 AGM region

Although AoD contains very few LTR-HSCs, there is no evidence of the production of LTR-HSCs by AoD when cultured as explant in either IMDM$^-$ or Myelocult (Figure 5.17; (Taoudi and Medvinsky, 2007). However, it is conceivable that AoD contains cells competent to form LTR-HSCs under the influence of AoV and/or UGRs or growth factors.

To test these hypotheses, E11.5 AGM regions from WT and GFP embryos (constitutively expressing GFP, Appendix 5.1, Gilchrist et al., 2003) were sub-dissected into UGR, AoD and AoV. Chimeric reaggregates were generated

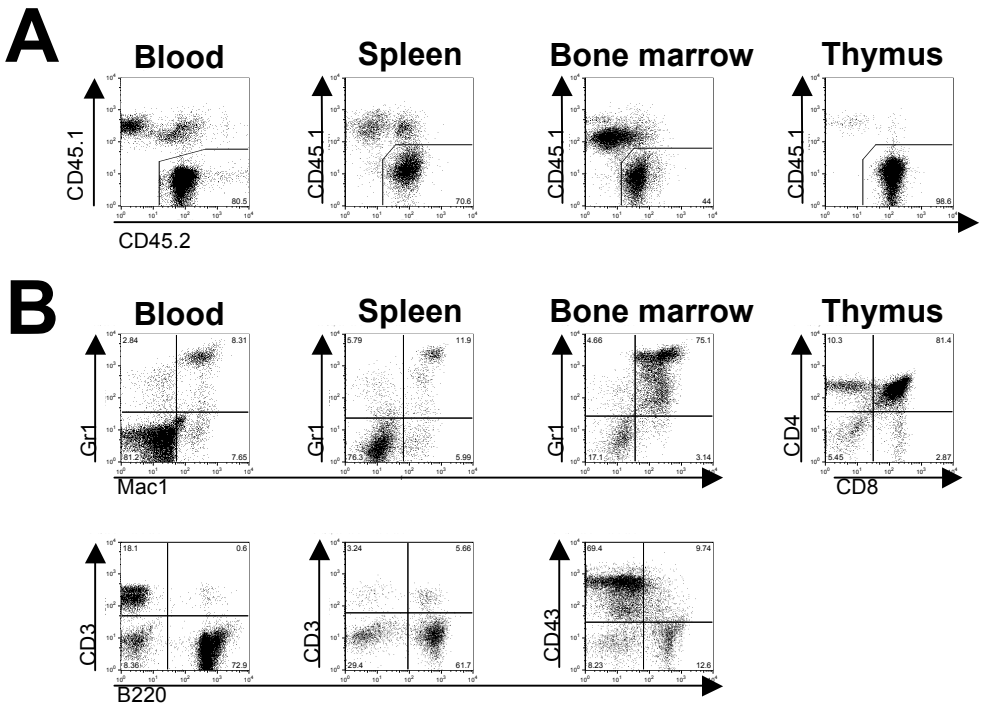

Figure 5.18: Long-term multilineage haematopoietic reconstitution by LTR-HSCs generated from E11.5 AGM explants cultured in IMDM$^-$.

A: Donor derived reconstitution in major haematopoietic organs (peripheral blood, spleen, bone marrow, and thymus) in recipients reconstituted with IMDM$^-$ explants cells.

B: Multilineage (myelo-lymphoid) contribution in major haematopoietic organs (peripheral blood, spleen, bone marrow, and thymus) of recipients reconstituted with IMDM$^-$ explants cells. Events were gated on donor cells exclusively.

Data were collected in high-level reconstituted recipients injected with 0.3 embryo equivalent of explant cells. Plots are representative of 2 recipient mice. Cell viability was determined by 7-AAD uptake. Quadrants are based on appropriate isotype control (Appendix 3.2) and values indicate percentages of cells.

and cultured in IMDM^{+} (Figure 5.19). DT was always left with AoD in reaggregates experiments.

5.3.5.1. Haematopoietic development from AoD in chimeric reaggregates

The contribution of AoD to chimeric reaggregates haematopoietic (CD45^{+}) cells was assessed. Reaggregates were cultured in IMDM^{+} for 4 and 5 days to investigate the potential dynamics of LTR-HSC emergence from AoD. Two independent experiments were performed in each condition and presented individually as their outcomes varied.

In 4 days chimeric AGM reaggregates, AoD-derived cells represented 26% and 21% of the viable cells in the 2 independent experiments (Figure 5.20A). Similar AoD contributions were obtained in 5 days chimeric reaggregates (26% and 24%)(Figure 5.20A). In 4 days chimeric Ao reaggregates, AoD-derived cells represented 47% and 53% of the viable cells in the 2 independent experiments (Figure 5.20A). Similar AoD contributions were obtained in 5 days chimeric reaggregates (51% and 43%) (Figure 5.20A).

AoD-derived haematopoietic (CD45^{+}) cell numbers were also assessed. 5 days AGM chimeric reaggregates contained more AoD-derived CD45^{+} cells compared to 4 days chimeric AGM reaggregates: 10670 and 7070 after 5 days (representing 44% and 40% of CD45^{+} cells) and 5810 and 4960 after 4 days (representing 34 % and 21% of CD45^{+} cells)(Figure 5.20B). In chimeric Ao reaggregates, numbers of AoD-derived CD45^{+} cells were similar after 4 and 5 days culture: 8890 and 16570 after 4 days (representing 44% and 58% of CD45^{+} cells) and 8800 and 8600 after 5 days (representing 43% and 44% of CD45^{+} cells)(Figure 5.20B).

Taken together, these data show that there is no obvious difference in CD45^{+} cell numbers between AGM and Ao chimeric reaggregates. In both AGM and Ao chimeric reaggregates, AoD underwent a gross 4-fold CD45^{+} cell expansion compared to the fresh tissue (Appendix 5.2). Thus, UGR does not influence

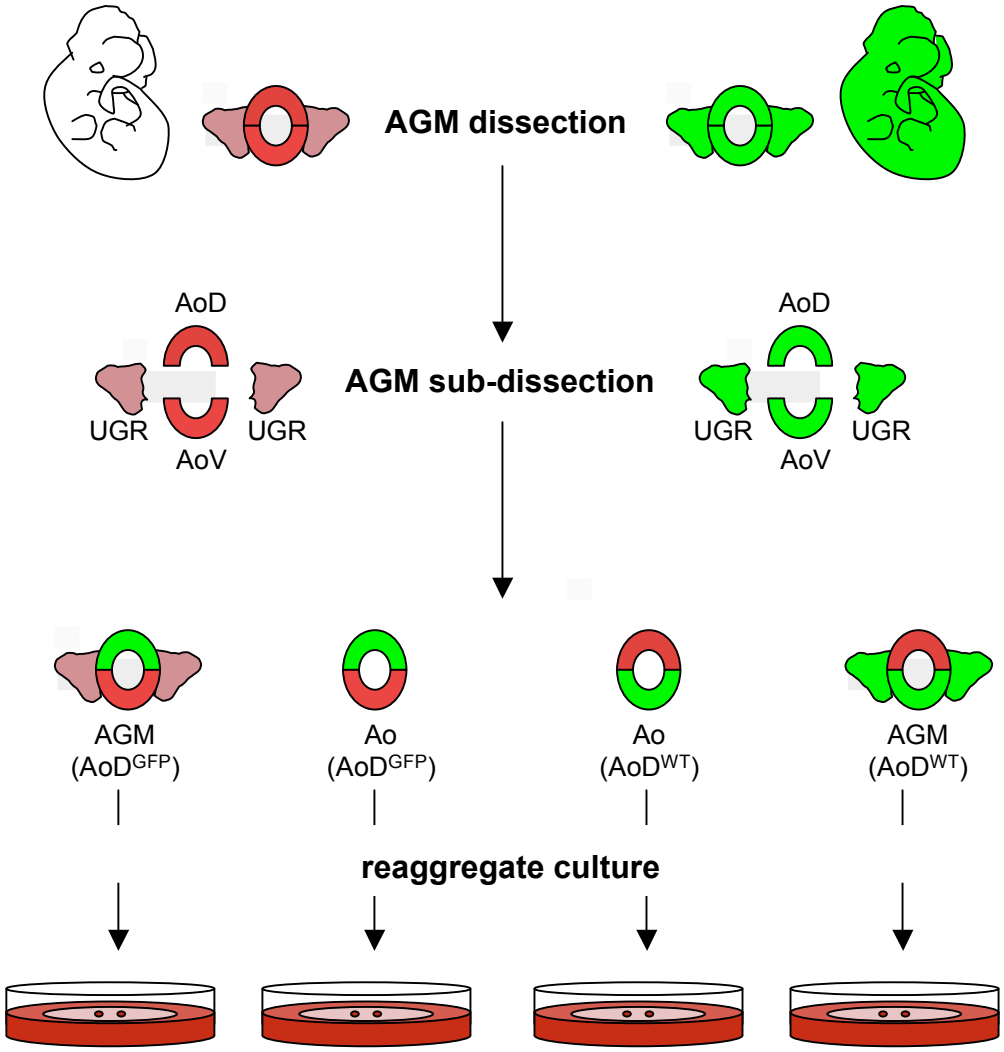

Figure 5.19: Experimental design to trace pre-HSCs in E11.5 AGM chimeric reaggregates.

Schematic representation of experimental design for chimeric reaggregates set-ups: WT and GFP AGM regions were sub-dissected into UGRs, AoD and AoV and cells from the 2 genotypes were mixed to produce chimeric reaggregates.

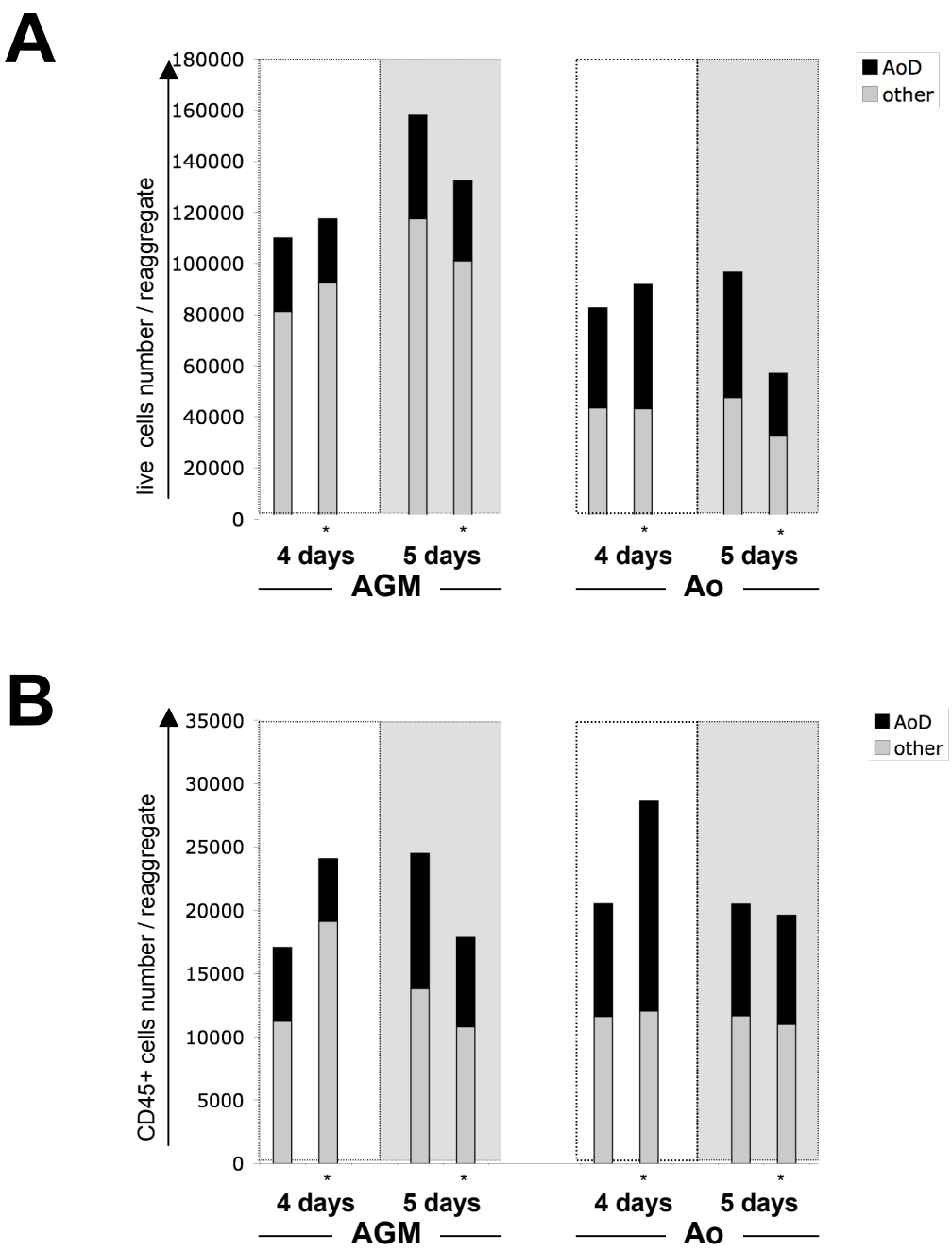

Figure 5.20: Haematopoietic expansion potential of AoD in E11.5 AGM region chimeric reaggregates.

A: AoD contribution to live cell numbers contained in 4 and 5 days chimeric reaggregates.

B: AoD contribution to haematopoietic ($CD45^+$) cell numbers contained in 4 and 5 days chimeric reaggregates.

Black: AoD; Grey: other (AoV and UGR when appropriate). Data is cumulative of 2 independent experiments, * mark experiment 2.

expansion of haematopoietic cells from AoD. AoD reaggregates would be required to conclude on the potential enhancing effects of AoV on haematopoietic cell expansion.

5.3.5.2. AoD contribution into the LTR-HSC compartment in E11.5 AGM chimeric reaggregates

After 4 or 5 days of culture, chimeric reaggregates were transplanted into recipients (0.1 rd/recipient).

When transplanted with 4 days AGM chimeric reaggregates, 6 out of 6 mice (100%) were reconstituted (mean PBC: 78.6%)(Figure 5.21A). AoD contribution in these recipients was assessed using the GFP genetic marker. AoD contribution to recipient's PBC was observed in 1 out of 2 experiments (stars in Figure 5.21A) and was on average smaller compared to AoV: 12% of the total PBC was AoD-derived (Figure 5.21A). When transplanted with 4 days Ao chimeric reaggregates, 4 out of 6 recipient mice (67%) were reconstituted (mean PBC: 20.2%) and AoD contribution represented 7.6% of the recipients' PBC (Figure 5.21A).

Similar analysis was performed with 5 days reaggregates. Unpublished data showed a plateau in LTR-HSCs numbers in reaggregates after 4 days of culture (S.Taoudi, unpublished). It has also been shown that maturation of pre-HSCs into LTR-HSCs mainly occurs between 3 and 4 days of culture (Taoudi et al., 2008). In view of these data, it was hypothesised that AoD-derived LTR-HSCs may take slightly longer to mature. Therefore, additional experiments were performed with 5 days cultures. 5 days chimeric AGM reaggregates (0.1 rd/recipient) reconstituted 6 out of 6 recipients (mean PBC: 67.62%) and a similar dose of chimeric Ao reaggregate reconstituted 2 out of 6 recipient mice (33%)(mean PBC: 52%)(Figure 5.21B). In this case, AoD contribution to recipient PBC was observed in the 2 experiments (Figure 5.21B). In AGM chimeric reaggregates, an average of 38.5% of the total PBC was AoD-derived; and in Ao chimeric reaggregates, an average of 9% of the total PBC was AoD-derived (Figure 5.21B). The fact that AoD-derived LTR-HSCs were present in 2 out of 2 experiments in 5 days reaggregates (compared to 1

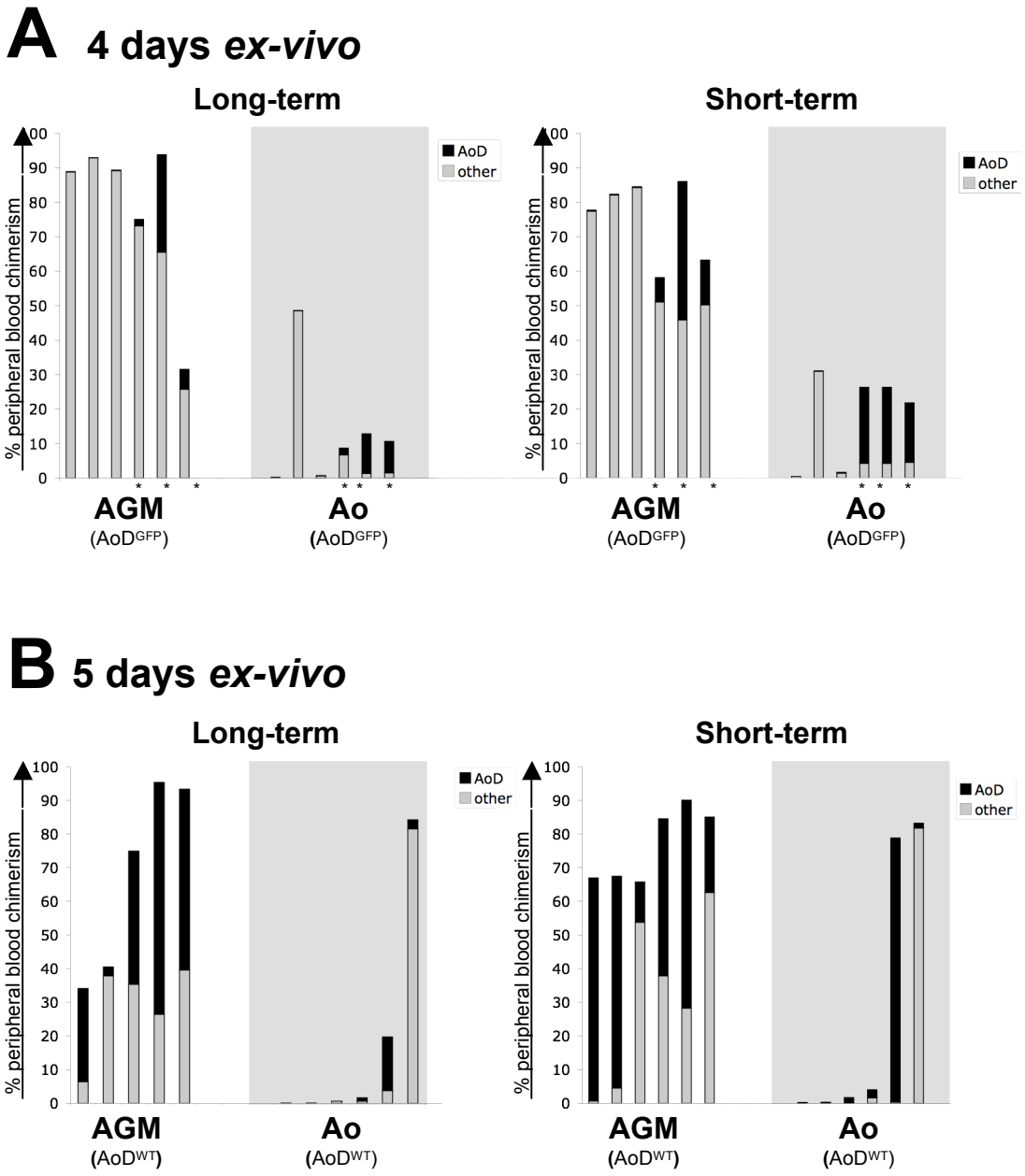

Figure 5.21: AoD contribution to LTR-HSC compartment in E11.5 AGM chimeric reaggregates.

Peripheral blood chimerism of recipients transplanted with 0.1 dose of reaggregates. Individual bars correspond to individual recipients.

A: AoD contribution to LTR-HSC compartment in 4 days chimeric reaggregates cultured for 4 days. Short (6 weeks) and long-term (16 weeks) analysis.

B: AoD contribution to LTR-HSC compartment in 5 days chimeric reaggregates. Short (6 weeks) and long-term (16 weeks) analysis.

Black: AoD; Grey: other (AoV and UGR when appropriate).

Data are cumulative of 2 independent experiments, * mark animals from experiment 2 transplanted with reaggregates cultured for 4 days

out of 2 with 4 days reaggregates) may indicate that AoD-derived LTR-HSCs indeed take slightly longer to mature. This hypothesis is supported by the fact that the AoD-derived chimerism was higher at 5 days than at 4 days (38.5% and 12% in AGM reaggregates respectively)(Figure 5.21B). However, additional experiments are required to establish whether this observation is a consistent phenomenon.

Interestingly, comparison of short-term (6 weeks post-transplant) and long-term (16 weeks-post transplant) showed that AoD-derived chimerism decreased with time (Figure 5.21). Reconstitution with 4 days AGM reaggregates showed 20.6% AoD-derived chimerism 6 weeks post-transplantation which decreased to 12% 16 weeks post-transplantation (Figure 5.21A). Similarly, reconstitution with 5 day reaggregates gave 45.3% AoD-derived chimerism 6 weeks post-transplantation and 38.5% 16 weeks post-transplantation (Figure 5.21B). Similar observations were made with Ao chimeric reaggregates.

Thus, these observations show that AoD contains cells which become LTR-HSCs in appropriate microenvironment, but they seem less competitive than those emerging from emerging in the AoV (Taoudi and Medvinsky, 2007). However, additional experiments are required to confirm this hypothesis. To assess the numbers AoD-derived LTR-HSCs quantitatively; limiting dilution experiments would be required.

5.3.5.3. Multilineage contribution of AoD-derived LTR-HSCs from AGM chimeric reaggregates

The multilineage haematopoietic reconstitution of AoD-derived cells in 4 days AGM and Ao reaggregates cultured was assessed by flow cytometry. More than 16 weeks post-transplantation, the presence of AoD-derived cells in primary recipients was checked by the expression of GFP in haematopoietic tissues (peripheral blood, spleen, bone marrow, and thymus). All tissues contained CD45.2 donor cells in high proportions (ranging from 12 to 90% in the peripheral blood, from 2 to 94% in the bone marrow, from 16 to 89% in the spleen, and from 9 to 99% in the thymus)(Figure 5.22A and B). Gating on GFP^+ cells assessed AoD

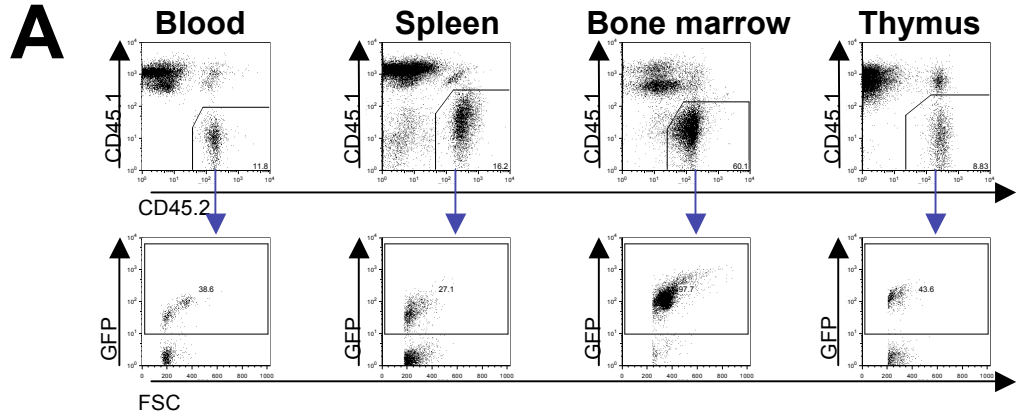
A
Blood
Spleen
Bone marrow
Thymus
CD45.1
CD45.2
GFP
FSC
11.8
16.2
60.1
8.83
38.6
27.1
87.7
43.6

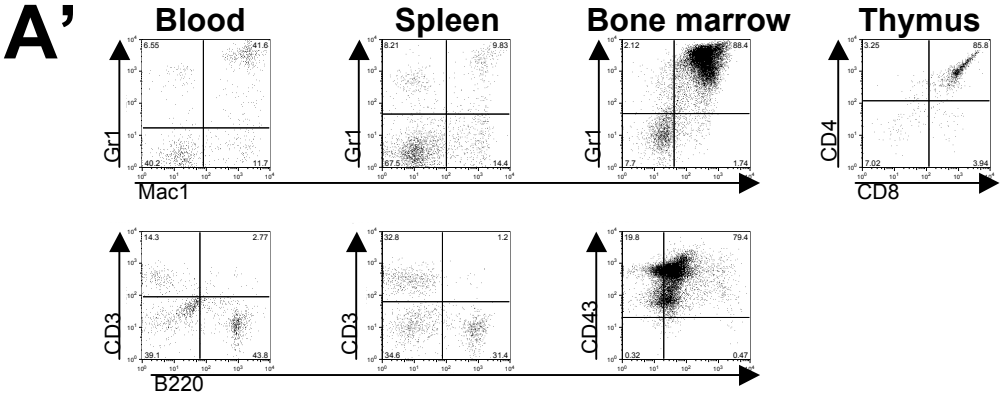
A'
Blood
Spleen
Bone marrow
Thymus
Gr1
Mac1
CD4
CD8
CD3
B220
CD43
6.55
41.6
40.2
11.7
8.21
9.83
67.5
14.4
2.12
88.4
7.7
1.74
3.25
85.8
7.02
3.94
14.3
2.77
39.1
43.8
32.8
1.2
34.6
31.4
19.8
79.4
0.32
0.47

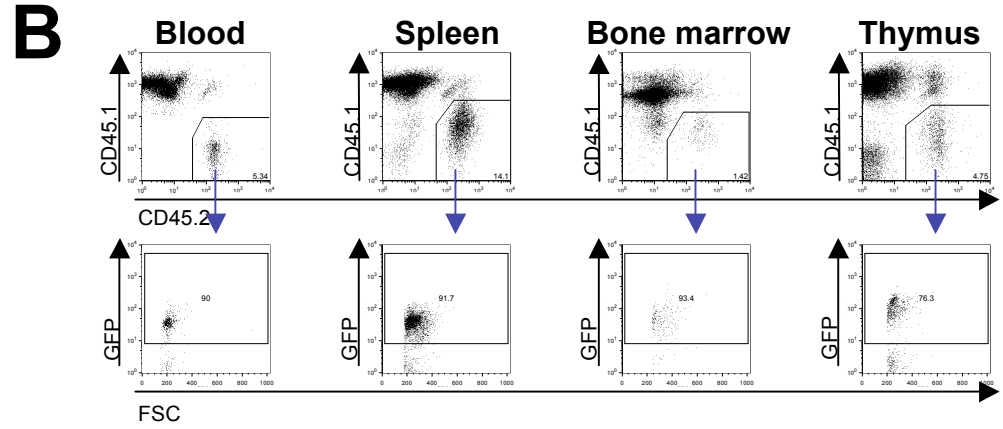
B
Blood
Spleen
Bone marrow
Thymus
CD45.1
CD45.2
GFP
FSC
5.34
14.1
1.42
4.75
90
91.7
93.4
76.3

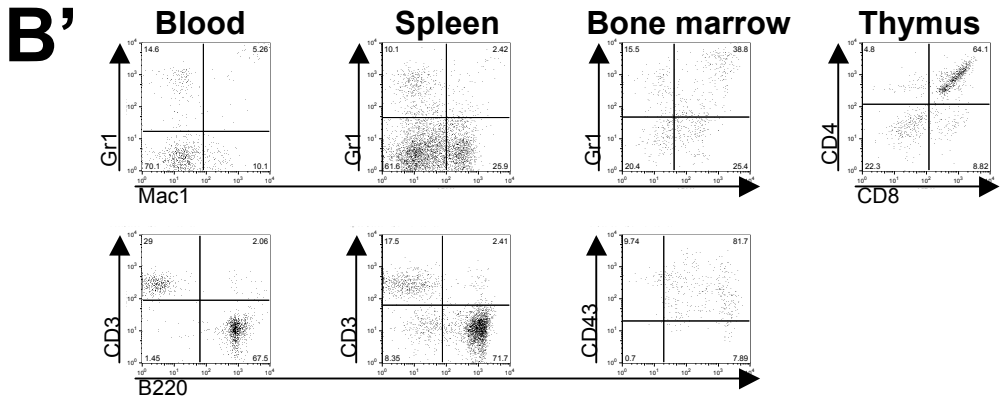
B'
Blood
Spleen
Bone marrow
Thymus
Gr1
Mac1
CD4
CD8
CD3
B220
CD43
14.6
5.26
70.1
10.1
10.1
2.42
61.6
25.9
15.5
38.8
20.4
25.4
4.8
64.1
22.3
8.82
29
2.06
1.45
67.5
17.5
2.41
8.35
71.7
9.74
81.7
0.7
7.89

Figure 5.22: Long-term multilineage haematopoietic reconstitution by AoD-derived LTR-HSCs generated in AGM and Ao chimeric reaggregates.

A: E11.5 AGM chimeric reaggregates donor and AoD derived reconstitution in major haematopoietic organs (peripheral blood, spleen, bone marrow, and thymus). AoD-derived contribution was determined based on GFP expression.

A': Multilineage (myelo-lymphoid) contribution of AoD-derived cells in major haematopoietic organs (peripheral blood, spleen, bone marrow, and thymus) of recipients. Events were gated on GFP^+ exclusively.

B: E11.5 Ao chimeric reaggregates donor and AoD derived reconstitution in major haematopoietic organs (peripheral blood, spleen, bone marrow, and thymus). AoD-derived contribution was determined based on GFP expression.

B': Multilineage (myelo-lymphoid) contribution of AoD-derived cells in major haematopoietic organs (peripheral blood, spleen, bone marrow, and thymus) of recipients. Events were gated on GFP^+ exclusively.

Data were collected in high level reconstituted recipients injected with 0.1 dose of reaggregate each. Plots are representative of 3 recipient mice. Cell viability was determined by 7-AAD uptake. Quadrants are based on appropriate isotype control (Appendix 3.2) and values indicate percentages of cells.

contribution (Figure 5.22A and B). Peripheral blood, spleen and bone marrow contained AoD-derived myeloid cells marked by Mac1 and Gr1 and lymphoid cells marked by CD3 (T cells), B220 and CD43 (B cells)(Figure 5.22A' and B'). In the thymus, the majority of AoD-derived cells were immature double-positive ($CD4^+CD8^+$) T cells (Figure 5.22A' and B'). Thus AoD-derived LTR-HSCs were functional, independently on whether AoD was cultured with AoV only (Ao reaggregates, Figure 5.22B and B') or AoV and UGR (AGM reaggregates, Figure 5.22A and A').

5.4. Discussion

5.4.1. Axio-lateral polarity of LTR-HSC development in E11.5 AGM reaggregates

LTR-HSCs localize solely in the Ao of the E11.5 AGM region (de Bruijn et al., 2000b; Taoudi and Medvinsky, 2007). However, the presence of LTR-HSCs in the E12.5 UGRs and their capacity at E11.5 to induce LTR-HSC formation (de Bruijn et al., 2000b) raises the possibilities that either UGR autonomously support LTR-HSC formation or pre-HSCs from the Ao have seeded UGRs. Co-culture of Ao and UGR as explants does not improve LTR-HSC production from either Ao or UGR (de Bruijn et al., 2000b) but does not exclude the possibilities of LTR-HSC induction in the Ao by UGRs and vice-versa. Reaggregate culture was used to address this question because it allows the production of chimeric "organoids" with enhanced cell-cell contacts, whilst maintaining the AGM capacity to produce high numbers of LTR-HSCs in response to growth factors. First, I showed that there was no axio-lateral polarity in the repartition of haematopoietic cells and progenitors in the uncultured E11.5 AGM region as they are evenly distributed between Ao and UGRs. Second, I investigated the autonomous haematopoietic potential of the E11.5 Ao and UGR reaggregates. Contrary to previous observations with explants, the E11.5 UGRs in our study were not capable of generating LTR-HSCs while the Ao maintained its ability to generate functional LTR-HSCs (from ≈1 to ≈45 in 4 days of

culture). This discrepancy could be due to either the mechanical dissociation of UGRs in our experiments or due to some contamination with the Ao in previous experiments. In my experiments, it was observed that AGM reaggregates consistently contained higher LTR-HSC activity than Ao reaggregates. Although evaluation of accurate numbers of LTR-HSCs requires limiting dilution experiments, these results suggested that both Ao and UGR are required to provide optimal LTR-HSC expansion in reaggregates.

Experiments with E11.5 AGM and Ao chimeric reaggregates were set up in order to answer whether the higher LTR-HSC expansion in AGM reaggregates compared to Ao reaggregates was due to either 1) stimulatory effects of UGRs on the LTR-HSC expansion from the Ao or 2) stimulatory effects of the Ao on LTR-HSC formation in the UGR. Tracing of Ao and UGR cells was allowed by using GFP expression as a genetic marker. The large majority of the PBC of recipients was Ao-derived, demonstrating that most pre-HSCs were located in the Ao region. This result has two implications: 1) it shows that exposure of the UGR to Ao cells did not trigger LTR-HSCs formation from the UGRs; 2) it suggests that UGRs are required to support optimal LTR-HSC expansion from Ao in reaggregates. To address the latter idea and rule out any "size" effect of the smaller Ao reaggregates, double-sized Ao|Ao reaggregates were set up. Similar LTR-HSC numbers were obtained in Ao and Ao|Ao reaggregates. This suggests that UGRs specifically enhance LTR-HSCs expansion from a single Ao.

In addition, my results contradict Myelcult explants data showing that juxtaposition of Ao and UGR in explant cultures did not influence LTR-HSC development from Ao (de Bruijn et al., 2000b). This discrepancy could have two explanations: 1) cell-cell contacts between Ao and UGR cells are required for the UGR to stimulate LTR-HSC expansion, or 2) the absence of growth factors in Myelocult medium fails to reveal the positive effects of UGR cells on LTR-HSC expansion. Near future experiments will address these questions by culturing chimeric reaggregates in $IMDM^{-}$.

5.4.2. Dorso-ventral polarity of LTR-HSC development in E11.5 AGM reaggregates

I have shown that Ao is the site containing the vast majority of pre-HSCs in the E11.5 AGM region. The second aspect of this study was to investigate the dorso-ventral repartition of these pre-HSCs using a similar strategy involving chimeric reaggregates.

In the fresh AGM region, there was no obvious dorso-ventral polarity in the repartition of haematopoietic cells and CFU-Cs, confirming previous observations (Taoudi and Medvinsky, 2007). More interestingly, there was no dorso-ventral polarity of $EGFP^+$ cells in the Ao, implying that AoV and AoD equally express Runx1. This argues with the ventral segregation of Runx1 expression in the E11.5 Ao (North et al., 1999). Although this discrepancy is likely due to a different Runx1 dose in the murine models used (haploinsufficient in $Runx1^{lz}$, full dose in $Runx1^{EGFP}$), my observation highlights the AoD as a potential haematopoietic site due to its Runx1 expression.

In previous experiments DT (containing somites remnants and the notochord) was left attached to the AoD. However, surrounding tissues are known to express factors, such as sonic hedgehog or VEGF for example, that can influence haematopoiesis in the AGM region (Pardanaud and Dieterlen-Lievre, 1999; Peeters et al., 2009). In view of these data, the influence of DT on LTR-HSC development was investigated in explants cultures. My results suggested that DAGM explants contained less LTR-HSCs than AGM explants, thus suggesting that DT has a negative influence on LTR-HSC development from the AGM region. Another group made a similar conclusion in a recently published paper (Peeters et al., 2009). It will be interesting to establish in future if the addition of IL-3, SCF, and Flt3l could by-pass the inhibitory effects of DT.

Suboptimal culture conditions at the time (observed by all lab members) most likely led to fewer LTR-HSCs in cultures and thus also probably explain the lack of reconstitution in AoV explants. The lack of reconstitution from AoD explants even when DT was stripped off suggested that AoD cannot generate LTR-HSCs.

However, transplantation experiments with higher doses of explants are required to detect very low numbers of LTR-HSCs and thus formally conclude on the effect of DT on AoD explants. Additionally, preliminary data indicate that DT might have an inhibitory effect on the fresh E11.5 AoD but this needs to be confirmed.

Evidence so far has shown that LTR-HSC activity is almost exclusively located in the E11.5 AoV and the explant culture revealed intrinsic properties of the AoV to induce LTR-HSC formation (Taoudi and Medvinsky, 2007). The haematopoietic response of AoV when exposed to the AoD or vice versa could not be assessed by the explant culture. However, such interactions are present *in vivo* and might play important roles. The reaggregate culture system bypasses such limitations and thus was used to assess the possible presence of cells competent to become LTR-HSCs in the AoD. Chimeric GFP and WT E11.5 AGM and Ao reaggregates were cultured in $IMDM^{+}$ for 4 days and 5 days. Whereas AoD-derived reconstitution was observed in 1 out of 2 experiments with 4 days reaggregates, it was observed consistently, at high level, in 5 days reaggregates. This suggests that: 1) AoD contains pre-HSCs that can mature into LTR-HSCs during reaggregate culture and 2) AoD-derived LTR-HSCs might take slightly longer to mature in culture. In addition, reconstitution data were similar in 4 and 5 days reaggregates, confirming S.Taoudi's unpublished observations. Interestingly, it also appeared that AoD-derived chimerism decreased between short and long term reconstitution analyses, while contribution of AoV remained fairly stable. This indicates that AoD-derived LTR-HSCs have different properties than AoV-derived LTR-HSCs. I also showed that AoD-derived LTR-HSCs are functional as they provide multilineage reconstitution in recipients. Although these results are promising, further experiments are required to generate a set of data that can be analyzed statistically. It will be interesting to investigate the numbers and properties of AoD-derived LTR-HSCs by isolating and transplanting them. Finally, removal of growth factors will be required to assess whether the generation of AoD LTR-HSCs occurs through the exposure of AoV microenvironment or the exposure to growth factors. Altogether, the results from this study are the first indication that AoD contains cells competent to develop into LTR-HSC.

6. Summary and Perspectives

6.1. Summary

This project focused on the reaggregate culture system as a method for studying the emergence and expansion of LTR-HSC in the E11.5 AGM region.

I first demonstrated the reproducibility of this culture system by showing its consistent ability for the extensive LTR-HSC expansion. I further characterised E11.5 AGM reaggregates by showing that the majority of the LTR-HSCs adopted a $CD45^{+}Sca1^{+}c\text{-}kit^{+}CD31^{med}$ immunophenotype and that IL-3, SCF, and Flt3l are all required to achieve maximal LTR-HSC expansion.

Second, I characterised EGFP expression in the *Runx1*^{EGFP} adult haematopoietic system and in the E11.5 AGM region. The reported pattern of Runx1 expression in the adult was in agreement with Runx1 reporter models previously published (Lorsbach et al., 2004; North et al., 2004). As Runx1 is thought to be required for the transition from endothelium to haematopoietic fate, I focused my analyses on EGFP expression in LTR-HSC compartment ($CD45^{+}c\text{-}kit^{+}CD34^{+}$VE-$cadherin^{+}$) and in non-haematopoietic compartment ($CD45^{-}$). I identified a population of $CD45^{-}$VE-$cadherin^{-}$ cells that express EGFP in the fresh E11.5 AGM but disappear after reaggregate culture. Additionally, preliminary analysis of the LTR-HSC content in the E11.5 AGM highlighted the possibility that the transgenic E11.5 AGM region contains fewer LTR-HSCs than in the WT.

In the third part of my project, the use of reaggregate culture system confirmed the Ao as the site harbouring the majority of pre-HSC in the E11.5 AGM. Interestingly, the close proximity of Ao and UGR cells enhanced the overall LTR-HSC expansion in chimeric reaggregates and preliminary data indicated that the UGRs provide support for Ao pre-HSC maturation. Additionally, the presence of DT appeared to inhibit LTR-HSC formation in AGM explant, supporting the idea that dorso-ventral positioning information is important for haematopoietic induction. Finally, dorso-ventral analysis of the Ao showed that the AoD contains pre-HSCs when cultured in reaggregates.

6.2. Ongoing work

6.2.1. The supportive role of the UGRs for LTR-HSC development

Preliminary data presented in Chapter 5 indicate that the UGRs provide support for LTR-HSC development from the Ao as the culture of multiple Ao did not result in the extensive LTR-HSC expansion that is observed with the AGM. Currently, I am trying to formally address the role of the UGR in pre-HSC development by setting up multiple Ao reaggregates and transplanting the cellular equivalent of 1 Ao. This should assess the potential of a single Ao when exposed to UGR, and hopefully confirm that UGR have a specific and positive influence.

In addition, I am addressing whether the presence of the UGR for maximal LTR-HSC expansion is still required in the absence of growth factors. Chapter 3 demonstrated that a significant LTR-HSC expansion could be achieved without growth factors. Because the absence of growth factors should be a situation closer to physiological conditions, it will be interesting to understand whether the UGR can achieve such positive effects on their own and perhaps will answer why our observations differed from what was previously observed (de Bruijn et al., 2000b).

Finally, I am also trying to identify the potential factors secreted by the UGRs that specifically improve pre-HSC maturation. This is currently assessed by culturing Ao as explants and reaggregates in the presence of various exogenous factors. Micro-array data from S. Rybtsov provided a list of candidate factors that are preferentially expressed by the UGR and some candidates are currently being tested.

6.2.2. The haematopoietic potential of AoD

Results presented in the second part of Chapter 5 are promising but require additional experiments to obtain a larger data set that can be statistically analysed.

I showed that the presence of dorsal tissue in AGM explants might inhibit LTR-HSC development. This result is currently being quantitatively assessed and AoD and DAoD explants are cultured with and without growth factors. In view of these results,

we also are currently trying to reproduce S. Taoudi data by transplanting fresh AoD and DAoD to understand whether DT could potentially inhibited AoD engraftment.

Additionally, chimeric reaggregates showed that AoD contains pre-HSC that could mature when exposed to the AoV microenvironment. My current experiments are repeating these experiments in the absence of growth factors to understand whether exposure to AoV microenvironment is sufficient to stimulate AoD pre-HSC maturation. Near future experiments will also focus on identifying the immunophenotype of the pre-HSCs in the AoD.

6.3. Perspectives

In the future, the reaggregate culture system could prove very useful for dissecting developmental processes involved in *de-novo* LTR-HSC development and the data presented in this thesis provide some examples of such applications. For example, identifying the immunophenotype of pre-HSCs in the E11.5 AGM region is a key to understand the dynamics by which LTR-HSCs emerge in the AGM region (Taoudi et al., 2008). Intrinsic proliferative properties of LTR-HSCs in the bone marrow have been extensively studied (Bowie et al., 2007b; Bowie et al., 2006; Cellot and Sauvageau, 2006; Wilson et al., 2008). However, the processes of LTR-HSC emergence and pre-HSC maturation are thought to occur exclusively in the embryo (Godin and Cumano, 2002). Whilst still subject to controversy, the AGM region is the first site harbouring LTR-HSCs during development (Muller et al., 1994) and has the capacity to support pre-HSC maturation and LTR-HSC expansion (Medvinsky and Dzierzak, 1996; Taoudi et al., 2008). While gene inactivation studies have shown that such processes are developmentally regulated by various genes such as Runx1, SCL, GATA-2, or Lmo-2 for example (Godin and Cumano, 2002), the exact developmental timepoints and cell types in which such signals are required are still unknown. Reaggregate culture system will allow the use of transgenic cells and tracing of their developmental potential, and as such will aid understanding the processes and stages at which these genes play important roles.

Similarly, the reaggregate system also allows identification and manipulation of key components of the LTR-HSC niche within the AGM region as shown in Chapter 5. Further characterisation of LTR-HSC niche components is of great interest in the HSC field because understanding external signals regulating HSC self-renewal, maintenance, expansion and differentiation is as important as understanding the intrinsic properties of HSCs. Studies of niche components in the adult bone marrow have highlighted the importance and the complexity of such extrinsic signals on LTR-HSCs (Arai et al., 2004; Calvi et al., 2003; Kiel and Morrison, 2008; Nilsson et al., 2001; Orford and Scadden, 2008; Warner et al., 2004; Zhang et al., 2003). In the AGM region more precisely, studies with explants and AGM cell lines have shown that the AGM microenvironment can support LTR-HSC maintenance, and probably induction and expansion (Matsuoka et al., 2001b; Medvinsky and Dzierzak, 1996; Taoudi et al., 2008; Xu et al., 1998). A recent study also highlighted the importance of dorso-ventral positioning for LTR-HSC expansion in the AGM region (Peeters et al., 2009). Importantly, the use of reaggregates in future studies will further assess which cells and signals in the AGM microenvironment promote either LTR-HSC induction, expansion, or differentiation.

Most importantly, dissecting biological processes that govern LTR-HSC emergence will provide an understanding of how to reproduce such developmental mechanisms and induce LTR-HSC formation from alternative sources such as ES cells. Despite many attempts to produce LTR-HSCs from ES cells (Tian and Kaufman, 2008), no one so far has been able to formally induce and expand LTR-HSCs. Such scientific advancements will hopefully provide alternative sources of LTR-HSCs for the treatments of HSC-related diseases such as leukeamia as well as providing insights into the complex genetic mechanisms underlying such disorders.

7. Appendixes

Appendix 3.1

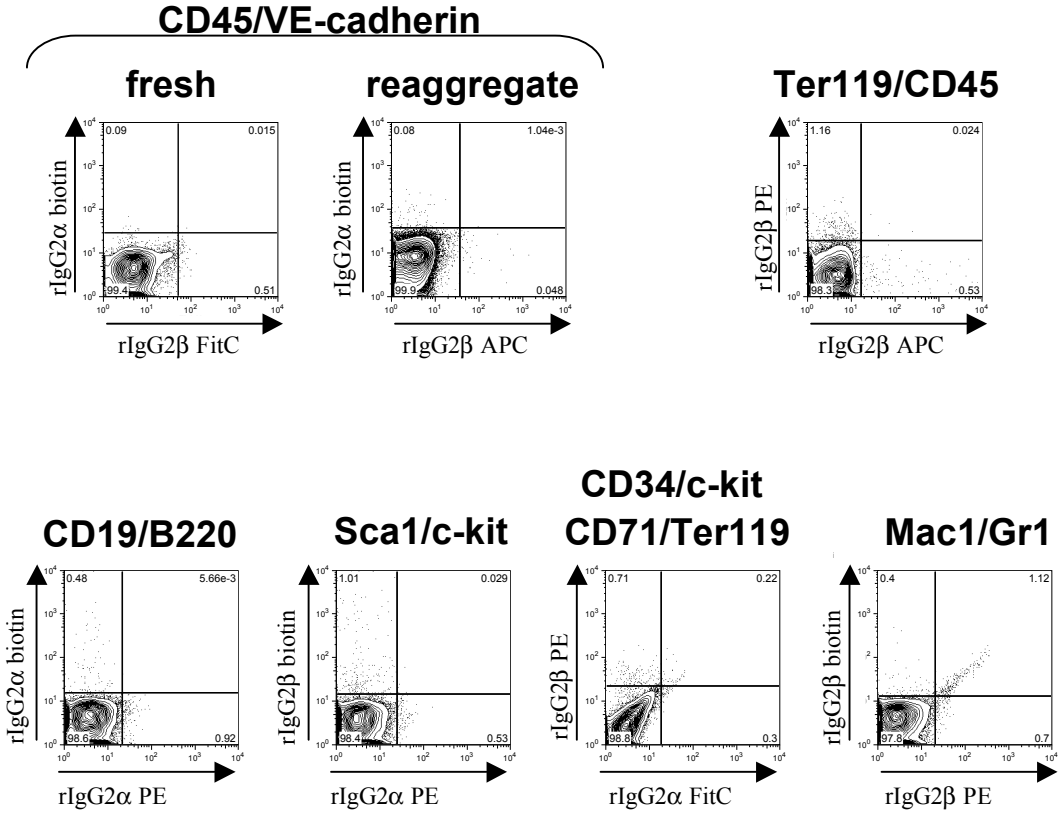

Appendix 3.1: E11.5 AGM reaggregate flow cytometry controls.
Single cell suspensions from E11.5 AGM reaggregates were obtained and incubated with the indicated isotype controls. Antibody stains corresponding to each isotype control are displayed on the top of each plot.
Cell viability was determined by 7-AAD uptake. Biotin conjugated antibodies were incubated with streptavidin APC. Values indicate percentages of cells.

Appendix 3.2

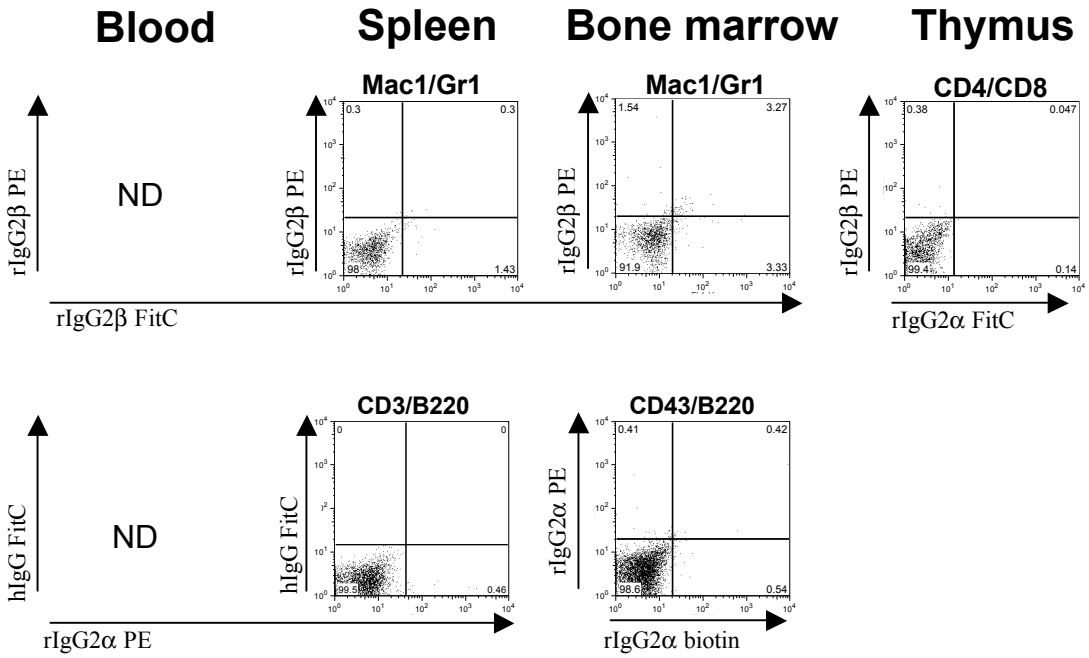

Appendix 3.2: Multilineage analysis flow cytometry controls.
Single cell suspensions from organs of primary recipient reconstituted with E11.5 AGM reaggregate cells were obtained and incubated with the indicated isotype controls. Antibody stains corresponding to each isotype control are displayed on the top of each plot.
Cell viability was determined by 7-AAD uptake. Biotin conjugated antibodies were incubated with streptavidin APC. Values indicate percentages of cells. ND: not done.

Appendix 4.1

A Lin sca1 c-kit

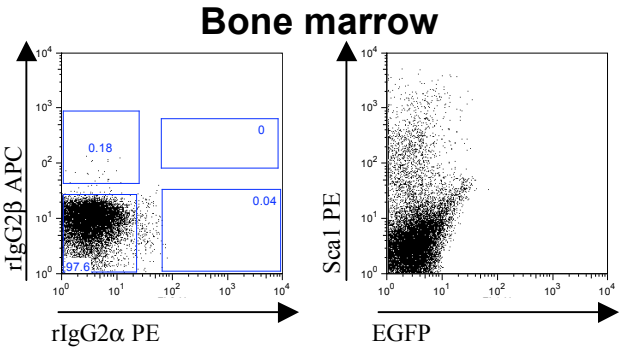

B Mac1 Gr1

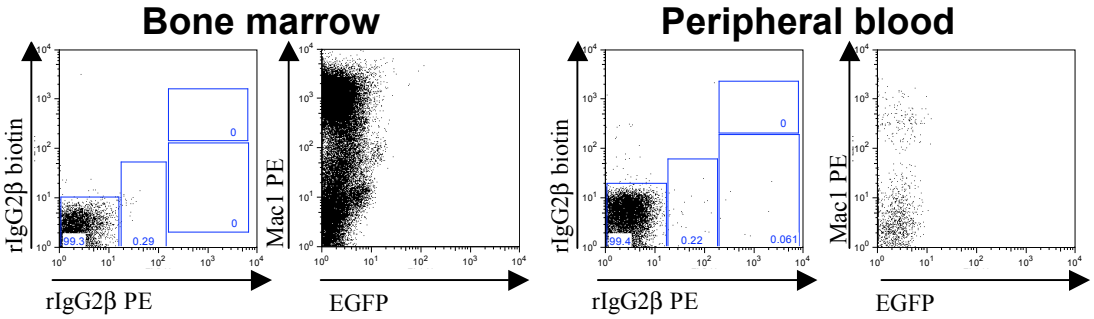

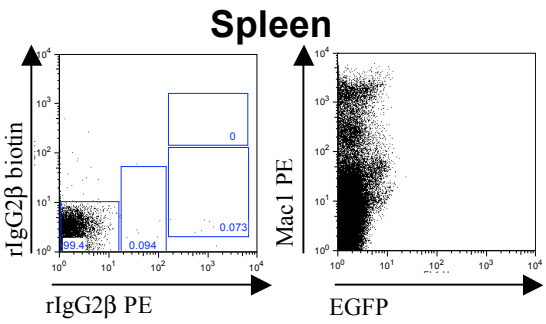

C CD45 Ter119

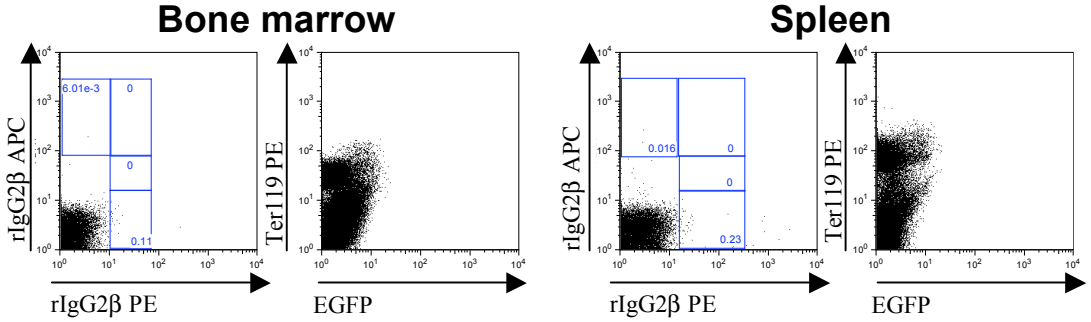

D CD4 CD8

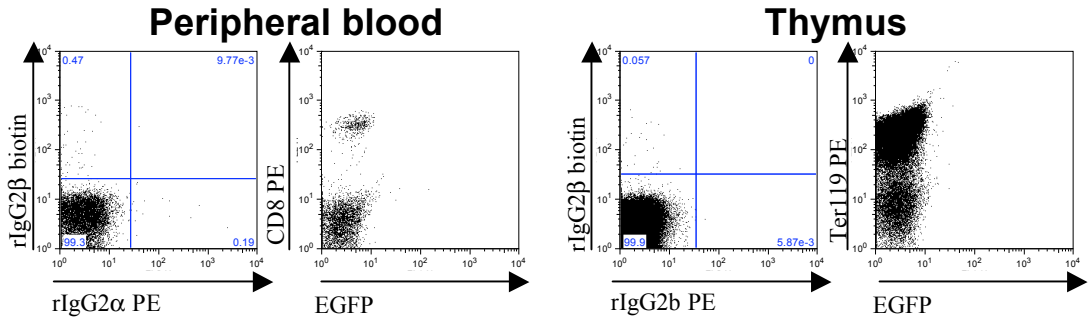

E CD3 B220

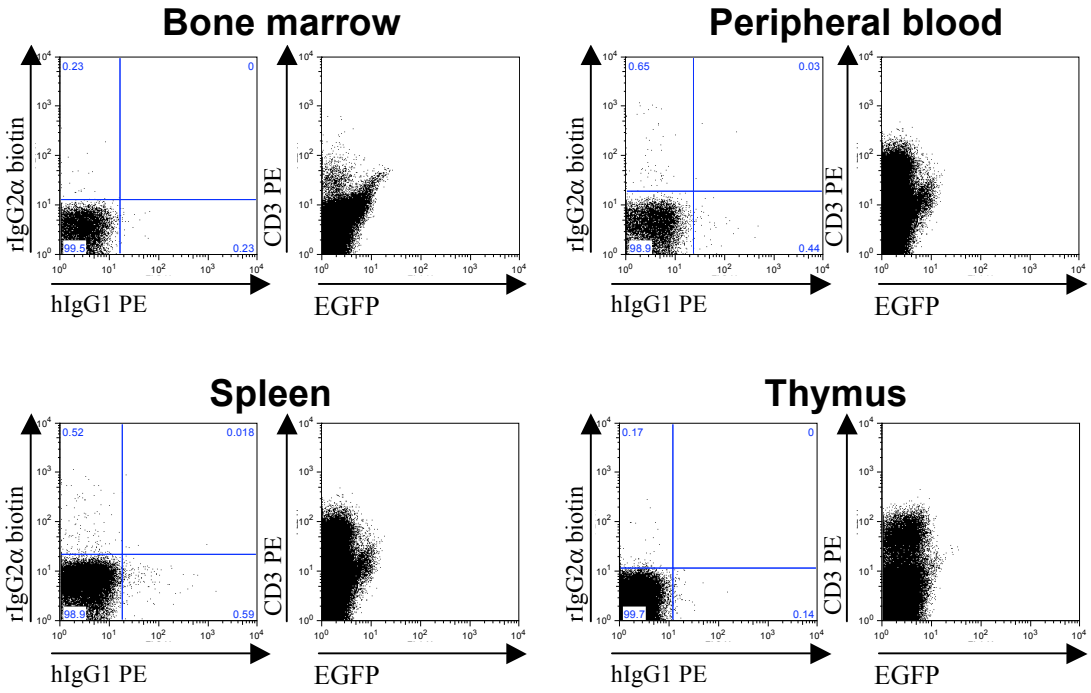

F CD19 B220

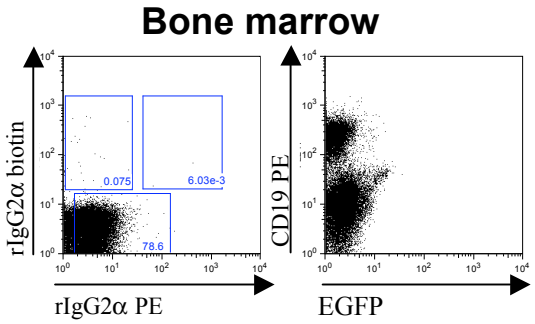

Appendix 4.1: Adult haematopoietic organs flow cytometry controls.

Single cell suspensions from *Runx1*$^{WT/WT}$ adult haematopoietic organs were obtained and incubated with the indicated isotype controls (left of each panel). Single PE stains against EGFP in *Runx1*$^{WT/WT}$ organs showing compensation between FL-1 and FL-2 channels (right of each panel)

A: Adult bone marrow Lin Sca1 c-kit stain flow cytometry controls. Live lin$^-$ cells only are displayed and were gated based on 7-AAD intake and lineage marker exclusion.

B: Adult bone marrow, peripheral blood, and spleen Mac1 Gr1 stain flow cytometry controls.

C: Adult bone marrow and spleen CD45 Ter119 stain flow cytometry controls.

D: Adult peripheral blood and thymus CD4 CD8 stain flow cytometry controls.

E: Adult bone marrow, peripheral blood, spleen and thymus CD3 B220 stain flow cytometry controls.

F: Adult bone marrow CD19 B220 stain flow cytometry controls.

Cell viability was determined by 7-AAD uptake. Biotin conjugated antibodies were incubated with streptavidin APC. Values indicate percentages of cells

Appendix 4.2

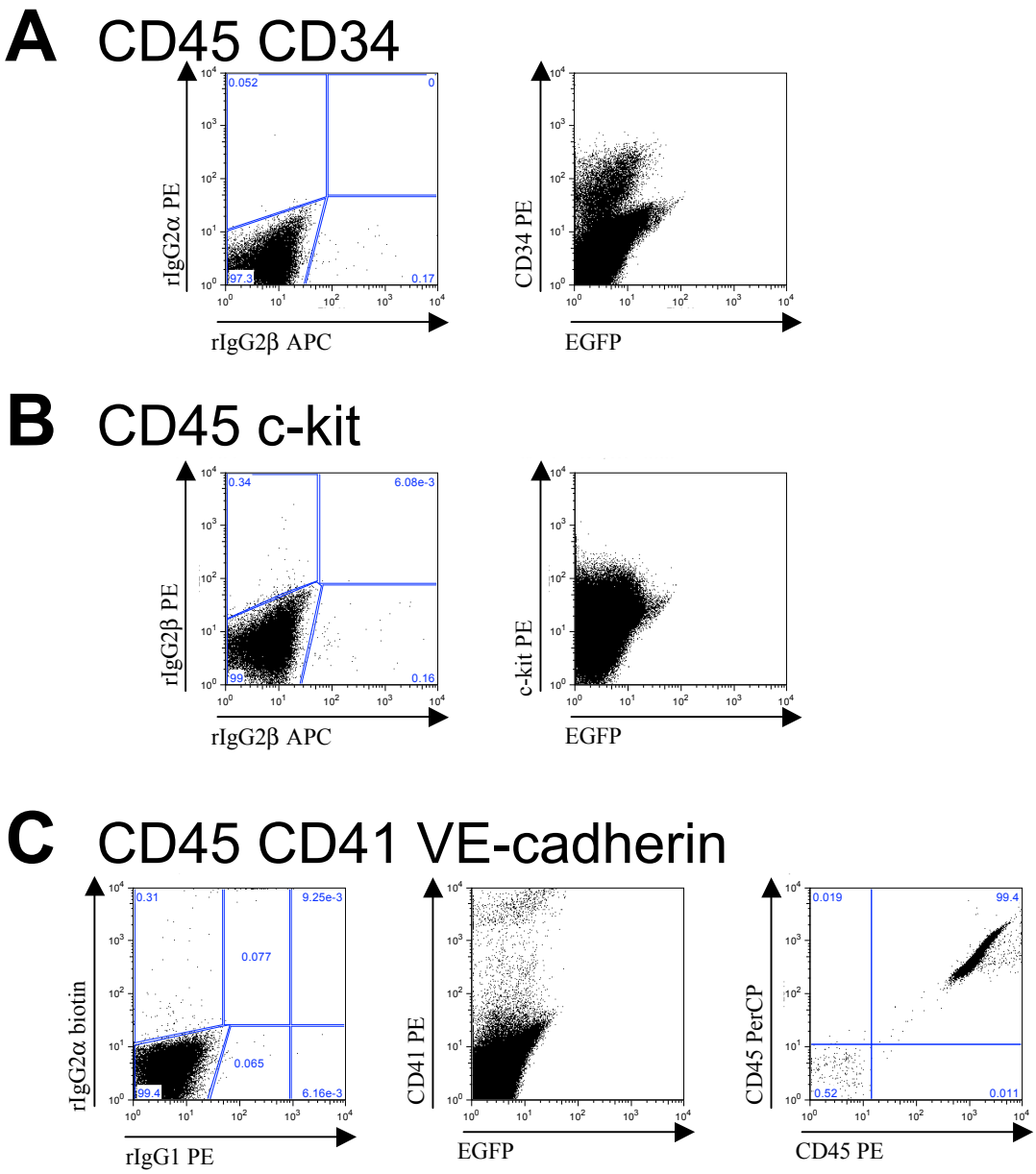

Appendix 4.2: E11.5 AGM region flow cytometry controls.

Single cell suspensions from *Runx1*$^{WT/WT}$ adult were obtained and incubated with the indicated isotype controls (left of each panel). Single PE stains against EGFP in *Runx1*$^{WT/WT}$ organs showing compensation between FL-1 and FL-2 channels (right of each panel and middle of C panel).

A: E11.5 AGM region CD45 CD34 stain flow cytometry controls.

B: E11.5 AGM region CD45 c-kit stain flow cytometry controls.

C: E11.5 AGM region CD45 VE-cadherin CD41stain flow cytometry controls. CD45^{+} cells were excluded using anti-CD45 PerCP antibody (right of the panel).

Cell viability was determined by 7-AAD uptake. Biotin conjugated antibodies were incubated with either streptavidin APC. Values indicate percentages of cells.

Appendix 4.3

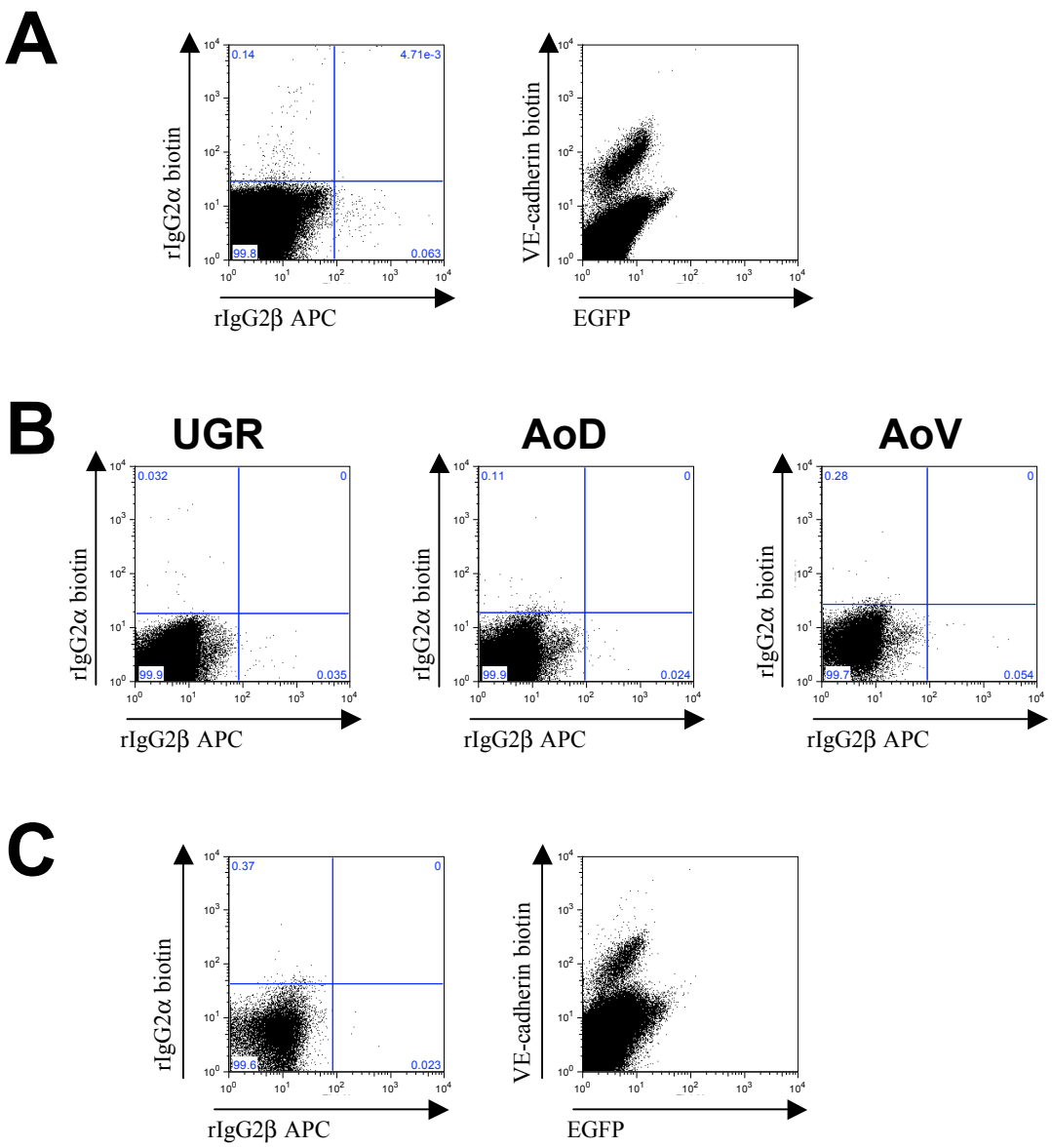

Appendix 4.3: E11.5 AGM region CD45 VE-cadherin flow cytometry controls.
Single cell suspensions from *Runx1*$^{WT/WT}$ adult haematopoietic organs were obtained and incubated with the indicated isotype controls (left of each panel). Single PE stains against EGFP in *Runx1*$^{WT/WT}$ organs showing compensation between FL-1 and FL-2 channels (right of panels A and C).
A: E11.5 AGM region CD45 VE-cadherin stain flow cytometry controls.
B: E11.5 AGM region sub-compartments (UGR, AoD, and AoV) CD45 VE-cadherin stain flow cytometry controls.
C: E11.5 AGM reaggregates CD45 VE-cadherin flow cytometry controls.
Cell viability was determined by 7-AAD uptake. Biotin conjugated antibodies were incubated with streptavidin PE. Values indicate percentages of cells.

Appendix 4.4

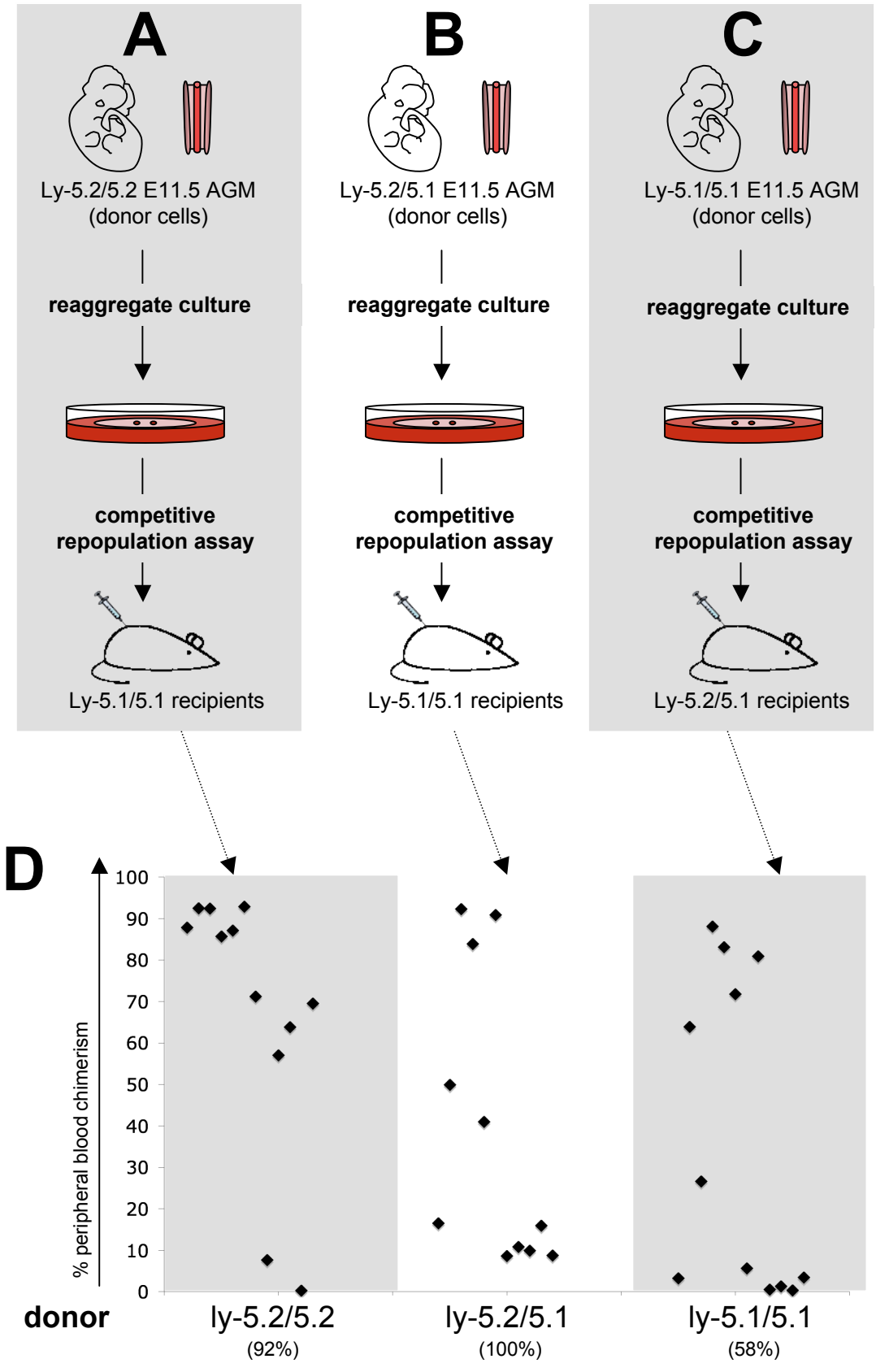
A
Ly-5.2/5.2 E11.5 AGM
(donor cells)
reaggregate culture
competitive
repopulation assay
Ly-5.1/5.1 recipients
B
Ly-5.2/5.1 E11.5 AGM
(donor cells)
reaggregate culture
competitive
repopulation assay
Ly-5.1/5.1 recipients
C
Ly-5.1/5.1 E11.5 AGM
(donor cells)
reaggregate culture
competitive
repopulation assay
Ly-5.2/5.1 recipients
D
% peripheral blood chimerism
100
90
80
70
60
50
40
30
20
10
0
donor
ly-5.2/5.2
(92%)
ly-5.2/5.1
(100%)
ly-5.1/5.1
(58%)

Appendix 4.4: Experimental design for a new lineage trace protocol and assessement of LTR-HSCs expansion potential of Ly-5.1 mice.

A: Control reaggregate system using Ly-5.2/5.2 E11.5 AGM derived donor cells and transplant into Ly-5.1/5.1 recipient mice.

B: Experimental reaggregates using Ly-5.2/5.1 E11.5 AGM derived donor cells and transplant into Ly-5.1/5.1 recipient mice.

C: Experimental reaggregates using Ly-5.1/5.1 E11.5 AGM derived donor cells and transplant into Ly-5.2/5.1 recipient mice.

D: LTR-HSCs expansion in reaggregates generated with Ly-5.2/5.2, Ly-5.2/5.1, and Ly-5.1/5.1 E11.5 AGM region.

Peripheral blood chimerism of recipients transplanted with 0.01 doses of reaggregates. Each point represents a single recipient mouse. Recipients were considered reconstituted when chimerism exceeded 5% at least 12 weeks after transplantation; percentages indicate proportion of reconstituted animals. Data is cumulative of 2 independent experiments.

Appendix 5.1

A

	WT	GFP
total cells	251081 ± 64147	268664 ± 58812
total live cells	123201 ± 50981	114316 ± 38303
total CD45+ cells	4091 ± 2434	4036 ± 2871
total DP cells	129 ± 11	160 ± 22

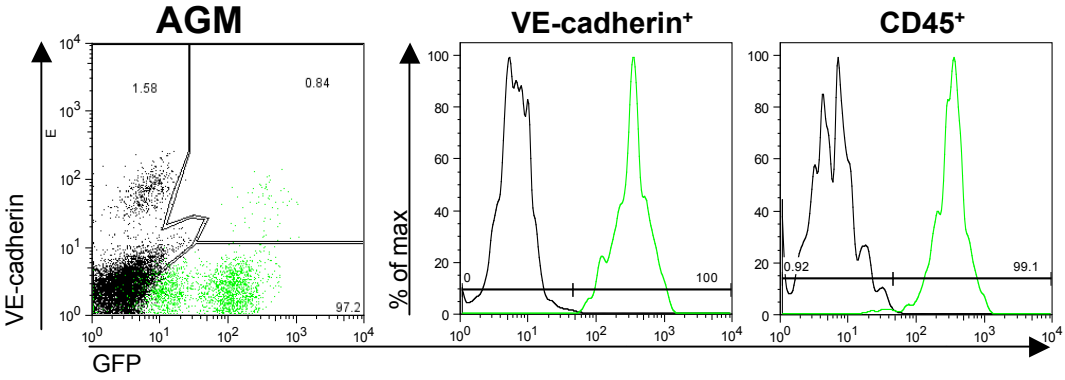

B

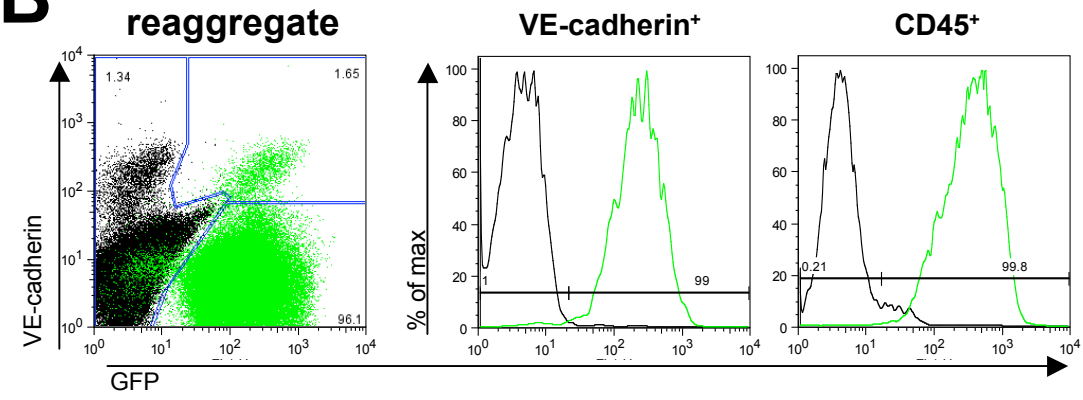

Appendix 5.1: Comparison between E11.5 AGM regions from WT and GFP embryos and GFP expression in fresh and cultured E11.5 AGM region.

A: Cell composition of E11.5 AGM regions in wild type and aGFP embryos. Data is representative of 5 independent experiments. Absolute numbers ± standard deviation.

B: Flow cytometric analysis of GFP expression in the endothelial (VE-cadherin$^+$) and haematopoietic (CD45$^+$) cell fractions of the fresh E11.5 AGM region.

C: Flow cytometric analysis of GFP expression in the endothelial (VE-cadherin$^+$) and haematopoietic (CD45$^+$) cell fractions of the E11.5 AGM reaggregate.

Black: WT mouse; Green: GFP mouse. Cell viability was determined by 7-AAD uptake. DP: CD45$^+$VE-cadherin$^+$

Appendix 5.2

Appendix 5.2: Cell composition of E11.5 fresh dAGM and dAoD.
dAGM and dAoD correspond to AGM and AoD including dorsal tissue (somites remnants and notochord).
Data is representative of 3-4 independent experiments; absolute numbers ± standard deviation.
Cell viability was determined by 7-AAD uptake. DP: $CD45^{+}$VE-$cadherin^{+}$; DN: $CD45^{-}$VE-$cadherin^{-}$

	dAGM	dAoD
total cells	401000 ± 64210	160333 ± 35170
total live cells	189621 ± 63287	116684 ± 22987
total CD45+ cells	5883 ± 3439	1969 ± 170
total VE cadherin+ cells	3012 ± 899	524 ± 42
total DP cells	84 ± 54	30 ± 14
total DN cells	180650 ± 59103	114444 ± 22776

8. Publication

Taoudi, S., Gonneau, C., Moore, K., Sheridan, J. M., Blackburn, C. C., Taylor, E. and Medvinsky, A. (2008). Extensive hematopoietic stem cell generation in the AGM region via maturation of VE-cadherin+CD45+ pre-definitive HSCs. *Cell Stem Cell* **3**, 99-108.

9. References

Akashi, K., Traver, D., Miyamoto, T. and Weissman, I. L. (2000). A clonogenic common myeloid progenitor that gives rise to all myeloid lineages. *Nature* **404**, 193-7.

Alvarez-Silva, M., Belo-Diabangouaya, P., Salaun, J. and Dieterlen-Lievre, F. (2003). Mouse placenta is a major hematopoietic organ. *Development* **130**, 5437-44.

Antonchuk, J., Sauvageau, G. and Humphries, R. K. (2001). HOXB4 overexpression mediates very rapid stem cell regeneration and competitive hematopoietic repopulation. *Exp Hematol* **29**, 1125-34.

Antonchuk, J., Sauvageau, G. and Humphries, R. K. (2002). HOXB4-induced expansion of adult hematopoietic stem cells ex vivo. *Cell* **109**, 39-45.

Arai, F., Hirao, A., Ohmura, M., Sato, H., Matsuoka, S., Takubo, K., Ito, K., Koh, G. Y. and Suda, T. (2004). Tie2/angiopoietin-1 signaling regulates hematopoietic stem cell quiescence in the bone marrow niche. *Cell* **118**, 149-61.

Argiropoulos, B. and Humphries, R. K. (2007). Hox genes in hematopoiesis and leukemogenesis. *Oncogene* **26**, 6766-76.

Aronson, B. D., Fisher, A. L., Blechman, K., Caudy, M. and Gergen, J. P. (1997). Groucho-dependent and -independent repression activities of Runt domain proteins. *Mol Cell Biol* **17**, 5581-7.

Basecke, J., Feuring-Buske, M., Brittinger, G., Schaefer, U. W., Hiddemann, W. and Griesinger, F. (2002). Transcription of AML1 in hematopoietic subfractions of normal adults. *Ann Hematol* **81**, 254-7.

Baumann, C. I., Bailey, A. S., Li, W., Ferkowicz, M. J., Yoder, M. C. and Fleming, W. H. (2004). PECAM-1 is expressed on hematopoietic stem cells throughout ontogeny and identifies a population of erythroid progenitors. *Blood* **104**, 1010-6.

Beddington, R. S. and Robertson, E. J. (1989). An assessment of the developmental potential of embryonic stem cells in the midgestation mouse embryo. *Development* **105**, 733-7.

Bee, T., Ashley, E. L., Bickley, S. R., Jarratt, A., Li, P. S., Sloane-Stanley, J., Gottgens, B. and de Bruijn, M. F. (2009a). The mouse Runx1 +23 hematopoietic stem cell enhancer confers hematopoietic specificity to both Runx1 promoters. *Blood* **113**, 5121-4.

Bee, T., Liddiard, K., Swiers, G., Bickley, S. R., Vink, C. S., Jarratt, A., Hughes, J. R., Medvinsky, A. and de Bruijn, M. F. (2009b). Alternative Runx1 promoter usage in mouse developmental hematopoiesis. *Blood Cells Mol Dis* **43**, 35-42.

Berman, J. W. and Basch, R. S. (1985). Thy-1 antigen expression by murine hematopoietic precursor cells. *Exp Hematol* **13**, 1152-6.

Bernex, F., De Sepulveda, P., Kress, C., Elbaz, C., Delouis, C. and Panthier, J. J. (1996). Spatial and temporal patterns of c-kit-expressing cells in WlacZ/+ and WlacZ/WlacZ mouse embryos. *Development* **122**, 3023-33.

Bertrand, J. Y., Giroux, S., Golub, R., Klaine, M., Jalil, A., Boucontet, L., Godin, I. and Cumano, A. (2005). Characterization of purified intraembryonic hematopoietic stem cells as a tool to define their site of origin. *Proc Natl Acad Sci U S A* **102**, 134-9.

Bhatia, M., Bonnet, D., Wu, D., Murdoch, B., Wrana, J., Gallacher, L. and Dick, J. E. (1999). Bone morphogenetic proteins regulate the developmental program of human hematopoietic stem cells. *J Exp Med* **189**, 1139-48.

Bijl, J., Thompson, A., Ramirez-Solis, R., Krosl, J., Grier, D. G., Lawrence, H. J. and Sauvageau, G. (2006). Analysis of HSC activity and compensatory Hox gene expression profile in Hoxb cluster mutant fetal liver cells. *Blood* **108**, 116-22.

Bowie, M. B., Kent, D. G., Copley, M. R. and Eaves, C. J. (2007a). Steel factor responsiveness regulates the high self-renewal phenotype of fetal hematopoietic stem cells. *Blood* **109**, 5043-8.

Bowie, M. B., Kent, D. G., Dykstra, B., McKnight, K. D., McCaffrey, L., Hoodless, P. A. and Eaves, C. J. (2007b). Identification of a new intrinsically timed developmental checkpoint that reprograms key hematopoietic stem cell properties. *Proc Natl Acad Sci U S A* **104**, 5878-82.

Bowie, M. B., McKnight, K. D., Kent, D. G., McCaffrey, L., Hoodless, P. A. and Eaves, C. J. (2006). Hematopoietic stem cells proliferate until after birth and show a reversible phase-specific engraftment defect. *J Clin Invest* **116**, 2808-16.

Bradley, A., Evans, M., Kaufman, M. H. and Robertson, E. (1984). Formation of germ-line chimaeras from embryo-derived teratocarcinoma cell lines. *Nature* **309**, 255-6.

Brasel, K., McKenna, H. J., Morrissey, P. J., Charrier, K., Morris, A. E., Lee, C. C., Williams, D. E. and Lyman, S. D. (1996). Hematologic effects of flt3 ligand in vivo in mice. *Blood* **88**, 2004-12.

Breier, G., Breviario, F., Caveda, L., Berthier, R., Schnurch, H., Gotsch, U., Vestweber, D., Risau, W. and Dejana, E. (1996). Molecular cloning and expression of murine vascular endothelial-cadherin in early stage development of cardiovascular system. *Blood* **87**, 630-41.

Brun, A. C., Bjornsson, J. M., Magnusson, M., Larsson, N., Leveen, P., Ehinger, M., Nilsson, E. and Karlsson, S. (2004). Hoxb4-deficient mice undergo normal hematopoietic development but exhibit a mild proliferation defect in hematopoietic stem cells. *Blood* **103**, 4126-33.

Bryder, D. and Jacobsen, S. E. (2000). Interleukin-3 supports expansion of long-term multilineage repopulating activity after multiple stem cell divisions in vitro. *Blood* **96**, 1748-55.

Buza-Vidas, N., Cheng, M., Duarte, S., Charoudeh, H. N., Jacobsen, S. E. and Sitnicka, E. (2009). FLT3 receptor and ligand are dispensable for maintenance and posttransplantation expansion of mouse hematopoietic stem cells. *Blood* **113**, 3453-60.

Cai, Z., de Bruijn, M., Ma, X., Dortland, B., Luteijn, T., Downing, R. J. and Dzierzak, E. (2000). Haploinsufficiency of AML1 affects the temporal and spatial generation of hematopoietic stem cells in the mouse embryo. *Immunity* **13**, 423-31.

Calvi, L. M., Adams, G. B., Weibrecht, K. W., Weber, J. M., Olson, D. P., Knight, M. C., Martin, R. P., Schipani, E., Divieti, P., Bringhurst, F. R. et al. (2003). Osteoblastic cells regulate the haematopoietic stem cell niche. *Nature* **425**, 841-6.

Cellot, S. and Sauvageau, G. (2006). In vitro stem cell expansion: stepping closer towards self-renewal. *Gene Ther* **13**, 1617-8.

Chadwick, K., Wang, L., Li, L., Menendez, P., Murdoch, B., Rouleau, A. and Bhatia, M. (2003). Cytokines and BMP-4 promote hematopoietic differentiation of human embryonic stem cells. *Blood* **102**, 906-15.

Chan, W. Y., Follows, G. A., Lacaud, G., Pimanda, J. E., Landry, J. R., Kinston, S., Knezevic, K., Piltz, S., Donaldson, I. J., Gambardella, L. et al. (2007). The paralogous hematopoietic regulators Lyl1 and Scl are coregulated by Ets and GATA factors, but Lyl1 cannot rescue the early Scl-/- phenotype. *Blood* **109**, 1908-16.

Chen, M. J., Yokomizo, T., Zeigler, B. M., Dzierzak, E. and Speck, N. A. (2009). Runx1 is required for the endothelial to haematopoietic cell transition but not thereafter. *Nature* **457**, 887-91.

Chen, X. D. and Turpen, J. B. (1995). Intraembryonic origin of hepatic hematopoiesis in Xenopus laevis. *J Immunol* **154**, 2557-67.

Choi, I., Cho, B. R., Kim, D., Miyagawa, S., Kubo, T., Kim, J. Y., Park, C. G., Hwang, W. S., Lee, J. S. and Ahn, C. (2005). Choice of the adequate detection time for the accurate evaluation of the efficiency of siRNA-induced gene silencing. *J Biotechnol* **120**, 251-61.

Choi, K., Kennedy, M., Kazarov, A., Papadimitriou, J. C. and Keller, G. (1998). A common precursor for hematopoietic and endothelial cells. *Development* **125**, 725-32.

Ciau-Uitz, A., Walmsley, M. and Patient, R. (2000). Distinct origins of adult and embryonic blood in Xenopus. *Cell* **102**, 787-96.

Collins, A., Littman, D. R. and Taniuchi, I. (2009). RUNX proteins in transcription factor networks that regulate T-cell lineage choice. *Nat Rev Immunol* **9**, 106-15.

Cumano, A., Dieterlen-Lievre, F. and Godin, I. (1996). Lymphoid potential, probed before circulation in mouse, is restricted to caudal intraembryonic splanchnopleura. *Cell* **86**, 907-16.

Cumano, A., Ferraz, J. C., Klaine, M., Di Santo, J. P. and Godin, I. (2001). Intraembryonic, but not yolk sac hematopoietic precursors, isolated before circulation, provide long-term multilineage reconstitution. *Immunity* **15**, 477-85.

de Bruijn, M. F., Ma, X., Robin, C., Ottersbach, K., Sanchez, M. J. and Dzierzak, E. (2002). Hematopoietic stem cells localize to the endothelial cell layer in the midgestation mouse aorta. *Immunity* **16**, 673-83.

de Bruijn, M. F., Peeters, M. C., Luteijn, T., Visser, P., Speck, N. A. and Dzierzak, E. (2000a). CFU-S(11) activity does not localize solely with the aorta in the aorta-gonad-mesonephros region. *Blood* **96**, 2902-4.

de Bruijn, M. F., Speck, N. A., Peeters, M. C. and Dzierzak, E. (2000b). Definitive hematopoietic stem cells first develop within the major arterial regions of the mouse embryo. *EMBO J* **19**, 2465-74.

Diehl, A., Stoelting, S., Nadrowitz, R., Wagner, T. and Peters, S. O. (2007). Improved hematopoietic stem cell engraftment following ex vivo expansion of murine marrow cells with SCF and Flt3L. *Cytotherapy* **9**, 532-8.

Dieterlen-Lievre, F. (1975). On the origin of haemopoietic stem cells in the avian embryo: an experimental approach. *J Embryol Exp Morphol* **33**, 607-19.

Durst, K. L. and Hiebert, S. W. (2004). Role of RUNX family members in transcriptional repression and gene silencing. *Oncogene* **23**, 4220-4.

Eichmann, A., Corbel, C., Nataf, V., Vaigot, P., Breant, C. and Le Douarin, N. M. (1997). Ligand-dependent development of the endothelial and hemopoietic lineages from embryonic mesodermal cells expressing vascular endothelial growth factor receptor 2. *Proc Natl Acad Sci U S A* **94**, 5141-6.

Eilken, H. M., Nishikawa, S. and Schroeder, T. (2009). Continuous single-cell imaging of blood generation from haemogenic endothelium. *Nature* **457**, 896-900.

Elagib, K. E., Racke, F. K., Mogass, M., Khetawat, R., Delehanty, L. L. and Goldfarb, A. N. (2003). RUNX1 and GATA-1 coexpression and cooperation in megakaryocytic differentiation. *Blood* **101**, 4333-41.

Ema, H. and Nakauchi, H. (2000). Expansion of hematopoietic stem cells in the developing liver of a mouse embryo. *Blood* **95**, 2284-8.

Emambokus, N. R. and Frampton, J. (2003). The glycoprotein IIb molecule is expressed on early murine hematopoietic progenitors and regulates their numbers in sites of hematopoiesis. *Immunity* **19**, 33-45.

Evans, M. J. and Kaufman, M. H. (1981). Establishment in culture of pluripotential cells from mouse embryos. *Nature* **292**, 154-6.

Evans, T. and Felsenfeld, G. (1989). The erythroid-specific transcription factor Eryf1: a new finger protein. *Cell* **58**, 877-85.

Fehling, H. J., Lacaud, G., Kubo, A., Kennedy, M., Robertson, S., Keller, G. and Kouskoff, V. (2003). Tracking mesoderm induction and its specification to the hemangioblast during embryonic stem cell differentiation. *Development* **130**, 4217-27.

Ferkowicz, M. J., Starr, M., Xie, X., Li, W., Johnson, S. A., Shelley, W. C., Morrison, P. R. and Yoder, M. C. (2003). CD41 expression defines the onset of primitive and definitive hematopoiesis in the murine embryo. *Development* **130**, 4393-403.

Fraser, S. T., Ogawa, M., Yokomizo, T., Ito, Y. and Nishikawa, S. (2003). Putative intermediate precursor between hematogenic endothelial cells and blood cells in the developing embryo. *Dev Growth Differ* **45**, 63-75.

Fraser, S. T., Ogawa, M., Yu, R. T., Nishikawa, S. and Yoder, M. C. (2002). Definitive hematopoietic commitment within the embryonic vascular endothelial-cadherin(+) population. *Exp Hematol* **30**, 1070-8.

Fujiwara, Y., Browne, C. P., Cunniff, K., Goff, S. C. and Orkin, S. H. (1996). Arrested development of embryonic red cell precursors in mouse embryos lacking transcription factor GATA-1. *Proc Natl Acad Sci U S A* **93**, 12355-8.

Garcia-Porrero, J. A., Godin, I. E. and Dieterlen-Lievre, F. (1995). Potential intraembryonic hemogenic sites at pre-liver stages in the mouse. *Anat Embryol (Berl)* **192**, 425-35.

Garcia-Porrero, J. A., Manaia, A., Jimeno, J., Lasky, L. L., Dieterlen-Lievre, F. and Godin, I. E. (1998). Antigenic profiles of endothelial and hemopoietic lineages in murine intraembryonic hemogenic sites. *Dev Comp Immunol* **22**, 303-19.

Gekas, C., Dieterlen-Lievre, F., Orkin, S. H. and Mikkola, H. K. (2005). The placenta is a niche for hematopoietic stem cells. *Dev Cell* **8**, 365-75.

Ghozi, M. C., Bernstein, Y., Negreanu, V., Levanon, D. and Groner, Y. (1996). Expression of the human acute myeloid leukemia gene AML1 is regulated by two promoter regions. *Proc Natl Acad Sci U S A* **93**, 1935-40.

Gilchrist, D. S., Ure, J., Hook, L. and Medvinsky, A. (2003). Labeling of hematopoietic stem and progenitor cells in novel activatable EGFP reporter mice. *Genesis* **36**, 168-76.

Gilliland, D. G. and Griffin, J. D. (2002). The roles of FLT3 in hematopoiesis and leukemia. *Blood* **100**, 1532-42.

Ginsburg, M., Snow, M. H. and McLaren, A. (1990). Primordial germ cells in the mouse embryo during gastrulation. *Development* **110**, 521-8.

Giroux, S., Kaushik, A. L., Capron, C., Jalil, A., Kelaidi, C., Sablitzky, F., Dumenil, D., Albagli, O. and Godin, I. (2007). lyl-1 and tal-1/scl, two genes encoding closely related bHLH transcription factors, display highly overlapping expression patterns during cardiovascular and hematopoietic ontogeny. *Gene Expr Patterns* **7**, 215-26.

Godin, I. and Cumano, A. (2002). The hare and the tortoise: an embryonic haematopoietic race. *Nat Rev Immunol* **2**, 593-604.

Goldfarb, A. N. (2009). Megakaryocytic programming by a transcriptional regulatory loop: A circle connecting RUNX1, GATA-1, and P-TEFb. *J Cell Biochem* **107**, 377-82.

Goodell, M. A., Brose, K., Paradis, G., Conner, A. S. and Mulligan, R. C. (1996). Isolation and functional properties of murine hematopoietic stem cells that are replicating in vivo. *J Exp Med* **183**, 1797-806.

Goyama, S., Yamaguchi, Y., Imai, Y., Kawazu, M., Nakagawa, M., Asai, T., Kumano, K., Mitani, K., Ogawa, S., Chiba, S. et al. (2004). The transcriptionally active form of AML1 is required for hematopoietic rescue of the AML1-deficient embryonic para-aortic splanchnopleural (P-Sp) region. *Blood* **104**, 3558-64.

Growney, J. D., Shigematsu, H., Li, Z., Lee, B. H., Adelsperger, J., Rowan, R., Curley, D. P., Kutok, J. L., Akashi, K., Williams, I. R. et al. (2005). Loss of Runx1 perturbs adult hematopoiesis and is associated with a myeloproliferative phenotype. *Blood* **106**, 494-504.

Hadland, B. K., Huppert, S. S., Kanungo, J., Xue, Y., Jiang, R., Gridley, T., Conlon, R. A., Cheng, A. M., Kopan, R. and Longmore, G. D. (2004). A requirement for Notch1 distinguishes 2 phases of definitive hematopoiesis during development. *Blood* **104**, 3097-105.

Huang, G., Shigesada, K., Ito, K., Wee, H. J., Yokomizo, T. and Ito, Y. (2001). Dimerization with PEBP2beta protects RUNX1/AML1 from ubiquitin-proteasome-mediated degradation. *EMBO J* **20**, 723-33.

Huber, T. L., Kouskoff, V., Fehling, H. J., Palis, J. and Keller, G. (2004). Haemangioblast commitment is initiated in the primitive streak of the mouse embryo. *Nature* **432**, 625-30.

Ichikawa, M., Asai, T., Saito, T., Seo, S., Yamazaki, I., Yamagata, T., Mitani, K., Chiba, S., Ogawa, S., Kurokawa, M. et al. (2004). AML-1 is required for megakaryocytic maturation and lymphocytic differentiation, but not for maintenance of hematopoietic stem cells in adult hematopoiesis. *Nat Med* **10**, 299-304.

Ichikawa, M., Goyama, S., Asai, T., Kawazu, M., Nakagawa, M., Takeshita, M., Chiba, S., Ogawa, S. and Kurokawa, M. (2008). AML1/Runx1 negatively regulates quiescent hematopoietic stem cells in adult hematopoiesis. *J Immunol* **180**, 4402-8.

Ikuta, K. and Weissman, I. L. (1992). Evidence that hematopoietic stem cells express mouse c-kit but do not depend on steel factor for their generation. *Proc Natl Acad Sci U S A* **89**, 1502-6.

Jaffredo, T., Gautier, R., Brajeul, V. and Dieterlen-Lievre, F. (2000). Tracing the progeny of the aortic hemangioblast in the avian embryo. *Dev Biol* **224**, 204-14.

Jaffredo, T., Gautier, R., Eichmann, A. and Dieterlen-Lievre, F. (1998). Intraaortic hemopoietic cells are derived from endothelial cells during ontogeny. *Development* **125**, 4575-83.

Jaffredo, T., Nottingham, W., Liddiard, K., Bollerot, K., Pouget, C. and de Bruijn, M. (2005). From hemangioblast to hematopoietic stem cell: an endothelial connection? *Exp Hematol* **33**, 1029-40.

Jones, R. J., Wagner, J. E., Celano, P., Zicha, M. S. and Sharkis, S. J. (1990). Separation of pluripotent haematopoietic stem cells from spleen colony-forming cells. *Nature* **347**, 188-9.

Jordan, H. E. (1917). Aortic Cell Clusters in Vertebrate Embryos. *Proc Natl Acad Sci U S A* **3**, 149-56.

Kennedy, M., Firpo, M., Choi, K., Wall, C., Robertson, S., Kabrun, N. and Keller, G. (1997). A common precursor for primitive erythropoiesis and definitive haematopoiesis. *Nature* **386**, 488-93.

Kiel, M. J. and Morrison, S. J. (2008). Uncertainty in the niches that maintain haematopoietic stem cells. *Nat Rev Immunol* **8**, 290-301.

Kiel, M. J., Yilmaz, O. H., Iwashita, T., Yilmaz, O. H., Terhorst, C. and Morrison, S. J. (2005). SLAM family receptors distinguish hematopoietic stem and progenitor cells and reveal endothelial niches for stem cells. *Cell* **121**, 1109-21.

Kim, I., He, S., Yilmaz, O. H., Kiel, M. J. and Morrison, S. J. (2006). Enhanced purification of fetal liver hematopoietic stem cells using SLAM family receptors. *Blood* **108**, 737-44.

Kina, T., Ikuta, K., Takayama, E., Wada, K., Majumdar, A. S., Weissman, I. L. and Katsura, Y. (2000). The monoclonal antibody TER-119 recognizes a molecule associated with glycophorin A and specifically marks the late stages of murine erythroid lineage. *Br J Haematol* **109**, 280-7.

Komori, T., Yagi, H., Nomura, S., Yamaguchi, A., Sasaki, K., Deguchi, K., Shimizu, Y., Bronson, R. T., Gao, Y. H., Inada, M. et al. (1997). Targeted disruption of Cbfa1 results in a complete lack of bone formation owing to maturational arrest of osteoblasts. *Cell* **89**, 755-64.

Kondo, M., Weissman, I. L. and Akashi, K. (1997). Identification of clonogenic common lymphoid progenitors in mouse bone marrow. *Cell* **91**, 661-72.

Krebs, L. T., Xue, Y., Norton, C. R., Shutter, J. R., Maguire, M., Sundberg, J. P., Gallahan, D., Closson, V., Kitajewski, J., Callahan, R. et al. (2000). Notch signaling is essential for vascular morphogenesis in mice. *Genes Dev* **14**, 1343-52.

Kumano, K., Chiba, S., Kunisato, A., Sata, M., Saito, T., Nakagami-Yamaguchi, E., Yamaguchi, T., Masuda, S., Shimizu, K., Takahashi, T. et al. (2003). Notch1 but not Notch2 is essential for generating hematopoietic stem cells from endothelial cells. *Immunity* **18**, 699-711.

Kumaravelu, P., Hook, L., Morrison, A. M., Ure, J., Zhao, S., Zuyev, S., Ansell, J. and Medvinsky, A. (2002). Quantitative developmental anatomy of definitive haematopoietic stem cells/long-term repopulating units (HSC/RUs): role of the aorta-gonad-mesonephros (AGM) region and the yolk sac in colonisation of the mouse embryonic liver. *Development* **129**, 4891-9.

Kyba, M., Perlingeiro, R. C. and Daley, G. Q. (2002). HoxB4 confers definitive lymphoid-myeloid engraftment potential on embryonic stem cell and yolk sac hematopoietic progenitors. *Cell* **109**, 29-37.

Lagasse, E., Connors, H., Al-Dhalimy, M., Reitsma, M., Dohse, M., Osborne, L., Wang, X., Finegold, M., Weissman, I. L. and Grompe, M. (2000). Purified hematopoietic stem cells can differentiate into hepatocytes in vivo. *Nat Med* **6**, 1229-34.

Lancrin, C., Sroczynska, P., Stephenson, C., Allen, T., Kouskoff, V. and Lacaud, G. (2009). The haemangioblast generates haematopoietic cells through a haemogenic endothelium stage. *Nature* **457**, 892-5.

Landry, J. R., Kinston, S., Knezevic, K., de Bruijn, M. F., Wilson, N., Nottingham, W. T., Peitz, M., Edenhofer, F., Pimanda, J. E., Ottersbach, K. et al. (2008). Runx genes are direct targets of Scl/Tal1 in the yolk sac and fetal liver. *Blood* **111**, 3005-14.

Lantz, C. S., Boesiger, J., Song, C. H., Mach, N., Kobayashi, T., Mulligan, R. C., Nawa, Y., Dranoff, G. and Galli, S. J. (1998). Role for interleukin-3 in mast-cell and basophil development and in immunity to parasites. *Nature* **392**, 90-3.

Lassila, O., Eskola, J., Toivanen, P., Martin, C. and Dieterlen-Lievre, F. (1978). The origin of lymphoid stem cells studied in chick yold sac-embryo chimaeras. *Nature* **272**, 353-4.

Lassila, O., Martin, C., Toivanen, P. and Dieterlen-Lievre, F. (1982). Erythropoiesis and lymphopoiesis in the chick yolk-sac-embryo chimeras: contribution of yolk sac and intraembryonic stem cells. *Blood* **59**, 377-81.

Ledbetter, J. A. and Herzenberg, L. A. (1979). Xenogeneic monoclonal antibodies to mouse lymphoid differentiation antigens. *Immunol Rev* **47**, 63-90.

Levanon, D., Bettoun, D., Harris-Cerruti, C., Woolf, E., Negreanu, V., Eilam, R., Bernstein, Y., Goldenberg, D., Xiao, C., Fliegauf, M. et al. (2002). The Runx3 transcription factor regulates development and survival of TrkC dorsal root ganglia neurons. *EMBO J* **21**, 3454-63.

Levanon, D., Brenner, O., Negreanu, V., Bettoun, D., Woolf, E., Eilam, R., Lotem, J., Gat, U., Otto, F., Speck, N. et al. (2001a). Spatial and temporal expression pattern of Runx3 (Aml2) and Runx1 (Aml1) indicates non-redundant functions during mouse embryogenesis. *Mech Dev* **109**, 413-7.

Levanon, D., Glusman, G., Bangsow, T., Ben-Asher, E., Male, D. A., Avidan, N., Bangsow, C., Hattori, M., Taylor, T. D., Taudien, S. et al. (2001b). Architecture and anatomy of the genomic locus encoding the human leukemia-associated transcription factor RUNX1/AML1. *Gene* **262**, 23-33.

Li, X., Zhao, X., Fang, Y., Jiang, X., Duong, T., Fan, C., Huang, C. C. and Kain, S. R. (1998). Generation of destabilized green fluorescent protein as a transcription reporter. *J Biol Chem* **273**, 34970-5.

Ling, K. W., Ottersbach, K., van Hamburg, J. P., Oziemlak, A., Tsai, F. Y., Orkin, S. H., Ploemacher, R., Hendriks, R. W. and Dzierzak, E. (2004). GATA-2 plays two functionally distinct roles during the ontogeny of hematopoietic stem cells. *J Exp Med* **200**, 871-82.

Lorsbach, R. B., Moore, J., Ang, S. O., Sun, W., Lenny, N. and Downing, J. R. (2004). Role of RUNX1 in adult hematopoiesis: analysis of RUNX1-IRES-GFP knock-in mice reveals differential lineage expression. *Blood* **103**, 2522-9.

Lu, J., Maruyama, M., Satake, M., Bae, S. C., Ogawa, E., Kagoshima, H., Shigesada, K. and Ito, Y. (1995). Subcellular localization of the alpha and beta subunits of the acute myeloid leukemia-linked transcription factor PEBP2/CBF. *Mol Cell Biol* **15**, 1651-61.

Lutterbach, B., Westendorf, J. J., Linggi, B., Isaac, S., Seto, E. and Hiebert, S. W. (2000). A mechanism of repression by acute myeloid leukemia-1, the target of multiple chromosomal translocations in acute leukemia. *J Biol Chem* **275**, 651-6.

Mach, N., Lantz, C. S., Galli, S. J., Reznikoff, G., Mihm, M., Small, C., Granstein, R., Beissert, S., Sadelain, M., Mulligan, R. C. et al. (1998). Involvement of interleukin-3 in delayed-type hypersensitivity. *Blood* **91**, 778-83.

Magli, M. C., Iscove, N. N. and Odartchenko, N. (1982). Transient nature of early haematopoietic spleen colonies. *Nature* **295**, 527-9.

Maillard, I., Koch, U., Dumortier, A., Shestova, O., Xu, L., Sai, H., Pross, S. E., Aster, J. C., Bhandoola, A., Radtke, F. et al. (2008). Canonical notch signaling is dispensable for the maintenance of adult hematopoietic stem cells. *Cell Stem Cell* **2**, 356-66.

Manaia, A., Lemarchandel, V., Klaine, M., Max-Audit, I., Romeo, P., Dieterlen-Lievre, F. and Godin, I. (2000). Lmo2 and GATA-3 associated expression in intraembryonic hemogenic sites. *Development* **127**, 643-53.

Mancini, S. J., Mantei, N., Dumortier, A., Suter, U., MacDonald, H. R. and Radtke, F. (2005). Jagged1-dependent Notch signaling is dispensable for hematopoietic stem cell self-renewal and differentiation. *Blood* **105**, 2340-2.

Martin, G. R. (1981). Isolation of a pluripotent cell line from early mouse embryos cultured in medium conditioned by teratocarcinoma stem cells. *Proc Natl Acad Sci U S A* **78**, 7634-8.

Matsuoka, S., Ebihara, Y., Xu, M., Ishii, T., Sugiyama, D., Yoshino, H., Ueda, T., Manabe, A., Tanaka, R., Ikeda, Y. et al. (2001a). CD34 expression on long-term repopulating hematopoietic stem cells changes during developmental stages. *Blood* **97**, 419-25.

Matsuoka, S., Tsuji, K., Hisakawa, H., Xu, M., Ebihara, Y., Ishii, T., Sugiyama, D., Manabe, A., Tanaka, R., Ikeda, Y. et al. (2001b). Generation of definitive hematopoietic stem cells from murine early yolk sac and paraaortic splanchnopleures by aorta-gonad-mesonephros region-derived stromal cells. *Blood* **98**, 6-12.

Matsuyoshi, N., Toda, K., Horiguchi, Y., Tanaka, T., Nakagawa, S., Takeichi, M. and Imamura, S. (1997). In vivo evidence of the critical role of cadherin-5 in murine vascular integrity. *Proc Assoc Am Physicians* **109**, 362-71.

McGrath, K. E. and Palis, J. (2005). Hematopoiesis in the yolk sac: more than meets the eye. *Exp Hematol* **33**, 1021-8.

McKenna, H. J., Stocking, K. L., Miller, R. E., Brasel, K., De Smedt, T., Maraskovsky, E., Maliszewski, C. R., Lynch, D. H., Smith, J., Pulendran, B. et al. (2000). Mice lacking flt3 ligand have deficient hematopoiesis affecting hematopoietic progenitor cells, dendritic cells, and natural killer cells. *Blood* **95**, 3489-97.

McKinney-Freeman, S. L., Naveiras, O., Yates, F., Loewer, S., Philitas, M., Curran, M., Park, P. J. and Daley, G. Q. (2009). Surface antigen phenotypes of hematopoietic stem cells from embryos and murine embryonic stem cells. *Blood* **114**, 268-78.

Medvinsky, A. and Dzierzak, E. (1996). Definitive hematopoiesis is autonomously initiated by the AGM region. *Cell* **86**, 897-906.

Medvinsky, A. and Dzierzak, E. (1999). Development of the hematopoietic stem cell: can we describe it? *Blood* **94**, 3613-4.

Medvinsky, A., Taoudi, S., Mendes, S. and Dzierzak, E. (2008). Analysis and manipulation of hematopoietic progenitor and stem cells from murine embryonic tissues. *Curr Protoc Stem Cell Biol* **Chapter 2**, Unit 2A 6.

Medvinsky, A. L., Gan, O. I., Semenova, M. L. and Samoylina, N. L. (1996). Development of day-8 colony-forming unit-spleen hematopoietic progenitors during early murine embryogenesis: spatial and temporal mapping. *Blood* **87**, 557-66.

Medvinsky, A. L., Samoylina, N. L., Muller, A. M. and Dzierzak, E. A. (1993). An early pre-liver intraembryonic source of CFU-S in the developing mouse. *Nature* **364**, 64-7.

Melchers, F. (1979). Murine embryonic B lymphocyte development in the placenta. *Nature* **277**, 219-21.

Mikkola, H. K., Fujiwara, Y., Schlaeger, T. M., Traver, D. and Orkin, S. H. (2003a). Expression of CD41 marks the initiation of definitive hematopoiesis in the mouse embryo. *Blood* **101**, 508-16.

Mikkola, H. K., Klintman, J., Yang, H., Hock, H., Schlaeger, T. M., Fujiwara, Y. and Orkin, S. H. (2003b). Haematopoietic stem cells retain long-term repopulating activity and multipotency in the absence of stem-cell leukaemia SCL/tal-1 gene. *Nature* **421**, 547-51.

Milner, L. A. and Bigas, A. (1999). Notch as a mediator of cell fate determination in hematopoiesis: evidence and speculation. *Blood* **93**, 2431-48.

Minegishi, N., Ohta, J., Yamagiwa, H., Suzuki, N., Kawauchi, S., Zhou, Y., Takahashi, S., Hayashi, N., Engel, J. D. and Yamamoto, M. (1999). The mouse GATA-2 gene is expressed in the para-aortic splanchnopleura and aorta-gonads and mesonephros region. *Blood* **93**, 4196-207.

Mitjavila-Garcia, M. T., Cailleret, M., Godin, I., Nogueira, M. M., Cohen-Solal, K., Schiavon, V., Lecluse, Y., Le Pesteur, F., Lagrue, A. H. and Vainchenker, W. (2002). Expression of CD41 on hematopoietic progenitors derived from embryonic hematopoietic cells. *Development* **129**, 2003-13.

Miyoshi, H., Ohira, M., Shimizu, K., Mitani, K., Hirai, H., Imai, T., Yokoyama, K., Soeda, E. and Ohki, M. (1995). Alternative splicing and genomic structure of the AML1 gene involved in acute myeloid leukemia. *Nucleic Acids Res* **23**, 2762-9.

Moore, M. A. and Metcalf, D. (1970). Ontogeny of the haemopoietic system: yolk sac origin of in vivo and in vitro colony forming cells in the developing mouse embryo. *Br J Haematol* **18**, 279-96.

Moore, M. A. and Owen, J. J. (1965). Chromosome marker studies on the development of the haemopoietic system in the chick embryo. *Nature* **208**, 956 passim.

Moore, M. A. and Owen, J. J. (1967). Chromosome marker studies in the irradiated chick embryo. *Nature* **215**, 1081-2.

Morrison, S. J., Hemmati, H. D., Wandycz, A. M. and Weissman, I. L. (1995). The purification and characterization of fetal liver hematopoietic stem cells. *Proc Natl Acad Sci U S A* **92**, 10302-6.

Mukouyama, Y., Chiba, N., Hara, T., Okada, H., Ito, Y., Kanamaru, R., Miyajima, A., Satake, M. and Watanabe, T. (2000). The AML1 transcription factor functions to develop and maintain hematogenic precursor cells in the embryonic aorta-gonad-mesonephros region. *Dev Biol* **220**, 27-36.

Muller, A. M., Medvinsky, A., Strouboulis, J., Grosveld, F. and Dzierzak, E. (1994). Development of hematopoietic stem cell activity in the mouse embryo. *Immunity* **1**, 291-301.

Niki, M., Okada, H., Takano, H., Kuno, J., Tani, K., Hibino, H., Asano, S., Ito, Y., Satake, M. and Noda, T. (1997). Hematopoiesis in the fetal liver is impaired by targeted mutagenesis of a gene encoding a non-DNA binding subunit of the transcription factor, polyomavirus enhancer binding protein 2/core binding factor. *Proc Natl Acad Sci U S A* **94**, 5697-702.

Nilsson, S. K., Johnston, H. M. and Coverdale, J. A. (2001). Spatial localization of transplanted hemopoietic stem cells: inferences for the localization of stem cell niches. *Blood* **97**, 2293-9.

Nishikawa, S. I., Nishikawa, S., Hirashima, M., Matsuyoshi, N. and Kodama, H. (1998a). Progressive lineage analysis by cell sorting and culture identifies FLK1+VE-cadherin+ cells at a diverging point of endothelial and hemopoietic lineages. *Development* **125**, 1747-57.

Nishikawa, S. I., Nishikawa, S., Kawamoto, H., Yoshida, H., Kizumoto, M., Kataoka, H. and Katsura, Y. (1998b). In vitro generation of lymphohematopoietic cells from endothelial cells purified from murine embryos. *Immunity* **8**, 761-9.

Noda, S., Horiguchi, K., Ichikawa, H. and Miyoshi, H. (2008). Repopulating activity of ex vivo-expanded murine hematopoietic stem cells resides in the CD48-c-Kit+Sca-1+lineage marker- cell population. *Stem Cells* **26**, 646-55.

North, T., Gu, T. L., Stacy, T., Wang, Q., Howard, L., Binder, M., Marin-Padilla, M. and Speck, N. A. (1999). Cbfa2 is required for the formation of intra-aortic hematopoietic clusters. *Development* **126**, 2563-75.

North, T. E., de Bruijn, M. F., Stacy, T., Talebian, L., Lind, E., Robin, C., Binder, M., Dzierzak, E. and Speck, N. A. (2002). Runx1 expression marks long-term repopulating hematopoietic stem cells in the midgestation mouse embryo. *Immunity* **16**, 661-72.

North, T. E., Stacy, T., Matheny, C. J., Speck, N. A. and de Bruijn, M. F. (2004). Runx1 is expressed in adult mouse hematopoietic stem cells and differentiating myeloid and lymphoid cells, but not in maturing erythroid cells. *Stem Cells* **22**, 158-68.

Nottingham, W. T., Jarratt, A., Burgess, M., Speck, C. L., Cheng, J. F., Prabhakar, S., Rubin, E. M., Li, P. S., Sloane-Stanley, J., Kong, A. S. J. et al. (2007). Runx1-mediated hematopoietic stem-cell emergence is controlled by a Gata/Ets/SCL-regulated enhancer. *Blood* **110**, 4188-97.

Nuchprayoon, I., Meyers, S., Scott, L. M., Suzow, J., Hiebert, S. and Friedman, A. D. (1994). PEBP2/CBF, the murine homolog of the human myeloid AML1 and PEBP2 beta/CBF beta proto-oncoproteins, regulates the murine myeloperoxidase and neutrophil elastase genes in immature myeloid cells. *Mol Cell Biol* **14**, 5558-68.

Ogilvy, S., Metcalf, D., Gibson, L., Bath, M. L., Harris, A. W. and Adams, J. M. (1999). Promoter elements of vav drive transgene expression in vivo throughout the hematopoietic compartment. *Blood* **94**, 1855-63.

Okada, H., Watanabe, T., Niki, M., Takano, H., Chiba, N., Yanai, N., Tani, K., Hibino, H., Asano, S., Mucenski, M. L. et al. (1998). AML1(-/-) embryos do not express certain hematopoiesis-related gene transcripts including those of the PU.1 gene. *Oncogene* **17**, 2287-93.

Okuda, T., Takeda, K., Fujita, Y., Nishimura, M., Yagyu, S., Yoshida, M., Akira, S., Downing, J. R. and Abe, T. (2000). Biological characteristics of the leukemia-associated transcriptional factor AML1 disclosed by hematopoietic rescue of AML1-deficient embryonic stem cells by using a knock-in strategy. *Mol Cell Biol* **20**, 319-28.

Okuda, T., van Deursen, J., Hiebert, S. W., Grosveld, G. and Downing, J. R. (1996). AML1, the target of multiple chromosomal translocations in human leukemia, is essential for normal fetal liver hematopoiesis. *Cell* **84**, 321-30.

Orford, K. W. and Scadden, D. T. (2008). Deconstructing stem cell self-renewal: genetic insights into cell-cycle regulation. *Nat Rev Genet* **9**, 115-28.

Orlic, D., Anderson, S., Biesecker, L. G., Sorrentino, B. P. and Bodine, D. M. (1995). Pluripotent hematopoietic stem cells contain high levels of mRNA for c-kit, GATA-2, p45 NF-E2, and c-myb and low levels or no mRNA for c-fms and the receptors for granulocyte colony-stimulating factor and interleukins 5 and 7. *Proc Natl Acad Sci U S A* **92**, 4601-5.

Osawa, M., Hanada, K., Hamada, H. and Nakauchi, H. (1996). Long-term lymphohematopoietic reconstitution by a single CD34-low/negative hematopoietic stem cell. *Science* **273**, 242-5.

Ottersbach, K. and Dzierzak, E. (2005). The murine placenta contains hematopoietic stem cells within the vascular labyrinth region. *Dev Cell* **8**, 377-87.

Palis, J., Robertson, S., Kennedy, M., Wall, C. and Keller, G. (1999). Development of erythroid and myeloid progenitors in the yolk sac and embryo proper of the mouse. *Development* **126**, 5073-84.

Pandolfi, P. P., Roth, M. E., Karis, A., Leonard, M. W., Dzierzak, E., Grosveld, F. G., Engel, J. D. and Lindenbaum, M. H. (1995). Targeted disruption of the GATA3 gene causes severe abnormalities in the nervous system and in fetal liver haematopoiesis. *Nat Genet* **11**, 40-4.

Pardanaud, L. and Dieterlen-Lievre, F. (1999). Manipulation of the angiopoietic/hemangiopoietic commitment in the avian embryo. *Development* **126**, 617-27.

Pardanaud, L., Luton, D., Prigent, M., Bourcheix, L. M., Catala, M. and Dieterlen-Lievre, F. (1996). Two distinct endothelial lineages in ontogeny, one of them related to hemopoiesis. *Development* **122**, 1363-71.

Peeters, M., Ottersbach, K., Bollerot, K., Orelio, C., de Bruijn, M., Wijgerde, M. and Dzierzak, E. (2009). Ventral embryonic tissues and Hedgehog proteins induce early AGM hematopoietic stem cell development. *Development*.

Peterkin, T., Gibson, A., Loose, M. and Patient, R. (2005). The roles of GATA-4, -5 and -6 in vertebrate heart development. *Semin Cell Dev Biol* **16**, 83-94.

Peters, S. O., Kittler, E. L., Ramshaw, H. S. and Quesenberry, P. J. (1996). Ex vivo expansion of murine marrow cells with interleukin-3 (IL-3), IL-6, IL-11, and stem cell factor leads to impaired engraftment in irradiated hosts. *Blood* **87**, 30-7.

Pevny, L., Simon, M. C., Robertson, E., Klein, W. H., Tsai, S. F., D'Agati, V., Orkin, S. H. and Costantini, F. (1991). Erythroid differentiation in chimaeric mice blocked by a targeted mutation in the gene for transcription factor GATA-1. *Nature* **349**, 257-60.

Phillips, D. R., Charo, I. F., Parise, L. V. and Fitzgerald, L. A. (1988). The platelet membrane glycoprotein IIb-IIIa complex. *Blood* **71**, 831-43.

Pimanda, J. E., Donaldson, I. J., de Bruijn, M. F., Kinston, S., Knezevic, K., Huckle, L., Piltz, S., Landry, J. R., Green, A. R., Tannahill, D. et al. (2007). The SCL transcriptional network and BMP signaling pathway interact to regulate RUNX1 activity. *Proc Natl Acad Sci U S A* **104**, 840-5.

Porcher, C., Swat, W., Rockwell, K., Fujiwara, Y., Alt, F. W. and Orkin, S. H. (1996). The T cell leukemia oncoprotein SCL/tal-1 is essential for development of all hematopoietic lineages. *Cell* **86**, 47-57.

Pozner, A., Lotem, J., Xiao, C., Goldenberg, D., Brenner, O., Negreanu, V., Levanon, D. and Groner, Y. (2007). Developmentally regulated promoter-switch transcriptionally controls Runx1 function during embryonic hematopoiesis. *BMC Dev Biol* **7**, 84.

Putz, G., Rosner, A., Nuesslein, I., Schmitz, N. and Buchholz, F. (2006). AML1 deletion in adult mice causes splenomegaly and lymphomas. *Oncogene* **25**, 929-39.

Radtke, F., Wilson, A., Stark, G., Bauer, M., van Meerwijk, J., MacDonald, H. R. and Aguet, M. (1999). Deficient T cell fate specification in mice with an induced inactivation of Notch1. *Immunity* **10**, 547-58.

Reed-Inderbitzin, E., Moreno-Miralles, I., Vanden-Eynden, S. K., Xie, J., Lutterbach, B., Durst-Goodwin, K. L., Luce, K. S., Irvin, B. J., Cleary, M. L., Brandt, S. J. et al. (2006). RUNX1 associates with histone deacetylases and SUV39H1 to repress transcription. *Oncogene* **25**, 5777-86.

Rhodes, K. E., Gekas, C., Wang, Y., Lux, C. T., Francis, C. S., Chan, D. N., Conway, S., Orkin, S. H., Yoder, M. C. and Mikkola, H. K. (2008). The emergence of hematopoietic stem cells is initiated in the placental vasculature in the absence of circulation. *Cell Stem Cell* **2**, 252-63.

Rich, I. N. (1995). Primordial germ cells are capable of producing cells of the hematopoietic system in vitro. *Blood* **86**, 463-72.

Robb, L., Lyons, I., Li, R., Hartley, L., Kontgen, F., Harvey, R. P., Metcalf, D. and Begley, C. G. (1995). Absence of yolk sac hematopoiesis from mice with a targeted disruption of the scl gene. *Proc Natl Acad Sci U S A* **92**, 7075-9.

Robert-Moreno, A., Espinosa, L., de la Pompa, J. L. and Bigas, A. (2005). RBPjkappa-dependent Notch function regulates Gata2 and is essential for the formation of intra-embryonic hematopoietic cells. *Development* **132**, 1117-26.

Robert-Moreno, A., Guiu, J., Ruiz-Herguido, C., Lopez, M. E., Ingles-Esteve, J., Riera, L., Tipping, A., Enver, T., Dzierzak, E., Gridley, T. et al. (2008). Impaired embryonic haematopoiesis yet normal arterial development in the absence of the Notch ligand Jagged1. *EMBO J* **27**, 1886-95.

Robin, C., Ottersbach, K., Durand, C., Peeters, M., Vanes, L., Tybulewicz, V. and Dzierzak, E. (2006). An unexpected role for IL-3 in the embryonic development of hematopoietic stem cells. *Dev Cell* **11**, 171-80.

Sabin, F. R. (1920). Studies on the origin of blodd vessels and red corpuscles as seen in the living blastoderm of chicks during the second day of incubation. *Contrib. Embryol.* **9**, 213-259.

Samokhvalov, I. M., Samokhvalova, N. I. and Nishikawa, S. (2007). Cell tracing shows the contribution of the yolk sac to adult haematopoiesis. *Nature* **446**, 1056-61.

Samokhvalov, I. M., Thomson, A. M., Lalancette, C., Liakhovitskaia, A., Ure, J. and Medvinsky, A. (2006). Multifunctional reversible knockout/reporter system enabling fully functional reconstitution of the AML1/Runx1 locus and rescue of hematopoiesis. *Genesis* **44**, 115-21.

Sanchez, M. J., Holmes, A., Miles, C. and Dzierzak, E. (1996). Characterization of the first definitive hematopoietic stem cells in the AGM and liver of the mouse embryo. *Immunity* **5**, 513-25.

Sasaki, K., Yagi, H., Bronson, R. T., Tominaga, K., Matsunashi, T., Deguchi, K., Tani, Y., Kishimoto, T. and Komori, T. (1996). Absence of fetal liver hematopoiesis in mice deficient in transcriptional coactivator core binding factor beta. *Proc Natl Acad Sci U S A* **93**, 12359-63.

Sauvageau, G., Thorsteinsdottir, U., Eaves, C. J., Lawrence, H. J., Largman, C., Lansdorp, P. M. and Humphries, R. K. (1995). Overexpression of HOXB4 in hematopoietic cells causes the selective expansion of more primitive populations in vitro and in vivo. *Genes Dev* **9**, 1753-65.

Sheridan, J. M., Taoudi, S., Medvinsky, A. and Blackburn, C. C. (2009). A novel method for the generation of reaggregated organotypic cultures that permits juxtaposition of defined cell populations. *Genesis*.

Shivdasani, R. A., Mayer, E. L. and Orkin, S. H. (1995). Absence of blood formation in mice lacking the T-cell leukaemia oncoprotein tal-1/SCL. *Nature* **373**, 432-4.

Simeone, A., Daga, A. and Calabi, F. (1995). Expression of runt in the mouse embryo. *Dev Dyn* **203**, 61-70.

Siminovitch, L., McCulloch, E. A. and Till, J. E. (1963). The Distribution of Colony-Forming Cells among Spleen Colonies. *J Cell Physiol* **62**, 327-36.

Simon, M. C., Pevny, L., Wiles, M. V., Keller, G., Costantini, F. and Orkin, S. H. (1992). Rescue of erythroid development in gene targeted GATA-1- mouse embryonic stem cells. *Nat Genet* **1**, 92-8.

Sitnicka, E., Bryder, D., Theilgaard-Monch, K., Buza-Vidas, N., Adolfsson, J. and Jacobsen, S. E. (2002). Key role of flt3 ligand in regulation of the common lymphoid progenitor but not in maintenance of the hematopoietic stem cell pool. *Immunity* **17**, 463-72.

Smith, A. G., Heath, J. K., Donaldson, D. D., Wong, G. G., Moreau, J., Stahl, M. and Rogers, D. (1988). Inhibition of pluripotential embryonic stem cell differentiation by purified polypeptides. *Nature* **336**, 688-90.

Souroullas, G. P., Salmon, J. M., Sablitzky, F., Curtis, D. J. and Goodell, M. A. (2009). Adult hematopoietic stem and progenitor cells require either Lyl1 or Scl for survival. *Cell Stem Cell* **4**, 180-6.

Spangrude, G. J., Heimfeld, S. and Weissman, I. L. (1988). Purification and characterization of mouse hematopoietic stem cells. *Science* **241**, 58-62.

Speck, N. A. and Gilliland, D. G. (2002). Core-binding factors in haematopoiesis and leukaemia. *Nat Rev Cancer* **2**, 502-13.

Spender, L. C., Whiteman, H. J., Karstegl, C. E. and Farrell, P. J. (2005). Transcriptional cross-regulation of RUNX1 by RUNX3 in human B cells. *Oncogene* **24**, 1873-81.

Sun, W. and Downing, J. R. (2004). Haploinsufficiency of AML1 results in a decrease in the number of LTR-HSCs while simultaneously inducing an increase in more mature progenitors. *Blood* **104**, 3565-72.

Suzow, J. and Friedman, A. D. (1993). The murine myeloperoxidase promoter contains several functional elements, one of which binds a cell type-restricted transcription factor, myeloid nuclear factor 1 (MyNF1). *Mol Cell Biol* **13**, 2141-51.

Szilvassy, S. J., Humphries, R. K., Lansdorp, P. M., Eaves, A. C. and Eaves, C. J. (1990). Quantitative assay for totipotent reconstituting hematopoietic stem cells by a competitive repopulation strategy. *Proc Natl Acad Sci U S A* **87**, 8736-40.

Takakura, N., Huang, X. L., Naruse, T., Hamaguchi, I., Dumont, D. J., Yancopoulos, G. D. and Suda, T. (1998). Critical role of the TIE2 endothelial cell receptor in the development of definitive hematopoiesis. *Immunity* **9**, 677-86.

Tanaka, K., Tanaka, T., Ogawa, S., Kurokawa, M., Mitani, K., Yazaki, Y. and Hirai, H. (1995). Increased expression of AML1 during retinoic-acid-induced differentiation of U937 cells. *Biochem Biophys Res Commun* **211**, 1023-30.

Tanaka, Y., Watanabe, T., Chiba, N., Niki, M., Kuroiwa, Y., Nishihira, T., Satomi, S., Ito, Y. and Satake, M. (1997). The protooncogene product, PEBP2beta/CBFbeta, is mainly located in the cytoplasm and has an affinity with cytoskeletal structures. *Oncogene* **15**, 677-83.

Taniguchi, H., Toyoshima, T., Fukao, K. and Nakauchi, H. (1996). Presence of hematopoietic stem cells in the adult liver. *Nat Med* **2**, 198-203.

Taoudi, S. (2006). Emergence and Expansion of Embryonic Definitive Haematopoietic Stem Cells. In *School of Biological Sciences* vol. PhD (ed., pp. 301. Edinburgh: University of Edinburgh.

Taoudi, S., Gonneau, C., Moore, K., Sheridan, J. M., Blackburn, C. C., Taylor, E. and Medvinsky, A. (2008). Extensive hematopoietic stem cell generation in the AGM region via maturation of VE-cadherin+CD45+ pre-definitive HSCs. *Cell Stem Cell* **3**, 99-108.

Taoudi, S. and Medvinsky, A. (2007). Functional identification of the hematopoietic stem cell niche in the ventral domain of the embryonic dorsal aorta. *Proc Natl Acad Sci U S A* **104**, 9399-403.

Taoudi, S., Morrison, A. M., Inoue, H., Gribi, R., Ure, J. and Medvinsky, A. (2005). Progressive divergence of definitive haematopoietic stem cells from the endothelial compartment does not depend on contact with the foetal liver. *Development* **132**, 4179-91.

Thomas, M. L. (1989). The leukocyte common antigen family. *Annu Rev Immunol* **7**, 339-69.

Thorsteinsdottir, U., Sauvageau, G. and Humphries, R. K. (1999). Enhanced in vivo regenerative potential of HOXB4-transduced hematopoietic stem cells with regulation of their pool size. *Blood* **94**, 2605-12.

Tian, X. and Kaufman, D. S. (2008). Differentiation of embryonic stem cells towards hematopoietic cells: progress and pitfalls. *Curr Opin Hematol* **15**, 312-8.

Till, J. E. and Mc, C. E. (1961). A direct measurement of the radiation sensitivity of normal mouse bone marrow cells. *Radiat Res* **14**, 213-22.

Ting, C. N., Olson, M. C., Barton, K. P. and Leiden, J. M. (1996). Transcription factor GATA-3 is required for development of the T-cell lineage. *Nature* **384**, 474-8.

Toles, J. F., Chui, D. H., Belbeck, L. W., Starr, E. and Barker, J. E. (1989). Hemopoietic stem cells in murine embryonic yolk sac and peripheral blood. *Proc Natl Acad Sci U S A* **86**, 7456-9.

Tsai, F. Y., Keller, G., Kuo, F. C., Weiss, M., Chen, J., Rosenblatt, M., Alt, F. W. and Orkin, S. H. (1994). An early haematopoietic defect in mice lacking the transcription factor GATA-2. *Nature* **371**, 221-6.

Tsai, S. F., Martin, D. I., Zon, L. I., D'Andrea, A. D., Wong, G. G. and Orkin, S. H. (1989). Cloning of cDNA for the major DNA-binding protein of the erythroid lineage through expression in mammalian cells. *Nature* **339**, 446-51.

Turpen, J. B., Kelley, C. M., Mead, P. E. and Zon, L. I. (1997). Bipotential primitive-definitive hematopoietic progenitors in the vertebrate embryo. *Immunity* **7**, 325-34.

Uchida, H., Zhang, J. and Nimer, S. D. (1997). AML1A and AML1B can transactivate the human IL-3 promoter. *J Immunol* **158**, 2251-8.

Uchida, N. and Weissman, I. L. (1992). Searching for hematopoietic stem cells: evidence that Thy-1.1lo Lin- Sca-1+ cells are the only stem cells in C57BL/Ka-Thy-1.1 bone marrow. *J Exp Med* **175**, 175-84.

Verkhusha, V. V., Kuznetsova, I. M., Stepanenko, O. V., Zaraisky, A. G., Shavlovsky, M. M., Turoverov, K. K. and Uversky, V. N. (2003). High stability of Discosoma DsRed as compared to Aequorea EGFP. *Biochemistry* **42**, 7879-84.

Vogeli, K. M., Jin, S. W., Martin, G. R. and Stainier, D. Y. (2006). A common progenitor for haematopoietic and endothelial lineages in the zebrafish gastrula. *Nature* **443**, 337-9.

Wagers, A. J., Sherwood, R. I., Christensen, J. L. and Weissman, I. L. (2002). Little evidence for developmental plasticity of adult hematopoietic stem cells. *Science* **297**, 2256-9.

Wang, Q., Stacy, T., Binder, M., Marin-Padilla, M., Sharpe, A. H. and Speck, N. A. (1996a). Disruption of the Cbfa2 gene causes necrosis and hemorrhaging in the central nervous system and blocks definitive hematopoiesis. *Proc Natl Acad Sci U S A* **93**, 3444-9.

Wang, Q., Stacy, T., Miller, J. D., Lewis, A. F., Gu, T. L., Huang, X., Bushweller, J. H., Bories, J. C., Alt, F. W., Ryan, G. et al. (1996b). The CBFbeta subunit is essential for CBFalpha2 (AML1) function in vivo. *Cell* **87**, 697-708.

Warner, J. K., Wang, J. C., Hope, K. J., Jin, L. and Dick, J. E. (2004). Concepts of human leukemic development. *Oncogene* **23**, 7164-77.

Warren, A. J., Colledge, W. H., Carlton, M. B., Evans, M. J., Smith, A. J. and Rabbitts, T. H. (1994). The oncogenic cysteine-rich LIM domain protein rbtn2 is essential for erythroid development. *Cell* **78**, 45-57.

Weiss, M. J., Keller, G. and Orkin, S. H. (1994). Novel insights into erythroid development revealed through in vitro differentiation of GATA-1 embryonic stem cells. *Genes Dev* **8**, 1184-97.

Weissman, I. L., Anderson, D. J. and Gage, F. (2001). Stem and progenitor cells: origins, phenotypes, lineage commitments, and transdifferentiations. *Annu Rev Cell Dev Biol* **17**, 387-403.

Weissman IL, P. V., Gardner R. (1978). Fetal hematopoietic origins of the adult hematolymphoid system. In *Differentiation of normal and neoplastic hematopoietic cells*, (ed. M. P. Clarkson B, Till JE), pp. 33-47. New York: Cold Spring Harbor, New York: Cold Spring Harbor Laboratory.

Westendorf, J. J., Yamamoto, C. M., Lenny, N., Downing, J. R., Selsted, M. E. and Hiebert, S. W. (1998). The t(8;21) fusion product, AML-1-ETO, associates with C/EBP-alpha, inhibits C/EBP-alpha-dependent transcription, and blocks granulocytic differentiation. *Mol Cell Biol* **18**, 322-33.

Wheeler, J. C., VanderZwan, C., Xu, X., Swantek, D., Tracey, W. D. and Gergen, J. P. (2002). Distinct in vivo requirements for establishment versus maintenance of transcriptional repression. *Nat Genet* **32**, 206-10.

Williams, R. L., Hilton, D. J., Pease, S., Willson, T. A., Stewart, C. L., Gearing, D. P., Wagner, E. F., Metcalf, D., Nicola, N. A. and Gough, N. M. (1988). Myeloid leukaemia inhibitory factor maintains the developmental potential of embryonic stem cells. *Nature* **336**, 684-7.

Wilson, A., Laurenti, E., Oser, G., van der Wath, R. C., Blanco-Bose, W., Jaworski, M., Offner, S., Dunant, C. F., Eshkind, L., Bockamp, E. et al. (2008). Hematopoietic stem cells reversibly switch from dormancy to self-renewal during homeostasis and repair. *Cell* **135**, 1118-29.

Wolber, F. M., Leonard, E., Michael, S., Orschell-Traycoff, C. M., Yoder, M. C. and Srour, E. F. (2002). Roles of spleen and liver in development of the murine hematopoietic system. *Exp Hematol* **30**, 1010-9.

Wood, H. B., May, G., Healy, L., Enver, T. and Morriss-Kay, G. M. (1997). CD34 expression patterns during early mouse development are related to modes of blood vessel formation and reveal additional sites of hematopoiesis. *Blood* **90**, 2300-11.

Xu, M. J., Tsuji, K., Ueda, T., Mukouyama, Y. S., Hara, T., Yang, F. C., Ebihara, Y., Matsuoka, S., Manabe, A., Kikuchi, A. et al. (1998). Stimulation of mouse and human primitive hematopoiesis by murine embryonic aorta-gonad-mesonephros-derived stromal cell lines. *Blood* **92**, 2032-40.

Yamada, Y., Warren, A. J., Dobson, C., Forster, A., Pannell, R. and Rabbitts, T. H. (1998). The T cell leukemia LIM protein Lmo2 is necessary for adult mouse hematopoiesis. *Proc Natl Acad Sci U S A* **95**, 3890-5.

Yan, J., Liu, Y., Lukasik, S. M., Speck, N. A. and Bushweller, J. H. (2004). CBFbeta allosterically regulates the Runx1 Runt domain via a dynamic conformational equilibrium. *Nat Struct Mol Biol* **11**, 901-6.

Yang, T. T., Cheng, L. and Kain, S. R. (1996). Optimized codon usage and chromophore mutations provide enhanced sensitivity with the green fluorescent protein. *Nucleic Acids Res* **24**, 4592-3.

Ying, Q. L., Nichols, J., Chambers, I. and Smith, A. (2003). BMP induction of Id proteins suppresses differentiation and sustains embryonic stem cell self-renewal in collaboration with STAT3. *Cell* **115**, 281-92.

Yoder, M. C. and Hiatt, K. (1997). Engraftment of embryonic hematopoietic cells in conditioned newborn recipients. *Blood* **89**, 2176-83.

Yoder, M. C., Hiatt, K., Dutt, P., Mukherjee, P., Bodine, D. M. and Orlic, D. (1997a). Characterization of definitive lymphohematopoietic stem cells in the day 9 murine yolk sac. *Immunity* **7**, 335-44.

Yoder, M. C., Hiatt, K. and Mukherjee, P. (1997b). In vivo repopulating hematopoietic stem cells are present in the murine yolk sac at day 9.0 postcoitus. *Proc Natl Acad Sci U S A* **94**, 6776-80.

Yokomizo, T., Hasegawa, K., Ishitobi, H., Osato, M., Ema, M., Ito, Y., Yamamoto, M. and Takahashi, S. (2008). Runx1 is involved in primitive erythropoiesis in the mouse. *Blood* **111**, 4075-80.

Yokomizo, T., Ogawa, M., Osato, M., Kanno, T., Yoshida, H., Fujimoto, T., Fraser, S., Nishikawa, S., Okada, H., Satake, M. et al. (2001). Requirement of Runx1/AML1/PEBP2alphaB for the generation of haematopoietic cells from endothelial cells. *Genes Cells* **6**, 13-23.

Yonemura, Y., Ku, H., Hirayama, F., Souza, L. M. and Ogawa, M. (1996). Interleukin 3 or interleukin 1 abrogates the reconstituting ability of hematopoietic stem cells. *Proc Natl Acad Sci U S A* **93**, 4040-4.

Yoshida, H., Takakura, N., Hirashima, M., Kataoka, H., Tsuchida, K. and Nishikawa, S. (1998). Hematopoietic tissues, as a playground of receptor tyrosine kinases of the PDGF-receptor family. *Dev Comp Immunol* **22**, 321-32.

Yu, C., Cantor, A. B., Yang, H., Browne, C., Wells, R. A., Fujiwara, Y. and Orkin, S. H. (2002). Targeted deletion of a high-affinity GATA-binding site in the GATA-1 promoter leads to selective loss of the eosinophil lineage in vivo. *J Exp Med* **195**, 1387-95.

Zeigler, B. M., Sugiyama, D., Chen, M., Guo, Y., Downs, K. M. and Speck, N. A. (2006). The allantois and chorion, when isolated before circulation or chorio-allantoic fusion, have hematopoietic potential. *Development* **133**, 4183-92.

Zhang, C. C., Kaba, M., Ge, G., Xie, K., Tong, W., Hug, C. and Lodish, H. F. (2006). Angiopoietin-like proteins stimulate ex vivo expansion of hematopoietic stem cells. *Nat Med* **12**, 240-5.

Zhang, C. C. and Lodish, H. F. (2008). Cytokines regulating hematopoietic stem cell function. *Curr Opin Hematol* **15**, 307-11.

Zhang, D. E., Fujioka, K., Hetherington, C. J., Shapiro, L. H., Chen, H. M., Look, A. T. and Tenen, D. G. (1994). Identification of a region which directs the monocytic activity of the colony-stimulating factor 1 (macrophage colony-stimulating factor) receptor promoter and binds PEBP2/CBF (AML1). *Mol Cell Biol* **14**, 8085-95.

Zhang, D. E., Hetherington, C. J., Meyers, S., Rhoades, K. L., Larson, C. J., Chen, H. M., Hiebert, S. W. and Tenen, D. G. (1996). CCAAT enhancer-binding protein (C/EBP) and AML1 (CBF alpha2) synergistically activate the macrophage colony-stimulating factor receptor promoter. *Mol Cell Biol* **16**, 1231-40.

Zhang, J., Niu, C., Ye, L., Huang, H., He, X., Tong, W. G., Ross, J., Haug, J., Johnson, T., Feng, J. Q. et al. (2003). Identification of the haematopoietic stem cell niche and control of the niche size. *Nature* **425**, 836-41.

Zhao, Y., Lin, Y., Zhan, Y., Yang, G., Louie, J., Harrison, D. E. and Anderson, W. F. (2000). Murine hematopoietic stem cell characterization and its regulation in BM transplantation. *Blood* **96**, 3016-22.

Zhong, R. K., Astle, C. M. and Harrison, D. E. (1996). Distinct developmental patterns of short-term and long-term functioning lymphoid and myeloid precursors defined by competitive limiting dilution analysis in vivo. *J Immunol* **157**, 138-45.

Zhou, Y., Lim, K. C., Onodera, K., Takahashi, S., Ohta, J., Minegishi, N., Tsai, F. Y., Orkin, S. H., Yamamoto, M. and Engel, J. D. (1998). Rescue of the embryonic lethal hematopoietic defect reveals a critical role for GATA-2 in urogenital development. *EMBO J* **17**, 6689-700.

Zovein, A. C., Hofmann, J. J., Lynch, M., French, W. J., Turlo, K. A., Yang, Y., Becker, M. S., Zanetta, L., Dejana, E., Gasson, J. C. et al. (2008). Fate tracing reveals the endothelial origin of hematopoietic stem cells. *Cell Stem Cell* **3**, 625-36.